University of Strathclyde

Department of Pure and Applied Chemistry

Study of SERS for the Detection of Drugs of Abuse

by

Sarah Louise Lamping

A thesis presented in fulfilment of the requirements for the degree of Doctor of Philosophy

October 2008

"The copyright of this thesis belongs to the author under the terms of the United Kingdom Copyright Acts as qualified by University of Strathclyde Regulation 3.49. Due acknowledgement must always be made of the use of any material contained in, or derived from, this thesis."

Dedicated to the memory of my Grandparents.

Acknowledgements

I would like to express my gratitude to Professor Andrew Mills, Professor Richard Lacey (Home Office Scientific Development Branch (HOSDB) and Professor Ewen Smith for their help and guidance throughout. I would also like to thank David Summers, Lynne Head and the whole Road Policing Team at HOSDB for their support.

To my family and friends, a big thank you for your tireless support and words of encouragement which have kept me going to the end.

Perfer et obdura; dolor hic tibi proderit olim

(be patient and persisting; some day this pain will be useful to you)

Abstract

A study of the use of Surface Enhanced Raman Spectroscopy (SERS) for the detection of illicit drugs in oral fluid using metal enhancement mechanisms was undertaken. Initial work investigated ecstasy tablet composition using Raman to identify what drugs and excipients might be present in oral fluid samples obtained from users. Overall, it is possible to identify the presence of phenethylamines and excipients in the seized tablets but not categorically distinguish between the phenethylamine derivative(s) especially when in a mixture. Comparison of the overall batch average peak positions and peak responses of the phenethylamine derivatives and excipients shows variability across the batches and reveals trends within the sub-batches. The Raman spectra appear to reflect the findings of the GC/MS analysis tentatively, implying this technique could be used for initial intelligence gathering applications whilst confirmatory analysis results are awaited.

Initial SERS research focused on achieving enhancement of aqueous drug solutions with silver and gold colloid. Overall a lack of reproducibility was observed. Therefore, alternative SERS enhancement mechanisms were sought.

Ag/TiO_2 substrates demonstrated low limits of detection and the possibility of detecting SERS enhancement of aqueous amphetamine solution at levels below $8x10^{-7}$ M. The work also showed that cotton swabs for sample application onto the surface of the substrate are a viable practical option for both experimental and field analysis.

Successful detection of methadone and buprenorphine, used to treat heroin addiction, was achieved with Ag/TiO_2 substrates at concentrations associated with therapeutic use, representing lower concentration drugs. The detection of MDMA in oral fluid following ecstasy use, not only showed promise for the detection of illicit drugs, but did so at the analytical cut-off concentration detailed in the draft type approval specification for roadside drug screening devices. This work confirms that SERS has a role for drug detection in oral fluid samples.

Abbreviations List

632.8 nm	Helium-Neon Laser
785 nm	Infra-red Laser
α	Inherent polarizability of the molecule
ACPO	Association of Chief Police Officers
ADD	Attention Deficit Disorder
ADHD	Attention Deficit Hyperactivity Disorder
AFM	Atomic Force Microscopy
Ag/TiO_2	Silver coated titanium dioxide substrate
AMNA	N-(1-methyl-2-phenyethyl)-2-mercaptopyridine-3-carboxaminde
APTMS	(3-Aminopropyl)trimethoxysilane
Aq	Aqueous
Au/TiO_2	Gold coated titanium dioxide substrate
BCS	British Crime Survey
BLB	Black Light Blue
BP	4,4'bipyridine
BPE	Trans-1,2 bis (4-pyridyl)-ethane
CCD	Charge Couple Device
CJACS	Criminal Justice and Court Services Act (2000)
CTT	Critical Tracking Task
$\delta\alpha/\delta Q_j$	The rate of changes of polarisability
DA	Dopamine
DCC	Dichlorohexylcarbodiimide
DDS	Drug Detection System
E	Incident electric field strength
E_{bg}	is the band-gap energy of TiO_2
EIA	Enzyme Immunoassay
E_0	Maximum value of the electric field strength
ESEM	Environmental Scanning Electron Microscopy
FFM	Friction Force Microscopy
FIT	Field Impairment Test
FME	Field Medical Examiner
GC/MS	Gas Chromatography/Mass Spectrometry
GM19	4(5'-azobenzotriazyl)-3,5-dimethoxyphenylamine
GSE	Gaseous Secondary Electron Detector
5-HT	Serotonin
λ	Wavenumber
IR	Infra-Red Spectroscopy
Intensity/a.u	Intensity/arbitrary units
LC/MS/MS	Liquid Chromatography/Tandem Mass Spectrometry
6-MAM	6-Mono-acetyl-morphine
MBDB	N-methyl-benzodioazoybutamine
MDA	Methylenedioxyamphetamine
MDEA	Methylenedioxyethylamphetamine
MDMA	Methylenedioxymethamphetamine
M^n	The metal

MMNA	N-methyl-N-(1-methyl-2-phenyethyl)-2-mercaptopyridine-3-carboxaminde
2-MNA	2-Mercaptonicotinic Acid
MvD	Metal Vapour Deposition
NaCl	Sodium Chloride
NAd	Noradrenaline
ng/ml	Nanogram per millilitre
OIM	Optical Imaging Microscope
P	Polarization
PACE 1984	Police and Criminal Evidence Act (1984)
pK_a	Dissociation Constant
PMA	4-Methoxyamphetamine
PVA	Polyvinyl Alcohol
Q_j	Normal modes of molecular vibration
RATSA 2003	Railways and Transport Safety Act (2003)
RPM	Revolutions per Minute
RSD	Relative Standard Deviation
RTA 1988	Road Traffic Act (1988)
RTA 1991	Road Traffic Act (1991)
SART	Sustained Attention to Response Task
SED	Sacrificial Electron Donor
SEM	Scanning Electron Microscopy
SERS	Surface Enhanced Raman Spectroscopy
S/P	Saliva/Plasma Ratio
t	Time
TiO_2	Titanium Dioxide
µg/ml	Microgram per millilitre
UV	Ultraviolet
UV/VIS	Ultraviolet/Visible
ν_0	Laser Frequency
XPS	X-ray Photoelectron Spectroscopy
γ_{lv}	Liquid Surface Tension
γ_{sv}	Solid Surface Tension
γ_{sl}	Solid-Liquid Interfacial Tension
γ_{sl}	Solid-Liquid Interfacial Tension
ZnTPP	Zinc Tetraphenylporphine

Contents

Abstract v

Abbreviations List vi

Contents viii

Chapter 1 - Overview

1.1 Introduction 1

1.1.1 Legislation 1

1.1.2 Roadside Screening Devices 4

1.2 Driving Impairment 6

1.3 Amphetamines and Substituted Amphetamines 10

1.3.1 Substituted Amphetamines 10

1.3.2 Methamphetamine 11

1.3.3 MDA 11

1.3.4 MDMA 12

1.3.5 Mechanism of Action 12

1.3.6 Routes of Administration 13

1.3.7 Drug Distribution in Blood and Oral Fluid and Half Life 14

1.3.8 Clinical Uses 16

1.3.9 Statistics 17

1.4 Functions of the Oral Cavity 20

1.4.1 The Oral Cavity 20

1.4.2 Xenobiotic Entry Into Oral Fluid 21

1.4.3 Oral Fluid Collection 22

1.4.4 Phenethylamines in Oral Fluid 23

Chapter 2 – Raman Spectroscopy

2.1 Introduction 26

2.2 Theory 26

2.3 Surface Enhanced Raman Spectroscopy (SERS) 31

2.3.1 Introduction 31

2.3.2 Field Enhancement Theory 31

2.3.3 Chemical Enhancement Theory 32

2.3.4 Metal Colloids 35

2.3.5 Metal Vapour Deposition 36

2.3.6 Photoreduced Metal Particles 37

2.3.7 SERS Detection of Illicit and Prescription Drugs 41

Chapter 3 – Raman Spectroscopy Analysis of Ecstasy Tablets

3.1 Introduction 47

3.2 Experimental 48

3.2.1 Tablet Preparation 48

3.2.2 Spectral Collection 48

3.2.3 Raman Analysis 49

3.2.4 Reference Samples 50

3.2.5 Ecstasy Tablet Samples 50

3.2.6 Spectral Processing 50

3.3 Results 51

3.3.1 Drug Reference Standards Peak Position Data 51

3.3.2 Excipient Reference Standards Peak Position Data 53

3.3.3 Seized Tablets Demographic 59

3.3.4 Seized Tablets Peak Position Data 59

3.3.5 Variations Within Tablets From the Same Batch 64

3.3.6 Between Tablets Batches 68

3.4 Conclusions 75

3.5 Future Work 77

Chapter 4 – SERS With Gold and Silver Colloid at 785 nm and 633nm Excitation

4.1 Introduction 78

4.2 Experimental Procedure 78

4.2.1 Silver Colloid Preparation 78

4.2.2 Gold Colloid Preparation 79

4.2.3 Raman Equipment 79

4.2.4 Wavelength Calibration Procedure 79

4.2.5 Raman Analysis 80

4.2.6 Infra-red Analysis 80

4.2.7 SERS Analysis 80

4.3 Results 83

4.3.1 Amphetamine 83

4.3.2 The Substituted Amphetamines 89

4.4 Conclusions 95

4.5 Future Work 97

Chapter 5 – Ag/TiO_2 Silver Substrate Surfaces – Initial Investigations

5.1 Introduction 98

5.2 Experimental Procedure 98

5.2.1 Ag/TiO_2 Substrate Preparation 98

5.2.2 Spectral Collection 98

5.2.3 Environmental Scanning Electron Microscopy (ESEM) 98

5.2.4 Optical Imaging Microscopy (OIM) 99

5.2.5 SERS Analysis 99

5.2.6 SERS Analysis Following Use of A Cotton Swab 100

5.3 Characterisation of Ag/TiO_2 Substrate Surfaces 100

5.4 Results 104

5.4.1 Amphetamine 104

5.4.2 Methamphetamine 112
5.4.3 MDEA 114
5.4.4 Cotton Swabs 115
5.5 Conclusions 116
5.6 Future Work 117

Chapter 6 – Comparison of Silver and Gold Substrates for SERS Enhancement of Aqueous Amphetamine Solution

6.1 - Introduction 118
6.2 Experimental 119
6.2.1 Ag/TiO_2 Substrate Preparation 119
6.2.2 Au/TiO_2 Substrate Preparation 119
6.2.3 Sputtered Silver Substrate Preparation 119
6.2.4 Silver PVA Substrate Preparation 119
6.2.5 Klarite Substrate Preparation 120
6.2.6 Spectral Collection 120
6.2.7 SERS Analysis 120
6.2.8 Klarite Substrate Collection Parameters 121
6.3 Results 122
6.3.1 UV Irradiation Pre-cleaned Ag/TiO_2 122
6.3.2 Ag/TiO_2 Silver Substrates 124
6.3.3 Establishing the Lower Limit of Detection for the Ag/TiO_2 Substrates 126
6.3.4 Sputtered Silver Substrates 128
6.3.5 Au/TiO_2 Substrates 130
6.3.6 Commercially Available Silver Klarite Substrates from Mesophotonics 131
6.4 Conclusions 135
6.5 Future Work 136

Chapter 7 – Drug User Oral Fluid Samples

7.1 - Introduction 137

7.2 Experimental 139

7.2.1 Oral Fluid Volunteers 139

7.2.2 SART Test 140

7.2.3 CTT Test 141

7.2.4 FIT Test 141

7.2.5 Ag/TiO_2 Substrate Preparation 141

7.2.6 Spectral Collection 141

7.2.7 Raman Analysis 141

7.2.8 SERS Analysis 142

7.2.9 Spectral Processing 142

7.2.10 GC/MS and LC/MS Analysis 142

7.3 Results 142

7.3.1 Crystalline Drug Spectra 142

7.3.2 SERS From Blank Oral Fluid 147

7.3.3 SERS from Oral Fluid Samples from Drug User Subject 14 147

7.3.4 SERS from Oral Fluid Samples from Drug User Subject 16 150

7.3.5 Control Oral Fluid Samples 153

7.3.6 SART and CTT Results 153

7.4 Conclusions 154

155

Chapter 8 – Conclusions and Future Work 156

References 160

Chapter 1

Overview

1.1 Introduction

1.1.1 Legislation

In the United Kingdom the term 'fit to drive' is encountered on a daily basis by police officers and police surgeons. However, interpretation of this term is subjective, rendering enormous scope for inconsistency in the way that drug drivers are dealt with by the legal system. Within the legislation the statutory offence relating to drugs and driving is embodied under section 3A and 4 of the Road Traffic Act (RTA) 1988 (as amended by S4 of the RTA 1991). The offence is as follows:

> **"If a person causes the death of another person by driving a mechanically propelled vehicle on a road or other public place without due care and attention, or without reasonable consideration for other persons using the road or place and –**
>
> **(a) He is, at the time when he is driving, <u>unfit</u> to drive through drink or drugs… he is guilty of an offence"**

Section 3A RTA 1988 as amended.

> **"A person who, when driving or attempting to drive a motor vehicle on a road or other public place, is <u>unfit</u> to drive through drink or drugs shall be guilty of an offence."**

Section 4 (1) RTA 1988 as amended.

> **"For the purposes of this section a person shall be taken as <u>unfit</u> to drive if his ability to drive properly is <u>impaired</u>."**

Section 3A(2) and 4(5) RTA 1988 as amended.

Difficulties in legislative enforcement by a police officer arise when they encounter an individual who is not over the limit for alcohol but have visible signs of impairment often associated with either mono- or polydrug use. This forces the officer to make a subjective decision as to whether the impairment being observed warrants further investigation. The decision made can be based upon a number of variables such as: any training the officer has received, personal knowledge, reaction of the custody officer and ultimately, the officer has to decide whether a Forensic Medical Examiner (FME) would agree with his/her observations.

With reference to the term 'unfit to drive' the legislation includes a definition of the term unfit to drive as outlined above. However, because of inter-individual variability of the interpretation of the terms 'unfit' and 'impaired' inconsistencies still arise.

Recent changes in the legislation, Railways and Transport Safety Act (RATSA) 2003, has enabled an officer to request the driver perform a field impairment test (FIT) and provide an oral fluid sample for analysis at the roadside using a suitable screening device. To date no suitable devices have been evaluated in the United Kingdom for use in the enforcement of this legislation. The new legislation states;

> **6C "A preliminary drug test is a procedure by which a specimen of sweat or saliva is-**
>
> **a) obtained and**
>
> **b) used for the purpose of obtaining, by means of a device of a type approved .... an indication whether the person to whom the test is administered has a drug in his body."**
>
> Section 107 (7) RATSA 2003 an amendment for section of the RTA 1998 (c.52) (testing for drink or drugs) substitute the above. 6B Preliminary impairment test and 6C Preliminary drug test.

The standard protocol for assessing drug drivers can be found in Figure 1.1.

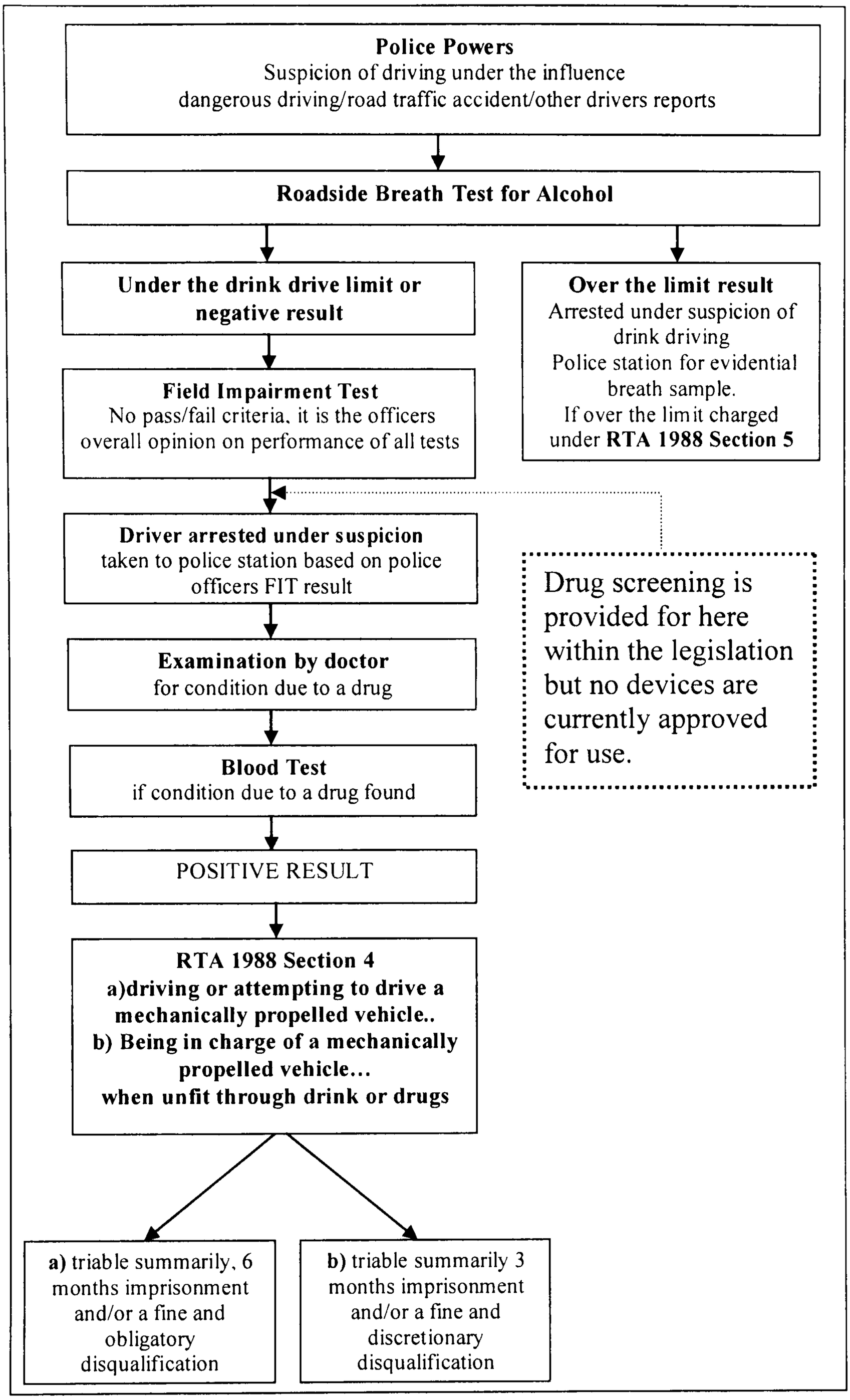

Figure 1.1: Summarising the UK procedural and legislative process for dealing with drug drivers.

1.1.2 Roadside Screening Devices

The practicalities of undertaking a drug screening test are complex. These devices are required to work in challenging environments including temperature ranges between -10 °C to 50 °C, in the rain and night time conditions. The 'time to result' from the start of sample collection must total less than fifteen minutes. This is essential because it is the last evidence gathering procedure pre-arrest. Minimal sample collection and transfer steps accompanied by automatic interpretation of the result are also necessary for non-technical users.

Surface Enhanced Raman Spectroscopy (SERS) is considered a viable method for this application because of its high sensitivity, capability to detect a wide range of substances simultaneously and quick analysis times. A simple three step process is envisaged, sample collection using a swab, transfer onto the SERS substrate through direct contact between the swab and the substrate, insertion into the machine and analysis within 1-2 minutes. It must be remembered that this is a screening technique that does not require a numerical output but just an indicative result of the presence of a drug.

Roadside screening devices would provide valuable support to a police officer as part of the standard officer's toolkit. A suitable device would indicate the presence of either single or multiple drugs which would aid the decision making process when impairment is suspected. Although, it must be borne in mind that the presence of a drug does not necessarily mean the driver is impaired.

Screening devices such as the Concateno/Cozart Rapiscan and Drug Detection System (DDS) (Abingdon, Oxford, UK) and Securetec DrugWipe (Munich, Germany) (Figure 1.2) are analytically based on immunochromatographic techniques [www.cozart.co.uk and www.securetec.net]. Generally, these devices utilise a lateral diffusion process within which the oral fluid sample is mixed with labelled antibodies contained in a buffer solution and passed over an area containing a linear array of immobilised drugs. The antibodies are either drug class specific e.g. opiates or are drug specific e.g. methadone. If drugs are present in the oral fluid sample,

they bind to the anti-drug antibodies, inhibiting their subsequent binding to the immobilised drug line. This produces a 'no line' response which indicates the presence of a drug in the sample. The presence of a line indicates the absence of a drug in the sample because the antibodies have bound to the immobilised drug line. The antibody's are typically labelled with colloidal gold or a phosphor allowing visualisation. The devices referred to above both use colloidal gold-labelled antibodies.

Cozart Rapiscan

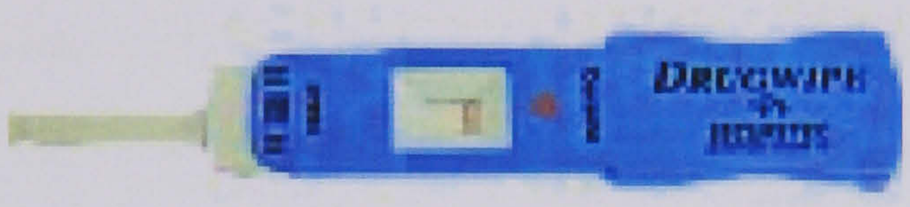

Securetech DrugWipe

Figure 1.2: Images of two commercially available drug screening devices.

The immunoassay devices typically rely upon a relatively large volume of sample being collected, approximately 1 ml, which is difficult to obtain from a drug user as the drugs often reduce oral fluid flow. They are very sensitive to the volume of sample loaded onto the reaction strip, too little or too much and they do not work properly. They also take on average 10 minutes to analyse the sample and produce a result. Detaining a suspected drug driver at the roadside for 10 minutes whilst a sample analyses is not practical or safe for either the officer or the suspected drug driver. Some of the devices only identify the presence of a drug class which prevents the user from determining if the drugs in the oral fluid are illicit or licit drugs. For example the presence of codeine could indicate the use of an over-the-counter anti-tussive or heroin.

The government has postponed the use of such devices until a type approval specification is agreed, defining the minimum operational requirements, electrical

interference tests and scientific standard that any device must perform to. The final report from the joint European and United States ROSITA II project concluded that they could not recommend any of the devices tested in both a laboratory and field trial setting for operational use for the enforcement of drug driving [Verstraete and Raes (2006)].

1.2 Driving Impairment

Driving a vehicle is a complex multi-functional task involving visual search and recognition, vigilance, information processing and the variable demand of decision making, risk taking and enough sense with motor control to carry out all these tasks correctly. It is also an overlearned task where critical high level demands are very infrequent. The different illicit drugs affect driving ability by differing degrees. Nevertheless, there lies a common core between all of the illicit drugs that will significantly modulate the drugs final effect on driving ability [Del Rio and Alvarez (1995)]. These include the following:

i) the amount of drug taken - with sustained drug consumption the drug dose increases especially if consumed in quick succession (within one evening etc.). Therefore, the greater the dose the more marked the influence on the different aspects of driving ability that are directly or indirectly affected by the drug.

ii) the route of administration – oral, smoked, intra-nasal, intravenous etc. (e.g. Heroin). The pharmacokinetic (absorption, distribution, elimination) and pharmacodynamic (effect of the drug on living organisms) properties of the drug will be influenced by the routes of administration and this could have a greater or lesser effect on driving ability.

iii) the onset of tolerance to a drug - which requires the dose to increase to experience the desired effects from that drug. However, despite the increase in dose to achieve the same physiological and psychological high it may not adversely affect the individual's driving behaviour beyond the level that

would be observed had they consumed a lower dose prior to the onset of tolerance.

iv) Overdose/withdrawal symptoms - produced by either an excessive amount of drug or when a purer than normal dose has been taken or withdrawal symptoms when the individual is without drug can produce extremes in the adverse effects of the drug on driving behaviour.

v) multiple drug taking - a behaviour often associated with individuals who frequently consume drugs. Alcohol is frequently imbibed in conjunction with the drugs and as will be demonstrated below with examples this can have additional deleterious effects.

Investigations focusing on the correlations between the concentration of a drug and the measured level of impairment are inconclusive. Previous studies [Research Technology Branch NIDA (1985)] have indicated broad ranges in drug concentration that can evoke similar levels of impairment between individuals. Many inter-individual variables contribute to the differences in drug concentration required to evoke the same level of impairment between individuals. These include; body weight, body composition, genetic and environmental influences that affect metabolic and eliminatory processes, prior exposure and the presence of other drugs that can cause pharmacokinetic and pharmacodynamic interactions. Currently it is not possible to define critical body fluid concentrations for drugs in the same way that they are defined for blood and breath alcohol. However, the ranges of concentrations of illicit drugs below (Table 1.1) were detected in the oral fluid of drug drivers in Scotland for a period of 22 months between 2001 and 2003 [Oliver *et al* (2006)]. Oliver *et al* (2006) reported that in 386 cases judged by the police to be impaired the examining FME agreed that the effects might be due to the presence of a drug in 297 (77%) of them. The majority of the drug positive cases were found to involve polydrug use with 4 illicit drugs and a prescription drug present in one subject. The drivers judged to be unimpaired at the roadside were asked to provide a voluntary oral fluid sample for analysis. 171 samples were collected and analysed.

Upon analysis 100 of these were found to have a drug(s) in the sample. Opioids and cannabis were most frequently detected indicating the drivers may have a tolerance to the drugs making it harder to detect them using FIT tests [Oliver *et al* (2006)].

Table 1.1 The range of drugs and concentration detected in oral fluid of drug drivers in Scotland compared to the therapeutic ranges detected in subjects and patients. (Conc. – concentration range, Thera. – therapeutic range).

Drug Detected	**Conc. Range (ng/ml)** [Oliver *et al* (2006)]	**Conc. Range (M)**	**Thera. Range (ng/ml)** [Moffat & Widdop (2004)]	**Thera. Range (M)**
Delta-9-tetrahydrocannabinol	0.002 – 49.3	6.36×10^{-12} – 1.56×10^{-7}	-	-
Amphetamine	69 – 96912	1.87×10^{-7} – 2.62×10^{-4}	1 – 10	2.73×10^{-9} – 2.71×10^{-8}
Methamphetamine	50 – 210	2.69×10^{-7} – 1.13×10^{-6}	-	-
Methylenedioxymethamphetamine	179 – 28942	1.17×10^{-6} - 1.61×10^{-4}	-	-
Methylenedioxyamphetamine	478	2.21×10^{-6}	-	-
Morphine	40 – 77000	1.40×10^{-7} – 2.69×10^{-4}	10 – 70	3.5×10^{-8} – 2.45×10^{-7}
Dihydrocodeine	97 – 4800	3.21×10^{-7} – 1.59×10^{-5}	94 – 156	3.11×10^{-7} – 5.17×10^{-7}
6-Monoacetylmorphine	8 – 70	2.44×10^{-8} – 2.13×10^{-7}	-	-
Methadone	16 – 16700	5.17×10^{-8} – 5.39×10^{-5}	50 – 1000	1.61×10^{-7} – 3.23×10^{-6}
Cocaine	7 – 2900	2.05×10^{-8} – 8.53×10^{-6}	-	-

Methylenedioxymethamphetmine (MDMA) is often used as a popular dance drug for its socially facilitating and euphoric effects. Morgan (1998) documented effects on cognitive performance (reduced accuracy) and Vollenweider *et al* (1998) reported a lack of concentration in subjects who had consumed MDMA. Schifano (1995)

observed extreme driving behaviour in MDMA users that increased the incidence of traffic accidents in this study.

Brookhuis *et al* (2000) investigated the effect of multiple doses of MDMA and various other psychotropic substances on driving performance. They assessed overall driving performance and decision making processes using a driving simulator programmed with different driving scenarios.

The driving simulator test included driving through a built up area and a motorway scenario. During the rides in the simulator, driving performance (longitudinal and lateral vehicle control) was measured and self reports on driving quality were recorded for each subject. Gap acceptance, the ability to follow speed changes of a lead car and responses to braking manoeuvres were also measured.

Speed variance increased both under the influence of MDMA and in the multiple drug conditions both in the city and on the motorway. Reaction time to braking manoeuvres by cars in front was not significantly affected in either of the drug conditions as compared to the control group.

Krueger and Vollrath (2000) observed similar findings of impairment in a simulator study investigating amphetamines. It was not possible to distinguish between the amphetamine users and MDMA users. However, two drug concentration groups could be defined; a low concentration group where the sum of the active substances was less than 50 ng/ml and a high concentration group whose sum of active substances exceeded 50 ng/ml.

The amphetamine/MDMA group exhibited an increased tendency to speed when under the influence of the higher concentration but without any adverse effect on lane keeping ability. The subject's performance of the secondary tasks (accidents at the crossroads, peripheral warning signal and stop sign reaction times) was also impaired. However, a combination of alcohol and the drugs at high concentration caused a converse effect on speed, lateral position and reaction. Krueger and

Vollrath (2000) likened this behaviour to the appearance of a sober driver. The low concentration group indicated no substantial alterations in driving behaviour when the drug was present alone. When the lower concentration was taken in conjunction with alcohol lane keeping performance deteriorated and secondary tasks were impaired. The observed impairment was similar to that expected and observed from the drivers who had consumed alcohol only.

These two studies indicate that both amphetamine and MDMA affect a drug user's ability to drive especially in terms of speed and risk taking behaviour. The impairment observed is altered when the drugs are taken in conjunction with alcohol or other drugs.

It is clear that the demand to identify drug induced impairment above and beyond alcohol impairment is ever increasing. This is imperative in cases where breath alcohol testing has indicated the presence of alcohol but not in excess of the legal limit. Under these circumstances the presence of alcohol could accompany illicit drugs and a simple and quick screening test would enable a police officer, when used in conjunction with a FIT test, to identify either the absence or presence of other substances that could be contributing to the observed impairment.

1.3 Amphetamines and Substituted Amphetamines

1.3.1 Substituted Amphetamines

All of the amphetamine derived analogues are produced from the precursor chemical phenethylamine, the generic name of amphetamine. Substitutions on the nitrogen and the ring system account for most of the structural variations. The most common examples of amphetamines include methamphetamine and the substituted amphetamines; MDMA, methlyenedioxyamphetamine (MDA), 4-methoxyamphetamine (PMA) and methylenedioxyethylamphetamine (MDEA) (Figure 1.3) which have no medical use [Drummer (2001)].

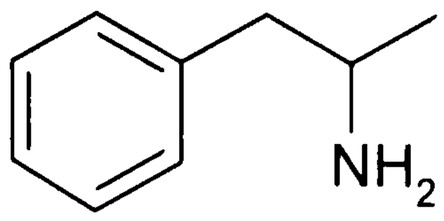

Amphetamine

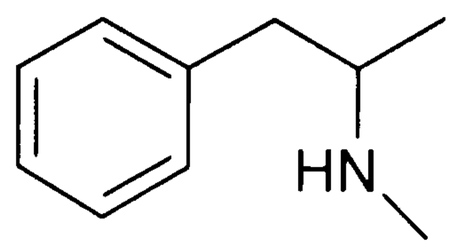

Methamphetamine

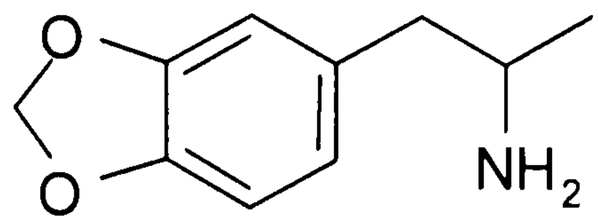

Methylenedioxyamphetamine (MDA)

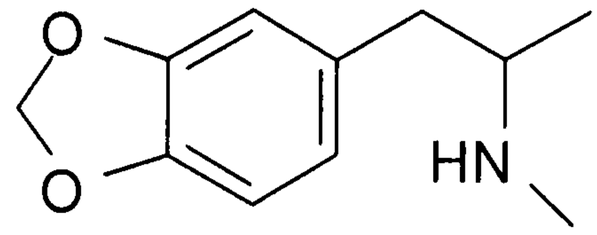

Methylenedioxymethamphetamine (MDMA)

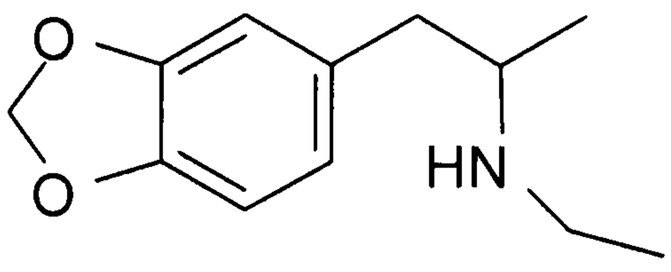

Methylenedioxyethylamphetamine (MDEA)

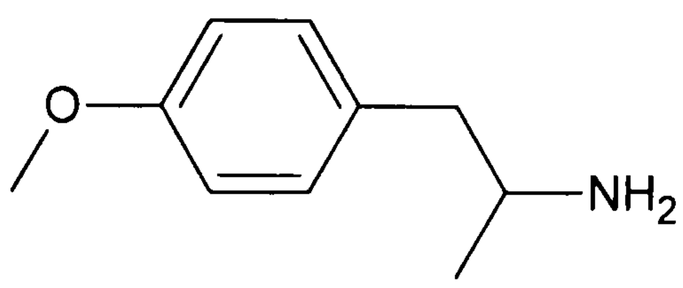

4-methoxyamphetamine (PMA)

Figure 1.3: The structures of common phenethylamine drugs.

1.3.2 Methamphetamine

Methamphetamine was first synthesised in Japan in 1919 by Ogata, patented in 1920 and later licensed to Burroughs Welcome who marketed it as the anorectic Methedrine® [Logan (2002)]. Methamphetamine has legitimate therapeutic use in the treatment of obesity, narcolepsey, Attention Deficit Hyperactivity Disorder (ADHD) and Attention Deficit Disorder (ADD).

1.3.3 MDA

MDA is readily available from several chemical suppliers. The illicit form is found as a freebase (ice) and is smoked in a similar fashion to crack cocaine. The use of

MDA is however rare in the UK [TICTAC (1999) & Valter and Arrizabalaga (1998)].

1.3.4 MDMA

Ecstasy, the street name for MDMA, was first synthesised in 1910 [Mannich and Jacobson (1910)] and was patented by the Merck company in 1914. The human pharmacology of MDMA was not presented until 1978 by Shulgin *et al* (1986). Ecstasy entered the UK with the arrival of American dance culture. It is classed as a hallucinogenic stimulant. MDMA is generally found as a racemic mixture. The d-isomer is more potent then the l-isomer in evoking the subjective effects of the drug [Schechter (1987), Glennon *et al* (1997)]. Frequently, drugs sold as ecstasy contain no MDMA but other illicit drugs usually stimulant drugs including methamphetamine, amphetamine, ketamine, MDA, MDEA and PMA [Bell *et al* (2003), Sonderman and Kower (1999)].

1.3.5 Mechanism of Action

Stimulants, amphetamine, methamphetamine and the designer drugs, have effects both within the central nervous system and the peripheral nervous system. Centrally they work by stimulating predominantly dopaminergic neurones and serotinergic neurones but they also stimulate noradrenergic neurones too. Peripherally they function by stimulating predominantly noradrenergic neurones but some dopaminergic neurones are also stimulated [Rang *et al* (1995), Raymon (2003)].

Dopaminergic neurones have dopamine as the neurotransmitter, serotonergic neurones have serotonin as their neurotransmitter and noradrenergic neurones have noradrenaline as their neurotransmitter. Dopamine is a catecholamine and is related to noradrenaline [Rang *et al* (1995), Raymon (2003)].

Stimulants all modify the behaviour of the nerves pre-synaptically by competitive antagonism [Logan (2002)]. Amphetamine and methamphetamine have the biggest effect on noradrenaline and then smaller effects on dopamine and serotonin respectively (Figure 1.4). High doses of methamphetamine administration cause

lower brain levels of dopamine and serotonin and decreases the activity of enzymes responsible for their synthesis [Logan (2002)]. MDMA, MDA and MDEA have the biggest effect on serotonin followed by dopamine and noradrenaline (Figure 1.4) [Rang *et al* (1995), Raymon (2003)]. Their affinity for different neurotransmitters accounts for their differing pharmacological effects. Amphetamine and methamphetamine have greater effects on the peripheral nervous system whereas MDMA, MDA and MDEA have a greater effect on the central nervous system overall, again accounting for their differences in pharmacological effects [Rang *et al* (1995), Raymon (2003)].

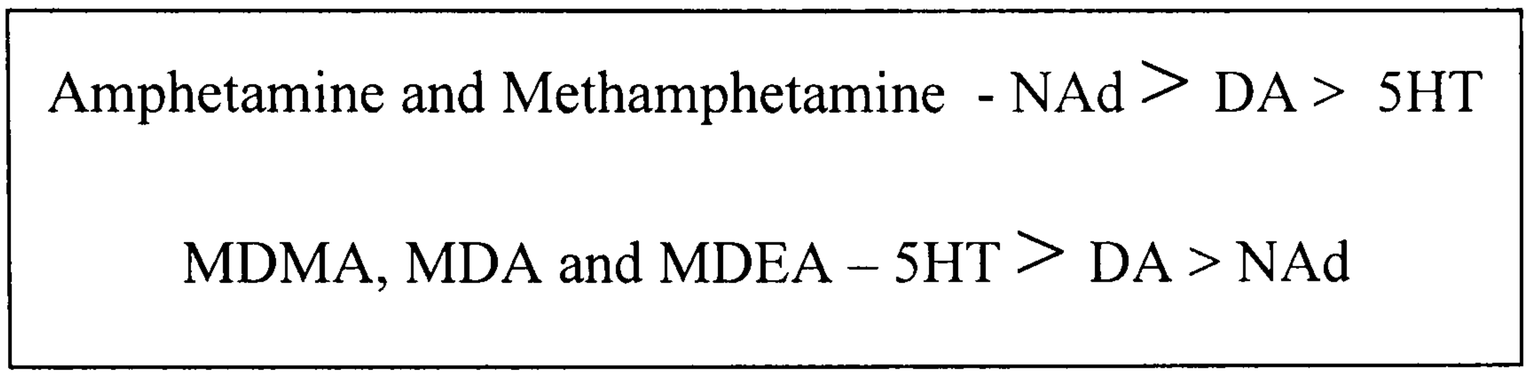

Figure 1.4: A flow diagram illustrating the decreasing affinity of the drugs for the neurotransmitters. 5HT (Serotonin), DA (Dopamine), NAd (Noradrenaline).

1.3.6 Routes of Administration

Intravenous injection, nasal insufflation, smoking or oral consumption of a tablet are the most common ways amphetamine is administered. Intravenous dosing provides the most efficient and quickest way of administering the drug.

Methamphetamine can be smoked as a hydrochloride salt by inhaling the vapours from a glass or aluminium pipe [Logan (2002), Cho (1990)]. The efficiency of this process is over 70% [Drummer (2001)]. Smoking produces a rapid absorption with peak blood concentrations within minutes. These concentrations are sustained for 3 - 4 hours before declining.

MDMA and MDA are administered orally in tablet form. Sometimes the tablet may be crushed, wrapped in toilet paper and swallowed for more rapid absorption [Logan and Couper (2003)].

1.3.7 Drug Distribution in Blood and Oral Fluid and Half Life

Amphetamine after a single oral dose is rapidly absorbed. It has low protein binding properties [Quinn *et al* (1997)] for both enantiomers, resulting in a higher amount of drug available in plasma for ready distribution into biological fluids and matrices with pH values lower than the plasma [Kidwell *et al* (1998)]. Studies with amphetamine dependent subjects have shown larger volumes of distribution implying that amphetamine may be sequestered in tissue compartments because of tolerance to the drug. Dependent users also have longer drug half life elimination (21.8 $\pm$ 1.4 hours) than non users (13.9 $\pm$ 3.4 hours) when administered the same 25 mg oral dose [Busto *et al* (1989)].

Amphetamine was identified in oral fluid following administration of d-amphetamine, l-amphetamine and d,l-amphetamine [Wan *et al* (1978)]. Martin *et al* (1977) and Wan *et al* (1978) reported higher amphetamine concentrations in oral fluid than in plasma and detection for 48 hours after oral administration of 10 mg of amphetamine hydrochloride to humans. Smith (1981) measured amphetamine by radio-immunoassay in oral fluid and oral fluid stains on a cigarette from a subject undergoing amphetamine therapy. The concentration of amphetamine in oral fluid (73 ng/ml) was similar to that found in whole blood (64.1 ng/ml) and semen (54 ng/ml) for the subject.

Methamphetamine has a blood half-life of 10 hours [Cook *et al* (1993)]. The volume of distribution for methamphetamine is similar to amphetamine and is also unaffected by route of administration [Samyn *et al* (2002)]. When smoked methamphetamine has a similar blood concentration versus time profile to intravenous administration. Peak blood concentrations of methamphetamine are close to 100 ng/ml following a smoked 30 mg dose. Oral fluid concentrations of methamphetamine are substantially higher than those in plasma which often relates to oral administration of the drug. Amphetamine, the main metabolite of methamphetamine, is produced only in small amounts following intravenous dosing or smoking. Plasma methamphetamine concentrations peak at 12 hours and are only 40 ng/ml [Cook *et al* (1993)]. Cook *et al* (1993) also showed some evidence that

methamphetamine kinetics may be dose dependent with slower clearances with higher doses, possibly due to the saturable excretion process in the kidney. This has important implications when considering chronic use.

Heavily drug dependent users of amphetamine and methamphetamine can exceed 2000 mg daily doses. While these doses are uncommon they will generate accordingly higher blood and tissue concentrations of drug. However, little research has been undertaken to demonstrate the linear relationship between dose and blood concentrations of these drugs following controlled high dose administration which leads to large errors in the predicted blood concentrations [De la Torre *et al* (2000)]. This is partly due to ethical concerns about administering high doses of stimulant drugs.

MDA has a blood half-life of 3 to 8 hours. Common abused doses are 50 - 250 mg. Blood concentrations can be up to approximately 400 ng/ml. It is highly toxic and has high abuse potential. It is the principle metabolite of MDMA [Drummer (2001)].

MDMA demonstrates stereo specific metabolism with an l- half life of 5.8 $\pm$ 2.2 hours and a d- half life of 3.6 $\pm$ 0.9 hours [Fallon *et al* (1999)] following administration of a 40 mg racemic mixture. This metabolic difference causes non-linear pharmacokinetics because the d- isomer is more pharmacologically active but is metabolised faster making the blood drug concentrations harder to interpret [Logan and Couper (2003)]. Upon administration of an oral dose effects can be observed within 25 - 30 minutes and remain present for an hour or more depending on the dose. De la Torre (2000) administered doses between 5 – 10 mg and observed peak plasma concentrations within 1.5 – 4 hours. The plasma MDA concentration was observed to peak later between 4 - 6 hours and did not exceed 5% of the parent compound concentration. Samyn *et al* (2002) reported an experimental saliva:plasma (S:P) that greatly exceeded the theoretical value following controlled administration of 75 and 100 mg doses. This accumulation of MDMA in oral fluid was thought to relate to the sympathomimetic effects of the drug affecting distribution. Navarro *et al* (2001) reported oral fluid concentrations that ranged from

1728.9 – 6510.6 ng/ml and plasma concentrations that ranged from 134.9 – 223 ng/ml 1.5 hours after administration of a single oral dose (100 mg) in 8 volunteers. The oral fluid and plasma concentration time profiles were in agreement despite considerably higher oral fluid concentrations. These may result from the low protein binding and basic nature of MDMA resulting in a higher free fraction available for diffusion into the acidic oral fluid.

1.3.8 Clinical Uses

Amphetamine derivatives have limited clinical usefulness owing to the number of side effects. However, derivatives such as fenfluramine and its d-isomer dexfenfluramine are used for the treatment of severe obesity inducing the state of anorexia but without introducing the side effects associated with amphetamine directly. Paradoxically it is also used in the treatment of hyperactive children but the mechanism behind the beneficial effects is currently unknown [Martindale (1993), Logan (2002)].

There are a number of legal stimulant drugs metabolised to amphetamine or methamphetamine such as Selegline, an antiparkinson drug, which is metabolised to a weakly active l-isomer of methamphetamine [Romberg *et al* (1995)], while others such as fenproporex and benzphetamine are metabolised to d- and l-methamphetamine and/or d- and l-amphetamine [Drummer (2001)].

All of these drugs are now controlled by The Misuse of Drugs Act 1971. This Act aims to prevent the unauthorised use of drugs which are being or are likely to be misused and if this misuse is having or appears capable of having harmful effects sufficient to constitute a social problem. However the Act does not control the consumption of these drugs. Within the Act these drugs are considered as Class B drugs except for methamphetamine which was recently re-classified as Class A [The Misuse of Drugs Act 1971 (Amendment) Order (2006)]. If an individual is found in possession of Class A methamphetamine they can be sentenced for up to seven years imprisonment and be given an unlimited fine. Trafficking offences can receive up to life imprisonment and an unlimited fine [The Misuse of Drugs Act 1971

(modification) Order 2001 and The Misuse of Drugs Act 1971 (Amendment) Order (2006)]. If an individual is found in possession of a Class B phenethylamine they receive a summary conviction, can be sentenced for up to three months and be given a fine of up to £1000. Possession on indictment receives up to five years imprisonment and an unlimited fine. Trafficking offences on summary conviction carry up to six months imprisonment and or a £2000 fine. An indictable trafficking offence can receive up to 14 years imprisonment and an unlimited fine [The Misuse of Drugs Act 1971 (modification) Order 2001].

1.3.9 Statistics

The total number of amphetamine and ecstasy users in the world is currently estimated to be 24.7 million (0.6% world population aged between 15-64 yrs) and 9 million (0.2% world population aged between 15-64 yrs) people respectively [World Drug Report (2008)]. Cannabis is the most widely used drug with amphetamine and ecstasy following closely behind. Global seizures of ecstasy were 5 metric tonnes in 2008 with the highest seizures being found in the United Kingdom as well as the USA, Belgium and others. However, global production based on estimated consumption figures, seizure data and precursor seizures is thought to range between 330 – 770 tonnes with the number of dismantled laboratories at 8245 in 2007 [World Drug Report (2008)]. Belgium and the Netherlands continue to be cited as the main countries of origin for ecstasy exportation. The United Kingdom continues to have the largest European market for amphetamines. The seizure rates for the United Kingdom in 2006 were 2038 kg of amphetamine and 2946000 units of ecstasy [World Drug Report (2006)]. In 2007 1 g of amphetamine was sold on average for £11 (range £3 to £45) and ecstasy on average for £4.50 per tablet (range £0.29 to £22) [World Drug Report (2008)]. In 1999, 667 million pounds of illicit drugs were seized in the UK by law enforcement agencies [Corkery (1999)]. This is a proportion of the amount that actually reaches the street for sale. Since the publication of Sir William Macpherson's report on the 'Stephen Lawrence Inquiry' [February (1999)] there has been a decrease in the number of individuals being stopped and searched which previously had accounted for more than half of drug offences brought to the attention of the police.

The British Crime Survey (BCS) 2002-2003 [Codon and Smith (2003)] indicated that of all 16-59 year old respondents 12% had taken an illicit drug. Figure 1.5 graphically represents the prevalence of the different drugs being taken by age group. Amphetamine and ecstasy were the second most commonly used drugs amongst the same age range, with 2% claiming to have tried them in the last year. In the 2005-2006 BCS [Roe and Man (2006)], 10% of 16-59 year old respondents reported taking an illicit drug within this period with cocaine use at 2.4%, amphetamine use at 1.3% and ecstasy use remaining stable at 1.6%. Figure 1.6 graphically represents the prevalence of the different drugs being taken by age group. If the 16-24 year olds in the 2002-2003 BCS [Condon and Smith (2003)] are looked at in more detail, the use of ecstasy and cocaine accounts for 5% and amphetamine 4%. In 2005-2006 BCS [Roe and Man (2006)] 16-24 year olds reported ecstasy use of 4.3%, cocaine use at 5.9% and amphetamines use at 3.3% slightly lower than in 2002-2003. The majority of amphetamine and ecstasy use is seen within the 16 – 34 year olds who are also considered to be the age group at most risk of being involved in road traffic accidents. Figures 1.5 and 1.6 compare the prevalence of drug misuse in 16-59 year olds in both the 2002-2003 and 2005-2006 BCS's respectively.

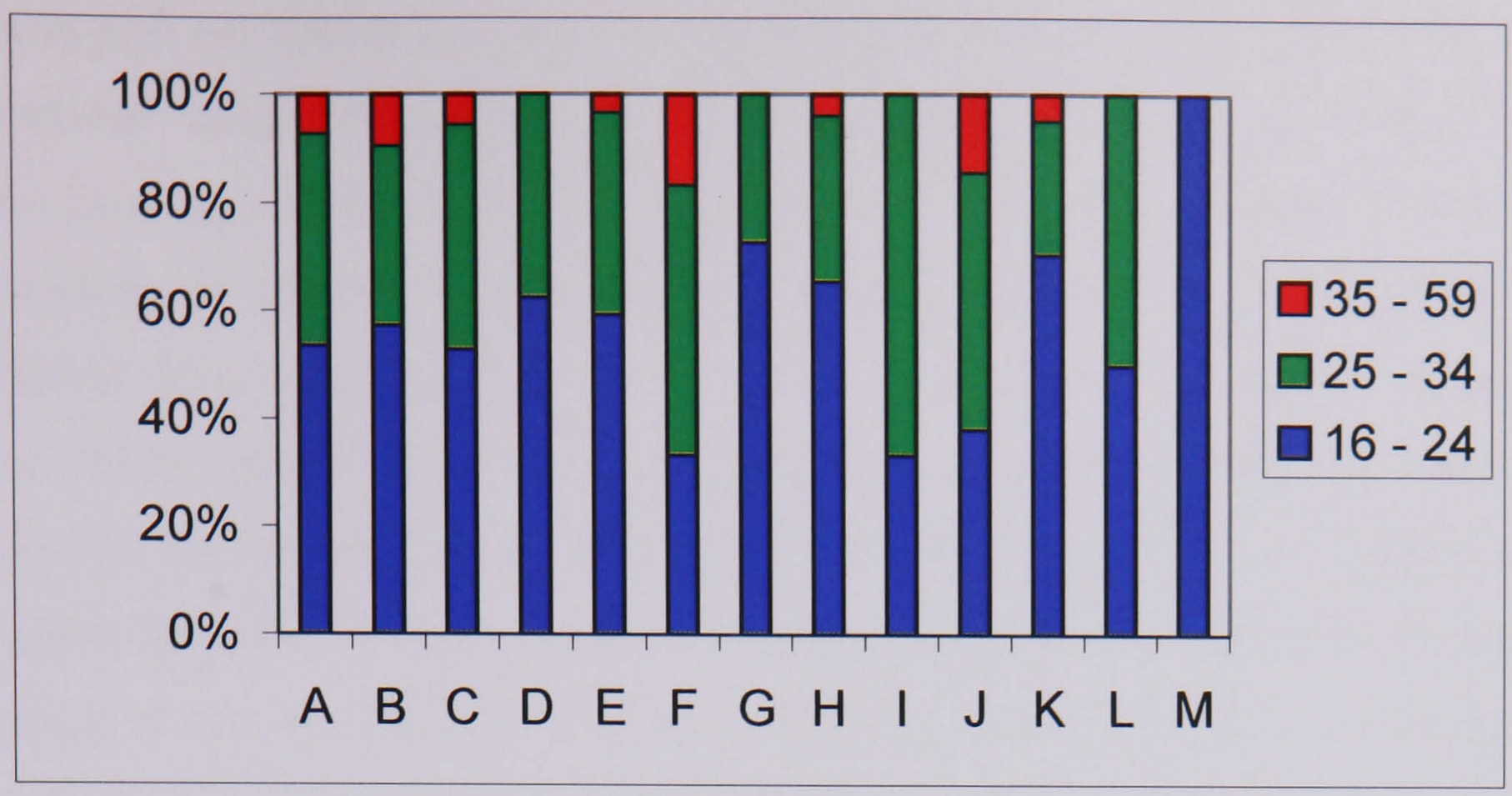

Figure 1.5: British Crime Survey 2002-2003 Prevalence of drug misuse in 16-59 year olds [Codon and Smith (2003)]. (X axis series names A- amphetamines, B- Cannabis, C-Cocaine, D- Ecstasy, E- Crack F- Heroin, G- LSD, H- Magic Mushrooms, I- Methadone, J-Tranquillisers, K- Amyl Nitrate, L- Anabolic Steroids, M- Glues).

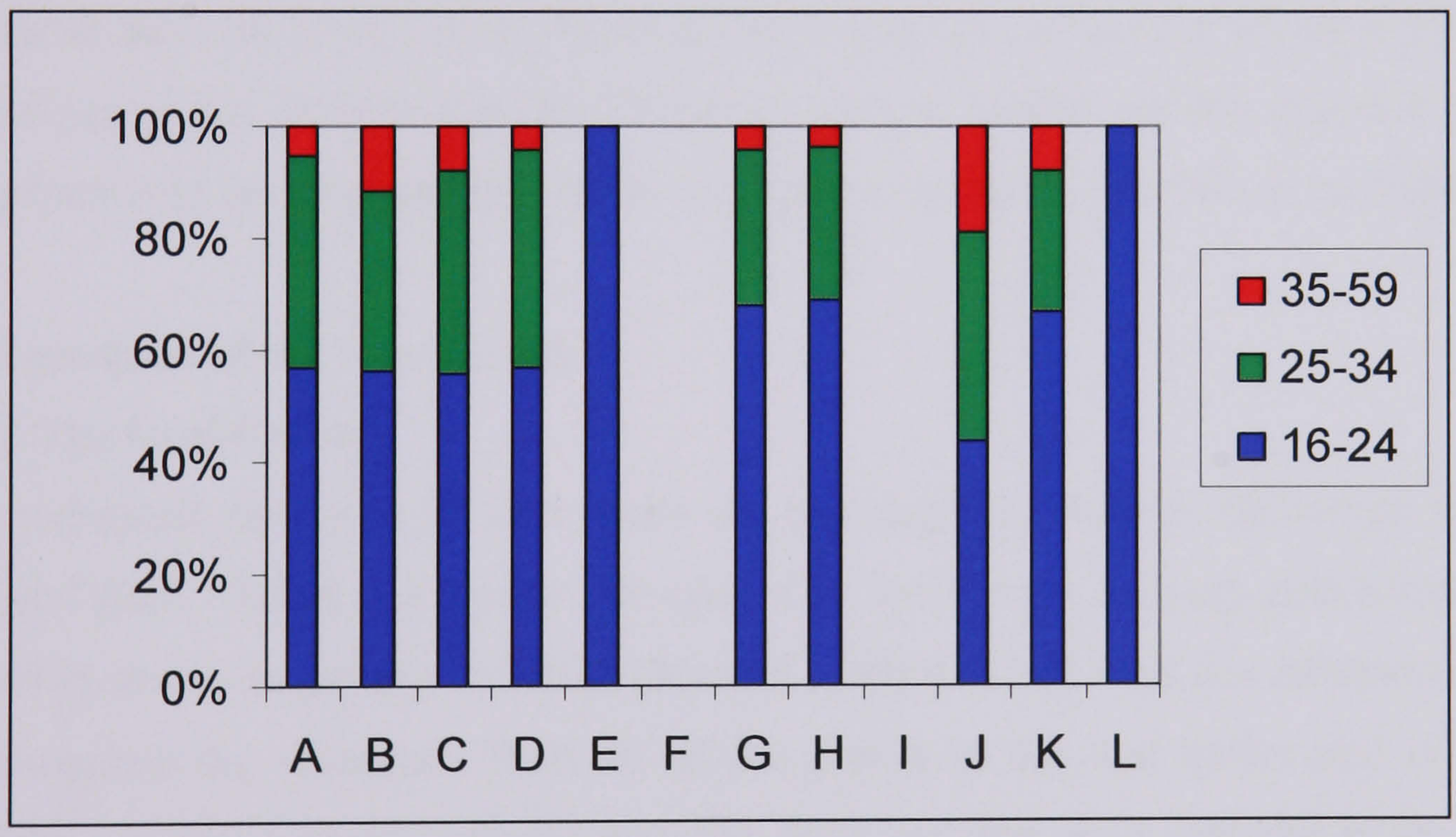

Figure 1.6: British Crime Survey 2005-2006 Prevalence of drug misuse in 16-59 year olds [Roe and Man (2006)]. (X axis series names A- amphetamines, B- Cannabis, C-Cocaine, D-Ecstasy, E- Crack F- Heroin, G- LSD, H- Magic Mushrooms, I- Methadone, J-Tranquillisers, K- Amyl Nitrate, L- Anabolic Steroids).

Surveys and newspaper articles also regularly indicate that more people are taking recreational drugs and driving having consumed them [Metro (London) 7th June 2006, Evening Standard 6th June 2006, The Times 3rd February 2006]. The Association of Chief Police Officers (ACPO) released the results of the 2006 Christmas drink and drug driving campaign. Throughout the month of December police forces undertook enforcement campaigns resulting in 666 FIT tests from which 251 arrests were made [ACPO Press Release (2007)]. It is important to remember that all of the 666 subjects passed a breath alcohol test thereby arousing suspicion of driving under the influence of a drug. However, subjects who recorded a positive, refused or failed the breath alcohol test following random stop, injury collisions or damage only collisions totalled 11,603 and it is unknown how many of these drivers were also under the influence of drugs as well as alcohol because they were dealt with only for their excess alcohol offence as prescribed by the RATSA amendment 2003 of RTA 1988.

Whilst it cannot be categorically stated that the use of drugs when driving causes accidents there are many factors that indicate that drugs may evoke impaired driving behaviour within an individual by affecting alertness, visual, activity, reaction time, judgement and decision making and so on thereby increasing the risk of accident.

1.4 Functions of the Oral Cavity

1.4.1 The Oral Cavity

The secretions present in the oral cavity can be categorised into two headings; saliva and oral fluid. Saliva is a secretion produced by the 3 major salivary glands and can be either mucus or watery in nature [Mandel (1990)]. Oral fluid is a substance that encompasses the secretions from all of the glands in the oral cavity and is very unclean. It also contains cellular material, food and any other material in the oral cavity [Mandel (1990)].

It is estimated that between 500 and 1500 ml of oral fluid is produced daily [Aps and Martins (2005)]. This is the equivalent to approximately one fifth of the total plasma volume. However, most of this will be swallowed and re-absorbed. Some of the

salivary components are derived from blood plasma but most are synthesised by the salivary glands.

Normal unstimulated salivary flow rate is between 0 - 6 ml/min [Aps and Martins (2005)]. A dry mouth reflex can be experienced by an individual when salivary flow is diminished to 40 - 50% of the normal value and not just when salivary flow is zero [Dawes (1987)].

1.4.2 Xenobiotic Entry Into Oral Fluid

Several theories have been proposed to explain the mechanism by which xenobiotics enter saliva. Smaller molecules such as ethanol can pass freely through membrane pores either into the saliva or directly into the oral cavity [Haeckel (1989)]. Most drugs seem to enter the saliva by a simple passive diffusion mechanism which depends on their physicochemial properties (pK_a, relative solubility in water and lipids which determines their free diffusibility, molecular weight and spatial configuration) or their link to the plasmatic proteins and the plasmatic and salivary pH values [Haeckel (1989)].

Slightly ionised, lipophilic substances penetrate the plasma-saliva barrier with ease because the concentration in the saliva is a reflection of the free molecule plasma concentration. They pass through the barriers at a rate roughly parallel to their oil/water partition coefficient [Jusko and Milsap (1993)].

In the case of slightly alkaline substances the salivary concentration is closely related to the pH of the saliva. If the constituents have a pK_a close to the salivary pH, a slight change in pH engineers a significant change in the degree of ionisation reflected by the saliva/plasma (S/P) ratio [Kidwell *et al* (1998)]. In accordance with the pH partition theory if a basic drug has a $pK_a > 6$ or an acidic drug has a $pK_a < 8$ this will alter considerably the total plasma and saliva concentrations.

The saliva drug concentrations reflect the free plasma fraction i.e. the active drug fraction. Therefore, it acts independently of any variations that may occur in the aqueous compartment [Jusko and Milsap (1993)].

1.4.3 Oral Fluid Collection

Oral fluid collection is considered a non-invasive procedure which can be undertaken under the direct supervision of trained police officers to reduce the risk of adulteration. It is easier and more expedient to obtain multiple oral fluid samples than blood. Furthermore, drawing blood requires the expertise of a medical professional and the subjects may experience fear, anxiety and discomfort [Siegel (1993)]. Although some training and explanation is necessary to assure proper gathering of oral fluid samples, it does not require the level of training needed for blood sampling. A sample of oral fluid can normally be taken by expectoration (spitting) into a container or by wiping the oral cavity with a cotton bud or similar item [Mandel (1990)]. If salivary flow is stimulated to increase the volume of fluid available for collection, the concentration of drug in saliva is liable to change due to a change in pH, affecting drug partitioning and the saliva:plasma ratio. Consequently oral fluid collection should be carried out without stimulating salivary flow. Studies with codeine show that oral fluid concentration is dependent upon the sampling protocol, with the highest concentration being observed following expectoration [O'Neal *et al* (2000)]. Consideration must also be given to the collection method and materials used and if its use directly affects the pH and therefore the detectable drug concentration [Crouch (2005)]. Equally the volume of oral fluid may be greatly reduced as a direct consequence of a reduction in resting level salivary flow. In a road safety context, all of these drawbacks need to be taken into account when collecting samples in situ. In addition, a dry mouth may be experienced by the subject due to the action of the drug itself or the release of adrenaline associated with being stopped by a police officer [Verstraete and Raes (2006), Kidwell *et al* (1998)].

1.4.4 Phenethylamines in Oral Fluid

A single administration of amphetamine and methamphetamine either through the oral cavity, intravenously or by a smoking method produces oral fluid concentrations at least 2 - 3 times greater than the recorded plasma concentrations [Kintz (1999)]. The drugs may be detectable in oral fluid for a period of time as long as two days if a sensitive analytical method is employed. A correlation between the oral fluid concentrations of methamphetamine and the presence of subjective and cardiovascular effects has not yet been established [Kintz (1999)]. Wylie *et al* (2005b) analysed oral fluid samples from 1396 drivers stopped randomly on UK roads with high accident rates. 16.8% of the samples were positive for at least one drug. The most frequently detected parent drug was MDMA which had a concentration range of 9 – 3144 ng/ml. Other detected phenethylamines included MDA (concentration range 4 – 275 ng/ml), amphetamine (concentration range 12 – 16414 ng/ml) and to a lesser extent MDEA and methamphetamine. Their presence may relate to intentional consumption, unknown consumption in the case of ecstasy tablets which are often found to contain multiple phenethylamine derivatives [Lamping (2006)] or as metabolites of ecstasy consumption. These results differ from other studies where samples have been collected from randomly stopped drivers [Wylie *et al* (2005b)]. This data may reflect the geographical usage of particular drugs within a country. This conclusion is supported by data obtained from blood samples collected from suspected driving under the influence of drugs cases from the west of Scotland where benzodiazepines were the most commonly detected drug followed by morphine and cannabis [Seymour and Oliver (2000)].

The use of stimulants (designer drugs) has increased but limited studies have been published on the measurement of MDA, MDMA and MDEA in oral fluid. This is possibly due to ethical constraints. Samyn *et al* (2002) report on a controlled MDMA study involving 12 experienced MDMA users. Each subject consumed 75 mg of MDMA on three separate occasions in a double blind cross over study. An in-dwelling venous catheter was used to obtain blood samples at 60 minute intervals from time 0 to 5 hours after administration. Oral fluid samples were also collected at the same time points. Plasma concentrations varied from 21 - 295 ng/ml reaching a

maximum concentration within 4 hours. The oral fluid concentrations were higher than the plasma concentrations but the inter-subject variability was three times higher with a larger range, 50 - 6982 ng/ml. However, if the average plasma and oral fluid concentrations are compared (Figure 1.7) there appears to be good correlation despite the large inter-subject variability.

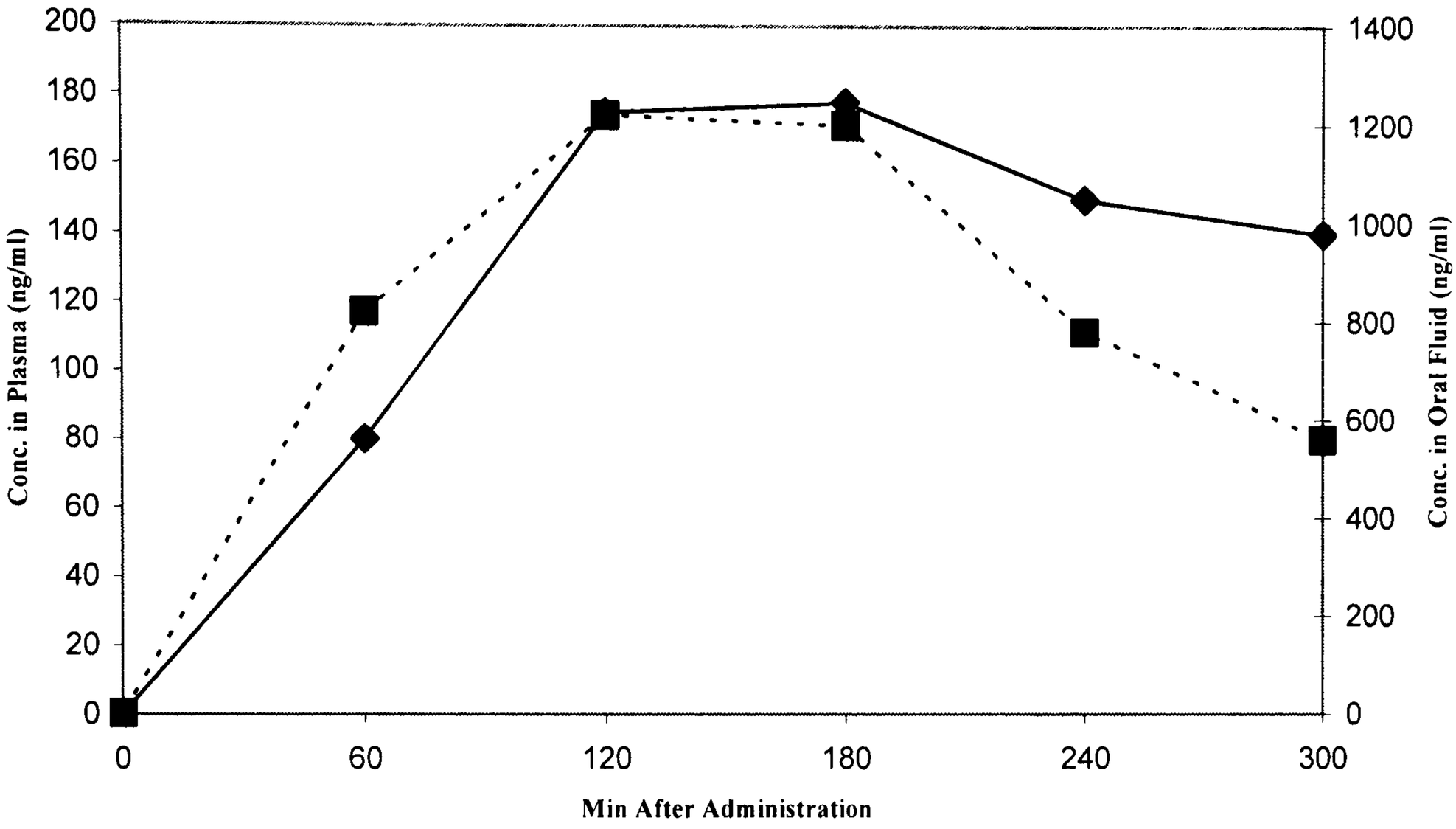

Figure 1.7: Average plasma (■) and oral fluid (◆) concentrations (ng/ml) in controlled dose MDMA volunteers [reproduced from Samyn *et al* (2002)].

Blood has always been regarded as the medium of choice for identifying cases of driving under the influence of xenobiotics. This is without an established concentration threshold beyond which impairment is substantial, in the same way for alcohol.

When it comes to preventative roadside testing blood sampling with its invasive procedures and cumbersome analysis is not suitable, but oral fluid sampling is a viable option. Consideration has to be given to the route by which the drug enters the oral fluid. This could occur during passage of the material through the mouth (food, drink, smoke, oral or nasal administration) or by secretion from the salivary glands (in which case the polarity and molecular size of the material will be important together with the factors listed previously) [Jusko and Milsap (1993). Research over the years has confirmed it is possible to detect amphetamine sulphate

and the substituted amphetamines in oral fluid using conventional methods such as liquid chromatography/mass spectrometry [Smith (1981), Schepers *et al* (2003), Samyn *et al* (2002), Wylie *et al* (2005a), Mortier *et al* (2001)]. The investigations detailed in this report have been conducted based on this with a view to finding a suitable technique which could be used at the roadside requiring little or no sample preparation and a fast analysis time.

Collection of mixed saliva has many disadvantages that can affect results. For example the drugs may bind to the inert materials used to collect an oral fluid sample [Siegel (1993)]. Orally administered drugs may leave drug residue in the mouth that will contaminate the oral fluid sample thereby influencing the detectable concentration of that drug. The drug may partition between the oral contents and oral mucosa and may then be slowly released back into the oral fluid as has been demonstrated for sulfamethizole resulting in false high oral fluid concentrations [Eatman *et al* (1977)]. Drugs may also enter the oral fluid from crevicular fluid. However, despite these problems, oral fluid generally contains unbound pharmacologically active parent drug [Siegel (1993)] which should give, in most cases, an indication of the level of drug consumed and therefore the potential impairing effects. The concurrent use of two or more drugs may alter drug binding [Siegel, (1993)] but polydrug profiles can be identified through the use of SERS because each drug has its own chemical fingerprint.

Chapter 2

Raman Spectroscopy

2.1 Introduction

The Raman effect was predicted by Smekcal in 1923 but first detected in 1928 by Sir C.V. Raman [Raman and Krishnan (1928)]. Initial experiments relied upon the focusing of sunlight and filters to observe visual colour changes in the scattered light [Gardiner and Graves (1989)]. Raman later investigated this effect using a mercury lamp and spectrograph on liquids including benzene and carbon tetrachloride which required a twenty-four hour period of exposure and a 600 ml sample volume [Raman and Krishnan (1928)].

The Raman effect is inherently weak, typically 10^{-10} of the incident radiation, making source stability and intensity an important part of collecting a spectrum [McCreery (2000)]. Maintaining the intensity and stability of the incident exciting radiation from the light sources available contributed to the difficulty in measuring the Raman effect until the early sixties when this was overcome by the harnessing of laser light. The use of laser light revolutionised Raman spectroscopy by providing a narrow beam, of high intensity and highly monochromatic light. This reduced interference from stray light and allowed the filtered removal of the incident radiation following exposure of the sample to ensure that only the scattered light was detected and analysed. This also reduced the time of sample exposure from hours to microseconds and enabled the recording of spectra from solid, liquid and gaseous samples, small sample volumes and coloured samples as well as those at high temperatures, under vacuum and in dilute solutions. Approaches used by others to review the theory of Raman spectroscopy have been used here [Gardiner and Graves (1989), McCreery (2000), Smith and Dent (2005)].

2.2 Theory

When a designated wavelength of incident radiation interacts with a sample molecule, that molecule will scatter the light in two principle ways (Figure 2.1)

[Gardiner and Graves (1989)]. The first is Rayleigh scattering and involves elastic scattering of the incident light in all directions. This occurs when the electrons in the molecule vibrate at the same frequency as the incident radiation and so emit the scattered light at the same frequency as the incident light. The second type of scattering is known as Raman scattering which is inelastic scattering of the incident light. It is subdivided into two processes which are explained below. This investigation will concentrate on the detection of Stokes Raman.

Inelastic scattering involves the interaction of a photon of incident radiation with a molecule. When the energy of the photon is too low to cause excitation of the electrons in the molecule to a higher electronic state, the photon is scattered. Inelastic scattering of the incident photon can occur in one of two ways; by either donation of its energy to or removal of energy from the molecule that it interacts with. This donation or removal of energy to or from the molecule produces two sets of lines on the spectrum. If the photon donates its energy to the molecule this results in Stokes lines. If the photon gains energy from the molecule Anti-Stokes lines arise (Figure 2.1) [Gardiner and Graves (1989)].

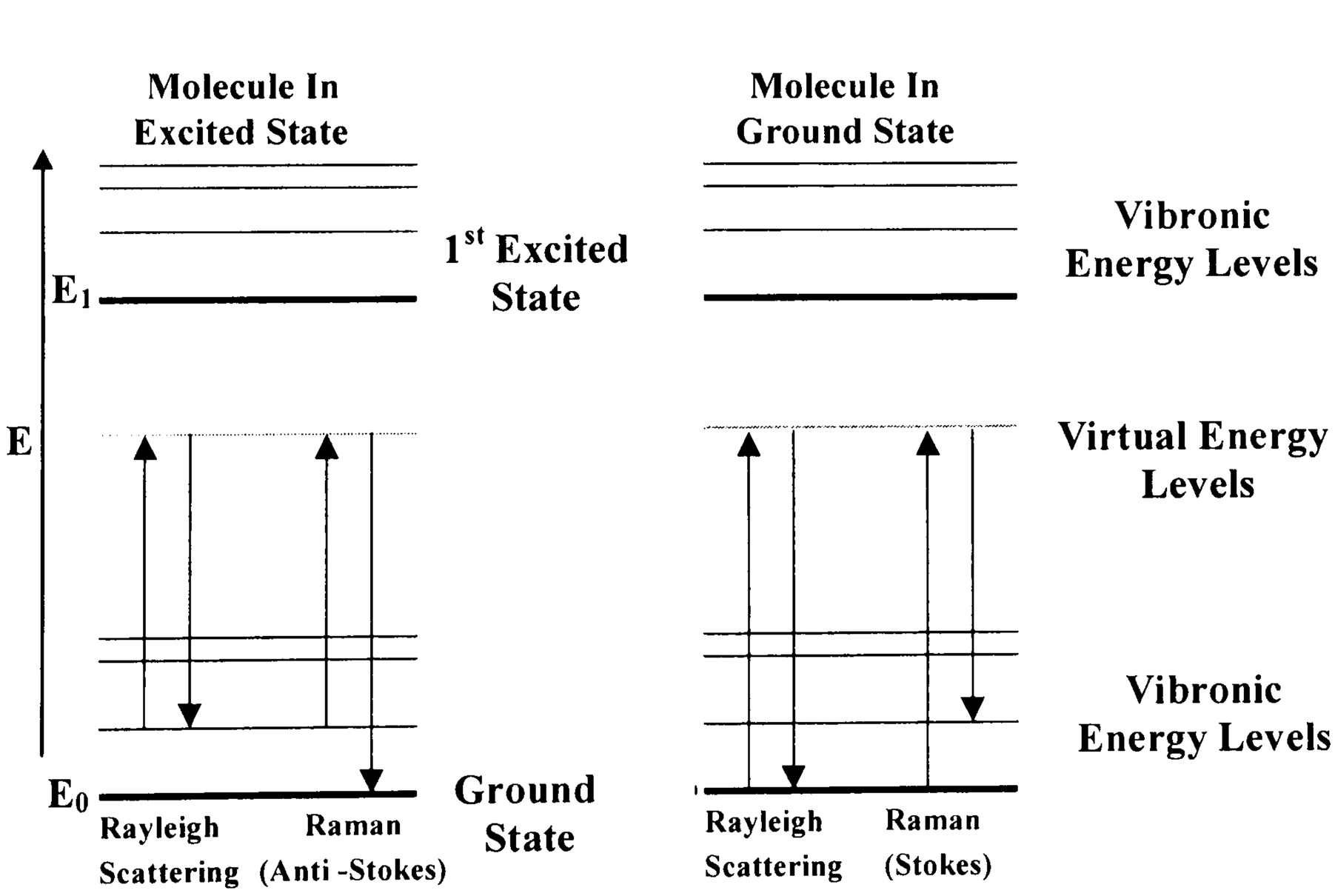

Figure 2.1: A diagram to illustrate Rayleigh and Raman Scattering [Gardiner and Graves (1989)].

Most collisions of the incident photons with a recipient molecule result in elastic Rayleigh scattering. However, approximately 1 in every million collisions results in the excited molecules undergoing polarizability changes provided during inelastic Raman scattering. If the molecule re-emits radiation following incident photon radiation collision and does not return to the original vibrational state but to an excited vibrational level of the ground state the emitted radiation is of lower energy than the incident radiation. It is the molecules natural vibrational frequency in the ground state that is responsible for this difference in energy. The lines produced from this process correspond to the Stokes Raman spectrum lines (Figure 2.2). However, if a molecule initially absorbs some of the radiation following incident photon collision while in an excited vibrational state and then decays to an energy level that is lower, the frequency of the Raman radiation is higher than the incident radiation. The resulting spectral lines correspond to the Anti-Stokes lines (Figure 2.2) which are usually much weaker than the Stokes lines.

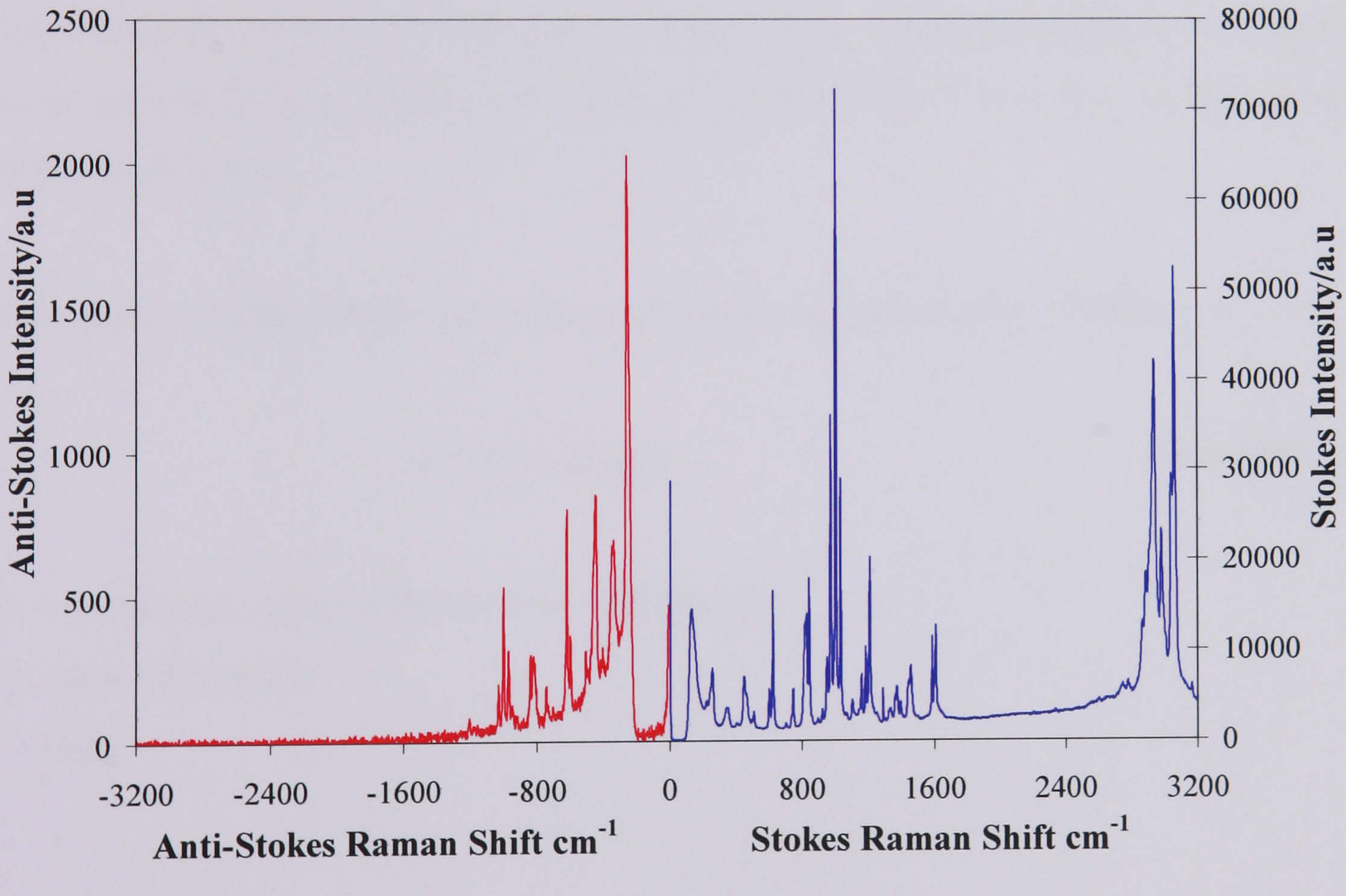

Figure 2.2: A typical Raman Spectrum illustrating the Anti-Stokes and Stokes spectrum of crystalline amphetamine sulphate.

For a vibration to be active in the Raman effect the polarizability of the molecule has to change during the vibration. Polarizability is the consequence of the applied electric field strength and involves a biased deformation of the electron cloud that surrounds the molecule at one end of the vibration over the other relative to its nuclei. This is known as an induced dipole moment.

If one considers the classical theory of the Raman effect, polarization strength is given by Equation 2.1 [McCreery (2000)];

$$P = \alpha E \qquad \textbf{(Equation 2.1)}$$

P = polarization

α = inherent polarizability of the molecule

E = incident electric field strength

This equation refers to the ease of distortion of the electron cloud surrounding the molecule and the magnitude of the induced dipole moment as related to the strength of the electric field.

The optical electric field is governed by Equation 2.2 [McCreery (2000)];

$$E = E_0 \cos 2\pi\nu_0 t \qquad \textbf{(Equation 2.2)}$$

E_0 = maximum value of the electric field strength

ν_0 = laser frequency

t = time

The molecular vibrations are composed of normal modes, Q_j, of which there are $3N$-6 in a molecule with N atoms (Equation 2.3) [McCreery (2000)];

$$Q_j = Q^o_j \cos 2\pi \nu_j t \qquad \textbf{(Equation 2.3)}$$

Q_j = normal modes of molecular vibration

ν_j = characteristic harmonic frequency of the jth normal mode

The molecular vibration adjusts the polarizability of electrons in the molecule (Equation 2.4) [McCreery (2000)];

$$\alpha = \alpha_0 + (\delta\alpha/\delta Q_j)\, Q_j + \ldots. \qquad \textbf{(Equation 2.4)}$$

$\delta\alpha/\delta Q_j$ = the rate of changes of polarisability

If the following mathematical relationship (Equation 2.5) is used and combined with all of the above equations (2.1 – 2.4) this gives rise to the polarizability equation (Equation 2.6) [McCreery (2000)];

$$\cos a \cos b = [\cos (a + b) + \cos (a - b)]/2 \qquad \textbf{(Equation 2.5)}$$

$$P = \alpha_0 E_0 \cos 2\pi \nu_0 t + E_0 Q^o_j (\delta\alpha/\delta Q_j) (\cos (\nu_0 + \nu_j) + \cos (\nu_0 - \nu_j))/2 \qquad \textbf{(Equation 2.6)}$$

The first term in Equation 2.6 has the frequency of the incident radiation and is the Rayleigh scattering. The second and third terms in Equation 2.6 represents the anti-Stokes ($\nu_0 + \nu_j$) and the Stokes ($\nu_0 - \nu_j$) Raman bands respectively [McCreery (2000)]. The primary selection rules for Raman scattering are found in Equation 2.5, which shows; firstly, a linear relationship between polarisation and scattering with laser intensity, and secondly, that Raman scattering is only generated by vibrations that modify the polarizability.

2.3 Surface Enhanced Raman Spectroscopy (SERS)

2.3.1 Introduction

SERS is observed when the molecule of interest is placed on a roughtened metal surface and a Raman spectrum is obtained. This Raman or SERS spectrum shows considerabley enhanced signal of the standard Raman and was first observed by Fleischmann *et al* (1974). The enhancement observed by SERS is attributable to two theoretical effects, the larger of which is field enhancement and the other chemical enhancement.

2.3.2 Field Enhancement Theory

Field enhancement occurs when metal particles or a roughened metal surface are exposed to an appropriate wavelength of laser light. If the optical properties of the metal surface are suitable, such as that seen with electrochemically roughtened silver or gold then the field enhancement of the incident light is increased at the particle surface, especially near the regions of curvature that occur on the small particles [Birke and Lombardi (1988), Zeman and Schatz (1987)]. The end result is an increase in the observed Raman scattering of approximately 10^6 under optimum conditions [McCreery (2000)]. However, this effect is strongly dependent upon several conditions. Field enhancement is strongest in metals with high reflectivity at the laser and Raman shifted wavelengths. This can be observed clearly with gold, silver and copper metals [McCreery (2000)]. Field enhancement has a longer range of enhancement capabilities than chemical enhancement in that it extends some several tens of nanometres away from the metal surface [McCreery (2000)]. Hence, the molecule has no need to be in direct contact with the surface to exhibit SERS. However, the magnitude of the field enhancement observed is dependent upon the optical properties of the metal and the chosen wavelength of excitation. McCreery (2000) states that the greatest enhancement properties of silver are observed in conjunction with a wavelength of excitation of 514 nm or 532 nm. It has also been observed that at excitation wavelengths greater than 600 nm gold and copper have their greatest enhancement. A significant magnitude of field enhancement is observed [McCreery (2000)] when the metal particles are several tens of nanometres

in diameter which makes them smaller than the laser wavelength. The metal particle shape also affects the observed field enhancement magnitude. This will differ depending upon the metal, laser wavelength and shifted Raman light. For example, the radii of curvature of spherical and elliptical particles are different but the average size and diameter of the particles may be the same. The outcome is a difference in the magnitude of the field enhancement effect [McCreery (2000)].

A roughened metal surface can consist of spheres, ellipsoids and irregular particles covering a range of sizes (in the nanometer range) so the magnitude of field enhancement will vary across a metal surface. Contributing to this are two phenomena; plasmon resonance and the antenna effect which are affected by the particle shape, size and distance between the particles. Plasmon resonance occurs when the metal particles are smaller than the laser wavelength. The incident light excites the metal conduction electrons inducing excitation of surface plasmons resulting in enhancement. At the plasmon frequency the metal polarises resulting in large field-induced polarisation [Ritchie (1957), Vo-Dinh (1998)]. If the metal has high optical cross section at this wavelength of excitation then the electrons will oscillate with the incident field creating dipolar surface plasmons. This causes the local electric field required for field enhancement. Detailed discussions have been presented by Zeman and Schatz (1987).

Moskovits *et al* (2007) demonstrated the importance of the gap distance between 2 nanoparticles and its effect on observed SERS enhancement. Using a series of hexagonally periodic Ag nanostructures constructed with gap distances between 10 – 35 nm, the intensity of the SERS enhancement factor varied by a factor of over 200. Xu *et al* (1999) also showed that electromagnetic enhancement factor of 10^{10} are present between two nanospheres separated by 1 nm.

2.3.3 Chemical Enhancement Theory

Chemical enhancement is the product of an interaction between the adsorbate molecule and the metal substrate often involving an electronic interaction such as

charge transfer. The adsorbate-substrate interactions, depending on the strength of the bond, can be loosely classified as physisorption and chemisorption. Physisorption is the weak and non-specific attraction of the adsorbate-substrate, such as a dipole-dipole, electrostatic or hydrophobic interaction. Chemisorption is more specific involving a site on the molecule such as a lone pair of electrons, or a site on the metal substrate. The interaction involves bond formation between the adsorbed molecules and the surface. This disturbs the molecular orbits and electron distribution in both the adsorbate and substrate. This interaction is specific to the adsorbed molecules thereby modifying their optical properties, and scattering cross section, in comparison to the free state adsorbate molecules. Overlap of the metal and adsorbate orbitals allows electron transfer from the molecules to the metal and vice versa. This theory is often referred to as the charge transfer theory [Zemen and Schatz (1987), Meier and Wokaun (1983), Otto (1978), Persson and Ryberg (1981), Adrian (1982), Pandey and Schatz (1984)].

Chemical enhancement can be observed beyond silver and gold metal surfaces. This is possible because the process requires the interaction of the substrate and adsorbate only and not on the optical properties of the substrate. However, the extent of this form of enhancement is limited to the first layer of the adsorbed molecules unlike field enhancement which can stretch several tens of nanometres from the surface [McCreery (2000)].

Overall the SERS effect is seen to provide a 10^6 enhancement factor to the Raman signal recorded. As a rough rule of thumb the contributions from the two enhancement effects attributable to SERS are often quoted as a 10^4 from field enhancement and 10^2 from chemical enhancement [McCreery (2000), Persson and Ryberg (1981), Adrian (1982), Pandey and Schatz (1984)].

A common analytical approach to SERS involves the preparation of SERS substrates by one of several methods that will be detailed below. The active substrate is exposed to a liquid or gaseous sample. The subsequent SERS spectrum is a snapshot

of the adsorbed layer undergoing field and chemical enhancement through the adsorbate-substrate interaction.

There are five principle ways to produce a SERS surface; electrochemical roughening, metal vapour deposition, metal colloids, etched metal surfaces and photoreduced metal particles [McCreery (2000), Vo-Dinh (1998)]. Figure 2.3 provides a schematic representation of how some of the surfaces are thought to be structured. Metal colloids, metal vapour deposition and photoreduced metal particles are three SERS methods that have been used in the work reported here and will be described in detail.

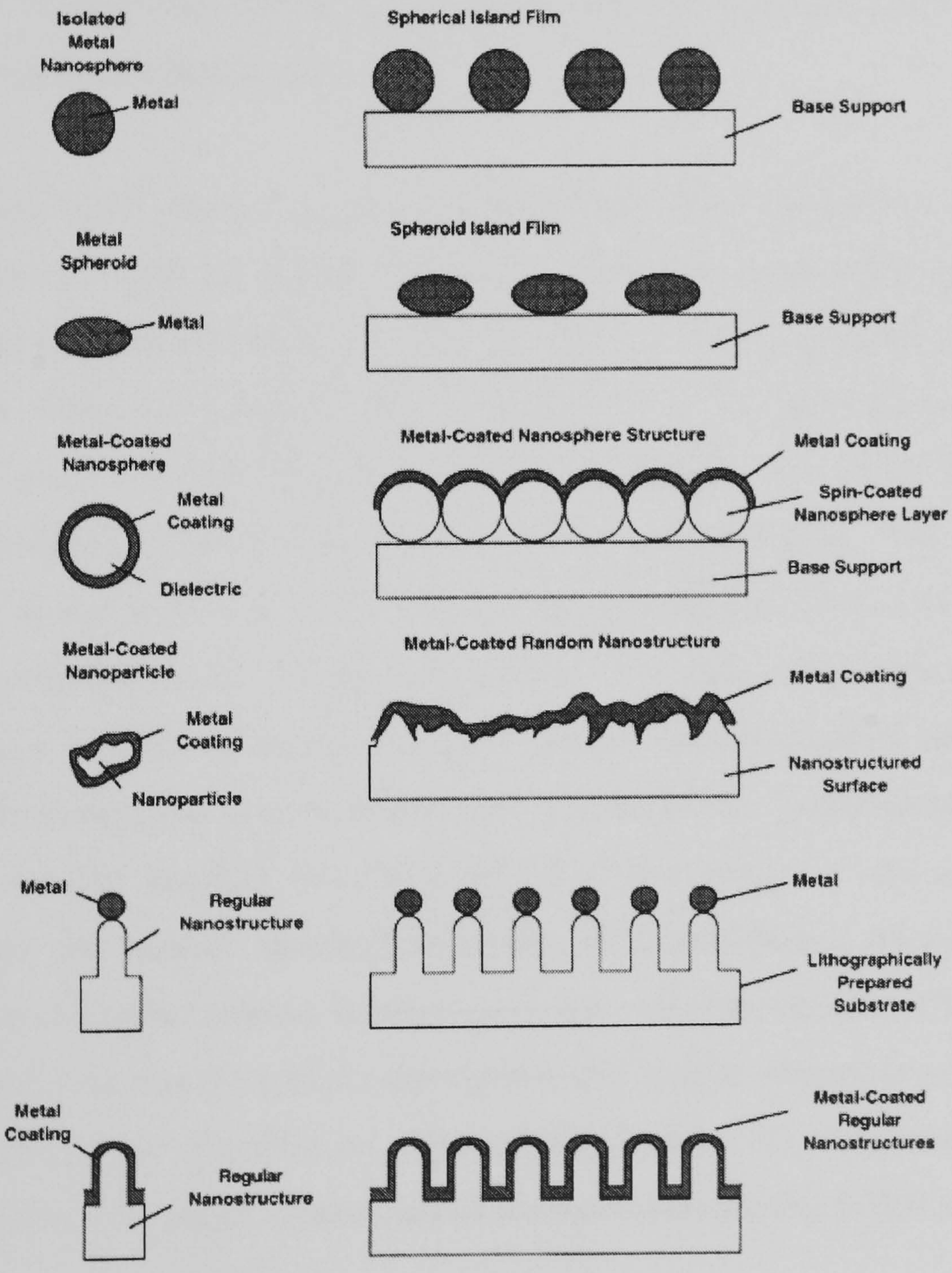

Figure 2.3: A schematic representation of the variety of nanostructures surfaces available for facilitation of SERS. Reproduced from Vo-Dinh (1998).

2.3.4 Metal Colloids

Colloidal suspensions are produced through the chemical reduction of a metal salt in water [Norrod *et al* (1997), Angebrranndt and Winefordner (1992), Sutherland *et al* (1990)]. The particle diameter distribution depends upon the conditions of synthesis but they can be controlled to produce a range suitable for both field enhancement and chemical enhancement. Silver and gold colloidal suspensions are available commercially (British Biocell International), with particle sizes of 40 mm (9.0×10^{10} particles/ml) and 80 mm (1.1×10^{10} particles/ml)) although the author has not observed any surface enhancement with these solutions. More usually for surface enhanced resonance Raman spectroscopy (SERRS) work they are prepared shortly before use. The colloidal particle size and density can be measured prior to use using UV/VIS absorption spectrometry.

The condition under which the colloid is produced dictates the particle size. If the particles are too small to exhibit field enhancement an aggregating agent can be added to the colloidal-adsorbate solution. However, this can introduce variability in the Raman intensities observed due to variations in the aggregation time and procedure. Jones *et al* (1999) compared several aggregation procedures to determine the reproducibility of SERS with resonant Raman dyes (SERRS). The aggregation agent used in this work was either added to the colloid-dye solution or the colloid was pre-aggregated before the dye was added. The Raman intensities were then observed as a function of aggregation time and the relative standard deviation was calculated from repeated spectral observation and the colloid preparations. Table 2.1 shows the relative standard deviations (RSD) of five spectra of the same colloid solution and the relative standard deviations of five different colloid solutions. Significantly the higher relative standard deviation was observed for different colloid solutions implying that the particle aggregation and analyte adsorption is sensitive to uncontrolled changes in conditions. The authors [Jones *et al* (1999)] concluded that pre-aggregation with poly-L-lysine yielded the most reproducible SERRS intensities.

Table 2.1: The relative standard deviations (RSD) of five spectra of the same colloid solution and the relative standard deviations of five different colloid solutions [Jones *et al* (1999)].

Aggregation Agent	**RSD 5 spectra of 1 colloid solution (%)**	**RSD 5 spectra from each of 5 colloid solutions (%)**
NaCl	14 – 18	28 - 35
Poly-L-lysine	1 – 4	17 - 18
Preaggregation with poly-L-lysine	1 – 3	3 - 5

2.3.5 Metal Vapour Deposition

Metal vapour deposition (MVD) of silver onto quartz and glass slides to create films with an estimated thickness of 20 to 30 nm was undertaken. MVD involves thermal decomposition of a measured quantity of silver using the instrument evaporation boat. There are three selectable sets of evaporation filaments located in an array within the chamber, positioned to achieve optimum coating uniformity. The system also contains a two stage rotary vane vacuum pump/mechanical booster vacuum pump combination and a high throughput diffusion pump. A low temperature stainless steel refrigerated cold finger is fitted to the chamber to ensure rapid pump down. Upon reaching sufficient pressurisation the silver is heated to molten consistency using an electric arc that generates charged species that bombard a silver target. The resultant mist of silver atoms is then deposited onto the appropriate glass surfaces located on the evaporation chamber roof by evacuating the chamber using the above pumping system resulting in uniform coverage of the slides. The size and shape of the metal nanoparticles can be influenced by varying the thickness of metal deposited [Vo-Dinh (1998)] which is monitored by a quartz crystal microbalance. The whole system is controlled and monitored by a computerised system.

Schlegel and Cotton (1999) examined the effect of deposition rate on the surface morphology and optical properties of silver films. They correlated the SER(R)S response using 10^{-3} M 4,4`bipyridine (BP) (non resonant) and 10^{-4} M zinc

tetraphenylporphine (ZnTPP) (resonant). The findings were that the BP SERS intensity is dependent upon the deposition rate. An exponential relationship between the deposition rate and the ZnTPP SERRS intensity was also observed. They concluded the deposition rate influences the morphology of the particles composing the metal film. This ultimately determines the optical properties of the films and the SERS enhancement achieved. Van Duyne *et al* (1993) however, using Atomic Force Microscopy (AFM) characterisation could not observe any changes in morphology or SERS activity as a function of deposition rate. Semin and Rowlen (1994) investigated these differences, using the same dyes, through the influence of a number of factors. They concluded that even small changes in the substrate deposition temperature can affect the silver form morphology and the optical characteristics. Additionally, the deposition geometry i.e. the angle between the source and the substrate during the deposition process is also important.

Mills *et al* (2004) used Ag sputtered films as SERS substrates in their study of benzotriazole dyes but found they exhibited a high residual standard deviation (ca. 45%). Faulds *et al* (2002) also used MVD silver and gold films. Spectra of aqueous amphetamine sulphate were recorded at concentrations from 10^{-2} to 10^{-5} M. The within film and between film precision was calculated to be 31.6% and 36.9% respectively for the silver films.

2.3.6 Photoreduced Metal Particles

The photoreduction of silver salts for SERS was based upon photographic emulsion production research. Several preparations have been developed including the photoreduction of silver nitrate solution prior to exposure to the analyte [Gao *et al* (1984)] or in the presence of the analyte [Ahern and Garrell (1987)]. When reduced in the presence of the analyte the level of SERS exhibited was four times greater than that for colloid produced through chemical reduction processes.

Silver particles have also been photoreduced onto titanium dioxide (TiO_2) substrates [Norrod *et al* (1997), Sudnik *et al* (1996)] and demonstrated a non-linear response to

trans-1,2-bis-(4-pyridyl)ethane (BPE) concentration with a detection limit of 2 μM in 3 μL of solution. Photoreduced films have demonstrated good reproducibility despite the non-linear response. This non-linear response has been attributed to analyte adsorption by the TiO_2 surface instead of the silver surface [Norrod *et al* (1997)].

The photocatalytic process has been extensively researched especially with TiO_2 powders [Litter (1999), Mills and Lee (2003)] and typically follows the summarised reaction pathways below (Equations 2.7 and 2.8). For the production of Ag/TiO_2 films the photocatalytic process can be summarised as follows [Litter (1999), Mills and Le Hunte (1997)]. Where M^n is the metal, SED is the sacrificial electron donor and E_{bg} is the band-gap energy of TiO_2 (3.2 eV for anatase titania. Thus, ultra band-gap irradiation of titania generates an electron-hole pair. The photo-generated electron is able to reduce silver ions at the surface of the titania to silver metal. The photo-generated hole is able to oxidatively mineralize methanol, which acts as a sacrificial electron donor (SED) [Mills *et al* (2004)].

$$M^{n^+} + SED \xrightarrow[Semiconductor]{h\nu \geq E_{bg}} M \downarrow + SED^{n+} \qquad \textbf{(Equation 2.7)}$$

$$6Ag^+ + CH_3OH + H_2O \xrightarrow[TiO_2]{h\nu \geq E_{bg}} 6Ag \downarrow + CO_2 + 6H^+ \qquad \textbf{(Equation 2.8)}$$

The second equation has been principally investigated with the photodeposition of metals such as platinum and palladium and to a lesser extent with Ag onto TiO_2. SERS success has been achieved by using the same approach to photocatalitically deposit other metals such as gold, copper and mercury onto TiO_2 [Litter (1999), Mills and Le Hunte (1997)]. Norrod *et al* (1997) compared the performance of five different Ag substrates for SERS including Ag/TiO_2 substrates produced by semiconductor photocatalysis. Although not found to be the most sensitive of the five films tested – this award went to post-deposition annealed Ag vapour films- the Ag/TiO_2 on glass substrstaes were found to be a sensitive SERS substrate showing

enhancement of BPE. As a consequence of this and other work most of the SERS substrate work reported in this thesis concerns Ag/TiO_2 substrates.

A study of photodeposited silver substrates on TiO_2 (Ag/TiO_2 substrates) looking at the effect of changing photodeposition time was performed by Mills *et al* (2004). Scanning Electron Microscopy (SEM) images can be used to estimate a silver photodeposited film of 150 nm was made [Mills *et al* (2004)]. Mills *et al* (2004) used such substrates to great effect as SERS substrates for the detection of the benzenetriazole dye, GM19. They found that the magnitude of the SERS signal increased with increasing photodeposition time and could be used for quantitative analysis of this dye over the range 10^{-6} to 10^{-7} (Figure 2.4).

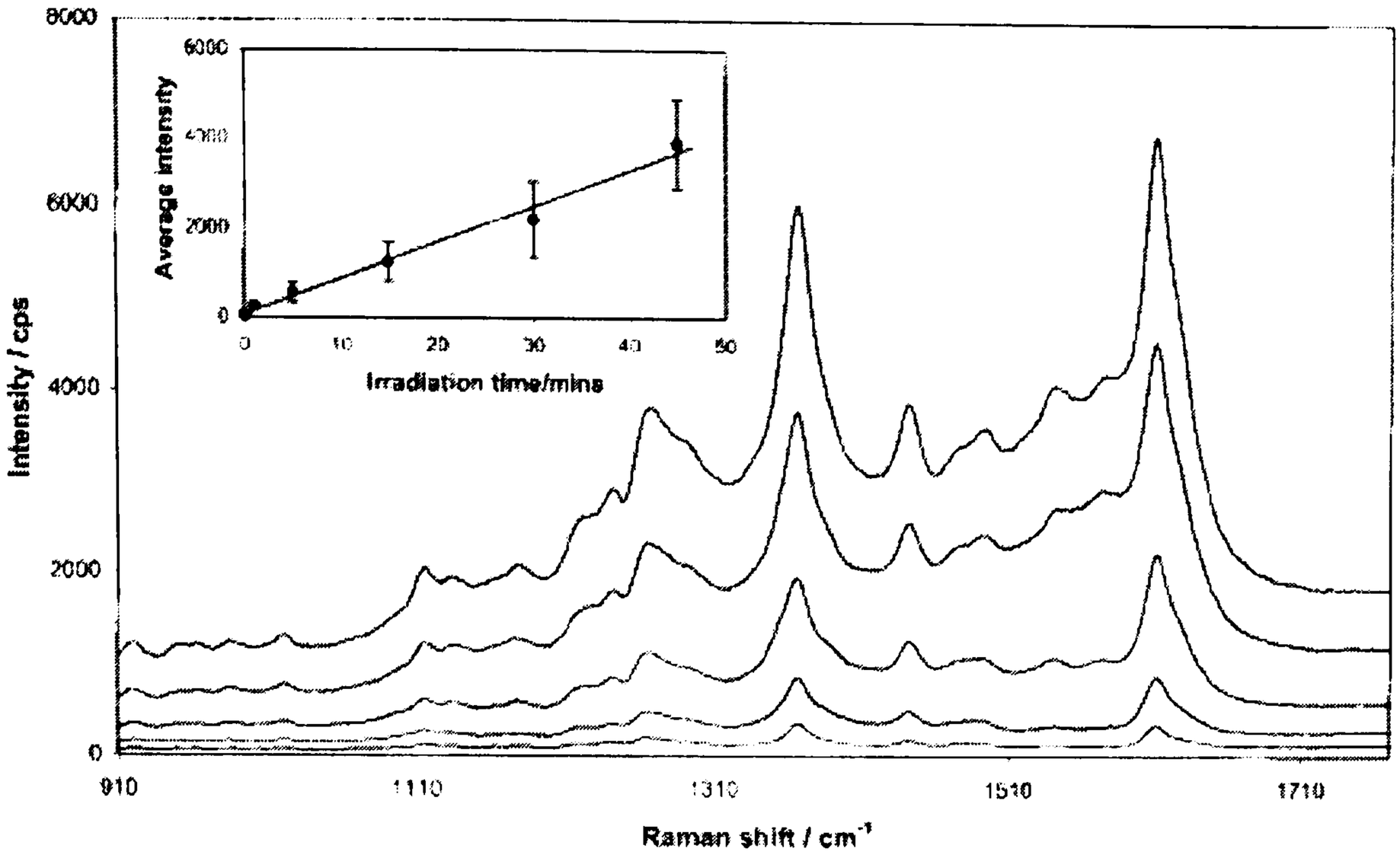

Figure 2.4: Recorded SERS spectra of Ag/TiO_2 substrates, where the Ag has been photodeposited using UV irradiation times that range from 1 to 45 min. The spectra are due to the dye GM19, which was deposited by soaking the substrates in a 10^{-6} M solution of the dye in methanol, before drying and subjecting them to analysis using the microprobe system. The inset shows the SERRS intensity of the 1615 cm^{-1} peak measured for the above substrates as a function of UV irradiation time [Mills *et al* (2004)]. The two major sets of peaks, which appear in all the SERRS spectra, are the quadrant stretch of the phenyl ring at 1615 cm^{-1} and the azo stretch at 1375 cm^{-1}. Reproduced from Mills *et al* (2004).

The Atomic Force Microscopy (AFM) images below (Figure 2.5) [Mills *et al* (2004)] show the Ag/TiO_2 substrates at different times through the photodeposition process, showing the growth of the silver on the TiO_2 surface. The images illustrate the changing size and shape of the silver islands but also that they remain separate entities and do not overlap even after 50 minutes photodeposition.

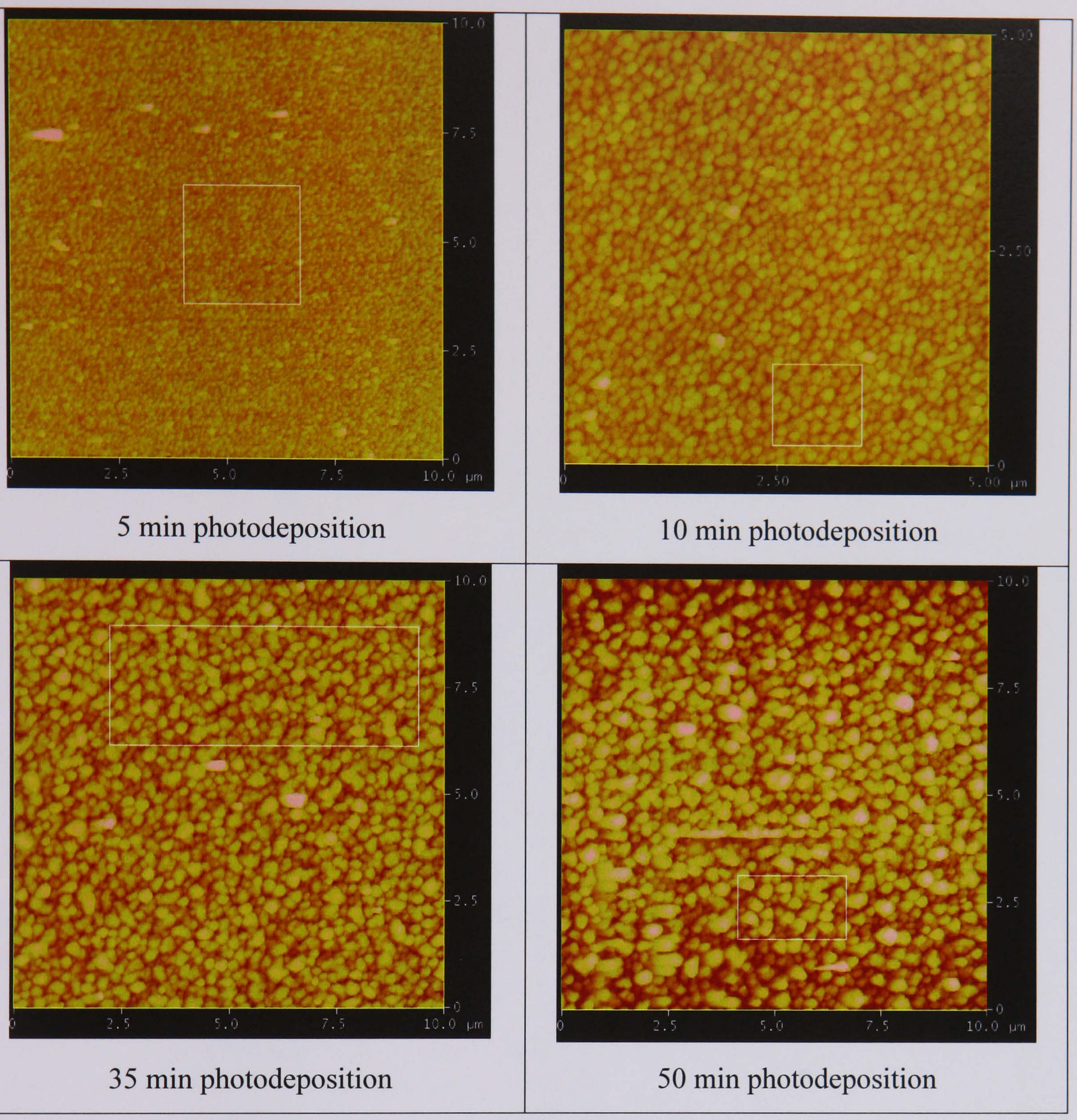

5 min photodeposition

10 min photodeposition

35 min photodeposition

50 min photodeposition

Figure 2.5: AFM images of photodeposited silver on TiO_2 substrates with increasing photodeposition time. The scales allow estimated measurement of the particle size.

2.3.7 SERS Detection of Illicit and Prescription Drugs

Table 2.2 provides a summary of peer reviewed literature involving the detection of illicit and prescribed drugs using a variety of SERS enhancement methods.

Table 2.2: A summary table of SERS papers involving various methods of facilitating SERS enhancement for the detection of illicit and prescription drugs.

Reference	Drugs	Concentration	SERS Method
Ruperez *et al* (1991)	Mefenorex Pentylenetetrazole L-amphetamine	$5x10^{-4}$ M $7x10^{-4}$ M $3x10^{-4}$ M	Silver hydrosols
Horvath *et al* (1997)	Heroin Codeine Cocaine	$4x10^{-3}$ M $4x10^{-3}$ M $4x10^{-3}$ M	TLC silver coated drug layer
Perez *et al* (1998)	Cocaine Triamterene Amiloride Methoxyphenamine Oxprenolol Acebutolol Atenolol Pemoline Propranolol	$2x10^{-6}$ M $2x10^{-7}$ M $8x10^{-7}$ M $5x10^{-7}$ M $4x10^{-7}$ M $4x10^{-6}$ M $3x10^{-6}$ M $1x10^{-7}$ M $2x10^{-7}$ M	Tetrahydroborate silver colloid Tetrahydroborate silver colloid Citrate silver colloid Citrate silver colloid Tetrahydroborate silver colloid Tetrahydroborate silver colloid Citrate silver colloid Tetrahydroborate silver colloid Citrate silver colloid
Sulk *et al* (1999)	Amphetamine Methamphetamine	$5x10^{-5}$ M $9x10^{-5}$ M	Roughened/etched silver foil
Cinta *et al* (1999)	Diazepam, Nitrazepam	$1x10^{-7}$ M $1x10^{-7}$ M	Borohydride silver colloid
Bell and Spence (2001)	Anti-cancer drug AQ4N	$1x10^{-6}$ M	Silver polymer-sol suspension
Faulds *et al* (2002)	Amphetamine Sulphate	$1x10^{-5}$ M	Citrate silver colloid Citrate gold colloid Vapour deposited silver films
Sagmuller *et al* (2003)	Amphetamine Methamphetamine Cocaine Tropane Procaine Diacetylmorphine Codeine Noscapine Papaverine	$1x10^{-3}$ M $1x10^{-3}$ M $1x10^{-3}$ M $1x10^{-3}$ M $1x10^{-3}$ M $1x10^{-3}$ M $1x10^{-3}$ M $1x10^{-3}$ M $1x10^{-3}$ M	Silver halide
Wang *et al* (2003)	Aspirin Salicylic Acid Acetaminophen	$8x10^{-6}$ M $1x10^{-5}$ M $1x10^{-3}$ M	Silver sol particles
Ryder (2005)	Cocaine Heroin Amphetamine Benzodiazepines	Review paper	

One of the first papers to report the detection of l-amphetamine at a concentration of $3x10^{-4}$ M was by Ruperez *et al* (1991) using silver colloid. Sulk *et al* (1999) reported the detection of amphetamine and methamphetamine using a roughened/etched silver

foil used to facilitate the SERS mechanism as a rapid screening method. The approach involved chemically removing the sulphate and hydrochloride salts from the amphetamine and methamphetamine respectively. The remaining amphetamine or methamphetamine was derivitised using a coupling reaction, whereby dichlorohexylcarbodiimide (DCC) acted as the coupling reagent, with 2-mercaptonicotinic acid (2-MNA) forming the amide compounds AMNA (N-(1-methyl-2-phenylethyl)-2-mercaptopyridine-3-carboxamide) and MMNA (N-methyl-N-(1-methyl-2-phenylethyl)-2-mercaptopyridine-3-carboxamide). These were coated onto the surface of the etched foil and a SERS spectrum recorded between 800 – 1650 cm^{-1} (Figure 2.6) using 647 nm and 633 nm excitation. Quantification of the drugs was achieved using a known quantity of internal standard coated onto the foil in addition to the drug sample and by comparing the Raman band relative intensities of the internal standard and drug peaks a concentration was determined. For both drugs strong ring breathing modes for both the phenyl ring and pyridinyl ring were observed and the amide stretch too. A summary of the peak positions for the different vibrational modes at 647 nm excitation is detailed in the Table 2.3.

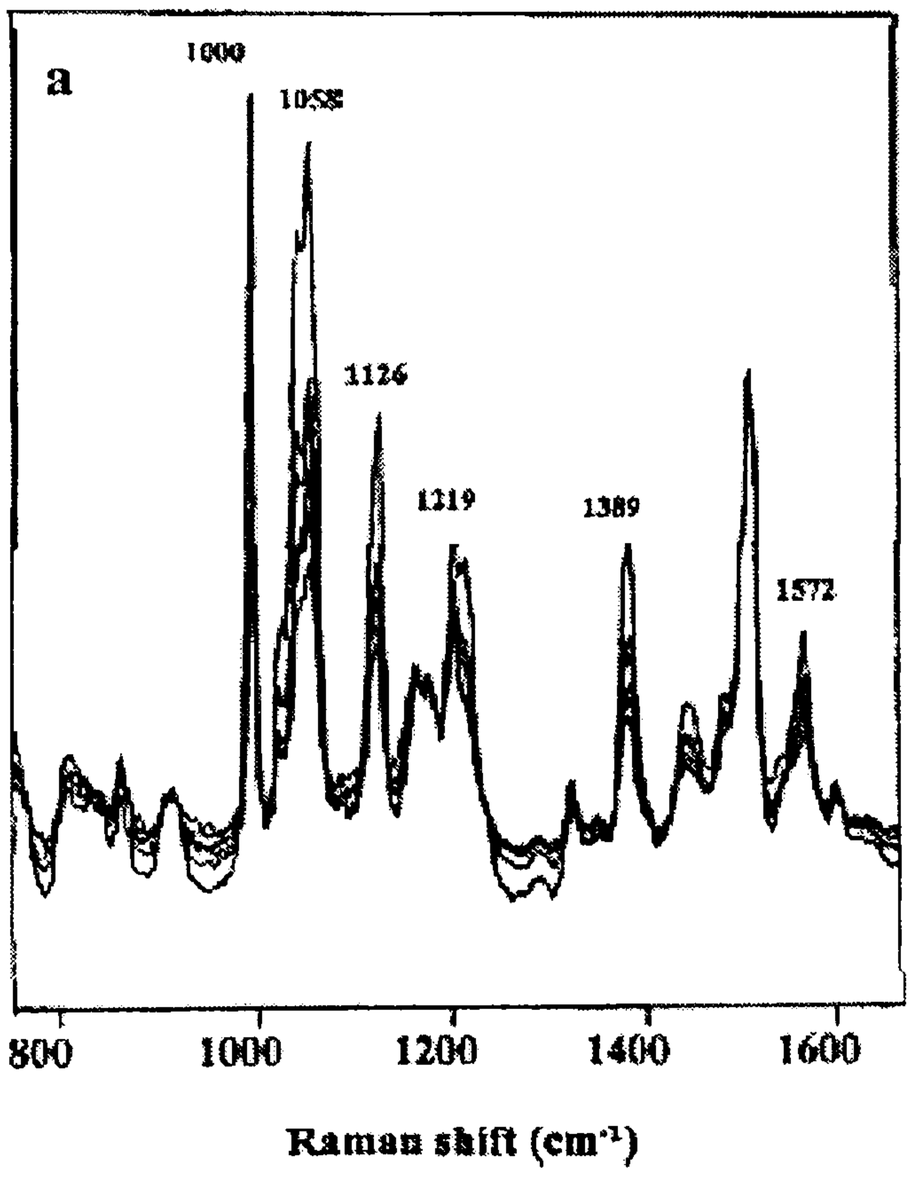

Figure 2.6: Taken from Sulk *et al* (1999), a SERS spectrum of MMNA recorded between 800 – 1650 cm^{-1}.

Table 2.3 Detailing the Raman modes in Sulk *et al* (1999) paper on the detection of amphetamine and methamphetamine using SERS.

Raman Mode	**Amphetamine Peak Position cm^{-1}**	**Methamphetamine Peak Position cm^{-1}**
Phenyl ring breathing	998	1000
Pyridinyl ring breathing	1055	1058
Asymmetric C-N-C stretch	1125	1126
Phenyl-C stretch	1205	
Pyridinyl C- stretch	1223	1219
Amide C-N stretch	1389	1389
Ring stretch	1569	1586.4

Detection limits of $5x10^{-5}$ M and $9x10^{-5}$ M for amphetamine and methamphetamine respectively were measured [Sulk *et al* (1999)]. These limits are much higher than the analytical concentration cut-off limits expected to be defined in the type approval specification for roadside testing. Traditional confirmatory analysis using standard Gas Chromatography/Mass Spectrometry or Liquid Chromatography/Mass Spectrometry methods would enable detection to $1x10^{-8}$ M to $2x10^{-9}$ M.

This work demonstrates the potential of SERS in the application of drug detection. However, the Sulk *et al* (1999) method involves lengthy (24 hours) complex chemical reactions to derivitise the drugs to force the attachment to the SERS substrate to facilitate the enhancement. Additionally, the spectra are from the derivitised drugs and not from the actual drugs themselves. If this method were expanded to enable detection of other drugs additional derivitisation methods would be required. Multiple analyses would then need to be performed if polydrug use was suspected, therefore, this method would not be suitable for roadside screening applications.

The work of Faulds *et al* (2002) assessed the use of gold and silver substrates for the detection of amphetamine sulphate by SERS. This work focused on several SERS methods including aggregated colloid suspensions, concentrated colloid and vapour deposited films. Samples of aqueous amphetamine sulphate solution at concentrations ranging between $1x10^{-2}$ M to $1x10^{-6}$ M were analysed using 785 nm excitation. The aggregated colloidal suspensions produced differing results depending on the combination of either gold or silver colloid with nitric acid, sodium chloride or poly-L-lysine as the aggregating agent. The lowest limit of detection was $1x10^{-5}$ M following gold colloid aggregation with sodium chloride. However, the spectral detail is very weak and whilst this concentration reflects those likely to be detected in drug users (Chapter 1.3) the lack of spectral detail will inhibit drug identification based upon the presence of a single peak. In contrast the vapour deposited silver films Faulds *et al* (2002) show better spectral resolution with multiple peaks present especially at $1x10^{-4}$ M. The increased spectral detail at $1x10^{-4}$ M versus the higher concentrations might reflect the onset of a true SERS enhancement at the surface-drug interaction site.

At higher concentrations, utilising a drop coat method, it is often possible to observe small crystal formations on the surface of the substrate. Often the density of the crystal structure prevents either excitation or recollection of the backscattered light from the substrate-drug interaction site so a weaker Raman scattering effect is observed [Faulds *et al* (2002)]. At lower concentrations the crystal formation is less dense allowing increased collection of the chemical and field enhanced backscattered light from the drug-surface interaction site resulting in increased spectral detail.

The within substrate and between substrate reproducibility of the vapour deposited substrates was found to be consistent when the RSD were calculated (approximately 30 - 35%). If multiple spectra were obtained from each film a RSD of under 6% was calculated. Additionally, based on the assumption that the drug distributes equally within the sample spot applied to the surface, the calculated concentration estimated to be under the beam at any sample site is estimated to be in the atto-gram region due

to the small beam diameter, illustrating the sensitivity of the SERS technique [Faulds *et al* (2002)].

There are many variables that determine the level of SERS enhancement effect observed. Chance exposure to contaminants can cause significant variation in the observed enhancement over time. The strength of the adsorbate-substrate interaction is reliant upon the surface chemistry and the molecular structure of the analyte. The analytes vary greatly in their interaction with the substrate and the slightest contamination can prevent this interaction from occurring altogether. Additionally, the nanoscale structure of the SERS substrate itself can influence the enhancement factor gained from a substrate.

Whilst SERS is still a developing analytical technique there are many benefits of using it; for firstly detecting aqueous amphetamine sulphate and the substituted amphetamines and secondly developing this for a roadside screening device for the detection of illicit drugs in oral fluid.

The work documented outlines the investigations undertaken so far regarding the potential use of SERS as a suitable technique for the detection of illicit drugs in oral fluid using one or more of the metal substrates described in this chapter. The investigations have concentrated on aqueous solutions of the phenethylamines, and the use of these illicit drugs spiked into oral fluid and samples of oral fluid collected from registered drug users. Work profiling the composition of ecstasy tablets was also undertaken to provide an in sight into what might be detected in the oral fluid of users.

Chapter 3

Raman Spectroscopy Analysis of Ecstasy Tablets

3.1 Introduction

The use of Raman spectroscopy with near infra-red excitation (785nm) applied to the analysis of Ecstasy tablets, (methylenedioxymethamphetamine) is well documented [Bell *et al* (2000a), Bell *et al* (2000b), Bell *et al* (2003), Bell *et al* (2004)]. Vibrational spectroscopic techniques lend themselves to this application readily owing to their ability to chemically fingerprint a compound based on its structural composition. The variance in structural composition is translated into the spectrum providing a unique substance identification system. Raman spectroscopy is the method of choice from the various spectroscopic techniques available. It requires no sample preparation, has reasonably short analysis times, typically less than a minute and produces information rich spectra without destroying the sample, making it ideal for tablet examination [Bell *et al* (2000a), Bell *et al* (2000b)].

Logos are commonly embossed onto the tablet surface and used for identification. These range from animals and birds to internationally recognisable brands such as Mitsubishi and Armani logos [Bell *et al* (2000b)]. However, the popularity of the logos amongst consumers often results in numerous clandestine laboratories adopting the same logo, preventing their use as markers of source or composition.

High sample throughput is essential if a technique is to be useful for operational analysis and intelligence gathering applications. Clandestine laboratory seizures often comprise several hundred thousand tablets and composition analysis of active drug and excipient components is required. Determining the degree of homogeneity between the seized tablets indicates if they are from a single source origin or if they were manufactured in different ways but made to look identical.

Traditionally, spectroscopic techniques have been used for drug screening rather than for drug intelligence applications [Bell *et al* (2000b)]. The latter is usually approached through impurity profiling using various chromatographic methods

[King *et al* (1994), Hubball (1992), Nic Daeid and Waddell (2005)]. GC-MS is considered the gold standard method for criminal prosecutions [King *et al* (1994)] to identify and quantify the active compounds present such as the phenethylamine derivatives [Hubball (1992)] but does not give any other information on tablet composition. A major disadvantage of GC-MS is the sample preparation requirements. The tablet must be dissolved and derivatised before analysis which is destructive and time consuming. Consequently only a few tablets from a single seizure can be analysed which may give a misleading batch composition picture [Bell *et al* (2000b)].

Assessment of the purity of the tablets is also of interest to identify what is present in the tablets. This information can be used to identify what might be found in the oral fluid of users. Analysis of the tablet composition will indicate what drugs and excipients should be considered during SERS analysis of oral fluid samples.

This work aims to determine if Raman spectroscopy can be used to distinguish between batches of tablets containing chemically similar ring-substituted phenethylamines and multiple excipients to give useful composition profiles for drug intelligence work. Tablets taken from several batches seized at different clandestine laboratory locations were analysed.

3.2 Experimental

3.2.1 Tablet Preparation

Prior to analysis each tablet was sprayed with compressed air to remove any loose particulate material. The tablet was mounted on a microscope slide and placed under the microscope where a white light photographic image was collected.

3.2.2 Spectral Collection

Raman spectra were recorded using a Renishaw System 1000 Raman Microscope (Renishaw Plc Gloucestershire UK) with near infra-red 785 nm compact diode laser excitation. The sample was mounted on a motorised XYZ stage. Scattered light was collected, passed through a Renishaw holographic notch filter and dispersed by a

Renishaw 1200 lines/mm grating onto a Rencam cooled charge-coupled device. A line focus accessory (Figure 3.1) was also used to increase the total area of the tablet analysed with each spectral collection.

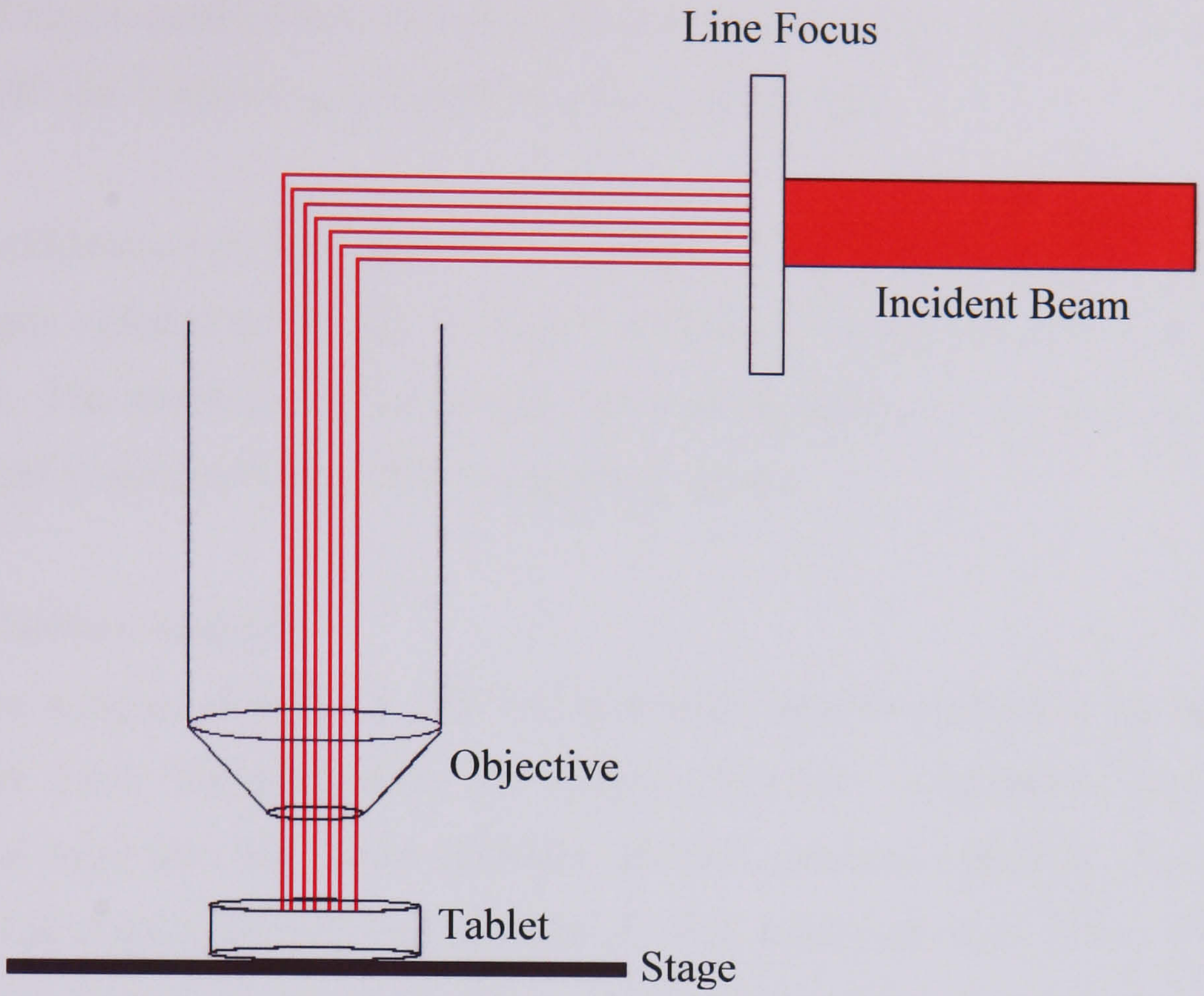

Figure 3.1: Graphical representation of the effect the line focus accessory has on the incoming incident laser beam and its presentation at the tablet surface.

3.2.3 Raman Analysis

Spectra were collected from three areas (top, middle and bottom) of the tablet to maximise the total area sampled and to compare any similarities and/ or differences across the tablet. The total analysis time per tablet was 15 minutes (5 minutes per area).

The laser was line focused (~400 μm (l) x 12 μm (w)) onto the sample through a x5 microscope objective. Using the software mapping function an area 0.16 mm^2 was defined on the tablet surface. This 400 μm by 400 μm area was divided into a grid. Incremental direction steps were defined; 12 μm imaging step size (Y), 30 μm mapping step size (X). The line focus accessory facilitates collection of a series of

line images. The 'line' itself is a series of 21 vertical spots with a diameter of approximately 12 μm each (Figure 3.1). Each image consists of 21 vertically aligned spectra. Spectra of the tablets were collected from 600 cm^{-1} to 1200 cm^{-1} for 10 seconds per incremental step using a rastered beam totalling 5 minutes collection per area. Reference standard spectra were collected using a single extended scan method (200 - 1600 cm^{-1}) and an accumulation time of 10 seconds.

A daily calibration of the laser was undertaken using a silicon wafer. Additional wavelength calibration checks were also undertaken using hydrogen peroxide and diamond. The resolution of the instrument is considered to be accurate to ± 2 cm^{-1} with regard to the positions of the strong sharp bands.

3.2.4 Reference Samples

Reference samples of MDMA, MDEA, and MDA as their hydrochloride salts were purchased from Sigma-Aldrich Ltd (Poole, Dorset). Commonly encountered excipients were also purchased (glucose, sorbitol, sucrose, cellulose) from Sigma-Aldrich Ltd (Poole, Dorset) and (powdered milk, talcum powder, flour, corn flour, baby milk) from a local supermarket. Multiple spectra from each sample were collected and used for peak position comparison.

3.2.5 Ecstasy Tablet Samples

Ecstasy tablets, seized from clandestine laboratory raids, were obtained from the Federal Police in Belgium. The samples were sent to the UK for initial Raman analysis and then returned for confirmatory GC/MS analysis.

3.2.6 Spectral Processing

Post collection, the spectra were subject to baseline correction (auto levelling), peak picking (across the whole spectra), peak fitting (Gaussian and Lorentzian mix) and exportation of the final peak tables using Advanced Chemistry Development Inc Spec Manager 2006 (v 9.15). Calculations were performed on Microsoft Excel 2002 (v 10.6501.6626) SP3 and SPSS 14.0 for windows 2005 (v 14.0.1).

3.3 Results

3.3.1 Drug Reference Standards Peak Position Data

Figures 3.2 to 3.4 and Tables 3.1 to 3.3 show the ring structures principle identifying vibrational modes for the reference standard phenethylamine derivatives. Although there are strong spectral similarities between the compounds (MDMA, MDEA, MDA) with their ring structures, the differences in the side chain functional groups, allow them to be distinguishable from each other especially in the fingerprint region of 700 - 1100 cm^{-1} (Figure 3.5).

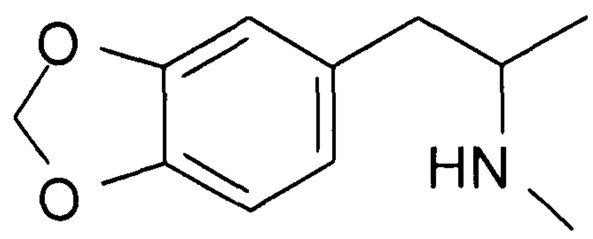

Figure 3.2: Structure of methylenedioxymethamphetamine (MDMA).

Table 3.1: The principal vibrational modes of MDMA.

Peak Position cm^{-1}	**Movement**	**Peak Position cm^{-1}**	**Movement**
771.16	Ring Vibration	881.30	C-C Skeletal Stretch
809.34	Ring Breathing	1012.75	1,3,5-Substituted Benzenes
832.84	Ring Breathing	1249.00	CH_2 Twist and Rock

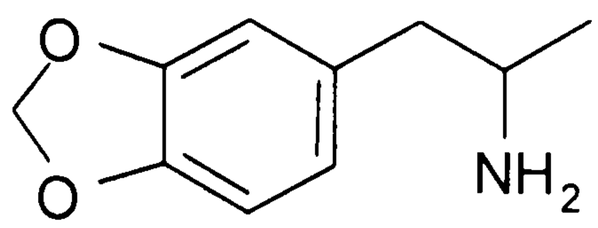

Figure 3.3: Structure of methylenedioxyamphetamine (MDA).

Table 3.2: The principal vibrational modes of MDA.

Peak Position cm^{-1}	**Movement**	**Peak Position cm^{-1}**	**Movement**
345.25	Chain Expansion	832.84	Ring Breathing
774.83	Ring Vibration	1255.81	CH Deformation
811.54	Ring Breathing		

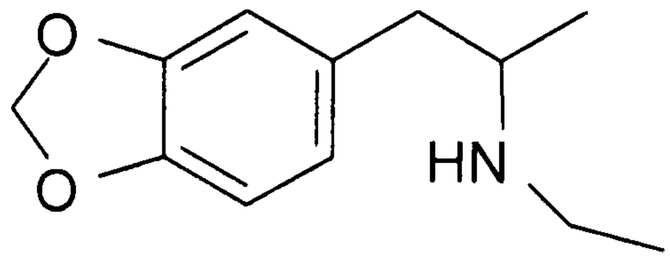

Figure 3.4: Structure of methylenedioxyethylamphetamine (MDEA).

Table 3.3: The principal vibrational modes of MDEA.

Peak Position cm^{-1}	**Movement**	**Peak Position cm^{-1}**	**Movement**
713.88	Ring vibration	843.85	C-C Skeletal Stretch
771.16	Ring vibration	1241.12	CH_2 Twist and Rock
802.73	Ring Breathing	1365.22	CH_3 Deformation
812.28	Ring breathing	1405.61	CH_2 Deformation

Figure 3.5: Overlaid reference spectra of the phenethylamine derivatives MDMA (green), MDA (blue) and MDEA (red).

3.3.2 Excipient Reference Standards Peak Position Data

Figures 3.6 to 3.13 and tables 3.4 to 3.7 present the structures, Raman spectrum and principle identifying vibrational modes within the mapping window of the excipients; cellulose, sucrose, glucose and sorbitol. Figure 3.14 presents four additional excipients, talcum powder, flour, corn flour and powdered milk, which were also considered but were subsequently not identified within the seized tablets.

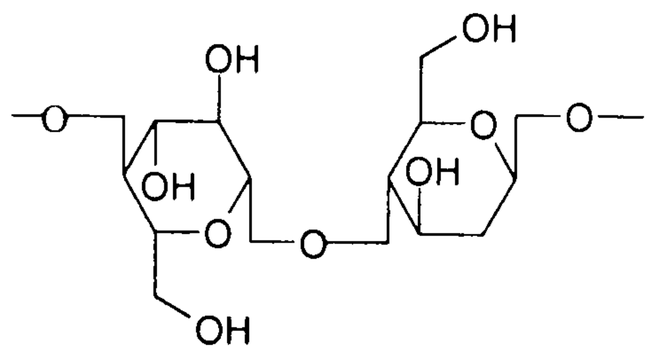

Figure 3.6: Structure of cellulose.

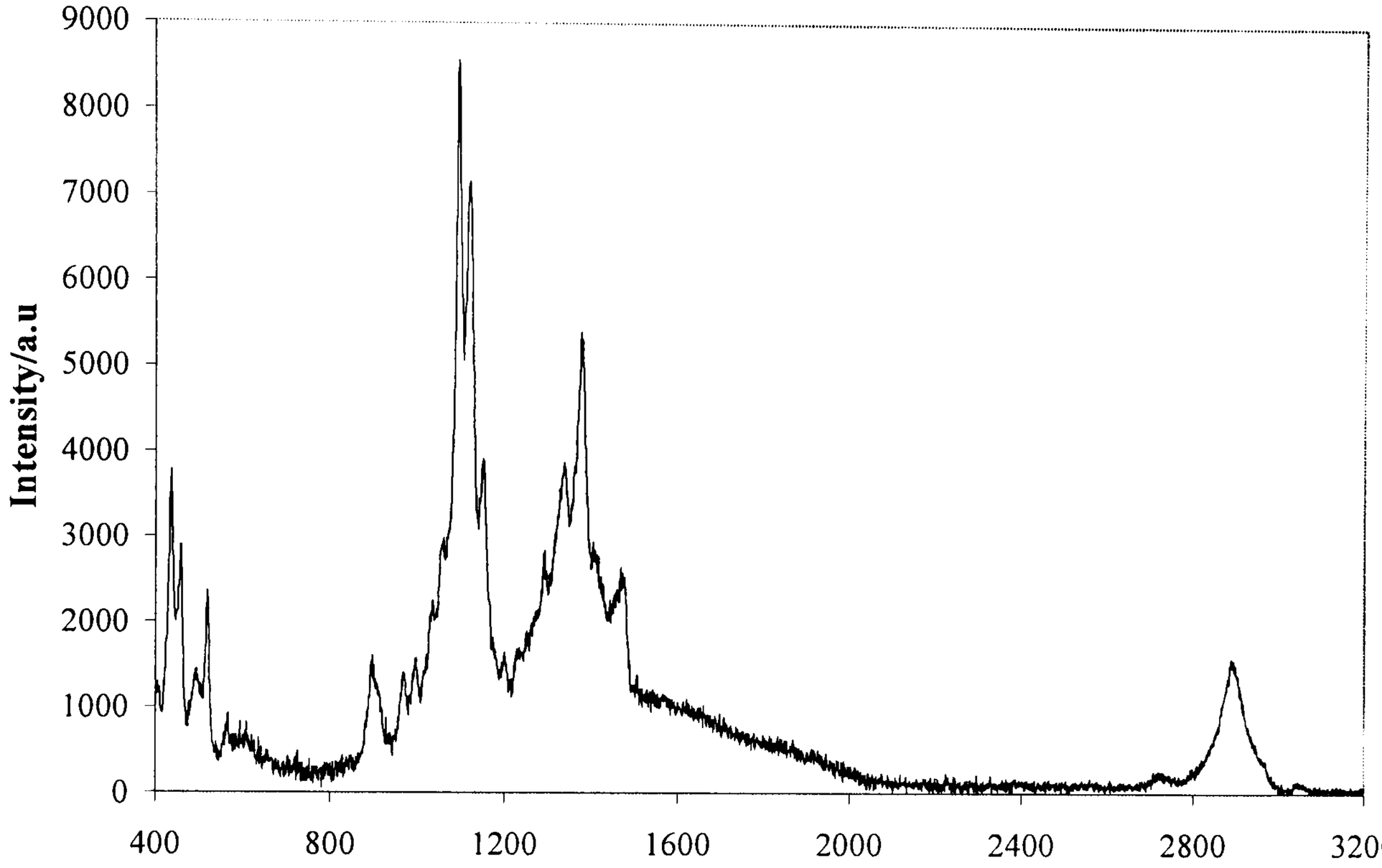

Figure 3.7: Raman spectrum of cellulose.

Table 3.4: The principal vibrational modes of cellulose within the mapping spectrum window.

Peak Position cm^{-1}	**Movement**	**Peak Position cm^{-1}**	**Movement**
896.18	Symmetric COC stretch	1377.18	Symmetric CO_2^- Stretch
1094.87	C-C Stretch	1469.29	OCH_2 Deformation
1334.05	CH Deformation		

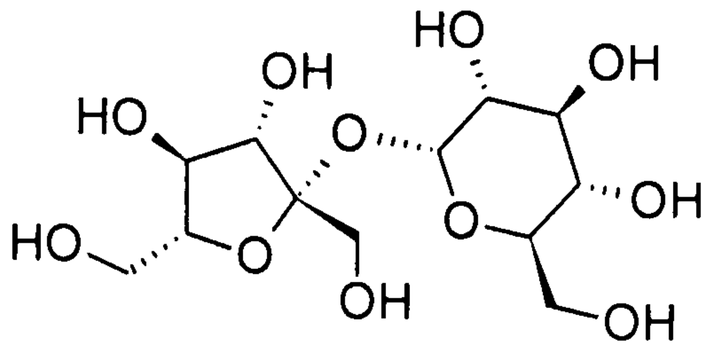

Figure 3.8: Structure of sucrose.

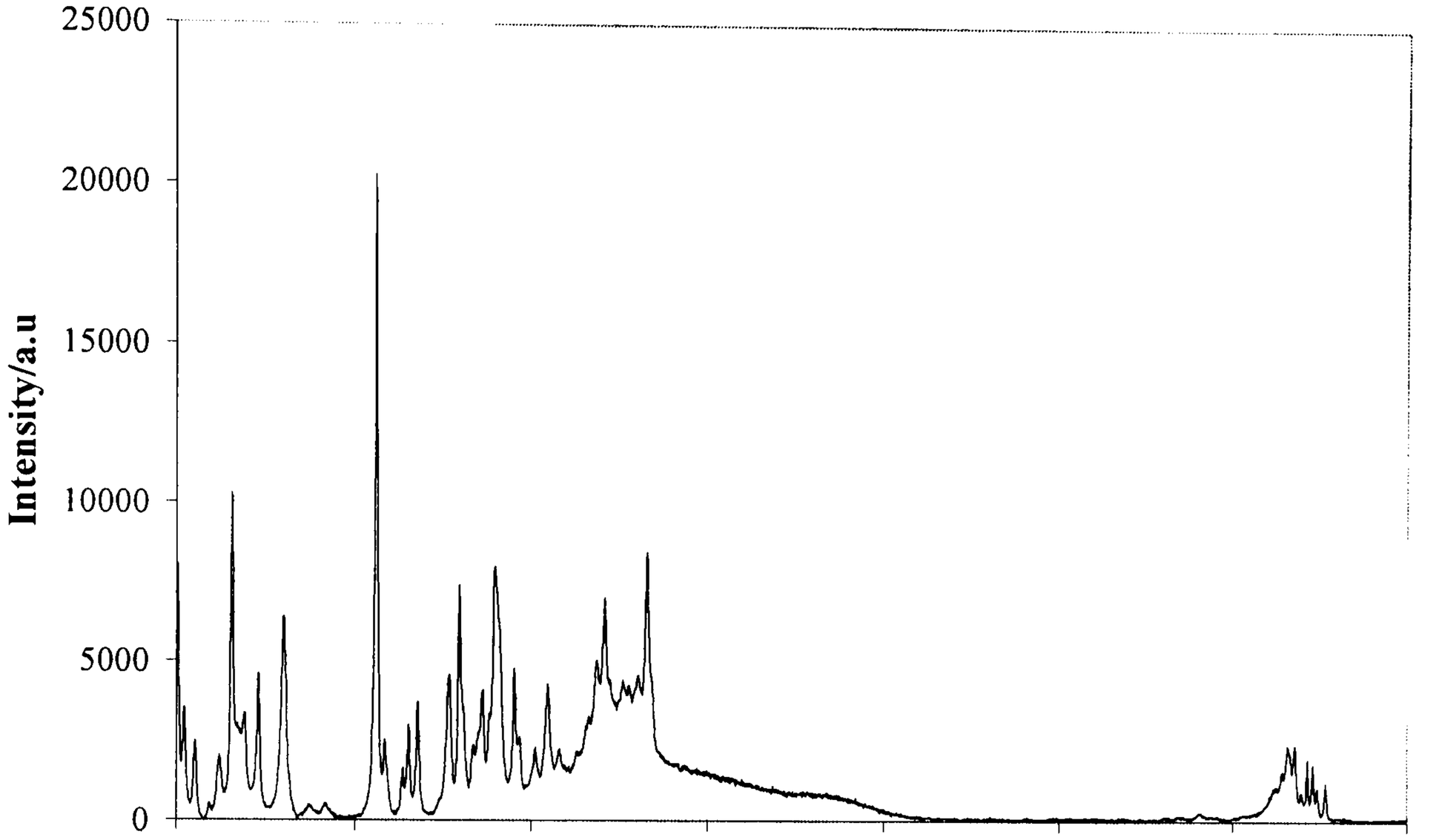

Figure 3.9: Raman spectrum of sucrose.

Table 3.5: The principal vibrational modes of sucrose within the mapping spectrum window.

Peak Position cm^{-1}	**Movement**	**Peak Position cm^{-1}**	**Movement**
847.20	C-C Skeletal Stretch	1088.44 – 1160.07	C-C Stretch
867.67-921.04	Symmetric COC Stretch	1364.76	Symmetric CO_2^- Stretch
1013.87-1035.07	Ring Vibration		

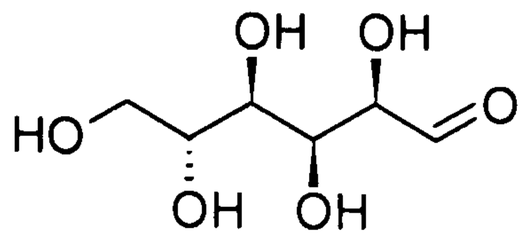

Figure 3.10: Structure of glucose.

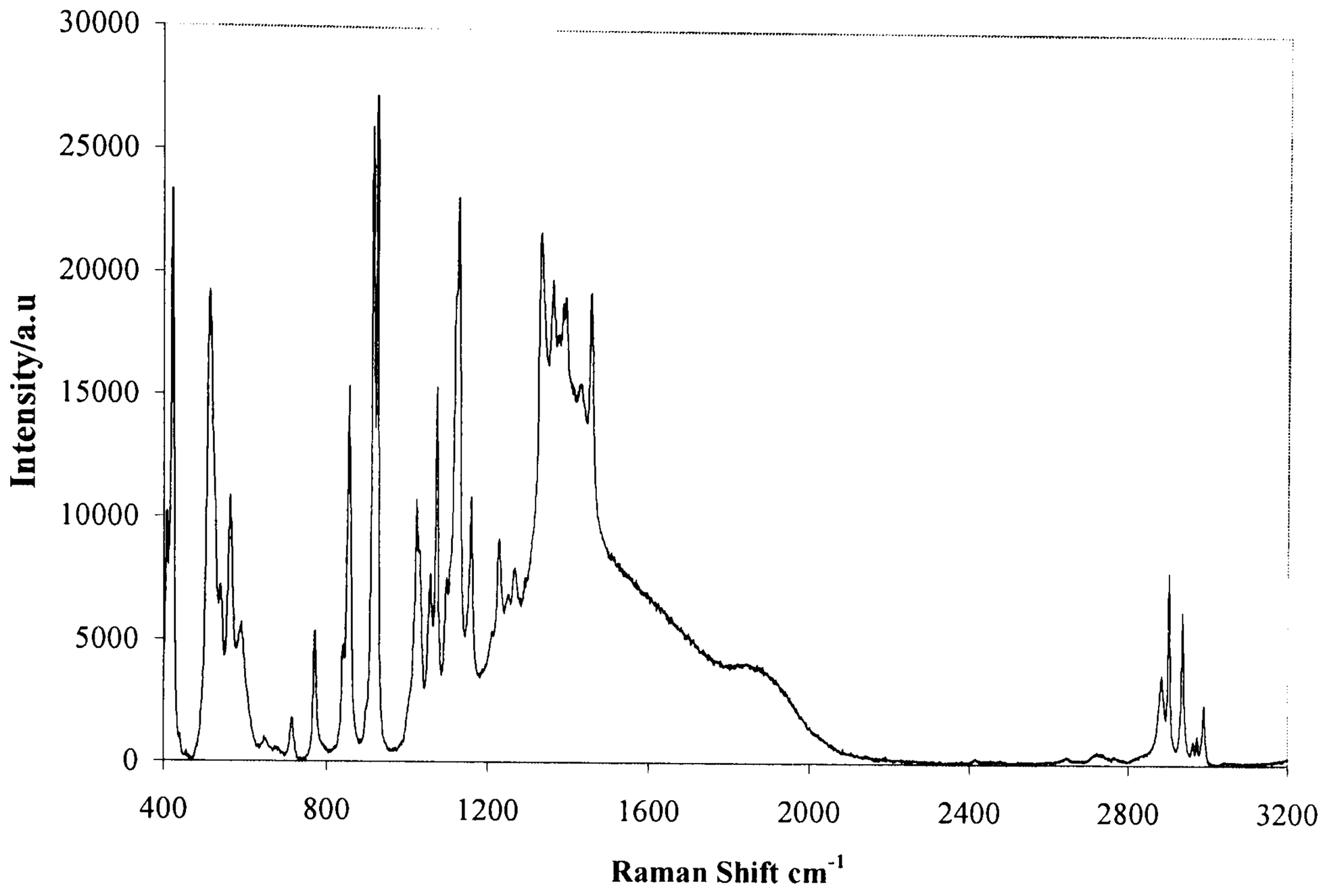

Figure 3.11: Raman spectrum of glucose.

Table 3.6: The principal vibrational modes of glucose within the mapping spectrum window.

Peak Position cm^{-1}	**Movement**	**Peak Position cm^{-1}**	**Movement**
855.86	C-C Skeletal Stretch	1022.53 – 1126.33	C-C Stretch
924.53	Symmetric COC Stretch		

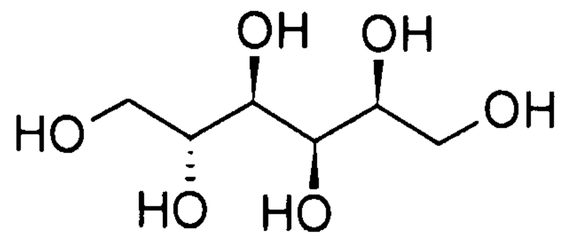

Figure 3.12: Structure of sorbitol.

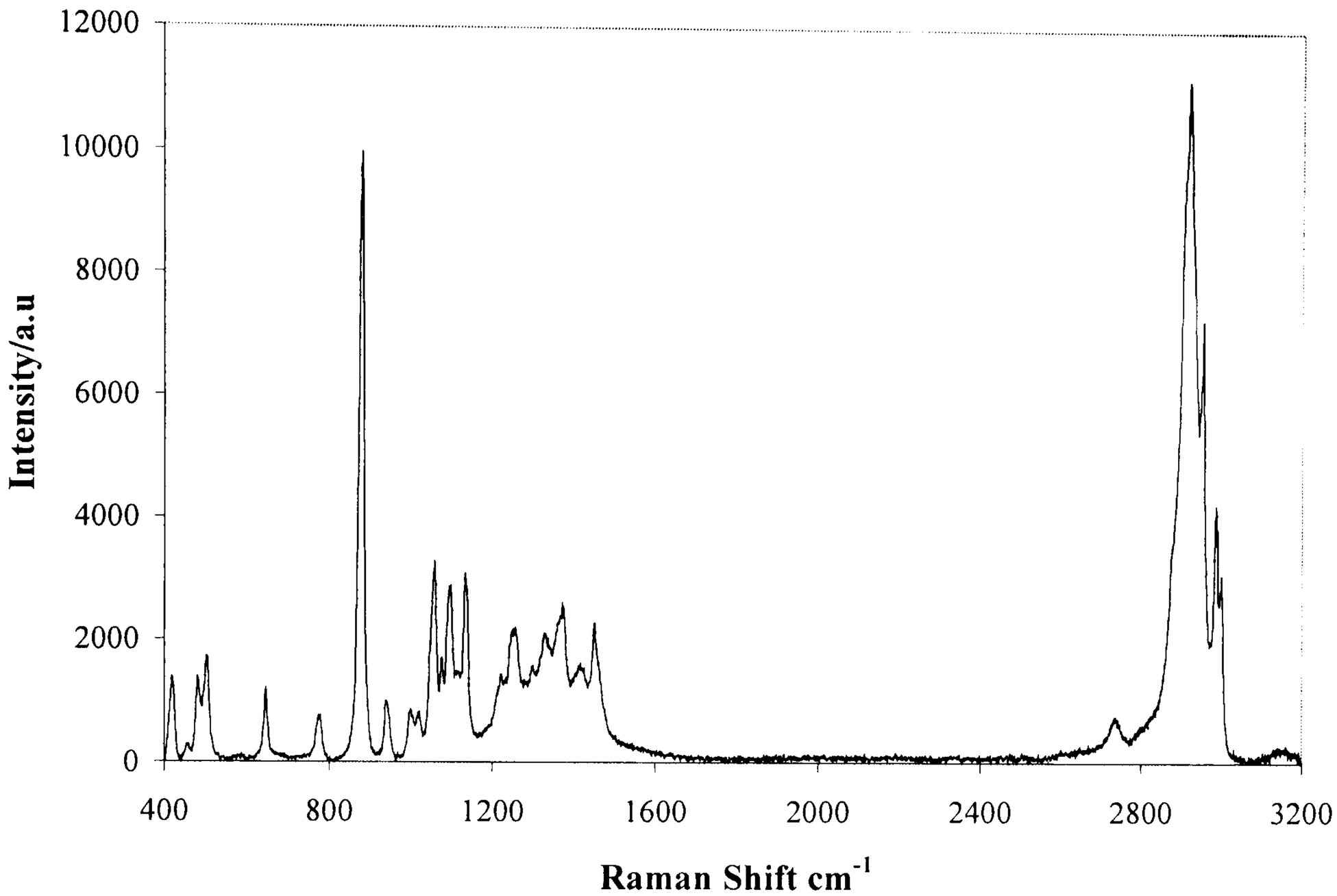

Figure 3.13: Raman spectrum of sorbitol.

Table 3.7: The principal vibrational modes of sorbitol within the mapping spectrum window.

Peak Position cm^{-1}	**Movement**	**Peak Position cm^{-1}**	**Movement**
880.42	C-C Skeletal Stretch	1020.6 – 1132.24	C-C Stretch

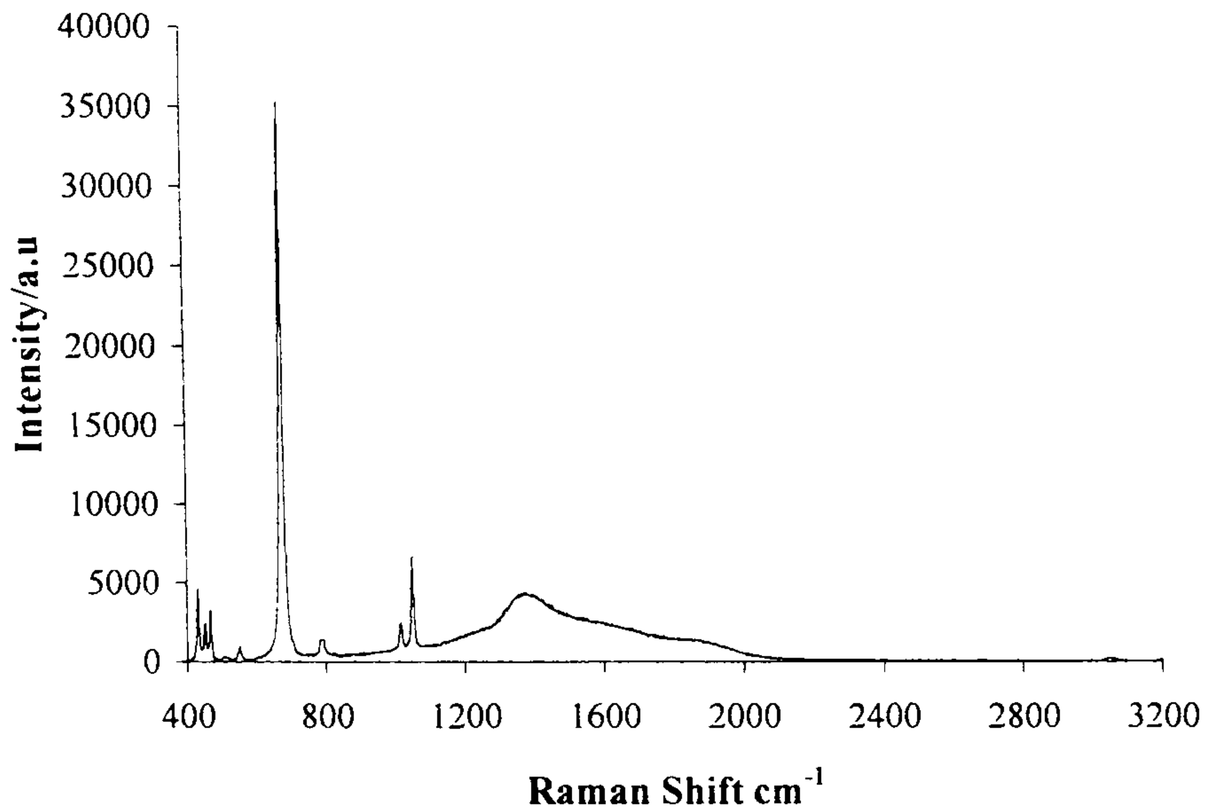

Talcum Powder

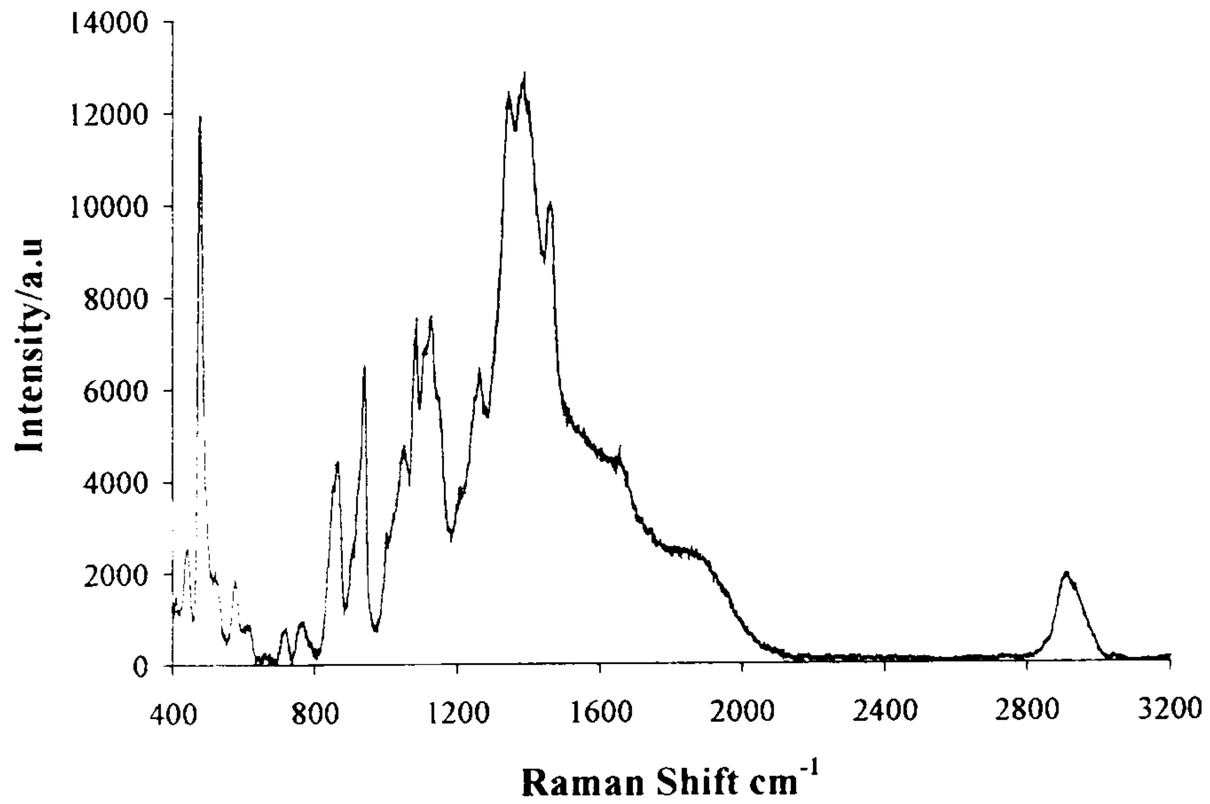

Flour

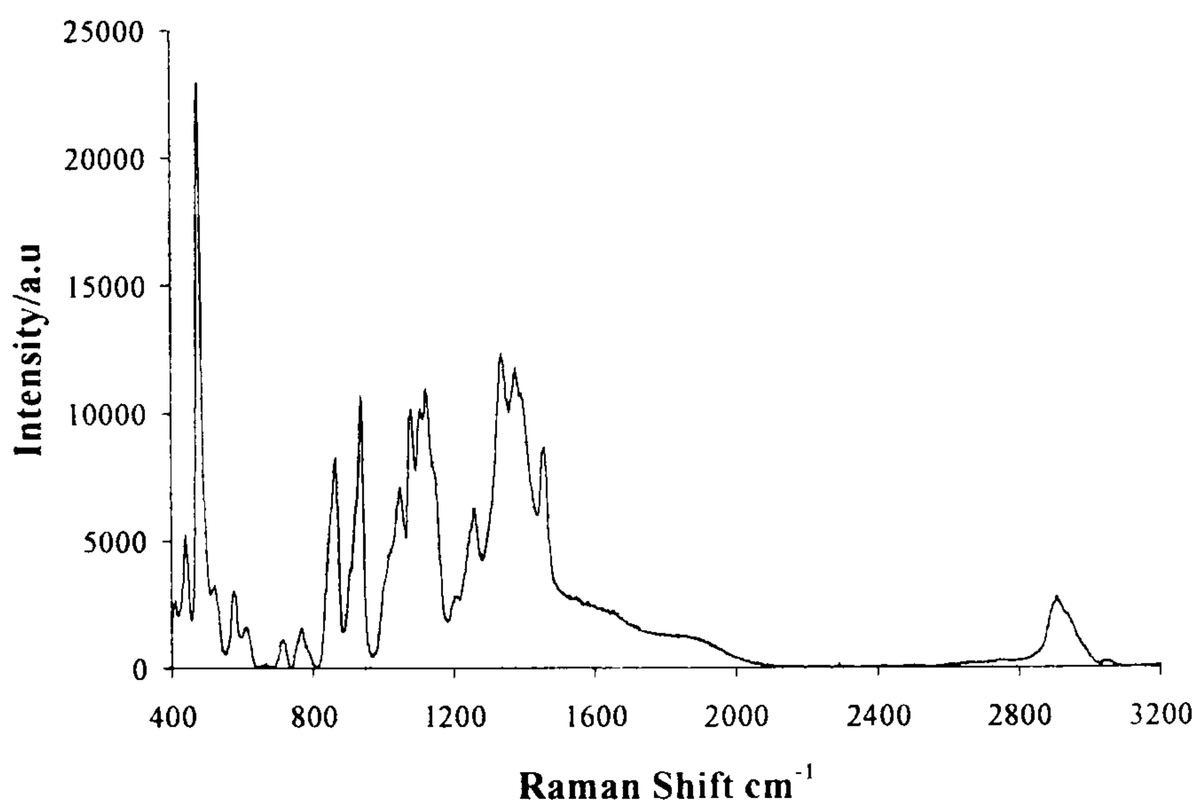

Corn Flour

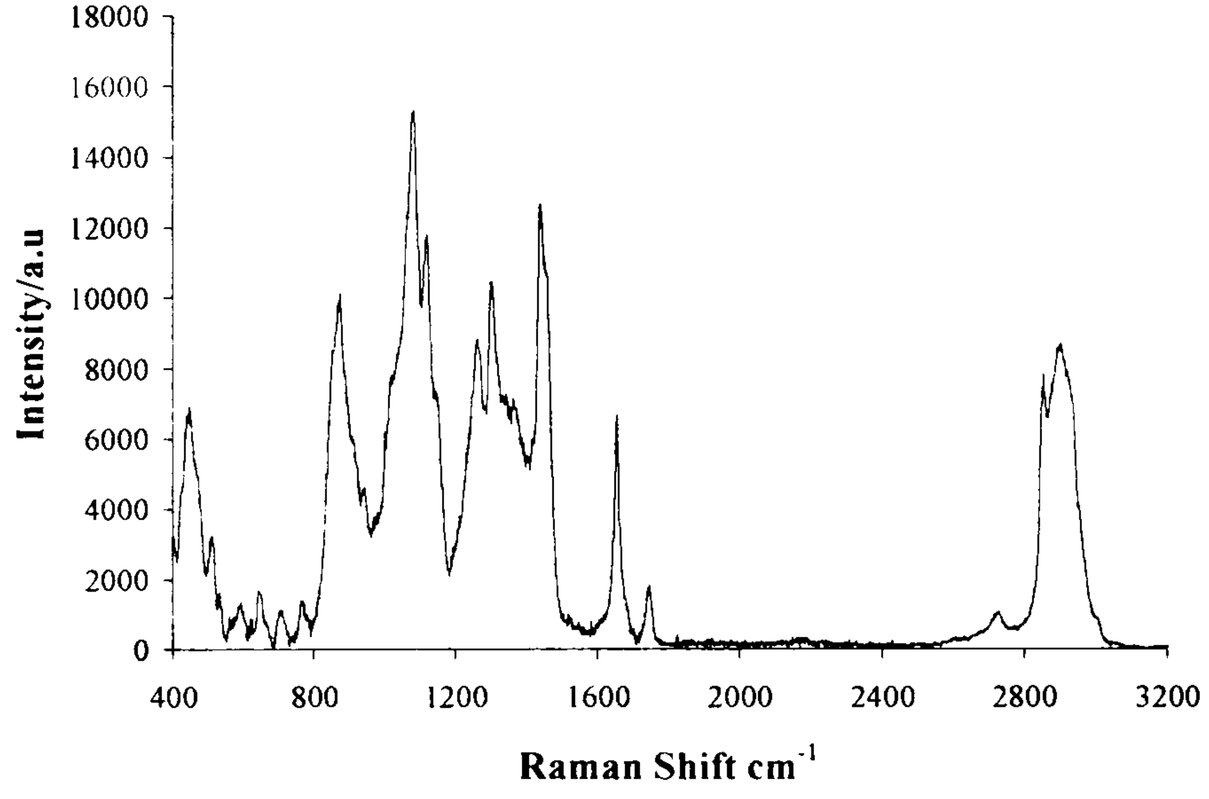

Powdered Milk

Figure 3.14: Other excipients considered but not found within the tablets analysed.

3.3.3 Seized Tablets Demographic

A total of seven batches of tablets were received from Belgium. In some instances multiple sub-batches of the batches were provided and had been categorised with a secondary number, e.g. 4-01. Each batch and sub-batch comprised 20 tablets individually stored in a plastic tube and marked with a unique identifier. All 260 tablets were analysed in sequential order with a batch of 20 tablets being completed on the same day. Table 3.8 provides a summary of the tablets supplied including information on the numbering system, logo, colour, shape and scoring, other observations and the average phenethylamine content (mg) as determined by GC/MS analysis by the partner laboratory in Ghent, Belgium.

3.3.4 Seized Tablets Peak Position Data

Table 3.8 shows the wide variety of tablets supplied. Despite the range of colours, shapes and particle packing of the tablets, these characteristics do not appear to have impeded the collection of Raman spectra. Attempts were made to try and obtain an average particle size for the tablet components using optical imaging microscopy to match to the incremental step of the motorised stage. However, following the removal of any loose particulate material from the surface, microscopic examination showed the particles to be smeared over each other and not as discrete entities. This smearing is thought to arise from the pill pressing mechanism used to cast the tablets.

Bell *et al* (2004) reported an average particle size of 40 μm in seized tablets but our loose particulate material measurements indicated an average particle size of 15 μm (range 1 – 35 μm). An incremental step size of 30 μm was chosen as a compromise to offset the desire to collect detailed spectra from the surface verses the additional time it would take to analyse the defined areas. Reducing the incremental step any further increases the overall collection time considerably. For example a 20 μm incremental step on a 0.16 mm^2 area has a 12 minute collection time period, totalling 36 minutes per tablet more than double the 30 μm incremental step, thereby reducing the throughput of tablets and the efficiency of the system.

Table 3.8: Summary table of the supplied tablets physical and chemical characteristics.

Batch/Sub-batch/Tablet number	Logo	Colour	Shape/ Scoring	Other Observations	Average phenethylamine content (mg)
1/-/0001-0020	AJ	White	Very flat surface, no scoring	Crumbly, softly packed particles, white light penetration	37.23 ± 1.70
2/-/0051-0070	AJ	White	Very flat surface, no scoring	Crumbly, softly packed particles, white light penetration	50.43 ± 3.73
3/-/0001-0020	Bacardi	Purple	Very flat surface, no scoring	Closely packed particles, very hard tablet, no white light penetration	22.57 ± 1.80
4/01/0001-0020 4/02/0001-0020 4/03/0001-0020	Flying Bird	White with brown and greys flecks	Curved surface, scoring on one side	Tightly packed particles, no white light penetration	18.18 ± 1.36 17.67 ± 0.39 18.17 ± 5.67
5/01/0001-0020 5/02/0001-0020	Armani	White flecked	Flat surface, scoring on one side	Closely packed particles, hard tablet, no white light penetration	6.09 ± 0.70 5.96 ± 0.73
5/03/0001-0020 5/04/0001-0020 5/05/0001-0020	Lips	White	Domed surface, no scoring	Slightly crumbly, soft tablet, white light penetration	23.07 ± 1.90 20.10 ± 3.34 21.88 ± 3.60
6/--/0001-0020	Dolphin	Purple	Flat surface, scoring on one side	Closely packed particles, hard tablet, no white light penetration	12.05 ± 1.17
7/01/0100-0119	Bird	Green	Flat surface, no scoring	Closely packed particles, no white light penetration	31.76 ± 4.19

Raman spectra (Figure 3.15) were captured from three areas on each tablet and the previously described data processing procedures undertaken. The extracted peak position data was used to compare the tablet peak positions with the reference standards peak positions (Table 3.9). The strongest peaks from the reference standards were chosen for comparison with the seized tablet spectra. Using this method the presence of a phenethylamine derivative, i.e. Ecstasy, could be detected. However, the peak resolution of the spectra collected from the tablets is less than the reference standards spectra due to a combination of the chosen magnification, the accumulation time per spectrum and the impurity of the sample.

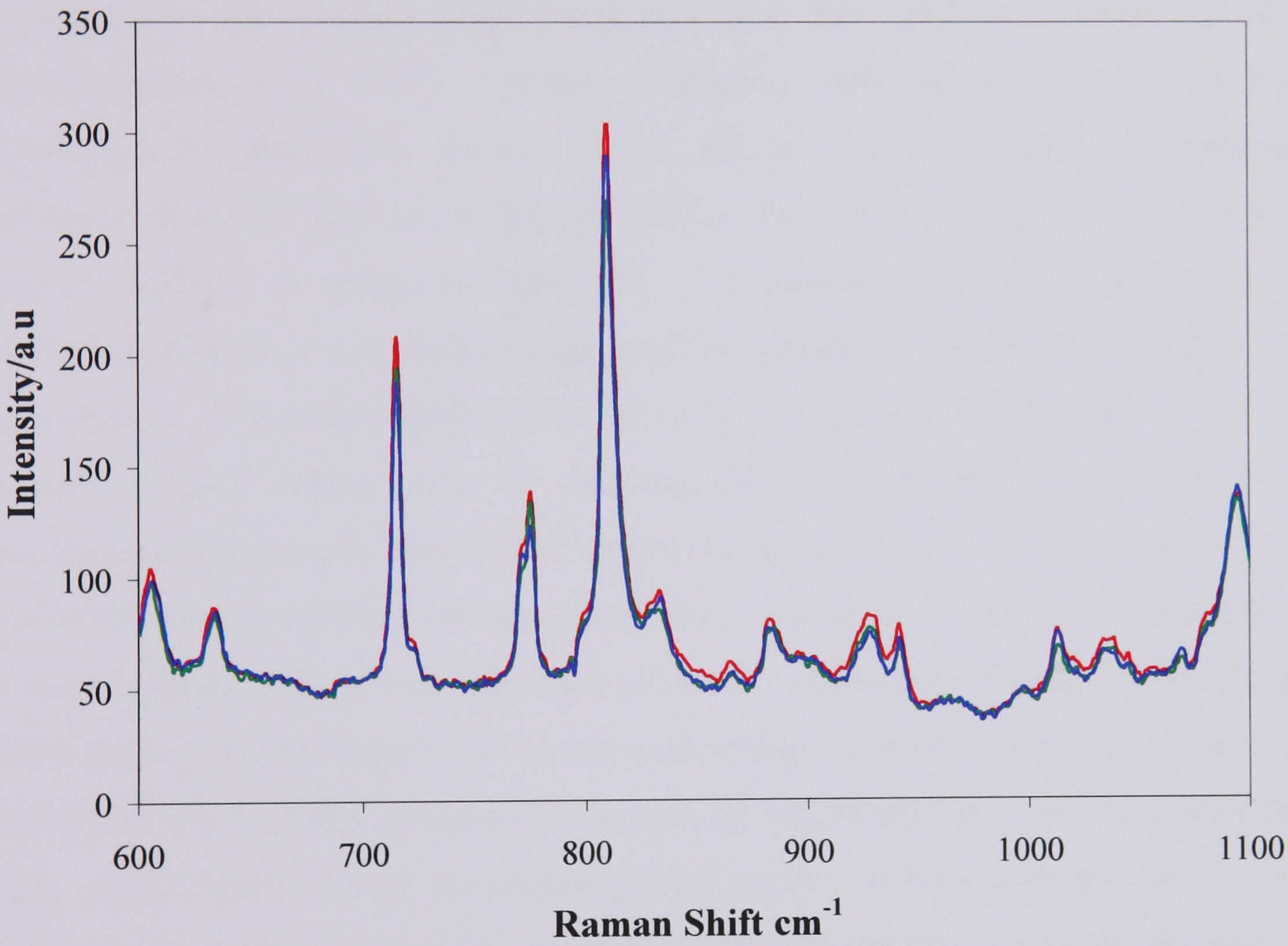

Figure 3.15: Averaged Raman spectra collected from 3 areas on tablet 022055. (Area A – Red, Area B – Blue, Area C – Green).

Table 3.9: Summary table of the reference samples peak positions for comparison with the seized tablets.

Reference Samples	Peak Positions cm^{-1}
MDMA	809.34
MDA	811.54
MDEA	812.28
Sucrose	847.20
Sorbitol	880.48
Glucose	924.53
Cellulose	1094.87

Consequently, the weaker peak resolution and the systematic errors of the instrumentation (± 2 cm^{-1}) preclude distinction between the spectra of the phenethylamine derivatives present in the tablets. In other words the spectral similarities between MDMA, MDA and MDEA when they are present as a mixture make it difficult to assign the presence of a specific drug. This difficulty is compounded by the crude methodology used to manufacture the tablets, resulting in the presence of multiple derivatives rather than simply MDMA itself which is typically sought. Additionally, the smearing effect of the tablet casting machines may amalgamate the particles further complicating the spectral representation. Bell *et al* (2000a) used a digital spectral subtraction method to compare the components of seized tablets with known reference standards. However, if components of the tablets share common functional groups subtracting the spectra out could lead to a mis-identification of the components present by artificially removing or excluding them. Additionally, visual comparison of the spectra without consideration of the absolute peak position can result in mis-assignment of the drug components present. Figure 3.16 shows three histogram plots from the three areas of tablet 1 Batch 5/01. All three graphs show the presence of and provide a visual representation of the spread of the phenethylamine derivatives peak positions detected within a single tablet. Consequently, the phenethylamine derivatives peak positions were averaged to facilitate comparison with the identified excipients [Bell *et al* (2000b), Ryder (2002)]. Interestingly the disparities in peak positions in the phenethylamine

derivatives were not observed with the excipients. It is thought this is related to the quality controlled production of these by licensed manufacturers.

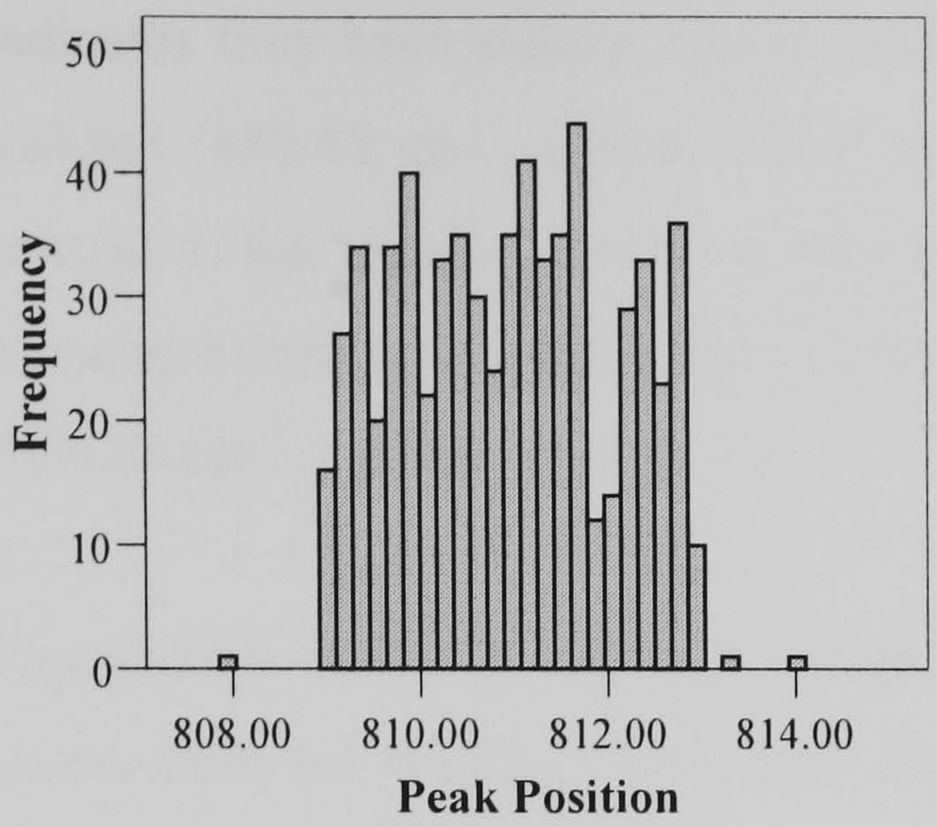

Area A: Mean 810.94 cm^{-1}, σ 1.12

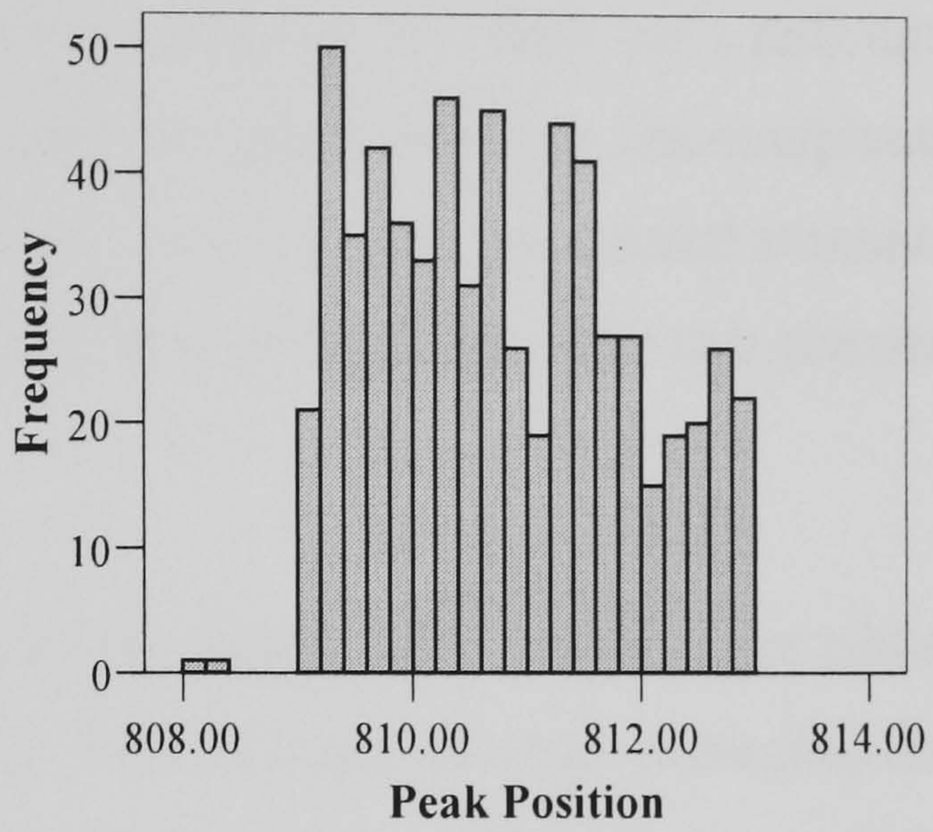

Area B: Mean 810.78 cm^{-1}, σ 1.10

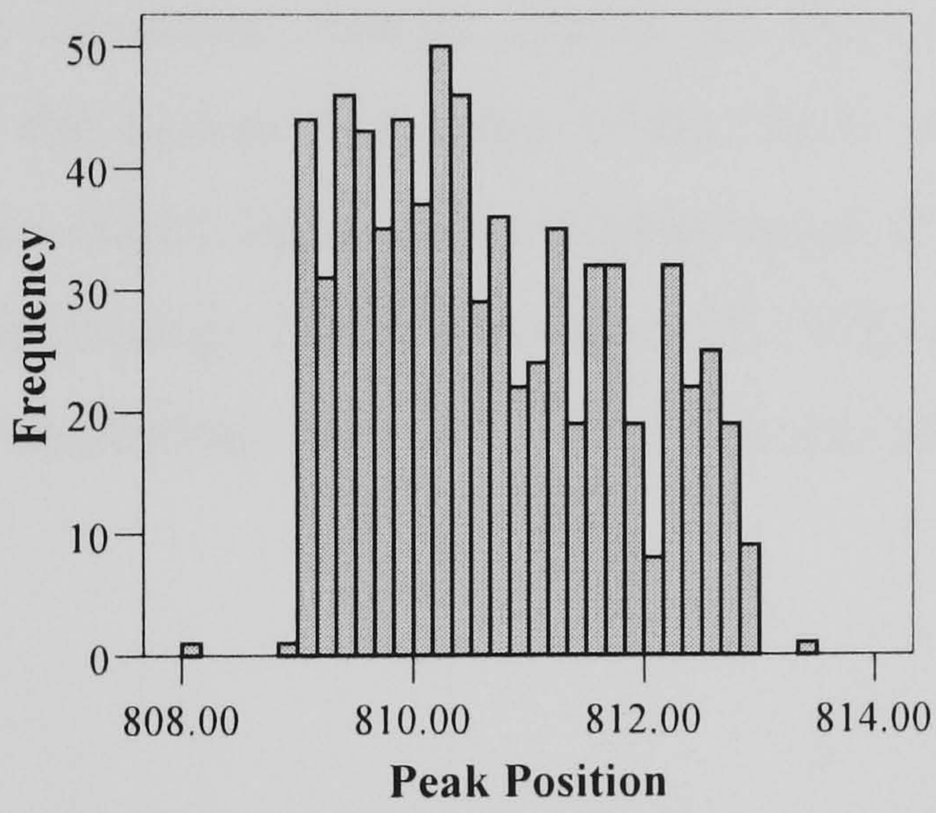

Area C: Mean 810.78 cm^{-1}, σ 1.10

Figure 3.16: Histogram plots of the spread and frequency of the phenethylamine peak position (cm^{-1}) across 3 areas (A, B, C) of tablet 1 in Batch 5-01.

3.3.5 Variations Within Tablets From the Same Batch

Figure 3.17 shows the average excipient peak intensity for three sub-batches (5/03, 5/04 and 5/05) normalised to 100%. All of the tablets in these batches have the same logo, physical dimensions and scoring. Comparison of the bar charts in Figure 3.17 indicates they have similar spectral intensities of cellulose (1094.87 cm^{-1}, red) and sorbitol (880.48 cm^{-1}, green) which can be taken as proportional to the excipients content of the tablets. However, sub-batches 5/04 and 5/05 also have small amounts of sucrose (847.2 cm^{-1}, blue) present but none of these sub-batches have any glucose (924.53 cm^{-1}, yellow) present.

Figure 3.18 shows the average phenethylamine derivative peak intensity per tablet across three sub-batches (5/03, 5/04 and 5/05). This was calculated by averaging the responses and standard deviations of the three areas of each tablet. The error bars represent the error of uncertainty. The response per tablet is variable across each batch but this is a consistent feature across all three sub-batches. This data tentatively supports the notion that these tablets have originated from the same clandestine laboratory based upon the phenethylamine derivative content and the cellulose and sorbitol content. The confirmatory GC/MS analysis results (Table 3.8) also corroborate the similarities between the sub-batches of average phenethylamine derivative content.

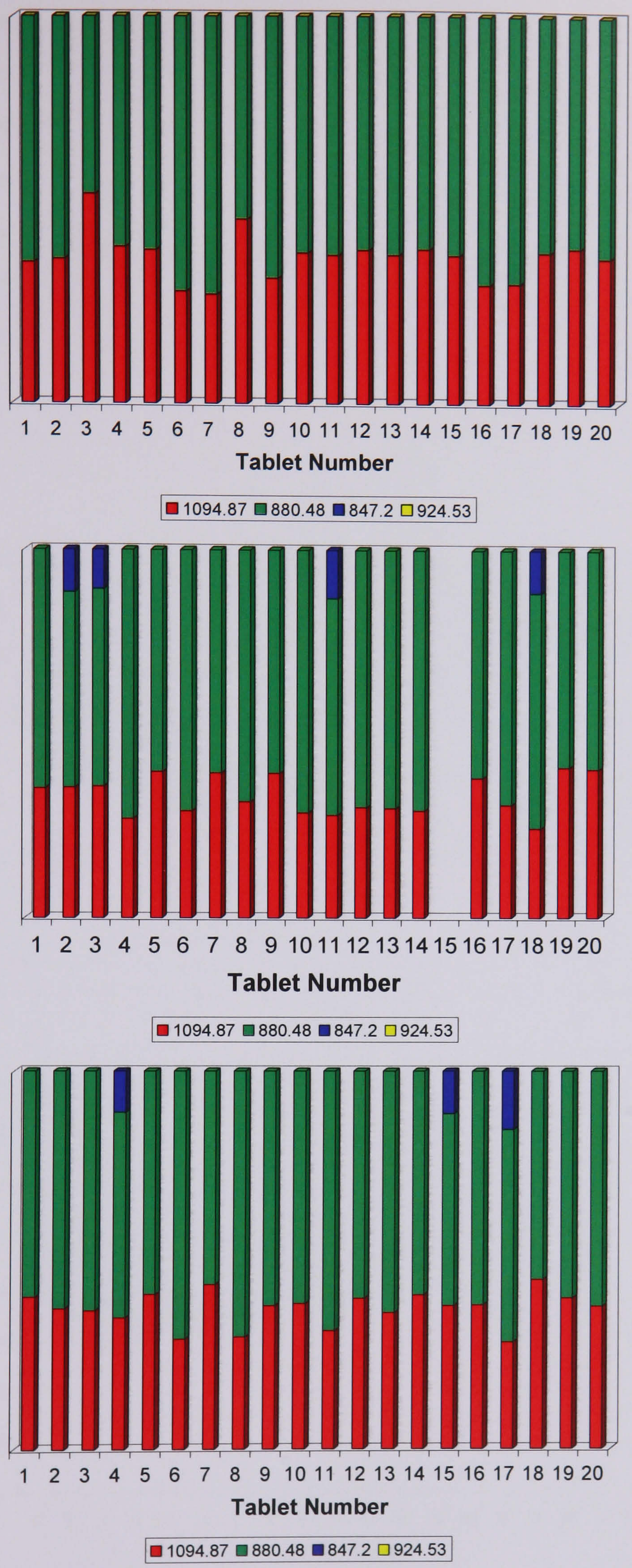

Figure 3.17: Average excipients(s); cellulose (red), sorbitol (green), sucrose (blue), glucose (yellow) peak intensity bar charts for Batches 5/03 (top) 5/04 (middle) and 5/05 (bottom) per tablet. Calculated by normalizing the average peak height for each excipient to 100%.

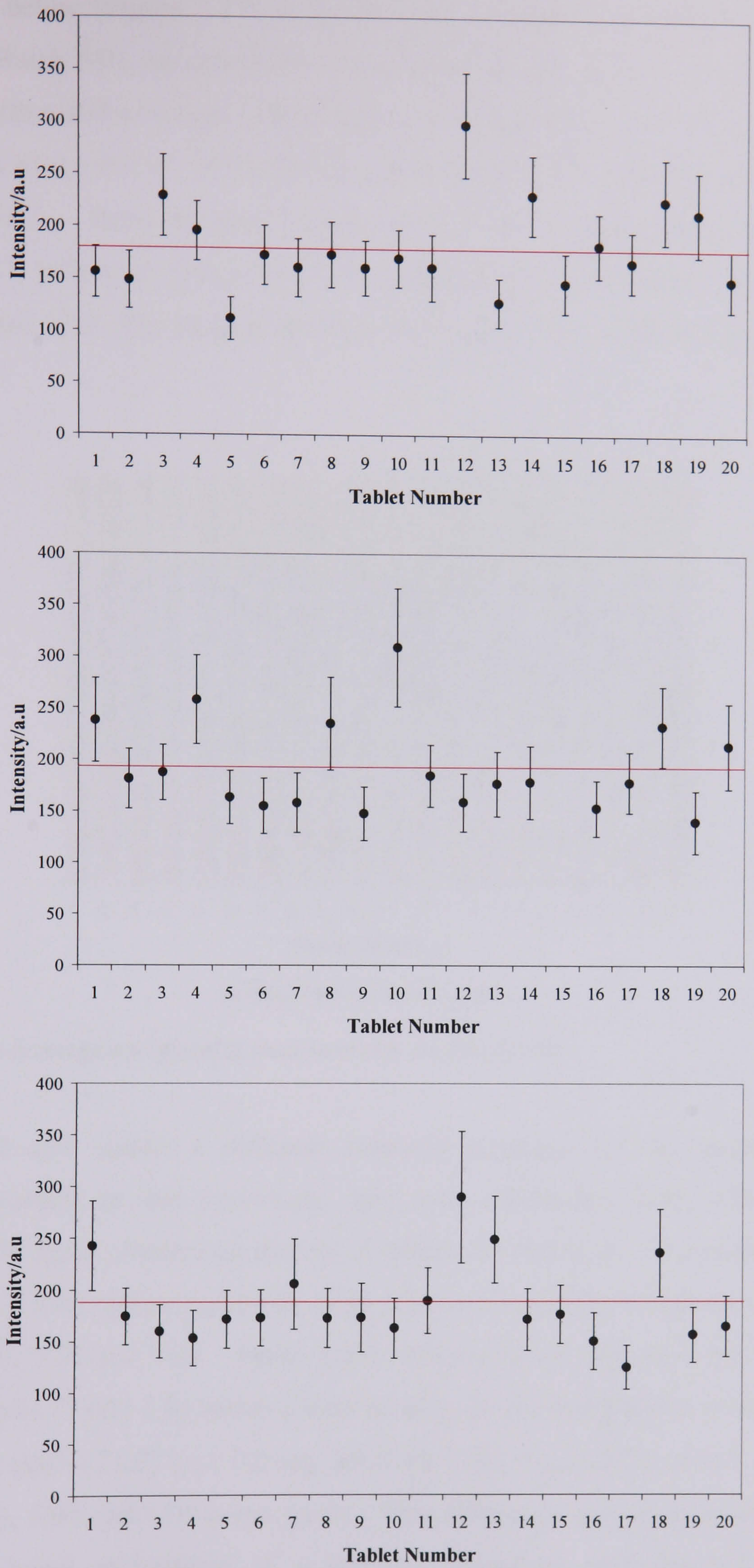

Figure 3.18: Average phenethylamine derivative peak intensity tables for Batches 5/03 (top) 5/04 (middle) and 5/05 (bottom) per tablet. The red line represents the average intensity for all of the tablets. The error bars represent the error of uncertainty.

The figure below (Figure 3.19) is the average excipients intensity, normalised to 100%, for Batch 5/01, recovered from the same location as Batches 5/03, 5/04 and 5/05 but, with a different logo. From the excipients intensity below the proportional components of the Batch 5/01 tablets are very different to those from Batches 5/03, 5/04 and 5/05. There is more sucrose (847.2 cm^{-1}, blue) present and glucose (924.53 cm^{-1}, yellow) is present in all of the tablets which was absent from Batches 5/03, 5/04 and 5/05. The proportions of each excipient are similar across the tablets.

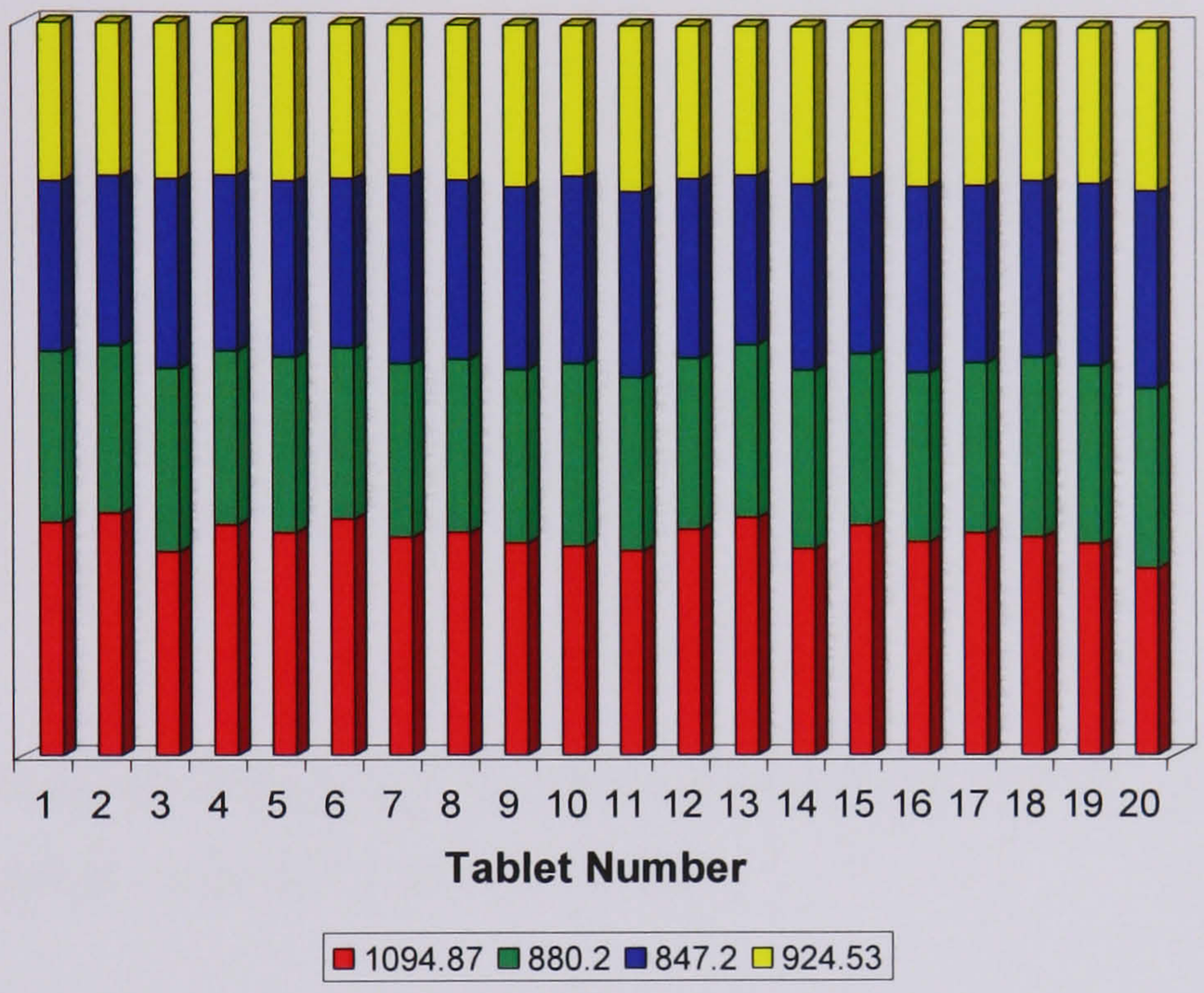

Figure 3.19: Average excipient(s) peak intensity for Batch 5/01.

Figure 3.20 also shows a different intensity response for the phenethylamine derivative content to that previously seen with sub-batches 5/03, 5/04 and 5/05 (Figure 3.18) again confirming that these tablets are different. The majority of the tablets have a lower phenethylamine derivative peak intensity than those seen in sub-batches 5/03, 5/04 and 5/05. Again, these differences are supported by the GC/MS analysis results (Table 3.8) which shows an average phenethylamine content of 6.09 (± 0.70) mg versus 23.07 (± 1.90) mg, 20.10 (± 3.34) mg, 21.88 (± 3.60) mg for sub-batches 5/03, 5/04 and 5/05 respectively. This difference may arise from; the tablet production being undertaken in a separate laboratory and the batches being amalgamated prior to distribution, the tablets being made at different times during

the laboratory lifespan reflecting the availability of the excipients and the batch of phenethylamine derivative produced at that time or two separate production lines operating concurrently within the laboratory manned by different individuals.

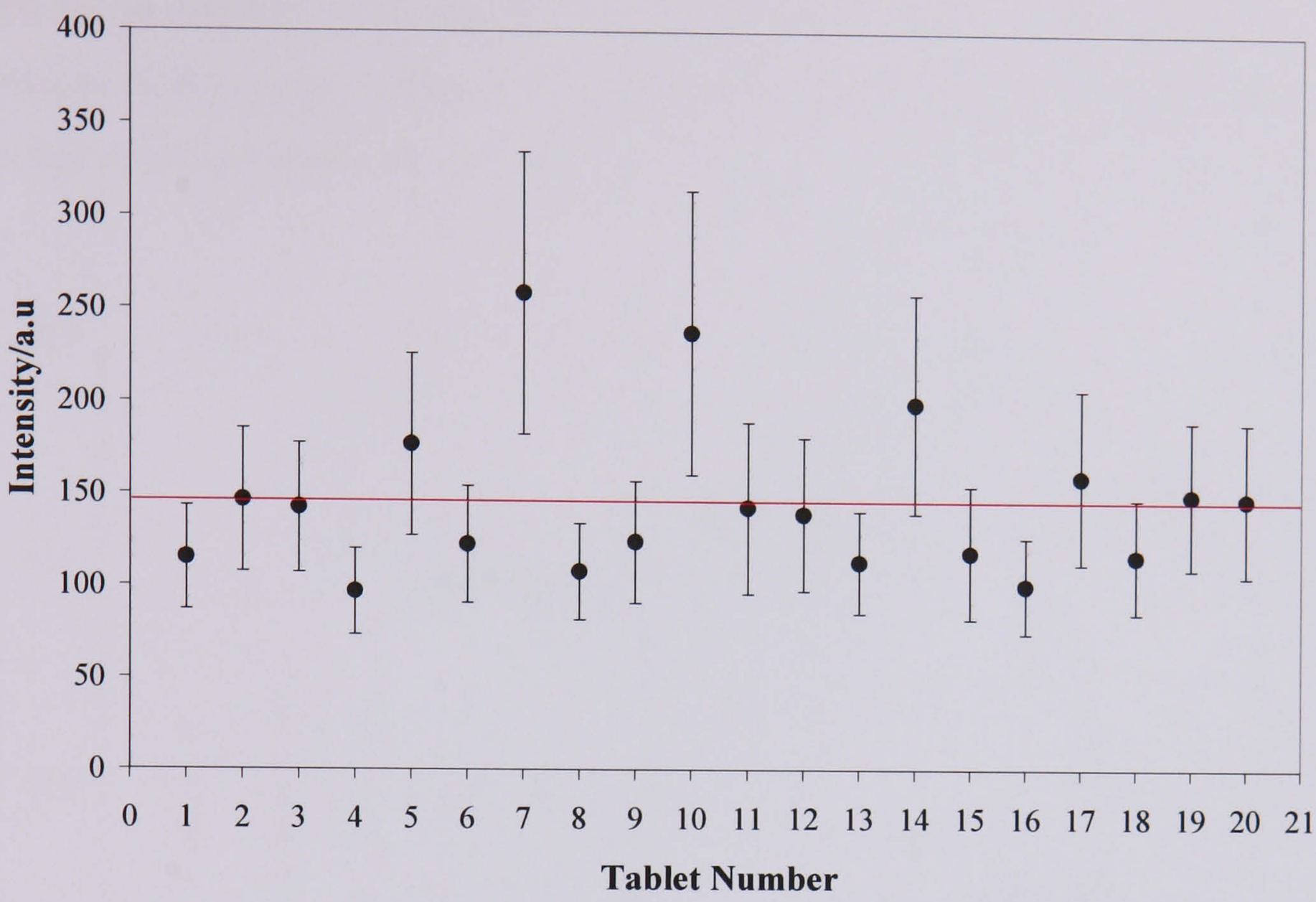

Figure 3.20: Average phenethylamine derivative peak intensity for Batch 5/01. The red line represents the average intensity for all of the tablets.

3.3.6 Between Tablet Batches

Figure 3.21 shows the average peak positions for the phenethylamine derivatives and illustrates the influence of the intrinsic instrumental errors in the peak position. Trends within the data can be observed within the sub-batches of 4 (4/01, 4/02, 4/03), 5 (5/01, 5/02) and 5 (5/03, 5/04, 5/05). Tablets in each of these sub-batches share the same logo and were recovered from the same location. These observations are also evident in Figure 3.22 comparing the average intensity of the combined phenethylamine Raman peak responses against the average MDMA content (mg) as determined by GC/MS analysis for each batch of tablets. Again there appear to be groupings of the data where the tablets are sub-batch related but there are no obvious relationships between the different batches of tablets. However, if the error of uncertainty is considered there is shared overlap across all the batches implying the

batches may not be as discrete as initially believed. It should be noted that more than the 20 tablets analysed by Raman spectroscopy were analysed for the GC/MS results. However, all of the 20 tablets were analysed as a composite of each batch and sub-batch of tablets. Although, caution should be applied because the intensity units quoted are an arbitrary scale and do not correlate with absolute concentration and can be influenced by crystal orientation in relation to the incident laser beam which will effect the observed spectrum intensity.

.

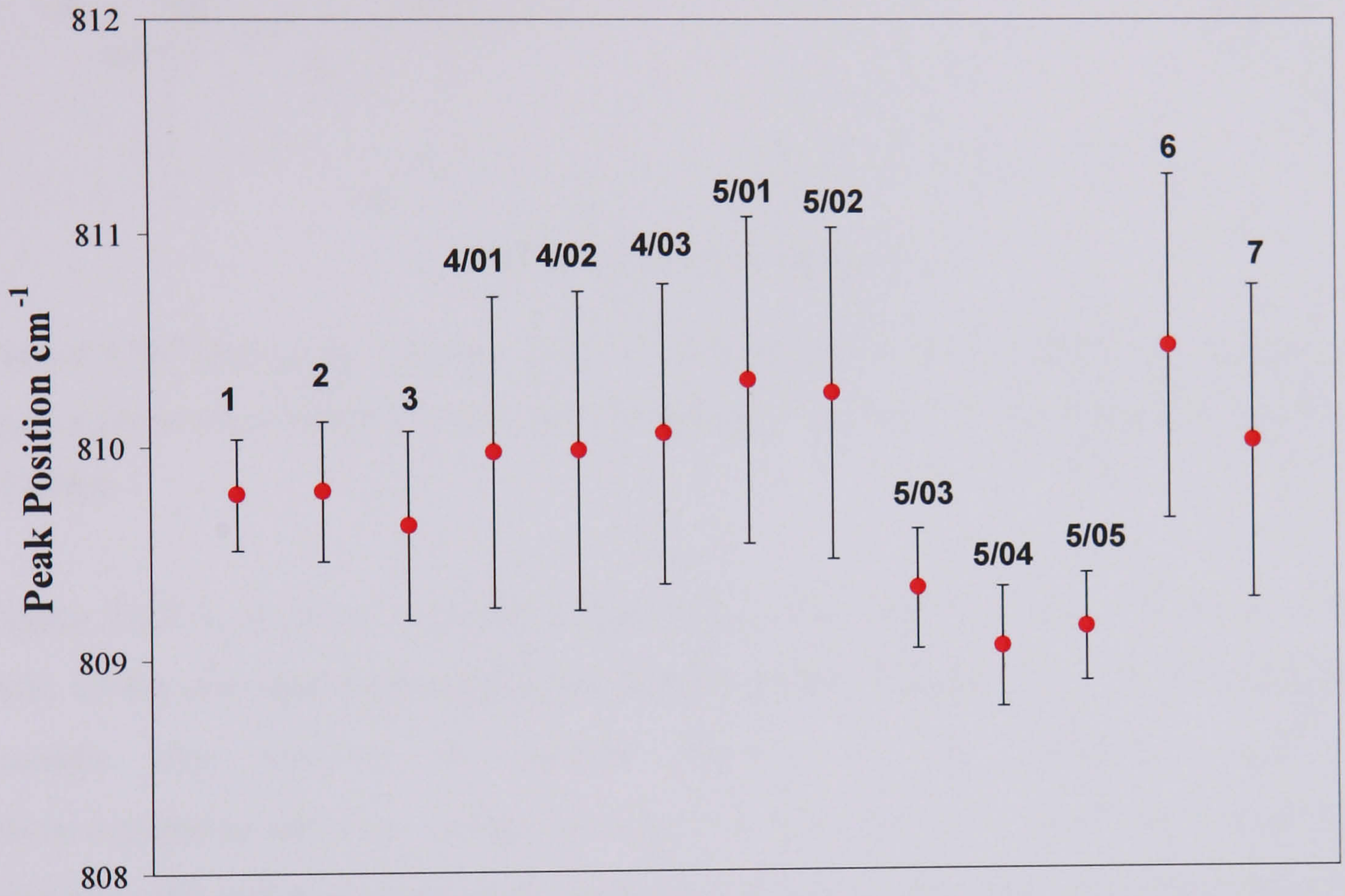

Figure 3.21: Average phenethylamine derivatives peak position for each batch of 20 tablets.

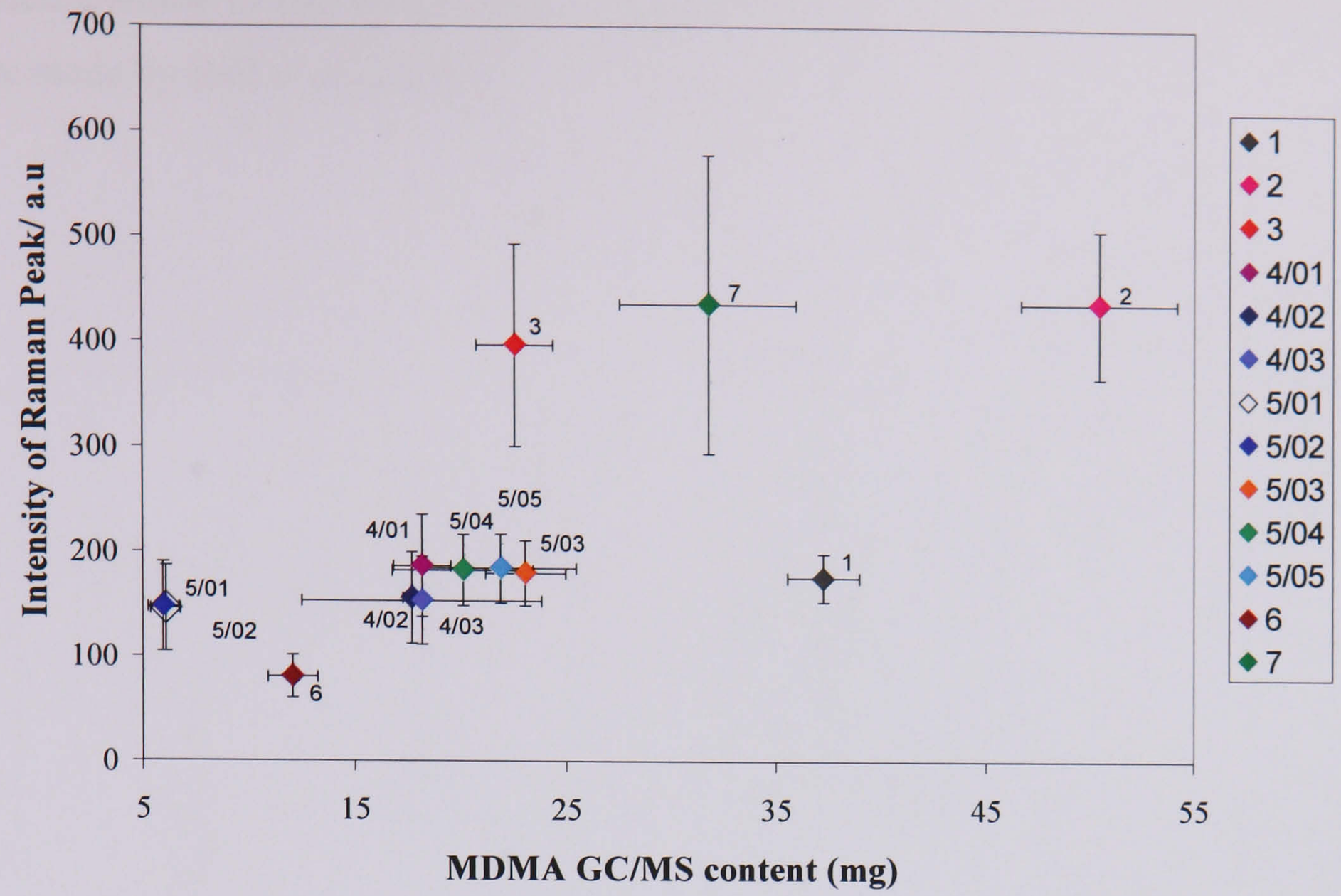

Figure 3.22: The average intensity of the combined phenethylamine Raman peak responses against the average MDMA content (mg) as determined by GC/MS analysis for each batch of tablets.

Figure 3.23 A, B and C provides information on the batch to batch variations in the ratio of the averaged phenethylamine/cellulose peak intensity data. Each histogram records the number of tablets found with a particular ratio of phenethylamine/cellulose composition and is overlaid with Gaussian curves that represent the mean and standard deviation of the same data. From the data the histograms show considerable variation in the ratio of drug/excipients across the batches which further supports the previous observations that these seized batches are not related. The sub-batch variability however, is smaller and similarities can be drawn from the ratios. For example Batch 5 subgroups 5/03, 5/04 and 5/05 all have similar mean values and frequency of tablets with the same ratios further supporting the previous evidence that these tablets stem from the same batch beyond the physical appearance of the tablet. The approximately normal distribution about the mean values for each batch further supports that the batches do not contain a mixture of tablets from different sources. This observation is based upon the combined

phenethylamine to one excipient ratio presence in the tablet. Similar observations were made by Bell *et al* (2000b).

A

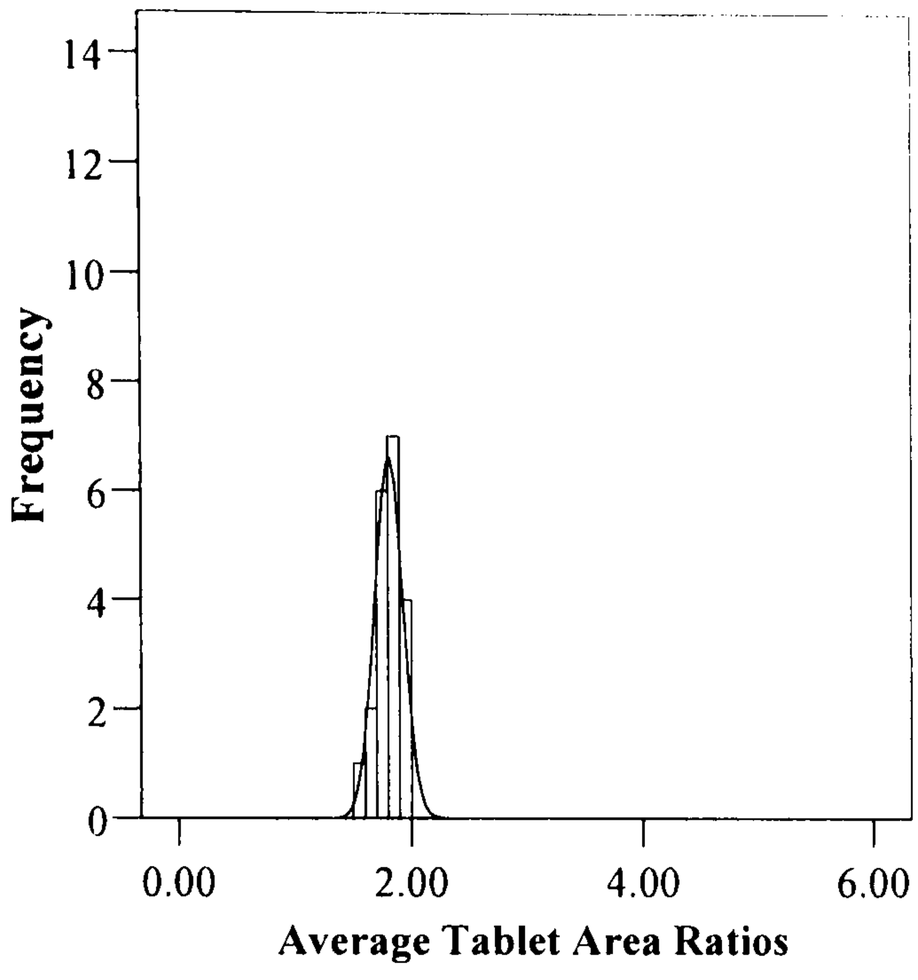

Batch 01

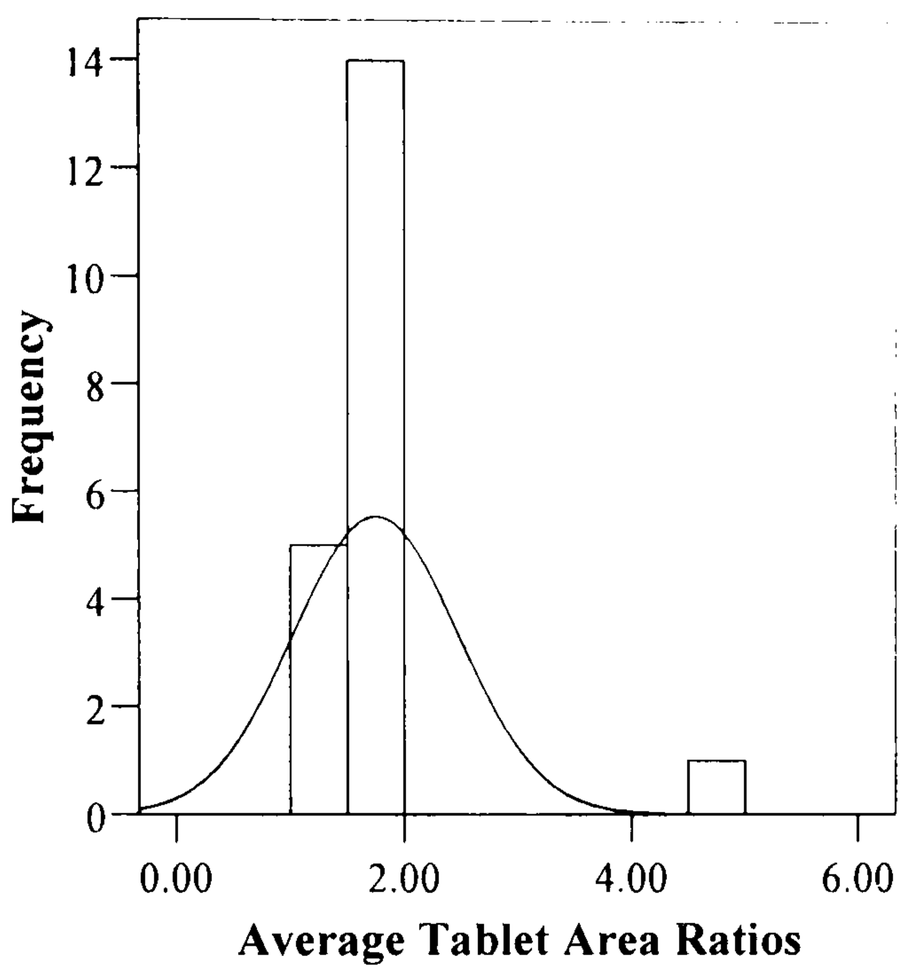

Batch 02

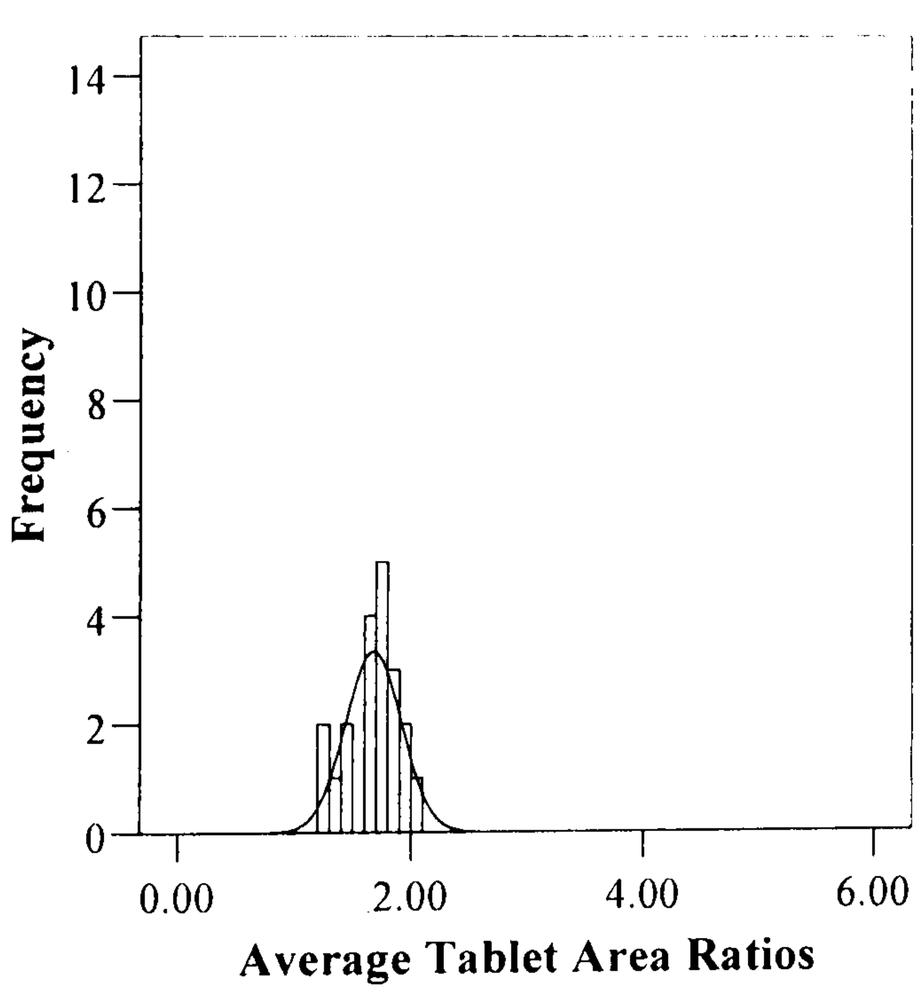

Batch 3

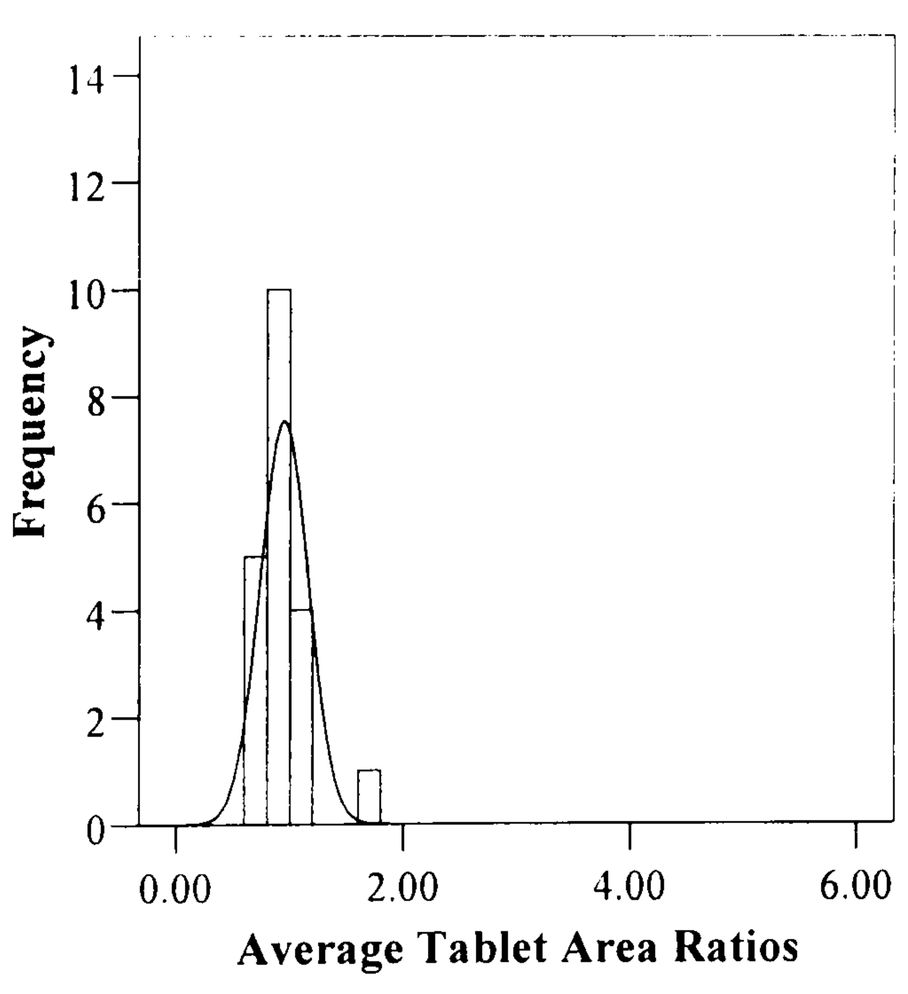

Batch 4/01

B

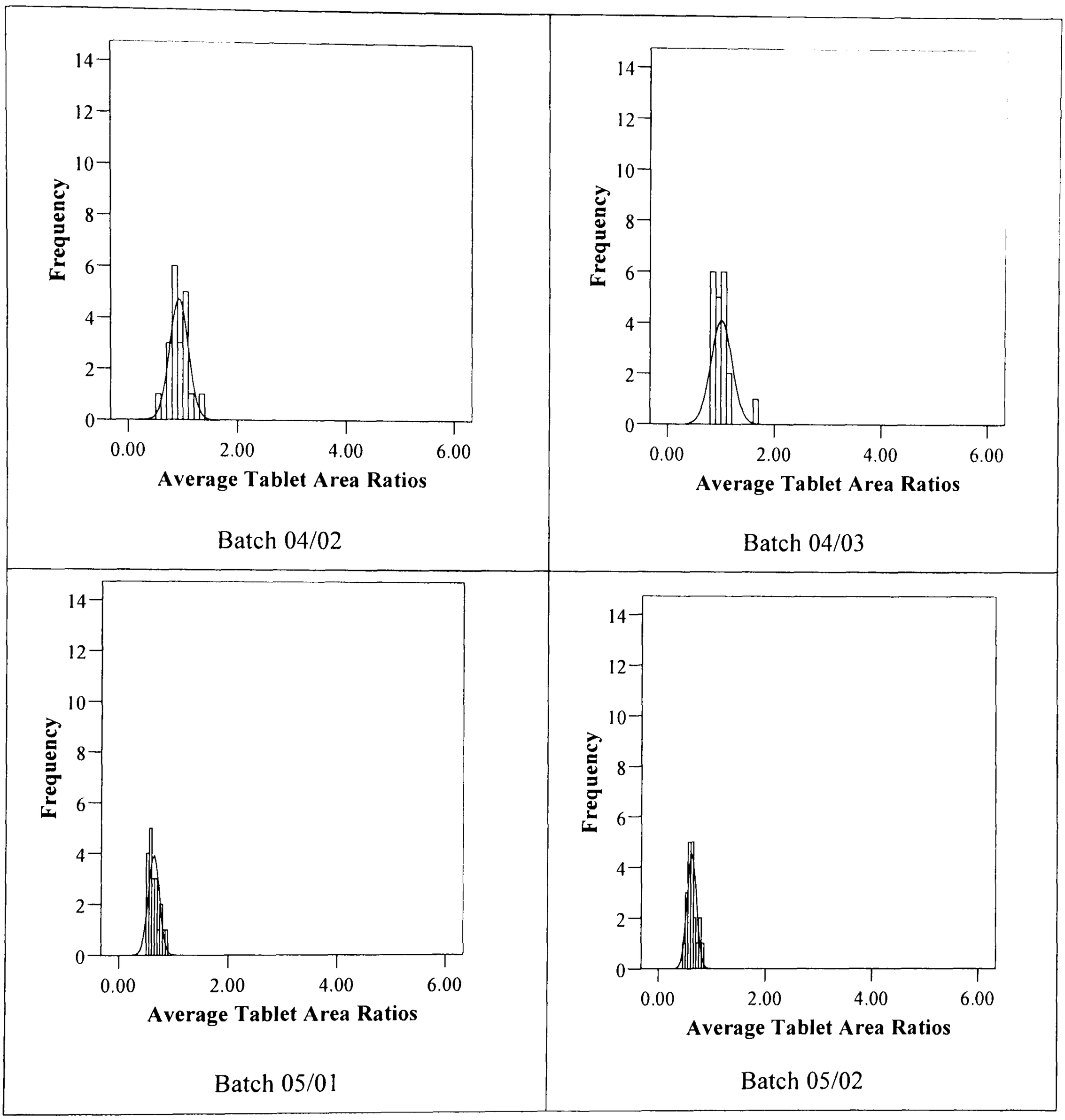

Batch 04/02

Batch 04/03

Batch 05/01

Batch 05/02

C

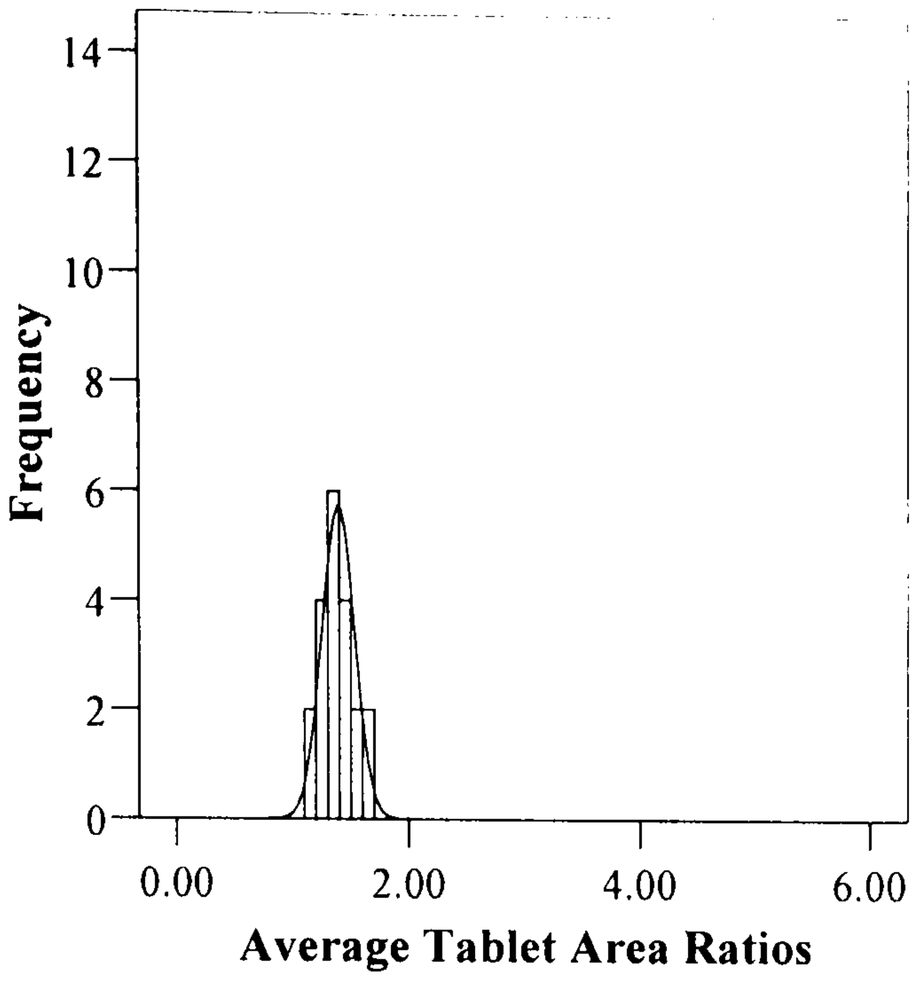

Batch 05/03

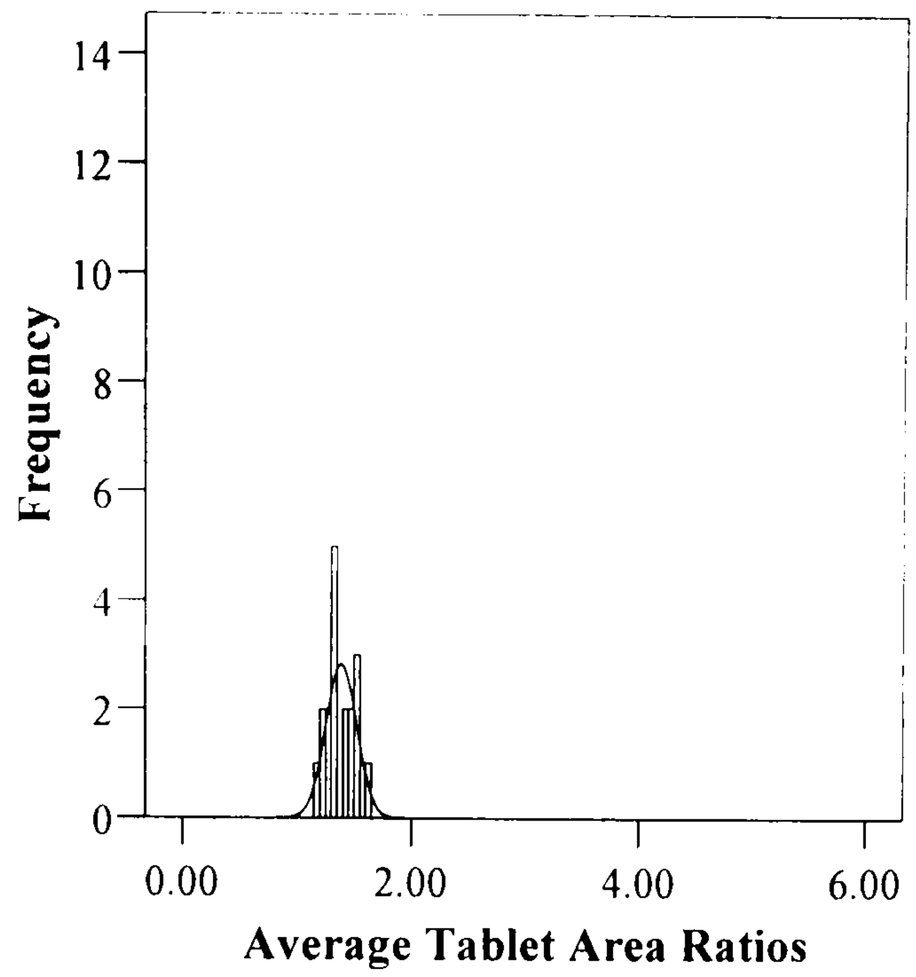

Batch 05/04

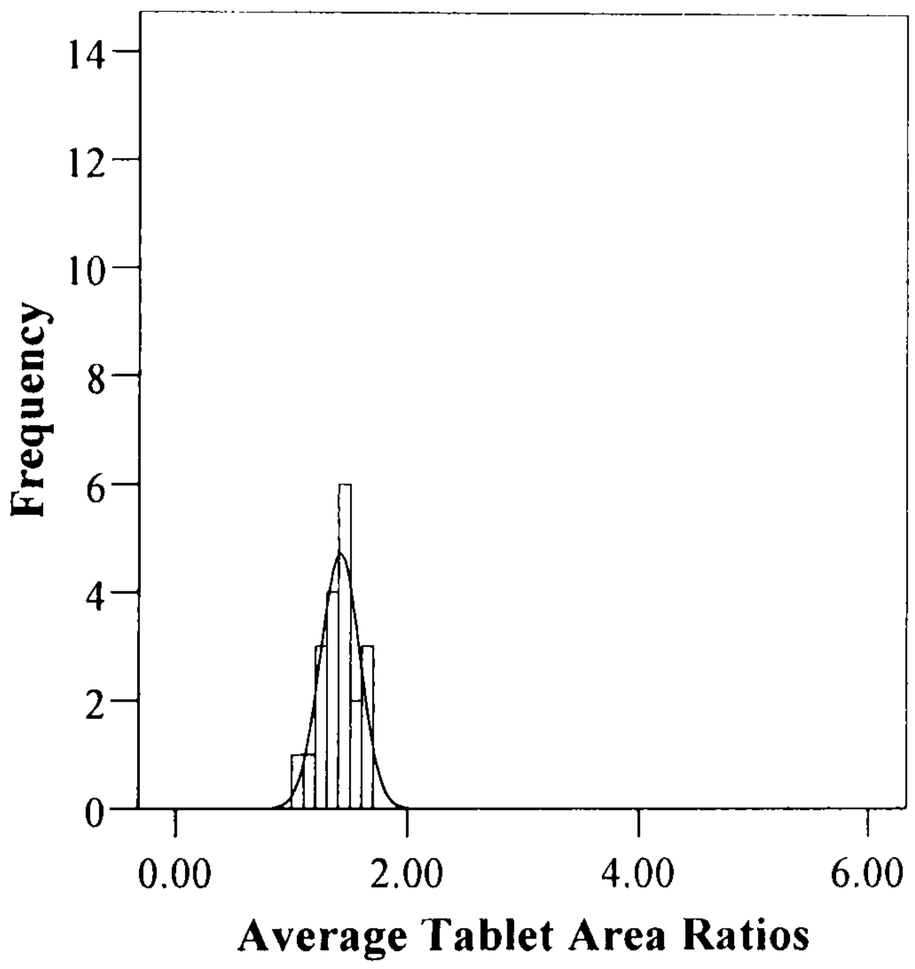

Batch 05/05

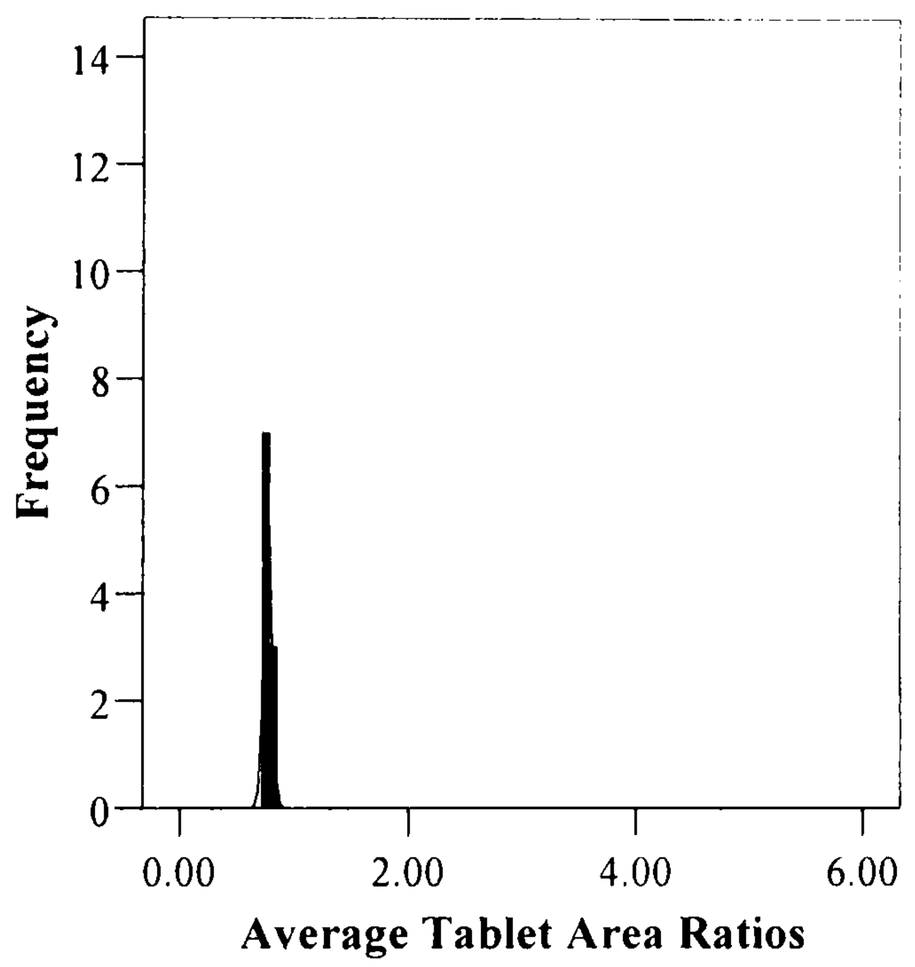

Batch 06

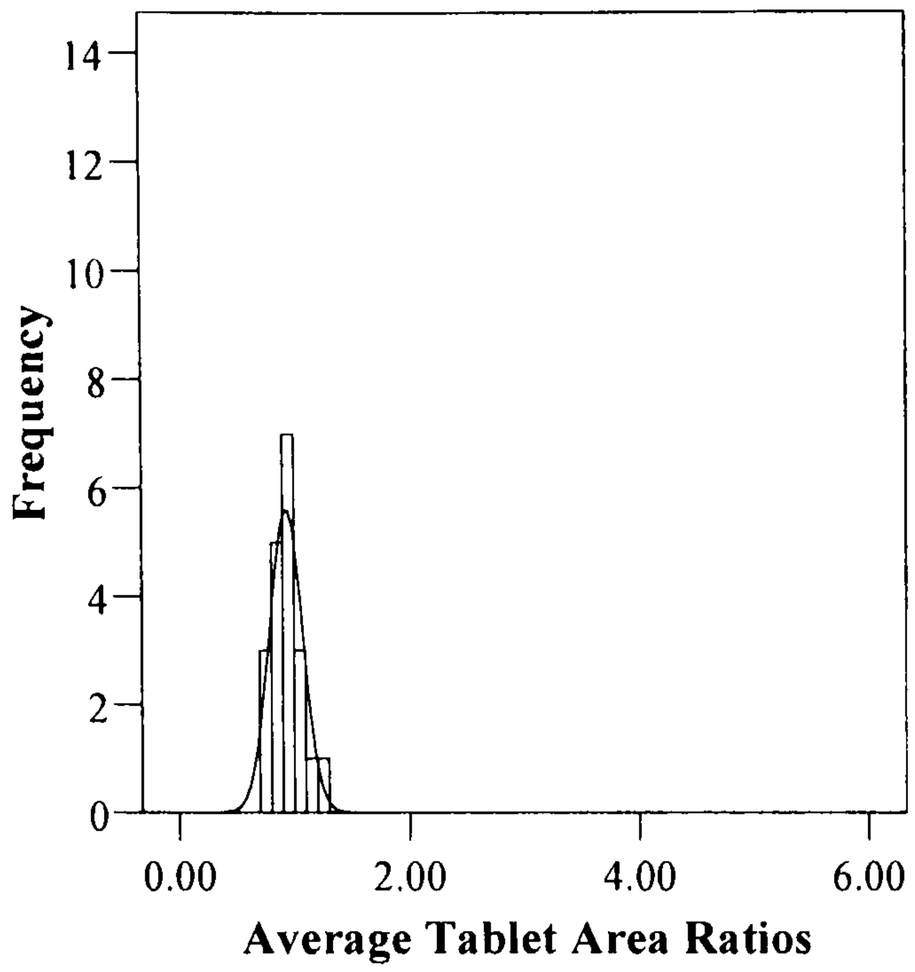

Batch 07

Figure 3.23 A, B and C: Histograms showing the number of tablets from each batch with a given phenethylamine/cellulose ratio drawn with Gaussian curves with the same mean and standard deviation as the data shown.

Figure 3.24 presents the data for the different tablets by batch and if applicable by sub-batch, plotted in a cluster diagram. The error bars represent the standard deviation of the ratio of phenylethylamine to cellulose (x-axis) and the peak height (y-axis). The data supports the conclusion that there are differences between the batches but trends within the sub-batches. Interestingly, all of the tablets seem to be grouped within each batch in terms of the ratio of average phenylethylamine derivative to cellulose but in some the intensity of the average phenylethylamine derivative peak intensity is varied. Good examples of this are batches 2 and 3 where the lowest peak intensity is 200 arbitrary units and the highest almost 600 arbitrary units. The errors of uncertainty are also large spanning almost 200 arbitrary units. Batch 2 also has one tablet with the highest ratio of average phenylethylamine derivative to cellulose which could have resulted from a blockage in the press filling machine causing more drug than filler to be added or the tablet could originate from another batch or laboratory.

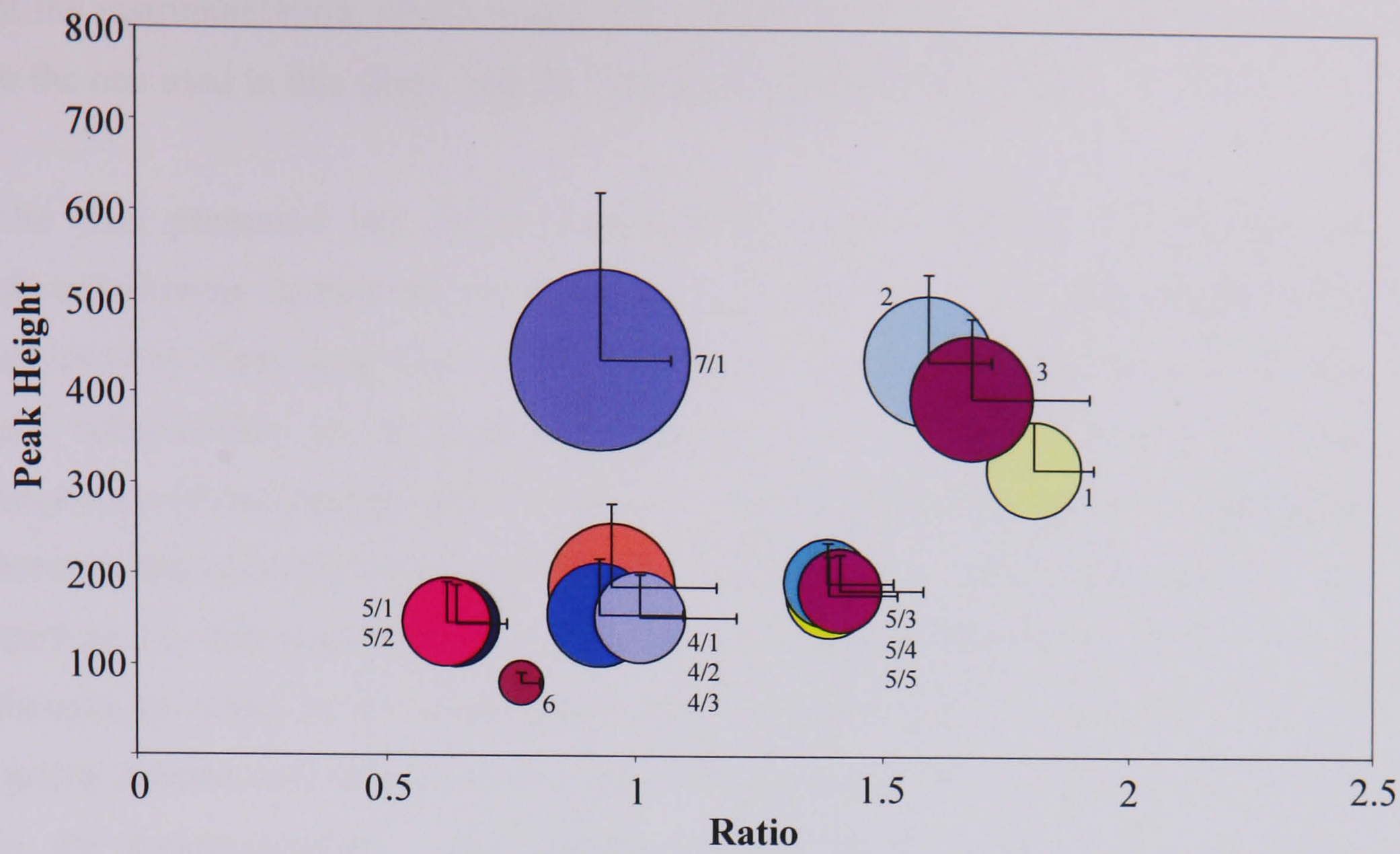

Figure 3.24: Cluster plot of the ratio of phenylethylamine/cellulose plotted against the average peak intensity for all the analysed tablets. The error bars present the standard deviation of the ratio of phenylethylamine to cellulose (x-axis) and the peak height (y-axis).

Comparison of the overall batch average peak positions and peak responses of the phenylethylamine derivatives and excipients shows the variability across the batches for example batch 1 versus batch 3 but also reveals trends within the sub-batches for example sub-batches 4/1, 4/2 and 4/3. However the error bars of the peak responses of the phenylethylamine derivatives overlap across all the batches implying they may not be as discrete as the data shows.

3.4 Conclusions

This work has demonstrated that there are advantages and disadvantages to the use of Raman spectroscopy to profile Ecstasy tablets. The principle advantages are; the absence of any sample preparation, beyond removing any loose particulate material, the non-destructive sample analysis, the efficiency of analysing large number of tablets faster than the standard methods employed currently and the information rich spectra that can be obtained from each sample. A major disadvantage to the widespread adoption of the Raman spectroscopy for routine analysis is often the cost

of the instrumentation, which ranges from ~£30K to £120K for a similar instrument to the one used in this study, and the running costs associated with it.

The data presented has shown that it is possible to identify the presence of phenethylamine derivatives and excipients in the seized tablets. Whilst this can be achieved by visual inspection of the spectra this must not be undertaken in isolation and consideration to the peak positions has to be given. However, on closer inspection of the absolute peak positions it is not possible to categorically distinguish between the phenethylamine derivative(s) present in the samples when they are in a mixture, i.e. differentiating between the presence of the MDMA from MDA. This is thought to relate to the crude production methodologies and associated lack of quality control used to produce the active drug component and the systematic errors in the instrumentation. The smearing effects of the tablet casting machines amalgamating the particles also complicate the spectral representation.

Analysing three areas per tablet and averaging the peak position and peak intensity data gives representative data that can be used to compare tablets within a batch and between batches. The phenethylamine derivatives average peak position data per tablet showed detectable variability in the intensity per batch but consistency within sub-batches, tentatively indicating that the tablets have originated from the same clandestine laboratory. This is further supported by the average peak responses of the excipients and the reproducibility observed within associated sub-batches.

Comparison of the overall batch average peak positions and peak responses of the phenethylamine derivatives and excipients shows the variability across the batches but also reveals trends within the sub-batches. Although the errors of uncertainty overlap across all the batches implying they may not be as discrete as the data shows.

Assessment of the phenethylamine derivatives to cellulose ratios shows an approximately normal distribution about the mean values for each batch. The histograms illustrate the variation in ratios across the batches but show the sub-batches to be closer aligned with each other.

Overall this study has shown that Ecstasy tablet composition profiling can be undertaken with some degree of success using Raman spectroscopy. Whilst it is not possible to specifically identify the type of phenethylamine present, using averages of the responses collated from multiple areas on the tablet and comparing these to the excipients can still produce useful data for comparison within batches and between batches. Analysis can be undertaken with virtually no sample preparation with higher throughput than traditional methods.

3.5 Future Work

Further work to investigate separation of the phenethylamine derivatives might include looking at other Raman fingerprint regions for alternative characteristic peaks to distinguish them. Additionally, cooling the sample to approximately 77 K might improve the peak resolution as temperature effects cause peak broadening [Otto (2006)]. Spatially Offset Raman [Matousek and Parker (2006)] is another method that could be tried. It analyses larger areas in a single analysis and enables penetration through the tablet facilitating analysis of different layers within the tablets. However, none of these methods will have an added advantage over the method described in this paper unless better separation of the phenethylamine derivatives is achieved.

Chapter 4

SERS with Gold and Silver Colloid at 785 nm and 633 nm Excitation

4.1 Introduction

Work was undertaken to investigate the suitability of the System 1000 Renishaw Raman Microscope coupled to 785 nm and 633 nm laser systems for SERS analysis of aqueous illicit drugs. Previous work has demonstrated that the 785 nm laser system will not generate the fluorescence that may be emitted from the illicit substances when shorter wavelength lasers are used [Sands *et al* (1998), Asher and Johnson (1984), Lewis (1995)]. The 785 nm laser system has also been identified as the optimum excitation wavelength for gold and silver colloid surface enhancement [McCreery (2000)].

The choice of aggregating agent also affects the SERS scattering observed. The aggregating agent facilitates the interaction of the illicit substance with the colloid. Faulds *et al* (2002) observed that amphetamine is weakly adsorbed onto colloidal surfaces. Coupling the colloid, aggregating agent and wavelength of the incident laser are essential to observe the greatest SERS enhancement factor. The experiments undertaken utilised silver and gold colloid, aggregated with either 0.1 M or 1 M sodium chloride solution coupled with excitation wavelengths of 633 nm and 785 nm.

4.2 Experimental Procedure

4.2.1 Silver Colloid Preparation

Silver colloid was prepared by the citrate reduction of silver nitrate as first reported by Lee and Meisel (1982), using conditions specified by Munro *et al* (1995). All glassware was vigorously cleaned by soaking in *aqua regia* and rinsed with de-ionised water before washing with detergent and rinsing thoroughly with de-ionised water. De-ionised water (500 ml) was placed in a round bottom, 3-neck flask. The de-ionised water was then stirred vigorously using a glass stirrer and heated to around 45 ^{o}C whereupon silver nitrate (90 mg Sigma Aldrich, 99.9999%) was added. The solution was heated to almost boiling (~96 ^{o}C) and sodium citrate

dihydrate (10 ml of a 1% solution, Aldrich, 99 + %) was added and the solution allowed to boil gently for 90 minutes. After this period, the heat was removed and the solution allowed to cool with constant stirring. The quality of the colloid was then assessed by measuring the electronic spectrum. The λ_{max} of the silver colloid prepared in this way was 404 nm [Faulds (2003)]. This colloid was supplied by Raman Spectroscopy Group, Strathclyde University, Scotland.

4.2.2 Gold Colloid Preparation

The gold colloid was prepared from a method described by Graber *et al* (1995). Sodium tetrachloroaurate (50 mg, BDH) was dissolved in 500 ml of water. The solution was brought to boiling whilst stirring constantly. Upon boiling, trisodium citrate (7.5 cm^3 of a 1% solution) (Sigma Aldrich) was added. The solution was maintained at boiling point for 15 minutes and then allowed to cool to room temperature with constant stirring. The λ_{max} of the gold colloid prepared in this way was 520 nm [Faulds (2003)]. This colloid was supplied by Raman Spectroscopy Group, Strathclyde University, Scotland.

4.2.3 Raman Equipment

A System 1000 Raman Microscope, with a charge couple device detector, Renishaw PLC (Wooten-Under-Edge, Gloucestershire, UK) was used. This was run by Renishaw Wire and Grams Software (Renishaw PLC). Experiments were conducted with a helium-neon laser (633 nm) and an infra-red (785 nm) laser.

4.2.4 Wavelength Calibration Procedure

Two forms of calibration procedure were undertaken. The first calibration procedure is undertaken every six months and involves the use of a neon lamp to check that the X-axis is calibrated in both the Stokes and Anti-Stokes regions. The neon lamp has a series of discrete lines with specific positions that are always the same along the spectrum. The positioning of these lines is compared with a reference table for the known neon spectrum and the software positions adjusted accordingly. The use of a neon lamp for calibration procedures is well known and it ensures a continuous and uniform standard of calibration.

The second procedure was undertaken on a daily basis prior to sample examination. A slab of silica chip mounted on a microscope slide is placed under the microscope objective (x50). Small scratches on the surface of the silicon chip are focused upon to ensure the correct surface is in view and that no dust particles are present which might interfere with the spectrum. The silicon chip is exposed to the laser light for a period of 1 and 5 seconds and spectra are captured containing a single peak positioned at 520 cm^{-1}. The positioning of the peak is very precise and was used to perform any required offset corrections within the software to ensure correct peak position assignment with the samples.

4.2.5 Raman Analysis

Raman spectra from crystalline samples of the illicit drugs were collected for peak position comparison with the SERS spectra. Several crystals were placed on a glass slide and spectra (400 – 3200 cm^{-1}) captured using a x50 objective and a 30 second accumulation time.

4.2.6 Infra-Red Analysis

Infra-red spectra of the crystalline drug was collected using a Bruker Optics Vector 33 spectrometer with the golden gate accessory. A small pile of crystals covering the diamond of the golden gate were analysed. Three spectra were accumulated between 600 – 3200 cm^{-1}, with a 30 second accumulation time.

4.2.7 SERS Analysis

Aqueous solutions of the illicit drugs were prepared at concentrations of $2.7x10^{-5}$ M (10 μg/ml), $2.7x10^{-6}$ M (1000 ng/ml) and $2.7x10^{-7}$ M (100 ng/ml). These concentrations were chosen, with the lowest value reflecting the levels commonly detected using GC/MS and liquid chromatography/tandem mass spectrometry (LC/MS/MS) confirmatory analysis [Wan *et al* (1978), Walsh (2003), Samyn *et al* (2002)]. The illicit drug solutions were amphetamine, methamphetamine (MA), MDA, MDMA, MDEA and PMA (Aldrich, 99 + %).

Each of the illicit drug solutions were investigated in turn immediately after the addition of the drug to the colloid - aggregating agent mixture and were looked at under the same conditions. Thus in a typical experiment, the illicit drug solution was mixed with the colloid and aggregating agent in a new glass chromatography vial. A sample of the colloid (900 μl) was transferred into a vial followed by 100 μl of illicit drug solution and 50 μl of the sodium chloride aggregating agent. The sample was mixed briefly in the vial before being transferred using a transfer pipette with a disposable tip to the well of a microtitre tray for analysis. The microtitre tray was placed on the microscope stage and focused on using the x20 objective. The spectrum was collected from 400 cm^{-1} - 2000 cm^{-1} shifted from the excitation line, over a 10 second accumulation time.

The centrifuged (900 μl) colloid was prepared as follows; the colloid was spun for 20 minutes at 3000 rpm. The supernatant was removed using a pasteur pipette to leave the centrifuged colloid pellet at the bottom. This was removed to a new chromatography vial and then 100 μl of illicit drug solution was added to the vial. The solution was mixed and pipetted into the microtitre tray for analysis with the Raman microscope system.

A summary table (Table 4.1) of all of the experimental conditions and the observations of surface enhancement of the drug solutions can be found below. When spectral peaks relating to the illicit drug under investigation were observed this was taken as the presence of SERS.

Table 4.1: Summary table of the experimental conditions and absence or presence of surface enhancement with the drugs solutions at different concentrations (Amphet – amphetamine, MA - methamphetamine).

Drug	Colloid	Wavelength (nm)	Centrifuged	Aggregating Agent	Concentration Aggregating Agent (M)	Volume (µl)	2.7 x10^{-5} M (10 µg/ml)	2.7 x10^{-6} M (1000 ng/ml)	2.7 x10^{-7} M (100 ng/ml)
Amphet	Gold	633	Centrifuged	None	0	0	■	X	■
	Gold	785		NaCl	1	50	✓	✓	✓
	Silver	633		NaCl	1	100	■	✓	✓
	Silver	633		NaCl	0.1	100	■	✓	■
	Silver	633		NaCl	0.1	75	✓	✓	✓
	Silver	633	Centrifuged	None	0	0	■	X	■
	Silver	785		NaCl	1	50	X	X	X
MA	Gold	785		NaCl	1	50	✓	X	X
	Silver	633		NaCl	1	50	X	■	■
	Silver	633		NaCl	1	30	X	■	■
MDA	Gold	785		NaCl	1	75	✓	✓	✓
MDMA	Gold	785		NaCl	1	50	X Some bronzing	✓ Some bronzing	✓ Some bronzing
MDEA	Gold	785		NaCl	1	50	X	✓	✓
PMA	Gold	785		NaCl	1	50	X	X	X

✓ (spectral peaks present), X (no spectral peaks present), ■ (not tested)

4.3 Results

4.3.1: Amphetamine

No SERS was observed for either the centrifuged silver or gold colloid solutions with 633 nm laser excitation. The silver colloid solution with 1 M sodium chloride aggregating agent was investigated with 785 nm laser excitation but no surface enhancement was seen with the amphetamine sulphate solutions with this laser wavelength, although similar work carried out by Faulds *et al* (2002) using silver and gold colloids had identified the characteristic peaks associated with amphetamine sulphate. This lack of SERS activity from the silver colloid with 785 nm excitation is probably due to silver's shorter wavelength plasmon resonance peak [Faulds *et al* (2002)]. Faulds *et al* (2002) work had also identified gold as providing better enhancement with 785 nm excitation. Confirmation of this observation was seen with the results for gold colloid with amphetamine sulphate which did demonstrate SERS (Figure 4.1). The characteristic doublet peak at 1002 $cm^{-1} \pm 2\ cm^{-1}$ associated with the presence of amphetamine whether in its sulphate form (Figure 4.1) or the substituted form of methamphetamine [Sagmuller *et al* (2003)] was observed here. This peak is attributed to a ring stretch breathing mode and/or ring vibration effect.

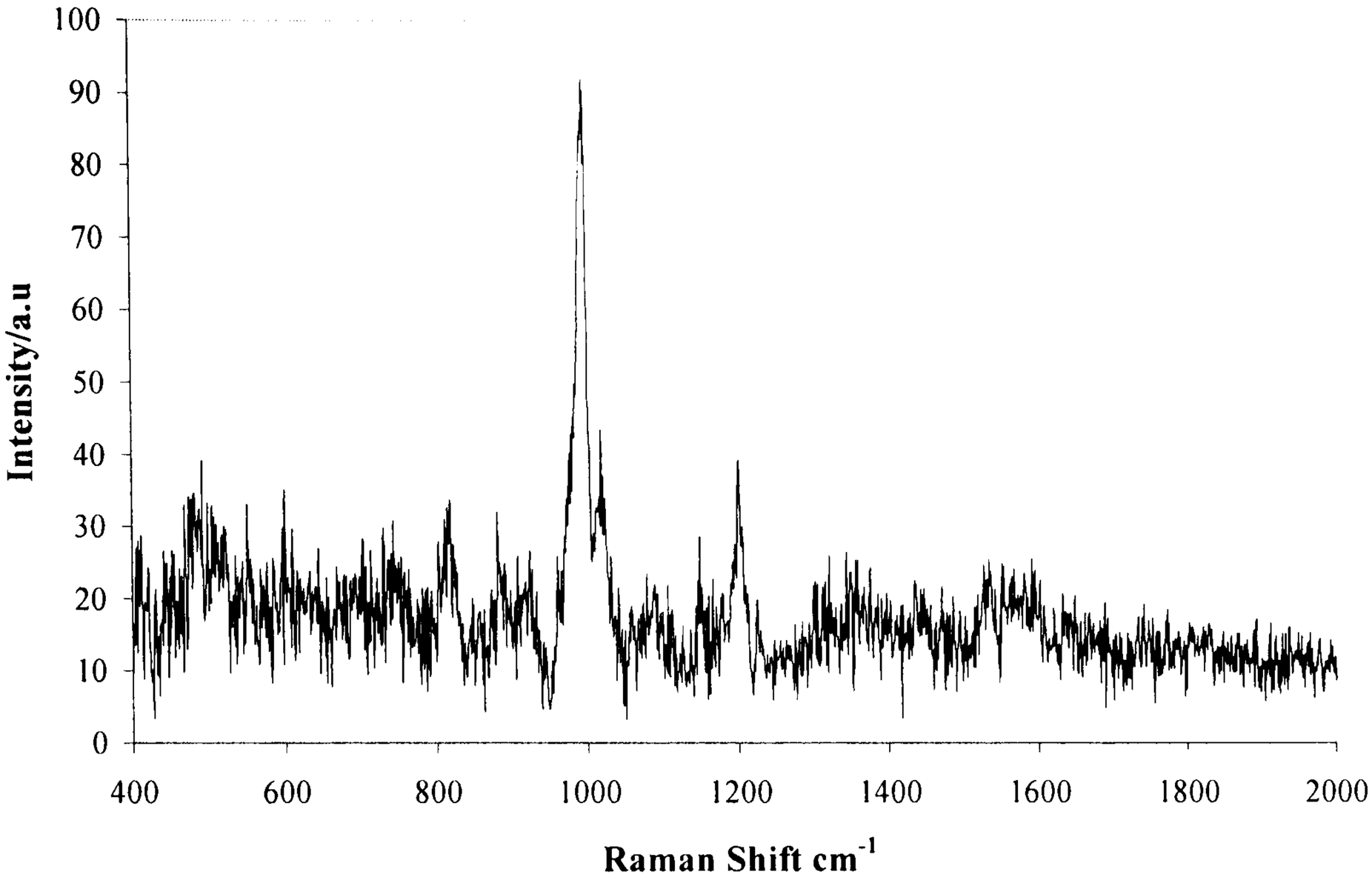

Figure 4.1: A SERS spectrum of aqueous amphetamine solution ($2.7x10^{-6}$ M) (using gold colloid (900 µl), aggregated with 1 M NaCl (50 µl), x20 objective, 10 seconds accumulation time).

Crystalline Raman and Infra-Red (IR) spectra (Figure 4.2) and the accompanying peak data table (Table 4.2) for amphetamine sulphate can be compared with the SERS spectra for peak identification.

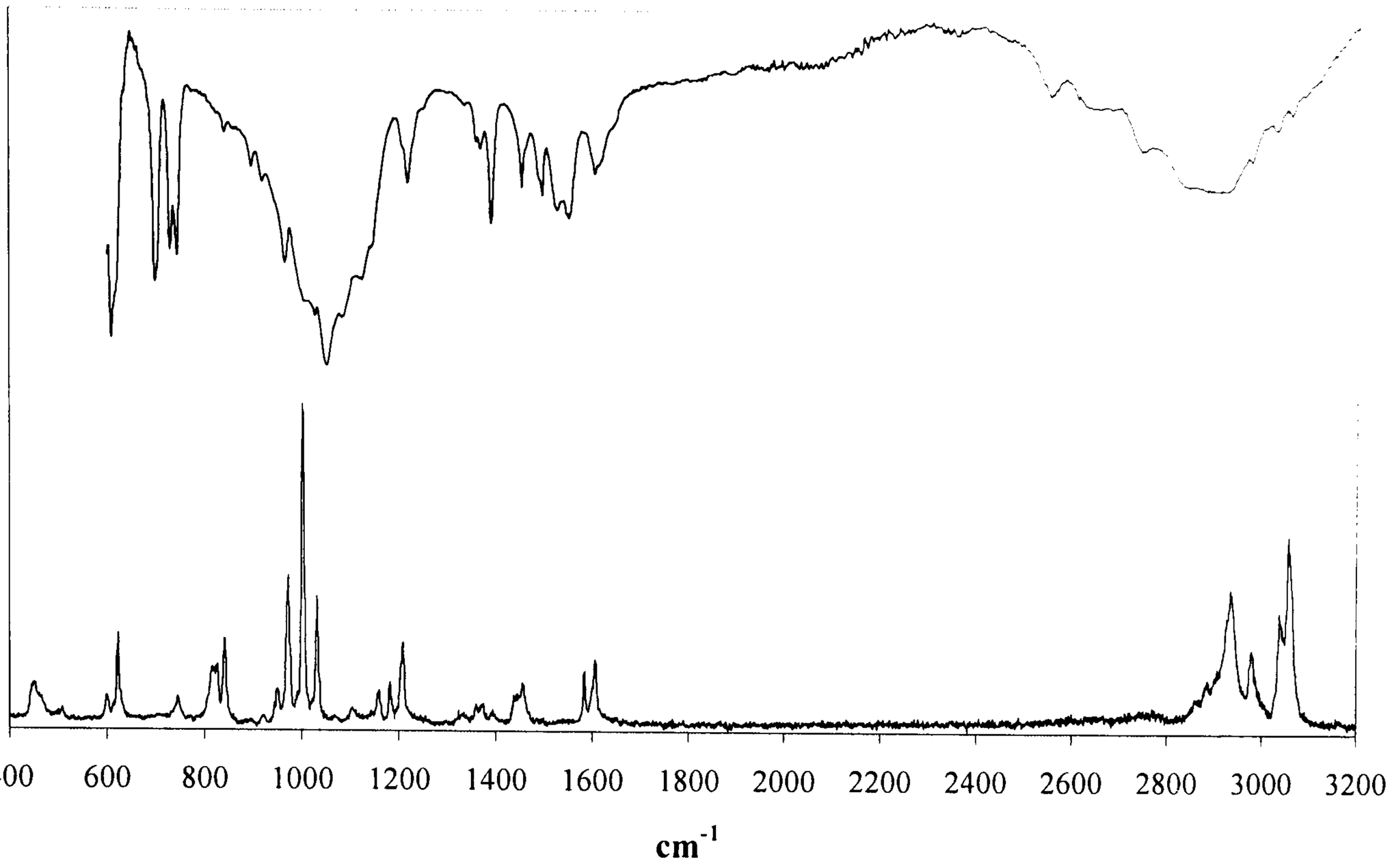

Figure 4.2: Raman (lower spectrum) and IR (upper spectrum) spectra of crystalline amphetamine sulphate.

Table 4.2: Raman and IR peak position data and the molecular vibration associated with that peak for amphetamine sulphate [Lin-Vien *et al* (1991), Moffat and Widdop (2004)].

Raman		**IR**	
Peak Position cm^{-1}	**Movement**	**Peak Position cm^{-1}**	**Movement**
622.5	Ring Deformation	700.00	Monosubstituted Benzene ring
841.4	N-H OR NH_2 stretch/wag	740.00	CH_2 / CH_3
972.8	Ring stretch breathing mode/ ring vibration	1495.00	Monosubstituted Benzene ring
1002.1	Ring stretch breathing mode/ ring vibration		
1032.1	Ring stretch breathing mode/ ring vibration		

Comparison of the Raman and SERS spectra for amphetamine shows the presence of a triplet peak at 1000 cm^{-1} in the Raman spectrum but a doublet peak in the SERS spectrum in the same position. This difference is attributed to firstly the sample

matrix. The Raman spectrum is a crystalline sample and the SERS a liquid sample. In the liquid SERS sample, the drug molecules are freely orientated within the aqueous media. This allows the functional groups to attach to the colloid surface in their preferred orientation giving rise to the doublet peak. The orientation of the molecule depends on the surface chemistry and the functional groups of the molecule. In the crystalline Raman spectrum the crystal packing motif dictates the orientation of the functional groups [Giccovazzo *et al* (1992)]. Additionally, the SERS effect results in a slight shift of the peak position and relative intensities of one peak to another.

Spectral peaks were observed with the $2.7x10^{-6}$ M and $2.7x10^{-7}$ M aqueous amphetamine solutions (Figure 4.3) at 633 nm following addition of 75 µl 0.1 M sodium chloride to a silver colloid. However, the $2.7x10^{-5}$ M solution presented no spectral detail. The concentration of the aggregating agent was decreased due to over-aggregation of the silver colloid solution which reduced the opportunity to observe the SERS effect. However, the reduction of the aggregating agent volume by 25% did not resolve this problem. The limit of detection using silver (excited by 633 nm) and gold (excited by 785 nm) colloids appeared similar at approximately $2.7x10^{-7}$ M (100 ng/ml).

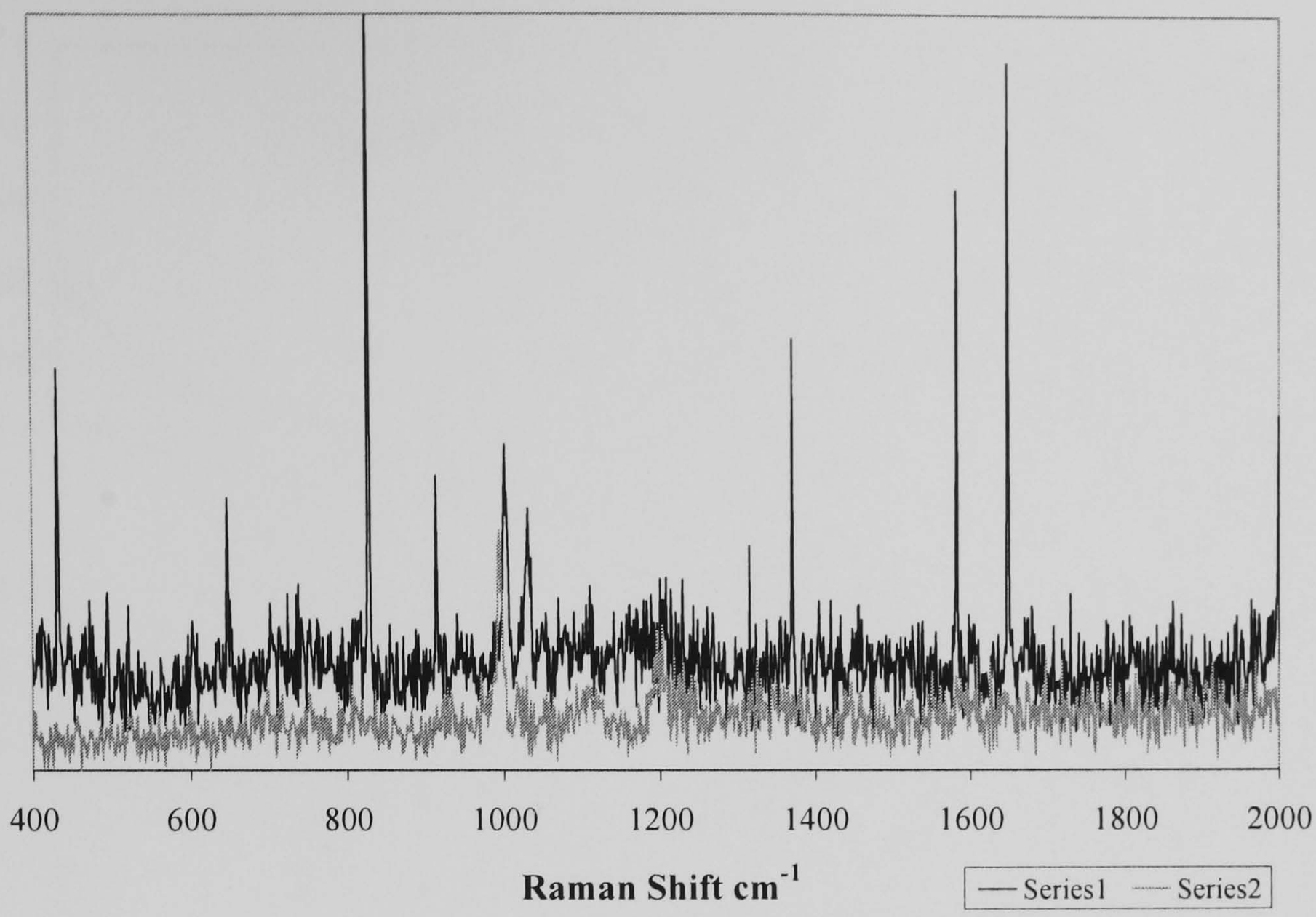

Figure 4.3: SERS Spectra of aqueous amphetamine solution comparing a $2.7x10^{-6}$ M (series 1) with $2.7x10^{-7}$ M (series 2) solution containing silver colloid aggregated with 0.1 M NaCl (75 µl).

Most of the drugs tested produced some SERS spectra using NaCl aggregated gold colloids and 785 nm laser excitation, which is related to gold colloids longer wavelength plasmon resonance peak [Faulds *et al* (2002)] (Figure 4.4) compared to silver colloid (Figure 4.5). The greatest enhancement is achieved when the laser wavelength overlaps with the plasmon resonance peak.

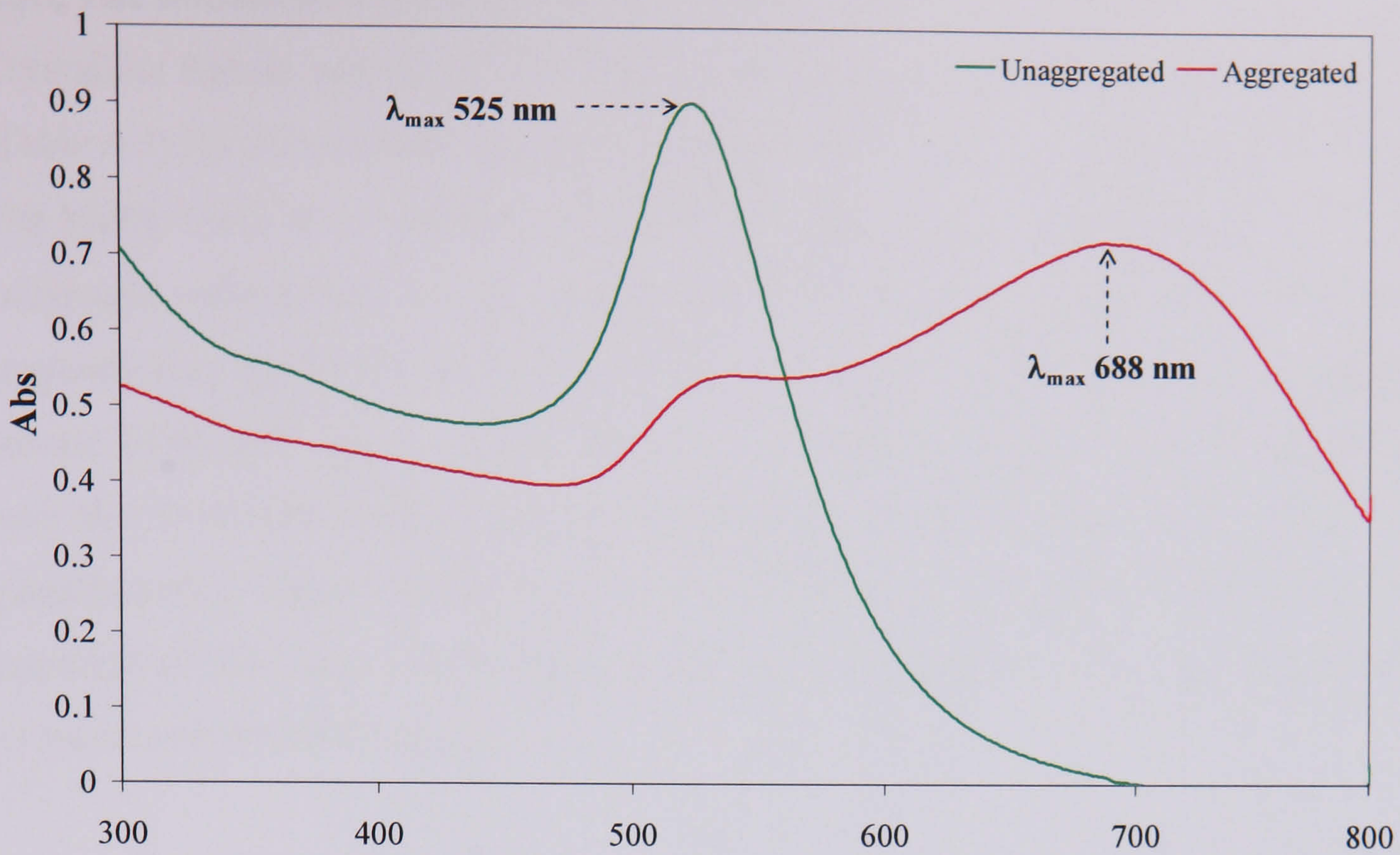

Figure 4.4: A UV/visible absorption spectrum of unaggregated and aggregated gold colloid illustrating the longer wavelength plasmon resonance peak.

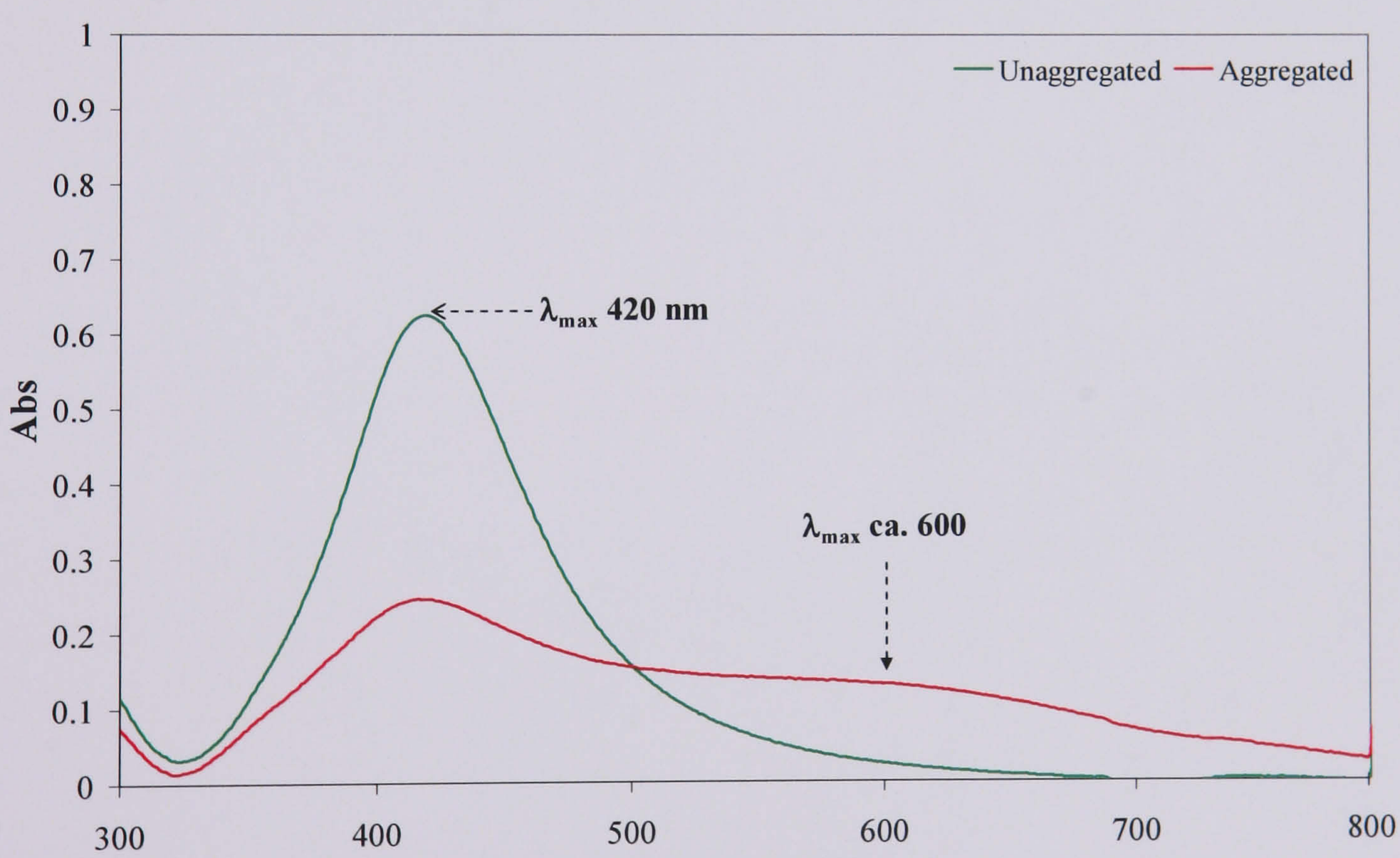

Figure 4.5: A UV/visible absorption spectrum of unaggregated and aggregated silver colloid illustrating the shorter wavelength plasmon resonance peak.

4.3.2 The Substituted Amphetamines

Crystalline Raman and IR spectra (Figure 4.6) and the accompanying peak data table (Table 4.3) for MDA can be compared with the SERS spectra for peak identification. The MDA SERS spectrum shows identifiable peaks at a concentration of 2.7×10^{-7} M using gold colloid (900 µl), aggregated with1M NaCl (50 µl) (Figure 4.7). Similar to amphetamine, the SERS spectrum of MDA is dominated by a characteristic doublet around 1000 cm^{-1} due to ring breathing and stretching vibrations. The peaks were such that it was possible to qualitatively identify the presence of this drug but not quantitatively. Other work showed that the sensitivity of SERS and, therefore, the detection of the lower concentration solutions, is dependent on the aggregation time to ensure reproducible results.

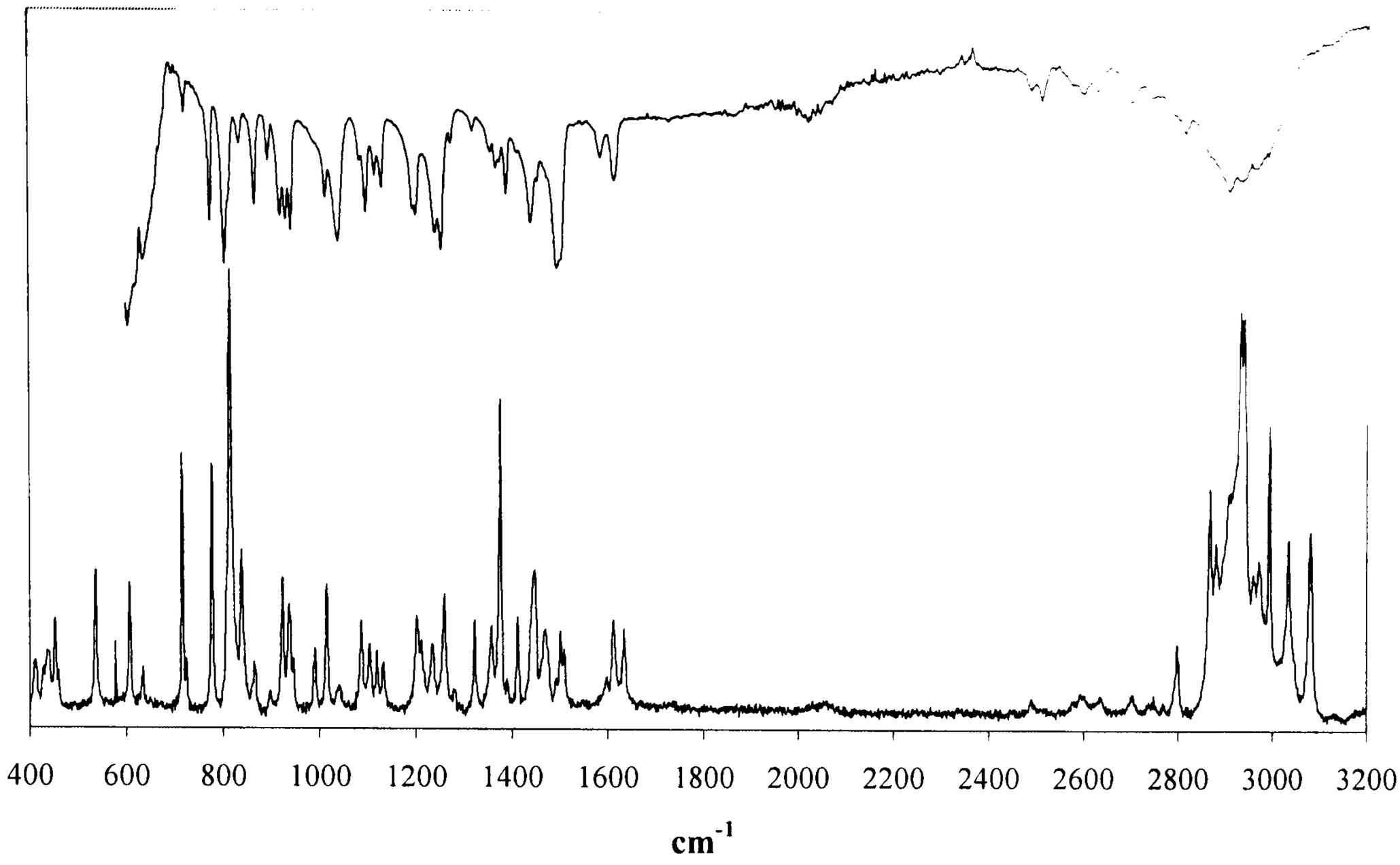

Figure 4.6: Raman (lower spectrum) and IR spectra (upper spectrum) of crystalline MDA.

Table 4.3: Raman and IR peak position data and the molecular vibration associated with that peak for MDA [Lin-Vien *et al* (1991), Moffat and Widdop (2004)].

Raman		**IR**	
Peak Position cm^{-1}	**Movement**	**Peak Position cm^{-1}**	**Movement**
246.4, 305.2, 344.0	Chain expansion n-alkanes	799.0	NH_2
715.3, 777.5	Ring vibration	1038.0	Aromatic ether
815.1	Ring breathing	1257.0	CH_3 / Aromatic ether
990.5, 1015.3	Trigonal ring breathing	1490.0	Aromatic vicinal tri-substituted benzene
1202.5, 1211.5, 1322.7	Ring vibration	1504.0	Aromatic vicinal tri-substituted benzene
1612.6, 1634.7	Ring stretches/ NH_2 scissors		
2867.5, 2880.7	Symmetric CH_2 / CH_3 stretches		
2924.1	Anti-symmetric CH_2 stretches		
3034.5, 3080.8	Aromatic CH stretch		

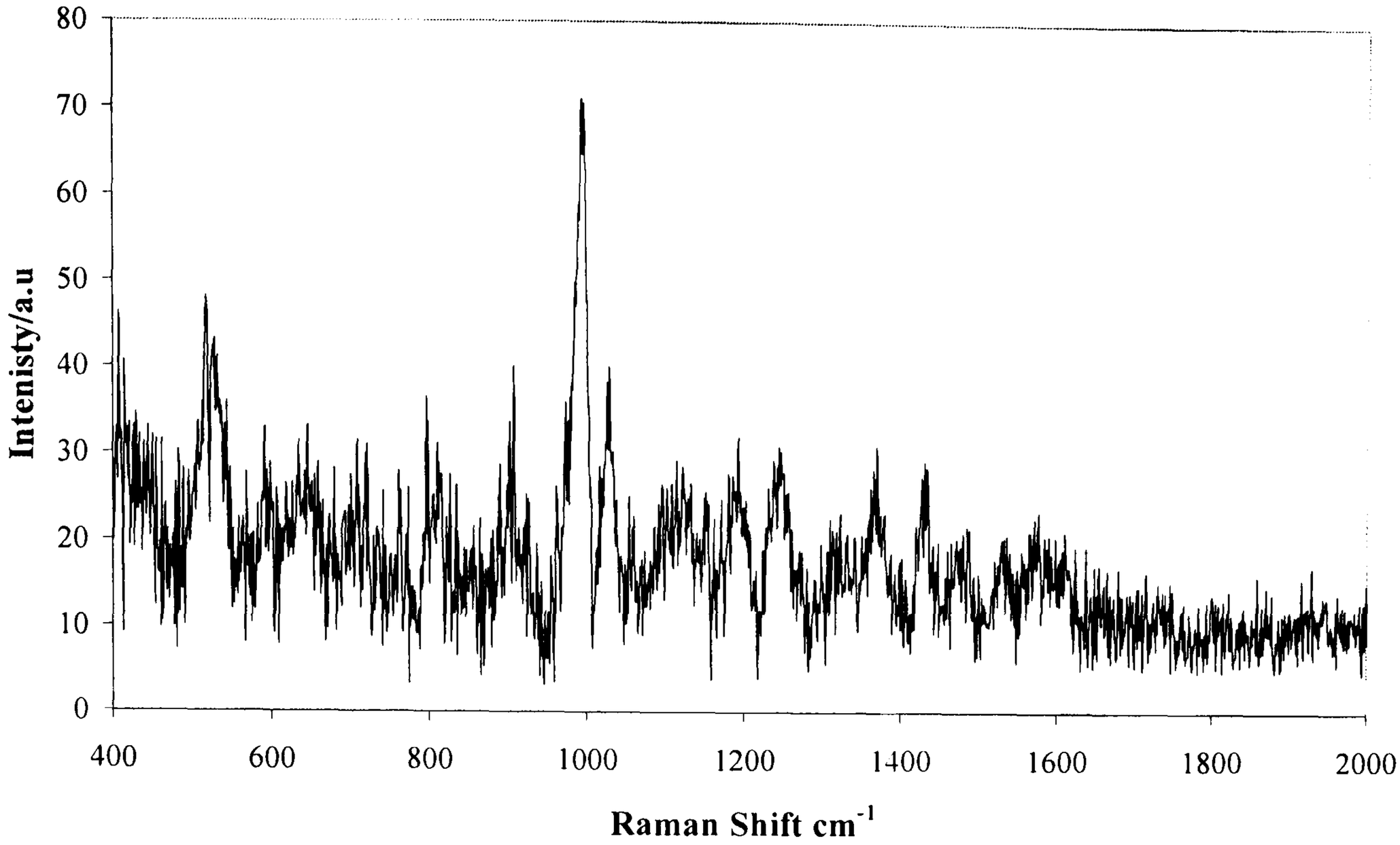

Figure 4.7: A SERS spectrum of aqueous MDA solution $2.7x10^{-7}$ M containing gold colloid aggregated with 0.1 M NaCl (75 μl).

MDEA, like MDA at a concentration of $2.7x10^{-7}$ M solution was detectable by SERS and produced a spectrum not dissimilar to that illustrated in Figure 4.7 for MDA. Curiously, at high ($2.7x10^{-5}$ M) concentrations no SERS spectrum could be observed for reasons which remain unclear. At lower concentrations good surface enhanced peak data were produced allowing qualitative identification of the drug.

Crystalline Raman and IR spectra (Figure 4.8) and the accompanying peak data table (Table 4.4) for MDMA can be compared with the SERS spectra for peak identification. MDMA solution suffered some colloidal bronzing effects at high concentrations ($2.7x10^{-5}$ M) (Figure 4.9) resulting in systematic peaks within the spectrum. The colloidal bronzing effect has not been thoroughly investigated and the underlying mechanisms are not understood to date [Karpov *et al* (1996)]. The $2.7x10^{-7}$ M concentration solution has a bigger signal to noise ratio, as would be expected due to the weaker concentration of the solution, but the doublet peak at 1000 cm^{-1} is identifiable (Figure 4.10). Colloidal bronzing at high concentrations could be due to the increased rate of onset of aggregation. It has been observed that

the stronger the concentration of the illicit drug solution the faster the aggregation process thus rapid onset of aggregation causes the silver or gold particles to clump together either with or without the attachment of the illicit drug particles. Therefore, the rate and extent of the surface attachment of the drug molecules to the gold or silver colloidal surface determines the surface enhancement observed in the spectra.

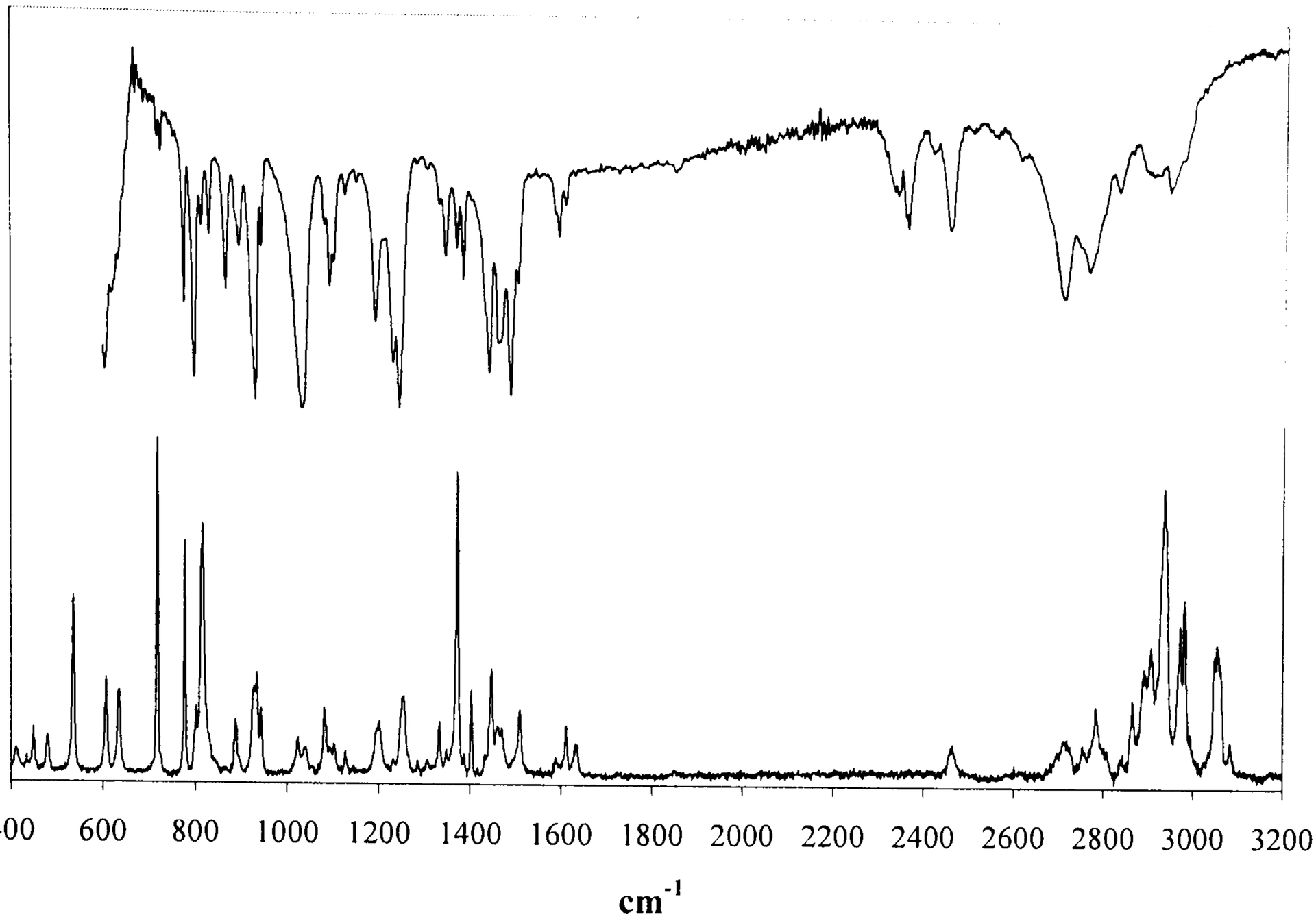

Figure 4.8: Raman (lower spectrum) and IR spectra (upper spectrum) of crystalline MDMA.

Table 4.4: Raman and IR peak position data and the molecular vibration associated with that peak for MDMA [Lin-Vien *et al* (1991), Moffat and Widdop (2004)].

Raman		**IR**	
Peak Position cm^{-1}	**Movement**	**Peak Position cm^{-1}**	**Movement**
254.1, 342.7	Chain expansion, n-alkanes	805.0	Unsymmetrical tri-substituted benzene / CH_2 rock
634.3	Ring deformation	1033.0	Unsymmetrical substituted benzene ring
777.2	Ring vibration	1189.0	CH_2 Wag
801.3, 814.9	Ring breathing	1442.0	Unsymmetrical substituted benzene ring
887.7	C-C Skeletal Stretch,	1489.0	CH_2-O / NCH_3
928.2	Symmetric COC stretch		
1251.8, 1254.7	In plane CH deformation		
1371.5, 1403, 1509.8	Ring stretch		
1611	NH_2 scissors		
2782.4	CHO group		
2981.1	Symmetric $=CH_2$ stretch		
3048, 3049.5, 3054.3	Aromatic CH stretch		

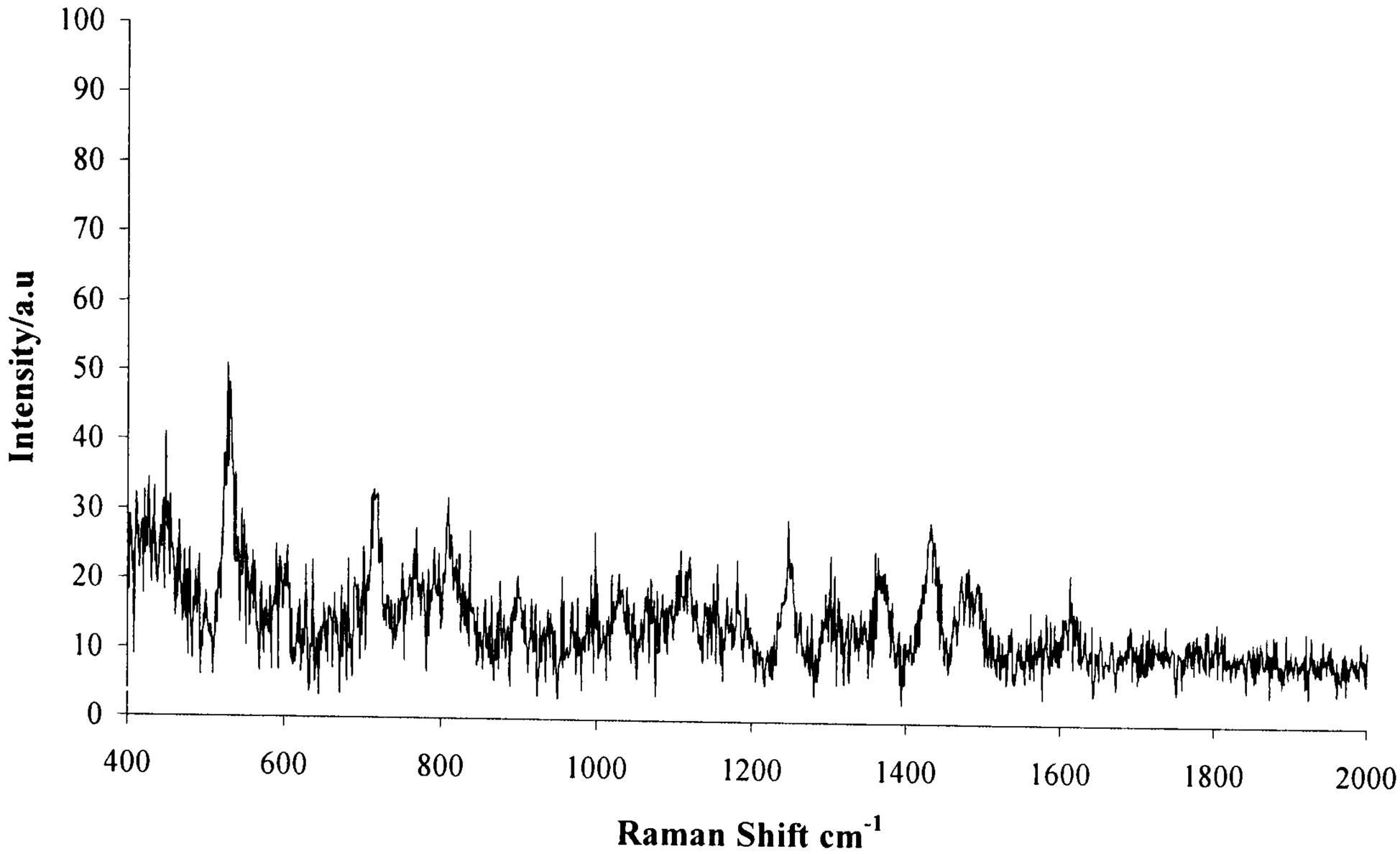

Figure 4.9: A SERS spectrum of aqueous MDMA solution ($2.7x10^{-5}$ M) containing gold colloid aggregated with 0.1 M NaCl (50 µl).

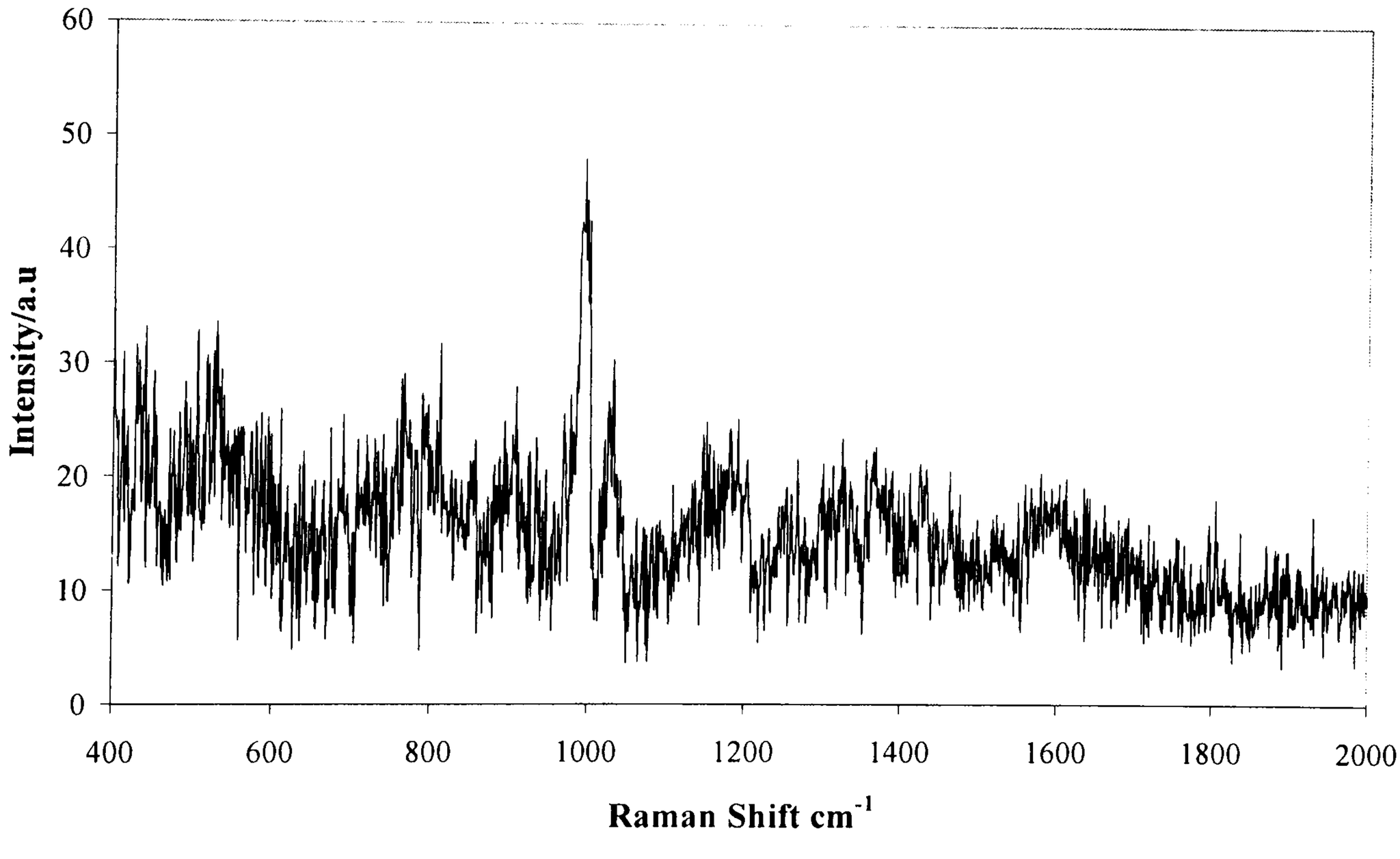

Figure 4.10: A SERS spectrum of aqueous MDMA solution ($2.7x10^{-7}$ M) containing gold colloid aggregated with 0.1 M NaCl (50 µl).

It is interesting to note that whereas the crystalline amphetamine Raman spectrum has the triplet peak at 1000 cm^{-1} ± 2 cm^{-1} and the SERS spectrum shows a doublet at 1000 cm^{-1} ± 2 cm^{-1}; in MDA and MDMA the strongest ring stretch/breathing mode is nearer 700 – 800 cm^{-1} but in the SERS spectra of these two compounds the doublet at 1000 cm^{-1}± 2 cm^{-1} is principally observed. This is thought to occur because the relative intensities of the bands change when moving from Raman to SERS, due to the orientation of these groups in the very localised electric field that gives rise to the SERS enhancement mechanism.

No SERS spectra were observed using the amphetamine derivative PMA. The lack of surface enhancement observed with the PMA is thought to be due to the electron rich or electron deficient functional groups on this amphetamine and its poor interaction with the positive gold colloidal surface and the aggregating agent.

4.4 Conclusions

This work has demonstrated the need for further research into the optimum working conditions of both the silver and gold colloid. It also illustrates that the use of the 785 nm laser systems is not the optimum wavelength of excitation when screening for the presence of amphetamine using silver colloid as the enhancement mechanism. Tentative results from experimental work carried out on the 633 nm laser system indicate this is a better wavelength of excitation for screening for the amphetamines and their substituted forms due to a greater spectral overlap with the plasmon resonance band for the silver colloidal particles.

This work also highlights the need to identify the most suitable aggregating agents for screening for the illicit drugs and their metabolites in aqueous samples because without an appropriate agent often no SERS signal is observed even if the drug is present. The electron donating/withdrawing nature of the functional groups need to be considered as well, as demonstrated through the lack of surface enhancement observed with the PMA solutions irrespective of their concentration. It is possible that the methoxy functional group within the PMA structure (Chapter 1.3 Figure 1.3) is affecting the overall polarisation state of the molecule. It is likely that the

methoxy functional group will be positioned closely to the substrate surface although the amine group may also be in close proximity. The consequence of the orientation is an effect the on the bond strength and the subsequent vibration frequency. The overall polarisation effect the PMA experiences is different due to its orientation on the substrate.

From the SERS work carried out using silver colloid, it is clear that the volume and concentration of the aggregating agent used has a direct influence on the SERS activity and therefore on the spectral data observed. Despite previous work [Lamping (1999)] indicating that 100 μl of aggregating agent was enough to instigate aggregation, in some of this experimental work addition of 100 μl of aggregating agent caused over-aggregation of the solution, preventing observation of any SERS signal.

The results of the above work also showed a lack of reproducibility when using both the silver and gold colloid. Consequently production of these two solutions has to be tightly controlled to ensure an acceptable degree of reproducibility between one batch and another. With the silver colloid the temperature at which the solution is refluxed at during its production is the key step and it has been found that a slight (one degree) variation can skew the enhancement capabilities of any particular batch [Faulds (2003)]. The same is true of the gold colloid however, its efficacy as a SERS substrate is not so temperature sensitive as that of silver colloid. Nevertheless, additional problems can manifest themselves when using the gold colloid such as the prevalent growth of bacteria within one month of exposing the solution to the air.

Both the silver and gold colloid contained visible particles both by eye and under the microscope indicating the self aggregating process is innate.

Colloidal bronzing was also evident if the length of time for sample exposure to the laser beam and SERS data capture ran into several minutes.

4.5 Future Work

The next chapter, Ag/TiO_2 Silver Substrate Surfaces – Initial Investigations, will investigate the suitability of silver coated titanium dioxide (Ag/TiO_2) substrates with amphetamine, methamphetamine and MDEA solutions to achieve SERS enhancement. Additionally, the use of cotton buds for the application of aqueous drug solutions to the Ag/TiO_2 substrate and the ability to undertake SERS analysis will be discussed.

Chapter 5

Ag/TiO_2 Silver Substrate Surfaces – Initial Investigations

5.1 Introduction

This work investigates the suitability of Ag/TiO_2 substrates as an alternative to using silver or gold colloid solutions. It also looks at establishing the solution volume required to achieve the greatest level of SERS to detect aqueous amphetamine and the substituted amphetamines. The accumulation time necessary to obtain the maximum enhancement was also explored.

5.2 Experimental Procedure

5.2.1 Ag/TiO_2 Substrate Preparation

The substrates were produced by the method described in Mills *et al* (2004). TiO_2, in the form of a nanocrystalline layer, was deposited onto a glass slide using a sol-gel process [Negishi *et al* (1995)]. The sol-gel was spin coated onto a 25 mm vitreosil quartz slide. After casting, the films were put into a preheated furnace (450 ^{0}C) for calcination (40 minutes) to produce a ca. 200 nm optically clear, robust nanocrystalline substrate of anatase titania on quartz. These films were then covered with 1 mM methanolic silver nitrate solution (ca. 10 cm^3) and irradiated using a black light blue (2 8W tubes) UVA lamp suspended 10 cm above. The substrates were air dried and stored in glass toped Petri dishes wrapped in aluminium foil to prevent exposure to light prior to use.

5.2.2 Spectral Collection

Raman and SERS spectra were recorded using the equipment described in Chapter 4.2.3.

5.2.3 Environmental Scanning Electron Microscopy (ESEM)

The samples were examined using a Phillips XL30 Environmental Scanning Electron Microscope, with a Large Field Gaseous Secondary Electron (GSE) detector (enabling the samples to be viewed without the need for a conductive coating), and water vapour as the imaging gas (~1.0 Torr). A 20kV accelerating voltage and a

30 μm final aperture was employed throughout, and the working distance was kept at approximately 10 mm. Each sample was held in place using an adhesive carbon pad, and was cleaned with compressed air prior to insertion in the microscope.

The samples were initially viewed at x25k magnification to gain an indication of sample homogeneity. Images were recorded at higher magnification from three randomly-chosen areas on each sample. Images were then typically recorded at magnifications of 50k, 100k and 200k.

5.2.4 Optical Imaging Microscopy (OIM)

The samples were examined using a Zeiss optical imaging microscope with bright field illumination. The x20 objective was used to capture digital images of the re-crystalisation of the aqueous samples.

5.2.5 SERS Analysis

Aqueous amphetamine solutions of $1x10^{-6}$ M (368.49 ng/ml) and $1x10^{-7}$ M (36.84 ng/ml) were used. A drop of aqueous amphetamine solution was placed, using a syringe, directly onto the silver surface. Unlike the colloid work, there is no sample mixing or preparation required when using the silver substrates. An initial volume of 10 μl of the $1x10^{-6}$ M aqueous amphetamine solution was used. The drop remained on the surface as a bead of liquid and did not spread. The volumes were reduced over the project time to 2 μl, 1 μl and 0.5 μl. The x20 microscope objective was used with the 1 μl volume and the x50 objective with the 0.5 μl volume on the 633 nm laser system. A standard collection time of 10 seconds was used unless otherwise indicated.

The substrates were also investigated with $1x10^{-2}$ M (3.68 mg/ml), $1x10^{-5}$ M (1856.9 ng/ml) $1x10^{-6}$ M (185.69 ng/ml) and $1x10^{-7}$ M (18.56 ng/ml) MA and $1x10^{-7}$ M (24.37 ng/ml) MDEA aqueous solutions.

5.2.6 SERS Analysis Following Use of A Cotton Swab

A cotton swab was dipped into 1 ml of $1x10^{-6}$ M amphetamine solution in a new glass vial until saturated. The cotton bud was spotted onto the surface of the substrate and analysed under the conditions previously described with a x50 microscope objective using the 40 minute photodeposited Ag/TiO_2 substrates.

5.3 Characterisation of Ag/TiO_2 Substrate Surfaces

Whilst NaCl aggregated silver colloid can result in SERS enhancement factors of 10^6 they require strict aggregation conditions to ensure reproducible signals. However, colloids are notoriously difficult to prepare and minor deviations in the production method can have significant impact on the particle size and ultimately affect the SERS enhancement factor. An alternative method showing reproducible SERS enhancement involves Ag/TiO_2 substrates.

Mills *et al* (2004) evaluated Ag/TiO_2 substrates for SERRS using GM19, a benzotriazole dye. GM19 typically forms a monolayer on most Ag/TiO_2 substrates at concentrations of 10^{-6} M [McLaughlin *et al* (2002)], thus, above this level use of the Ag/TiO_2 substrates typically produced SERS signals that decreased with increasing concentration. At lower concentrations of 10^{-6} - 10^{-7} M GM19 gave SERRS signals proportional to the concentration. The photodeposited substrates were also shown to be mechanically robust and had an indefinite shelf-life when stored in the dark under ambient conditions.

Mills *et al* (2004) noted an increasing degree of SERRS activity with an increasing level of silver deposition. Varying the photodeposition time directly affects the amount of silver deposited onto the TiO_2. Figure 5.1 illustrates the effect increasing photodeposition time has on the UV/VIS spectrum of the silver coated substrate. As the photodeposition time increases the substrate visibly darkens and the absorbance band attributed to the surface plasmon of silver increases in height accompanied by a slight shift in peak position (Figure 5.2).

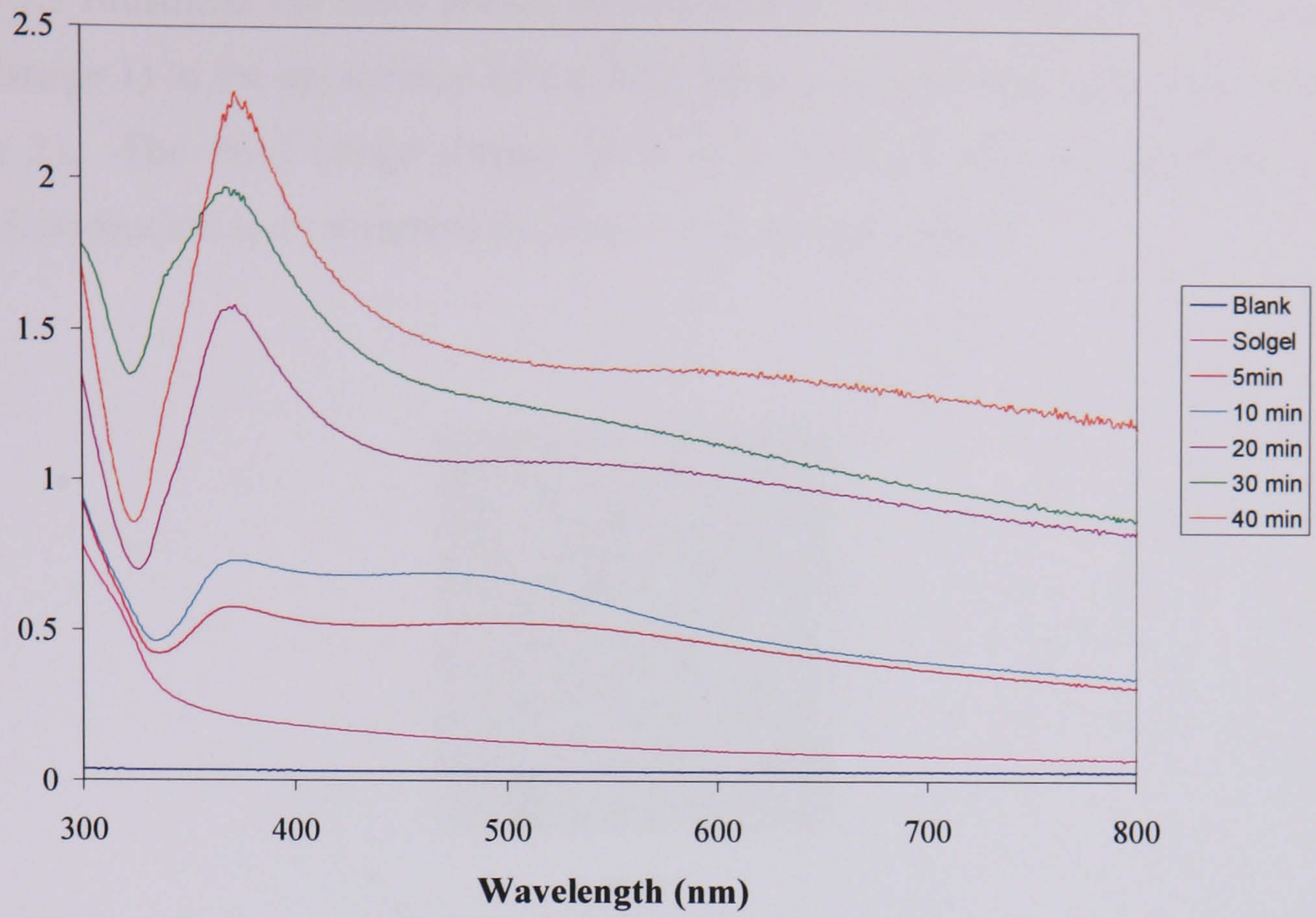

Figure 5.1: UV/VIS spectra of a blank quartz slide, quartz slide with calcinated TiO_2, and the quartz slides with calcinated TiO_2 and photodeposited silver with varying photodeposition time.

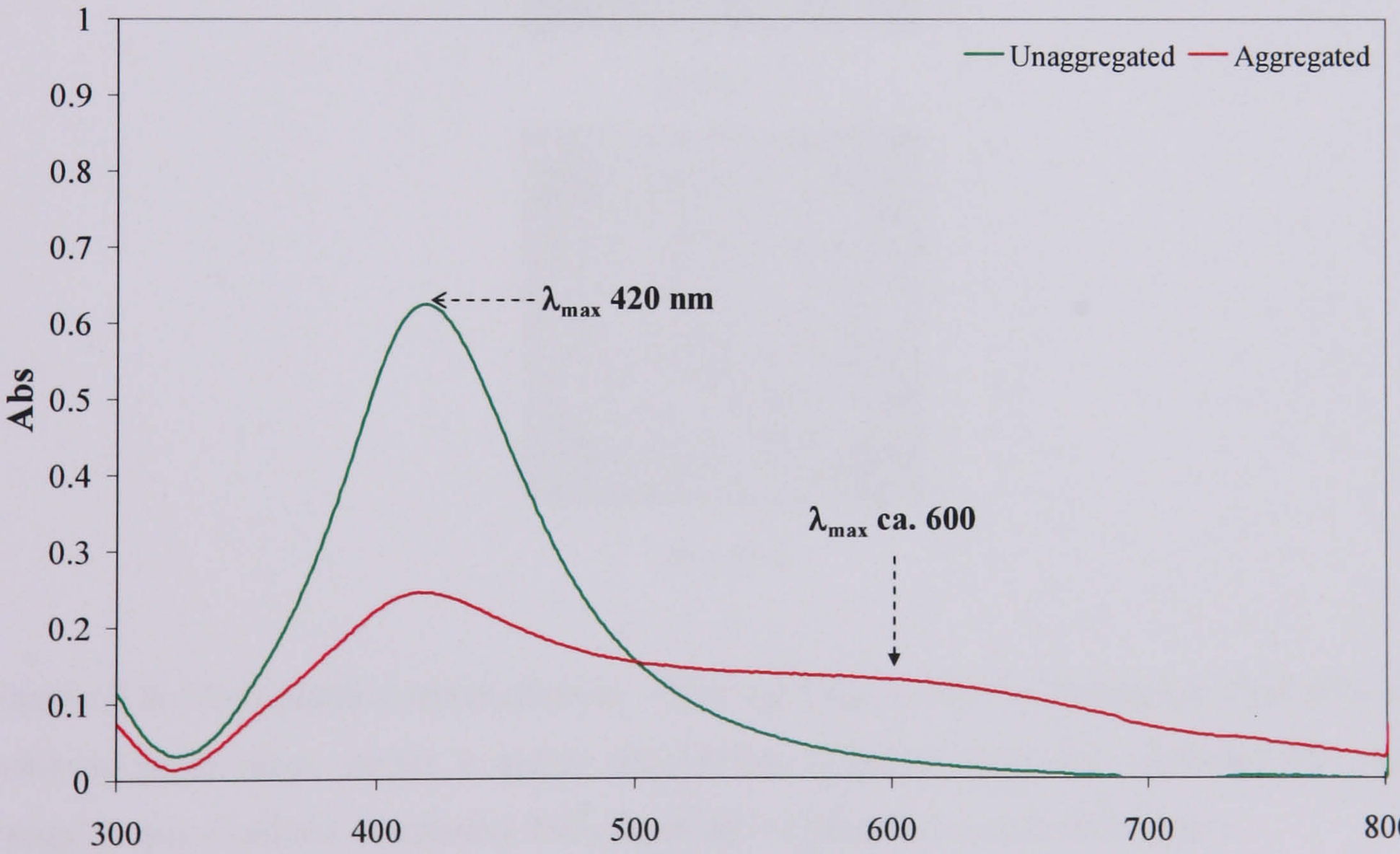

Figure 5.2: UV/VIS spectrum of citrate reduced silver colloid illustrating the shorter wavelength plasmon resonance peak.

Figure 5.3 illustrates the three phases of substrate production from the clean quartz slide (Image 1) to the appearance of the TiO_2 layer post spin coating and calcination (Image 2). The third image (Image 3) is of a substrate that has completed the production process and represents the final substrate appearance.

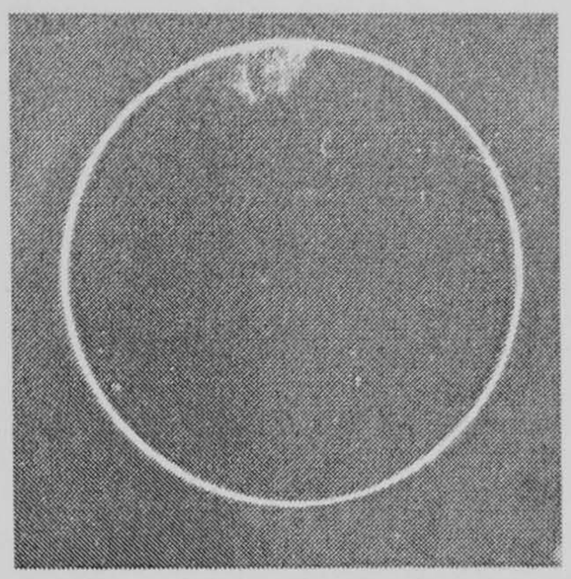

Image 1

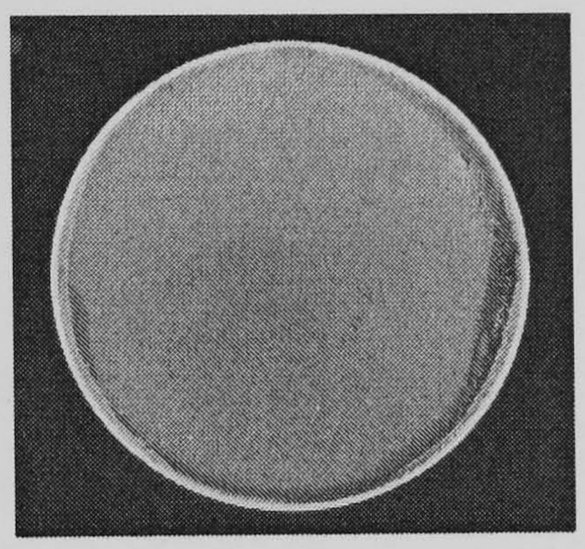

Image 2

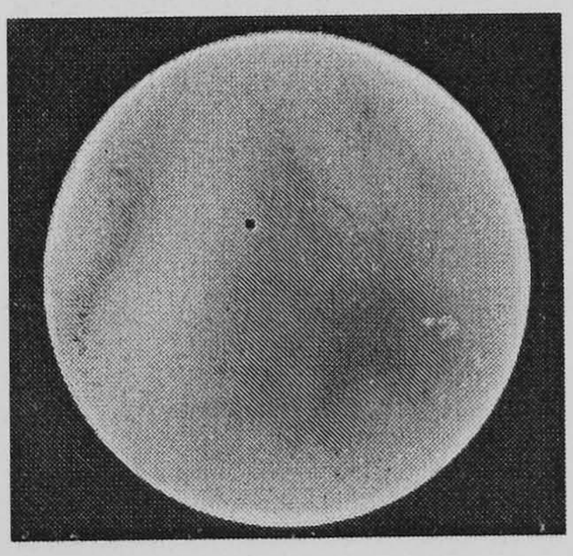

Image 3

Figure 5.3: Photographic representation of the Ag/TiO_2 substrates during the three phases of substrate production. Image 1: quartz slide, Image 2: quartz slide and calcinated TiO_2 layer, Image 3: quartz slides, calcinated TiO_2 layer with a photodeposited silver layer.

Figure 5.4 illustrates visibly the differences in depth profile between the photodeposited silver and the underlying TiO_2 layer. The upper ESEM image shows clearly that the silver deposits are discrete islands with gaps between the particles.

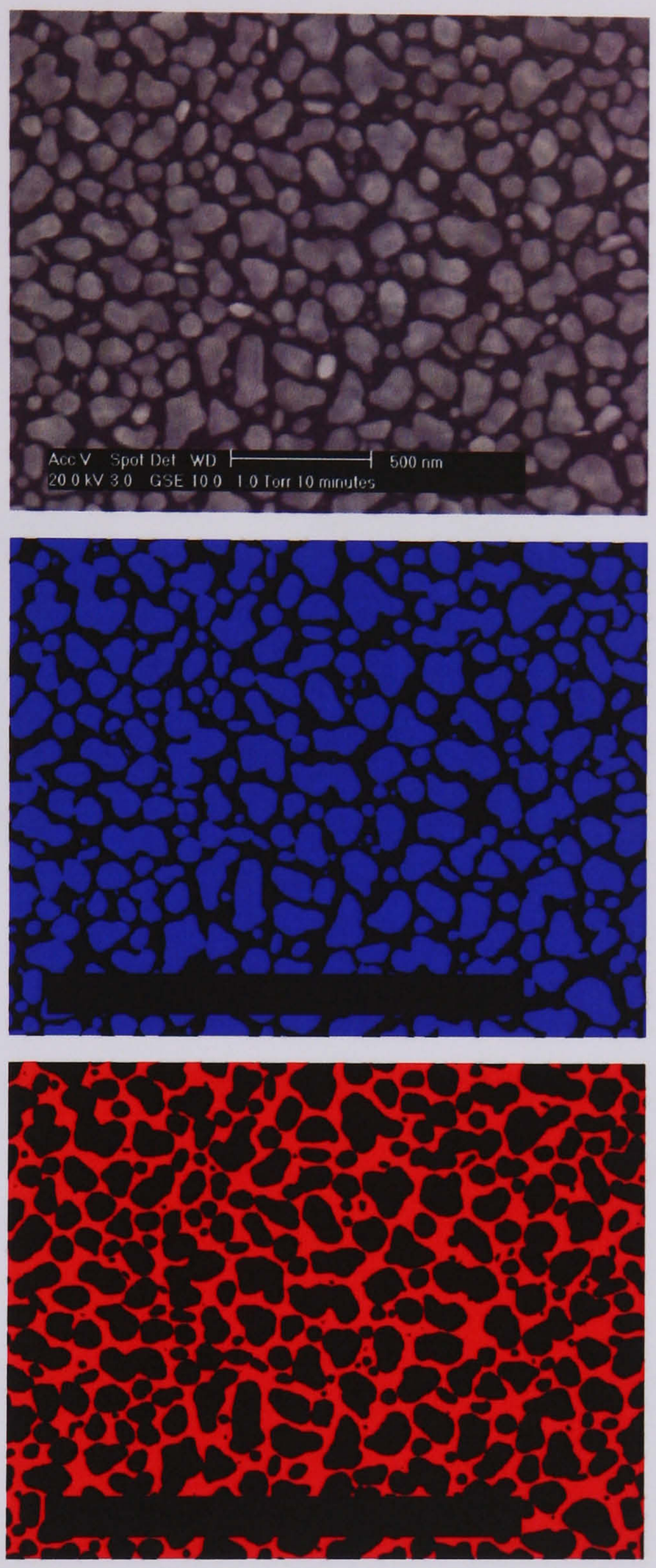

Figure 5.4: ESEM image of a substrate photodeposited for 10 minutes (top) and two images showing the area brighter with a threshold value above 67 nm, attributed to silver (blue, centre) and darker than a certain threshold value below 67 nm, attributed to substrate (red).

It is believed that the ratio of the size of the silver particles to the gap width between particles relates to the enhancement factor gained from a surface. Moskovits (2006) describes an illustration (Figure 5.5) of interparticle coupling between a molecule

residing within the interstice between two metal nanospheres. If the incoming incident beam is polarised along the interparticle axis this produces conjugate charges either side of the molecule. The proximity of the metal nanoparticle charges to the molecule induces polarisation effects within the molecule. The combination of polarised fields within the nanoparticles and the molecule results in an overall amplification of the polarisation effect across the system. Therefore, the enhancement factor achieved is d^{8} where d represents the gap between the two nanoparticles.

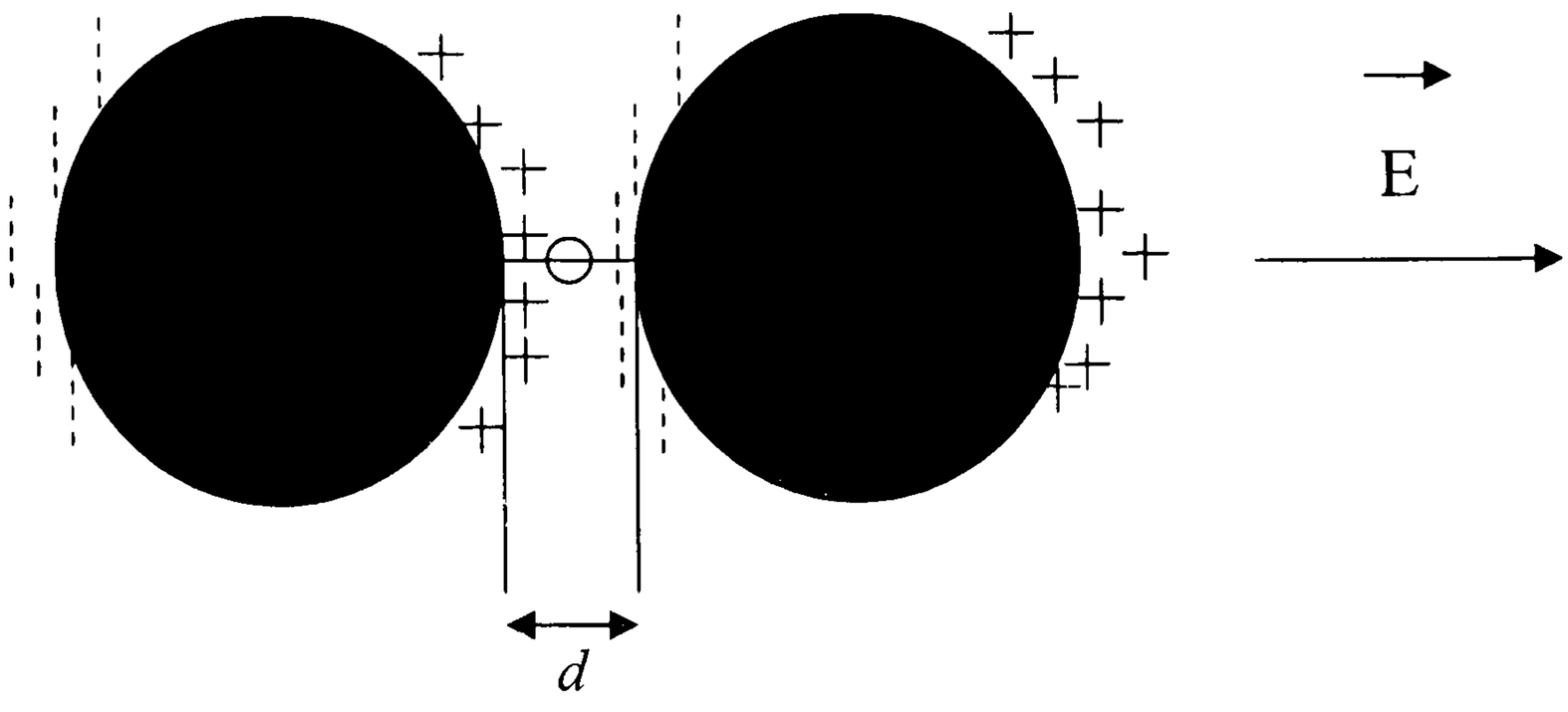

Figure 5.5: An illustration of the polarisation effects of two nanoparticles (black circles) on a molecule (white circle) when the incoming incident polarising light is polarised along the interparticle axis [Moskovits (2006)].

Consequently the suitability of these substrates for drug detection was explored in this work.

5.4 Results

5.4.1: Amphetamine

Several spectra were captured with a 10 µl volume of $1x10^{-6}$ M aqueous amphetamine but no spectral peak detail was resolved. It was apparent the volume of sample was perhaps too large for the laser beam (ca. 1 μm^2 diameter) to finely focus on the drug – substrate surface layer to observe the SERS enhancement taking place. Thus, some of the sample was wicked off using a paper towel so the final volume of

sample was approximated at 1 μl. The spot of sample was re-focused upon and exposed to the laser beam and a spectrum captured under the same conditions outlined previously.

The level of enhancement observed for the wicked sample far exceeded that observed with the silver and gold colloid solutions and the centrifuged silver and gold colloid. The spectrum captured recorded a surface enhancement figure of 32,000 counts (Figure 5.6) in comparison to the colloid spectra for the same drug which had enhancement to only a couple of thousand counts with the same concentration solutions. The SERS spectrum recorded for amphetamine showed the characteristic amphetamine doublet peak (1000 cm^{-1} $\pm$ 2cm^{-1}), along with other spectral peaks including the carbon-hydrogen stretch peaks in the range 2850 – 3000 cm^{-1}. Figure 5.7 is a spectrum of the same aqueous amphetamine solution captured from a glass surface without any silver present. Comparison of Figures 5.6 and 5.7 indicate the Ag/TiO_2 substrates are responsible for the SERS enhancement properties recorded from this solution.

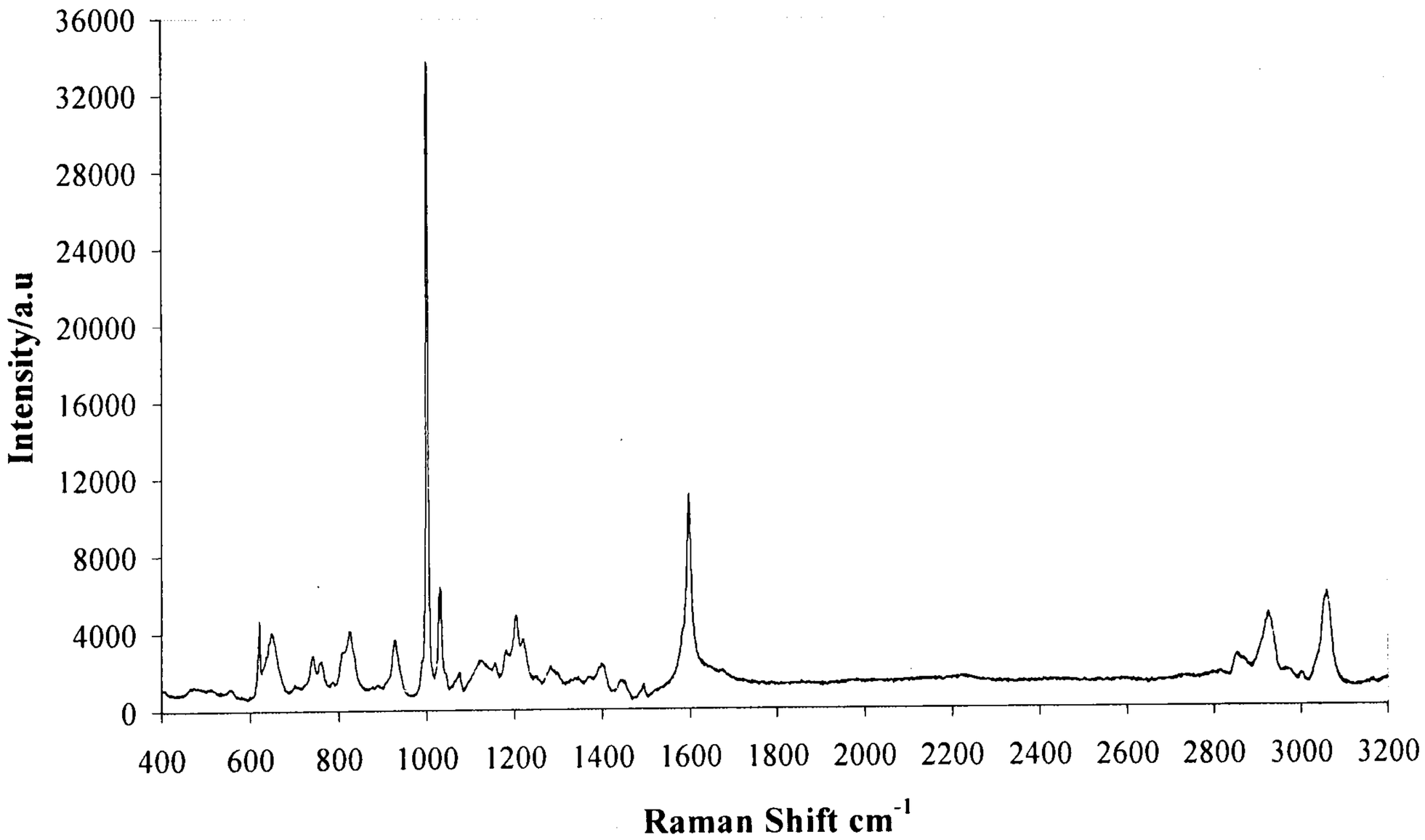

Figure 5.6: A SERS spectrum of approximately 1 μl (after wicking) of $1x10^{-6}$ M aqueous amphetamine following SERS with Ag/TiO_2 substrate.

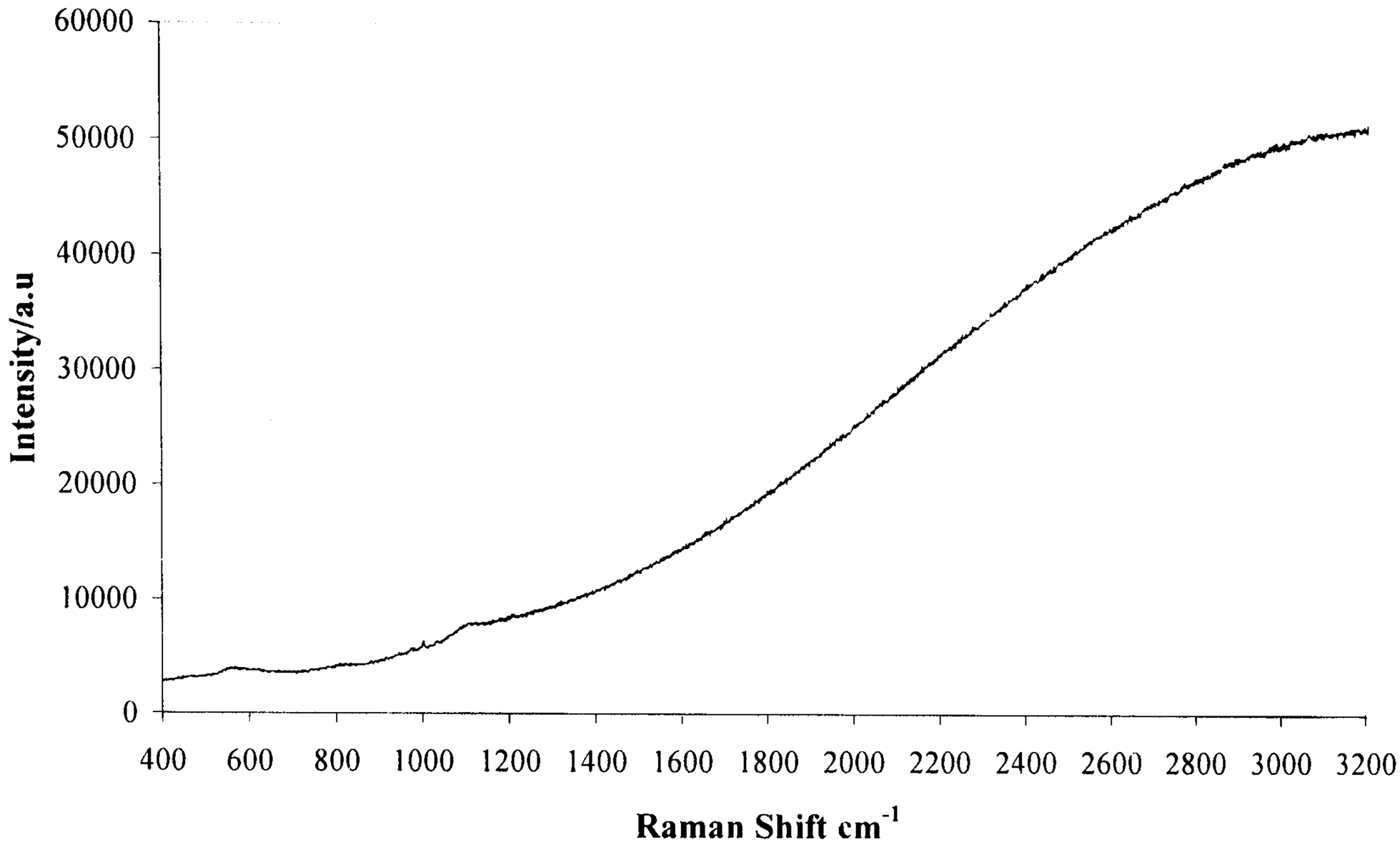

Figure 5.7: A spectrum of $1x10^{-6}$ M aqueous amphetamine recorded on a glass slide.

Figure 5.8 is an overlaid spectral presentation illustrating the background spectrum of the substrate prior to sample loading (series 1) and the peak positions from the first attempt (series 2) with approximately 1 µl (after wicking) of $1x10^{-6}$ M aqueous amphetamine solution following SERS with the Ag/TiO_2 substrates. Early indications are that the amphetamine can be identified using these types of substrates.

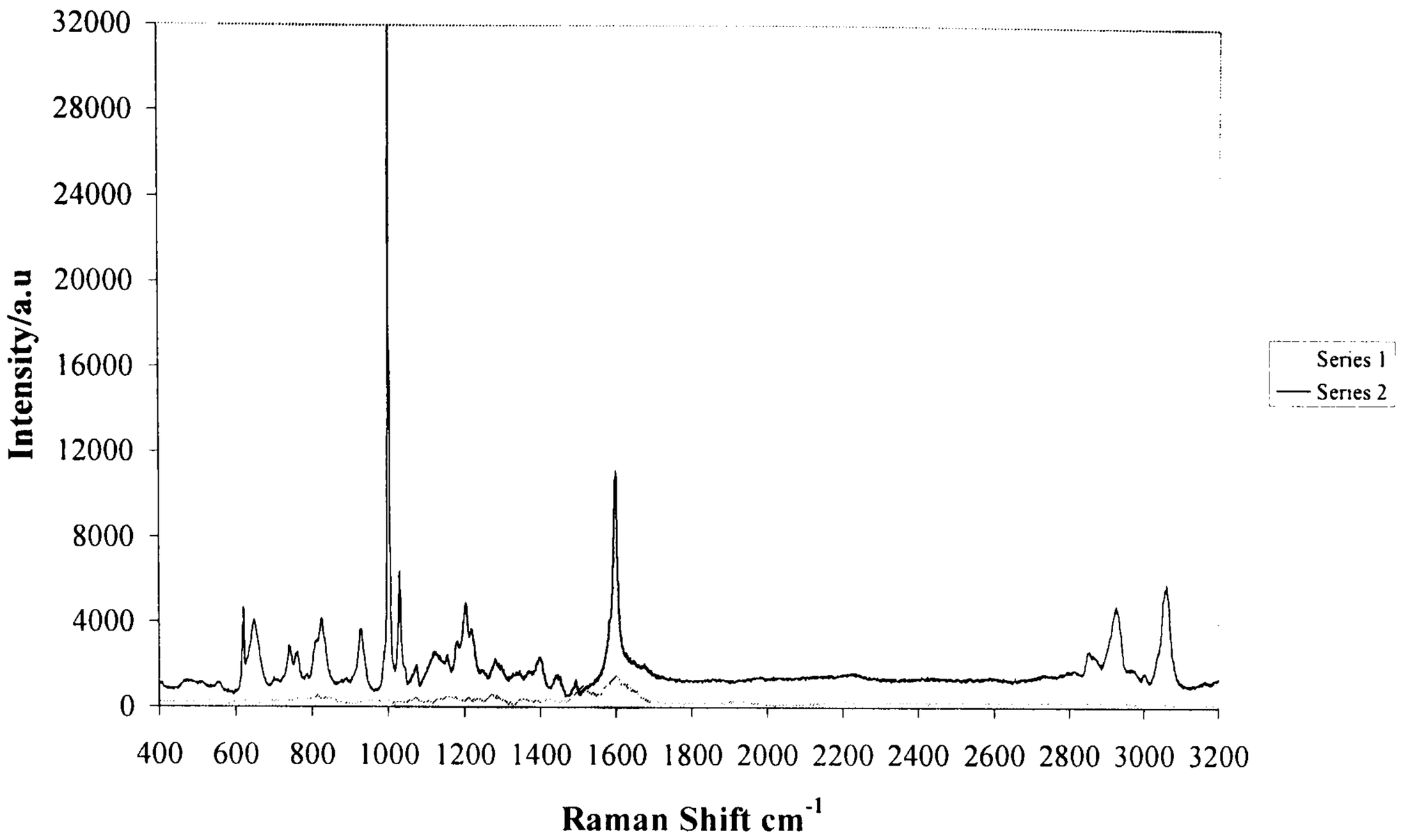

Figure 5.8: An overlaid spectral presentation of $1x10^{-6}$ M aqueous amphetamine following SERS with the Ag/TiO_2 substrates (series 2) and a background spectrum (series 2) of the substrate.

To evaluate this SERS effect further over a period of 6 minutes a $1x10^{-2}$ M amphetamine solution was analysed. Spectra were recorded from the 1 µl volume spotted onto the substrate surface initially (Figure 5.9) and then after 6 minutes (Figure 5.10) at which point the drop has evaporated sufficiently that the amphetamine is about to crystallise. It is at this point that the SERS signal is greatest (Figure 5.11).

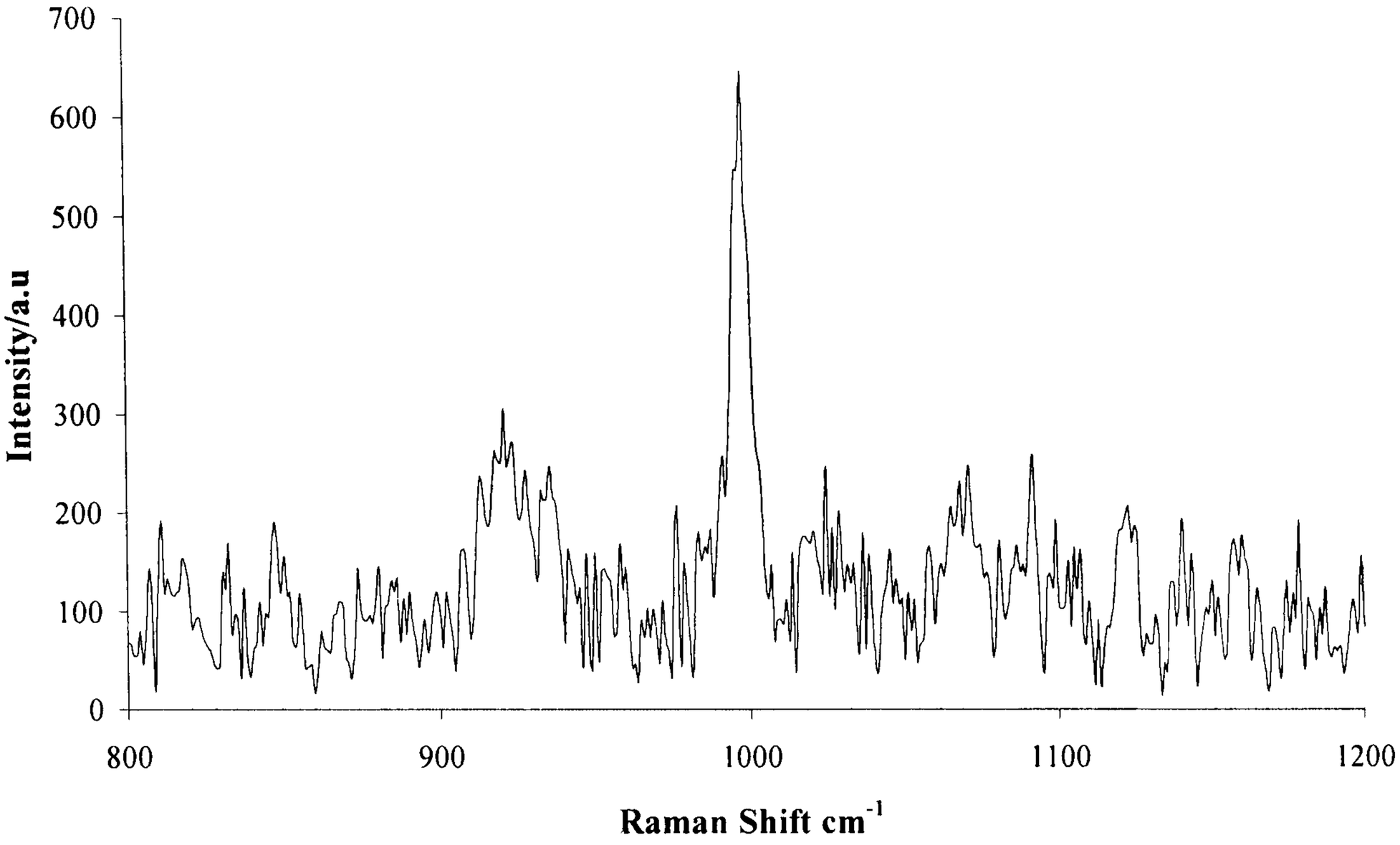

Figure 5.9: A SERS spectrum of a 1 μl volume of $1x10^{-2}$ M aqueous amphetamine solution following SERS with the Ag/TiO_2 substrates.

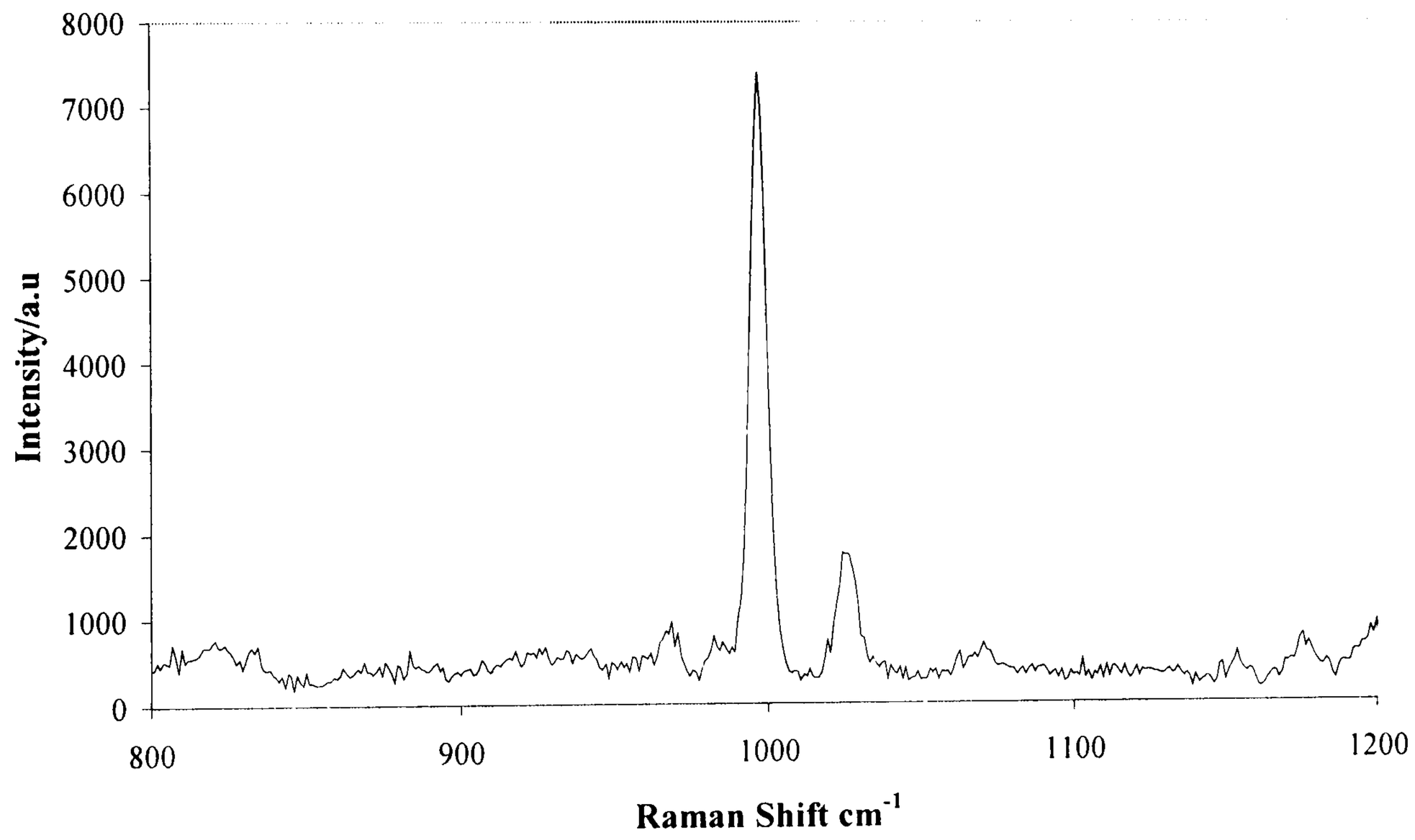

Figure 5.10: A SERS spectrum of a 1 μl volume of $1x10^{-2}$ M amphetamine just as the deposited sample begins to crystallise, 6 minutes after sample spotting.

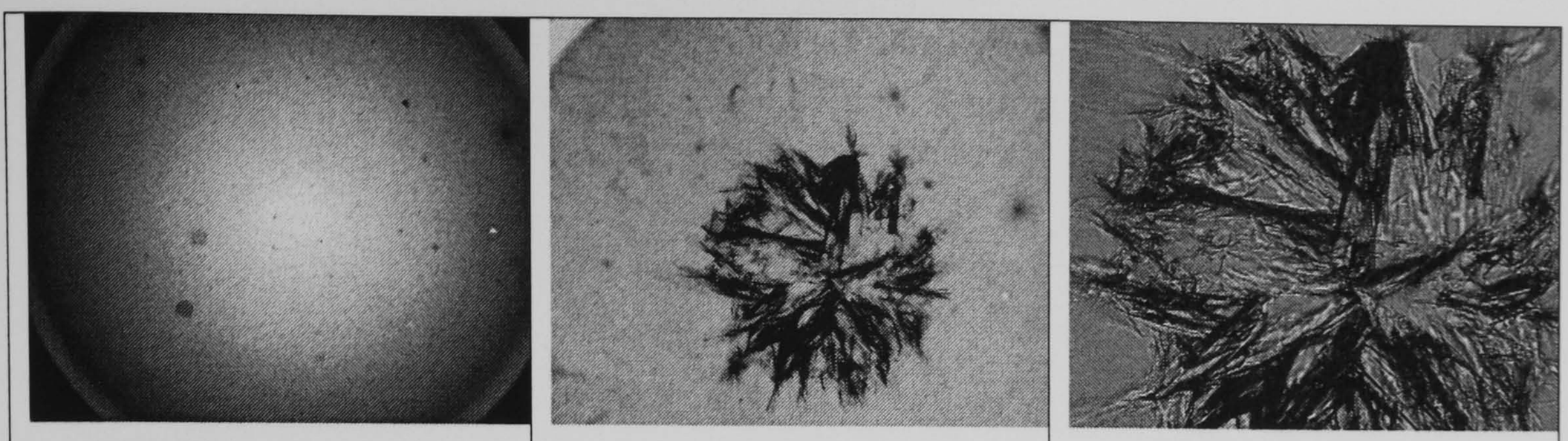

Spot of solution	Initial crystallisation surrounded by solution	Further crystallisation

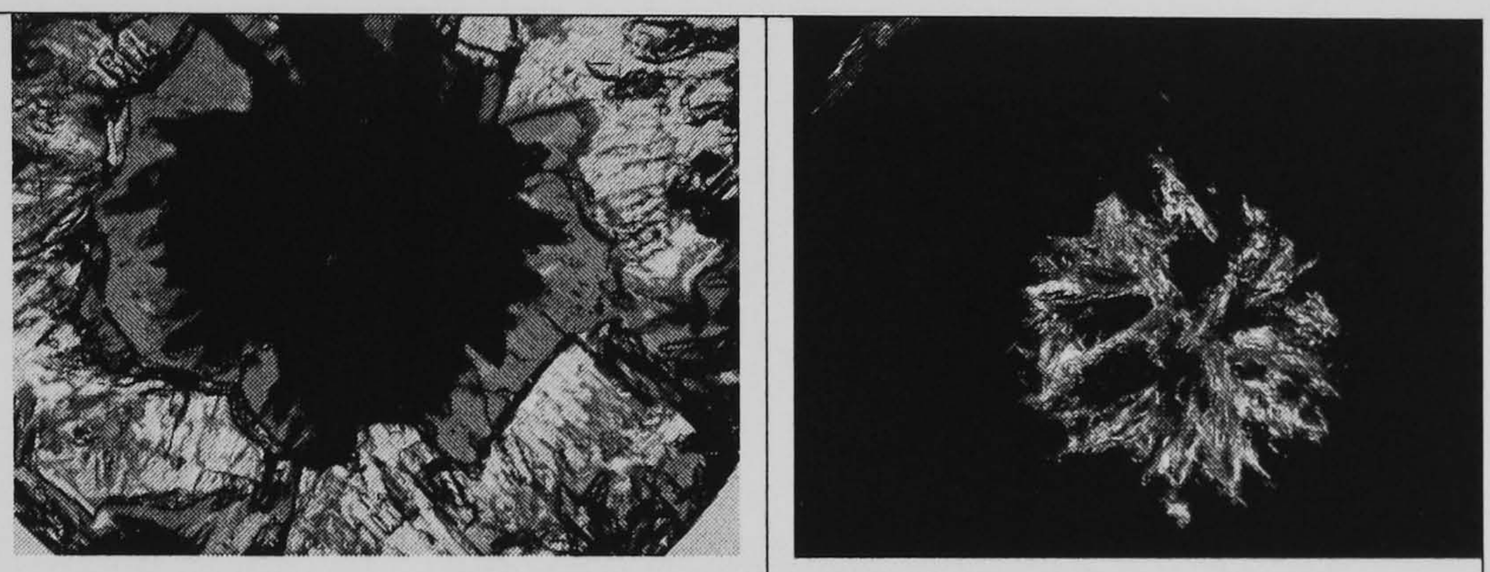

Complete crystallisation	Examination of the central crystallised area

Figure 5.11: Re-crystallisation images from a solution spot to full crystal formation. Each image is captured through the transition phases.

Figure 5.12 illustrates the change in intensity of the SERS enhancement for a 1 µl droplet of $1x10^{-2}$ M amphetamine solution on a Ag/TiO_2 substrate as a function of time and laser exposure. The change in intensity is due to solvent evaporation which causes the drug to eventually crystallise out. The maximum level of enhancement is reached when, from an optical microscopy observation, the drug is on the brink of crystallising out on the substrate surface. The laser beam is focused at the substrate surface and it is the enhanced Raman scattering from the drug mono-layer and the Ag/TiO_2 surface interaction that is responsible for the maximum enhancement. The observed enhancement is a combination of chemical enhancement, extending only to the first layer of adsorbed molecules and field enhancement which extends several tens of nanometers from the substrate surface [McCreery (2000)]. It is hypothesised that the decrease in sensitivity following this peak is caused by further layers of crystals of the drug forming which suppresses the field and chemical enhancement. Another possibility is that Raman scattering is only collected from the upper layers

of the crystals thereby giving a Raman spectrum of the drug without any surface enhancement.

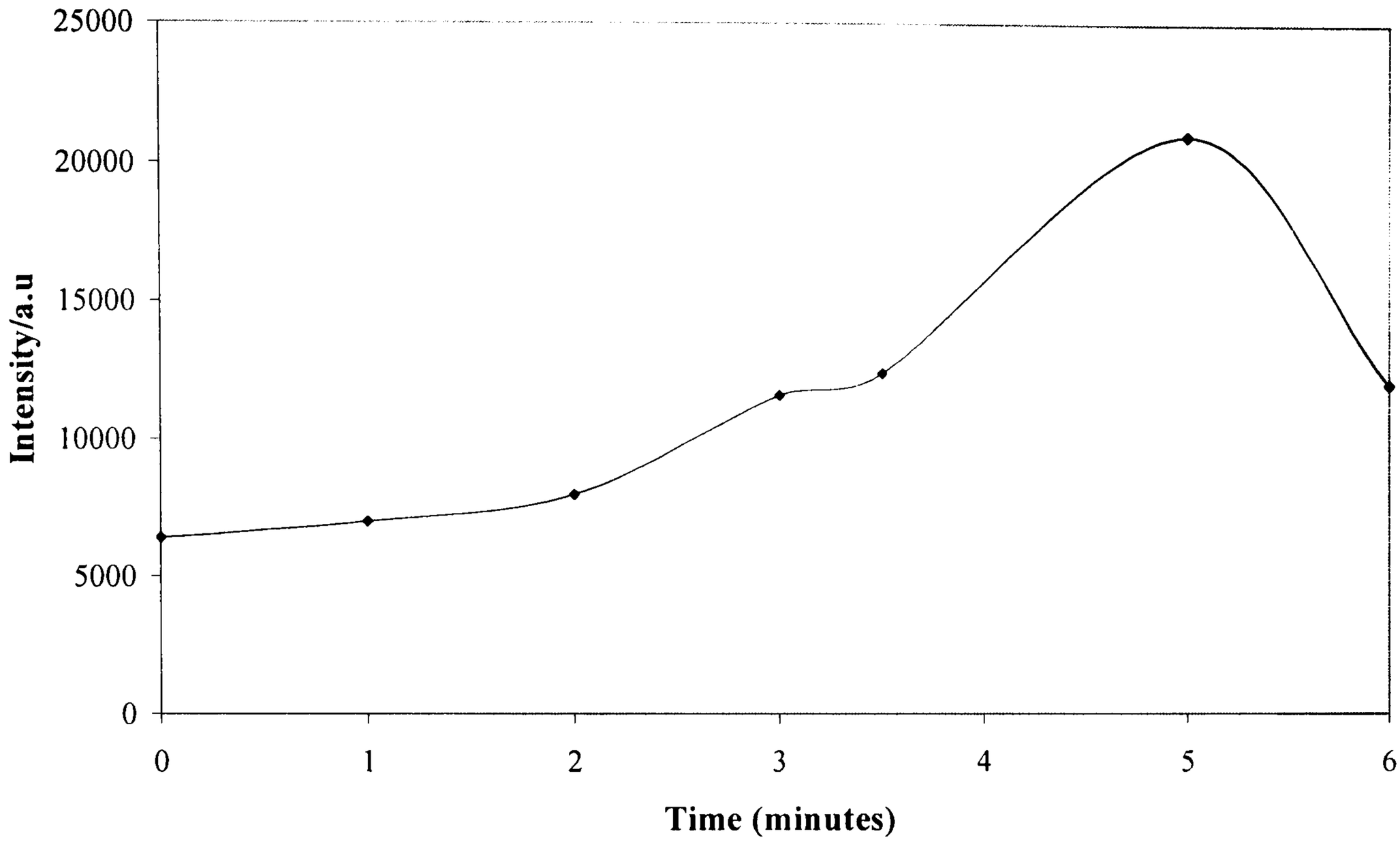

Figure 5.12: A plot of time versus SERS peak signal intensity of a 1 µl droplet of $1x10^{-2}$ M amphetamine solution peak (1000 $cm^{-1} \pm 2$ cm^{-1}) on a Ag/TiO_2 substrate.

When evaporation is complete spectra can still be recorded from the now crystalline spot but not with the same level of SERS intensity observed during the change from liquid to solid structure. A spectrum was captured from the crystalline spot area eight days later and the correct identification of the amphetamine was achieved from the peak data (Figure 5.13), although the SERS intensity was obviously very low. The reduction in sensitivity is due to the low vapour pressure of the amphetamine resulting in evaporation.

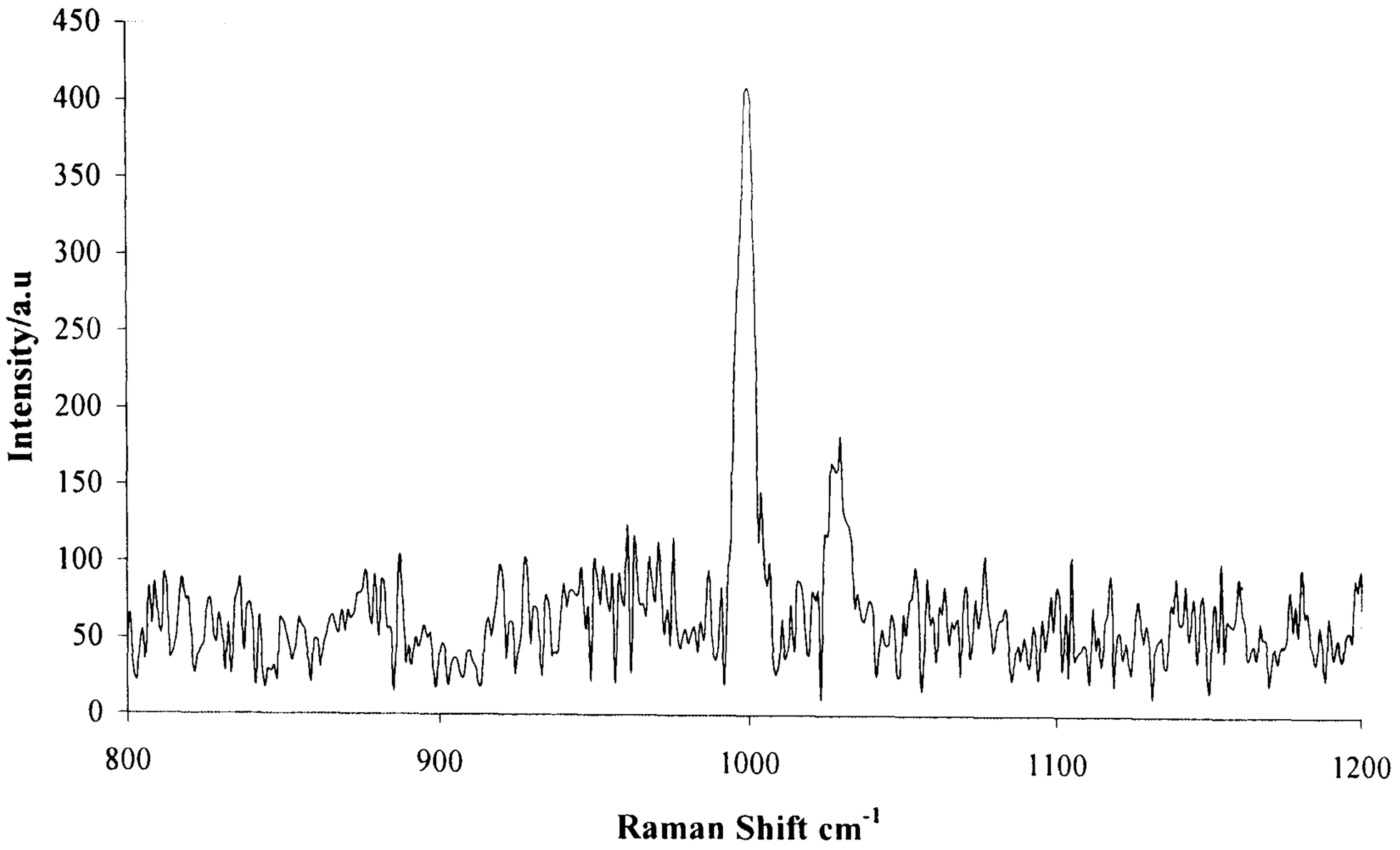

Figure 5.13: A SERS spectrum collected from an eight day old $1x10^{-2}$ M aqueous amphetamine crystalline pattern left on the Ag/TiO_2 substrate surface. The substrate had been exposed to the environment without any protection. The reduction in level of observed SERS can be seen when compared to Figure 5.10 when it was originally collected.

Subsequent attempts to reproduce the SERS spectra of amphetamine on Ag/TiO_2 substrates with similar levels of enhancement have proved difficult. Typically, signal peaks of 1000 counts were obtained in subsequent work and this is far short of values of 32,000 obtained initially. It is unclear why this is, although Ag/TiO_2 substrate reproducibility and sample delivery and sampling are possible causes.

Thus, in a typical experiment a 1 μl volume of aqueous amphetamine solution was dropped onto the surface of the substrate. The sample was exposed to the laser and a continuous spectrum was captured over a 5 second period. Over time when the 1000 $cm^{-1} \pm 2\ cm^{-1}$ peak was focused upon the spectral peaks began to sharpen in intensity as measured by the number of counts recorded (Figure 5.14). The sharpening of the peak was accompanied by a reduction in volume of the sample as it dehydrated under the laser beam. This finding indicates that the 1 μl volume of solution may still be too much to gather immediate spectral data from the sample and identify the illicit drug present. However, this could be due to a change in the microscope objective

from x50 to x20 for these experiments. It was changed because of problems focusing due to sample bead formation on the surface.

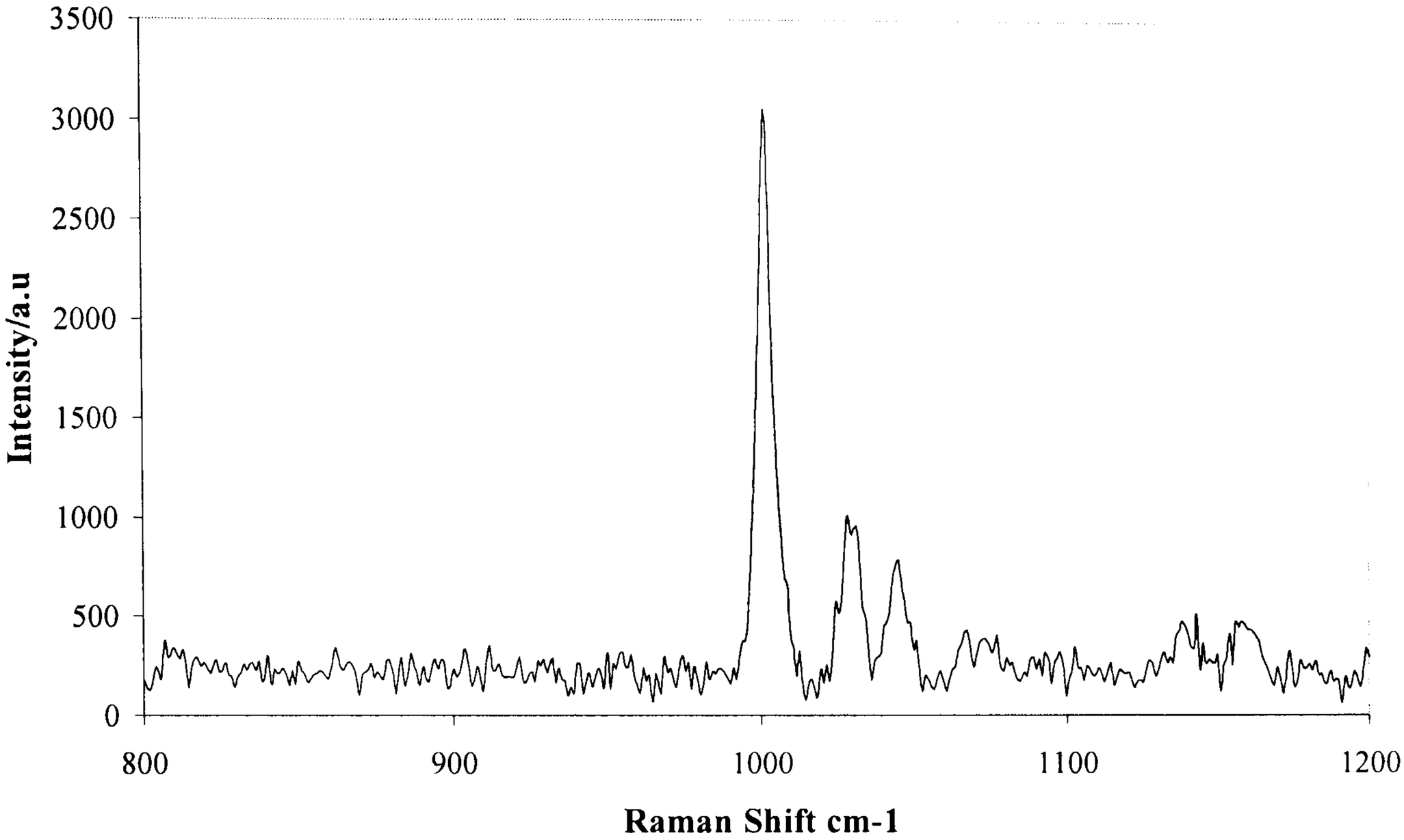

Figure 5.14: SERS spectrum from 1 µl volume of $1x10^{-6}$ M aqueous amphetamine solution on an Ag/TiO_2 substrate using a x20 microscope objective. Overall the enhancement observed is not as large in comparison to the levels previously observed (Figure 5.10).

5.4.2 Methamphetamine

The SERS spectra of methamphetamine was studied using the Ag/TiO_2 substrates. Crystalline Raman and IR spectra (Figure 5.15) and the accompanying peak data table (Table 5.1) for methamphetamine can be compared with the SERS spectra generated using the Ag/TiO_2 substrates for peak identification. 1 µl volumes of aqueous methamphetamine at concentrations of $1x10^{-5}$ M, $1x10^{-6}$ M and $1x10^{-7}$ M were investigated. The higher concentration solution produced a greater level of SERS with just under 40,000 counts (Figure 5.16) recorded for the doublet peak. The doublet peak is present in all of the substituted amphetamines along with other peaks depending on the illicit substance being detected and is due to ring-breathing transitions. The $1x10^{-6}$ M concentration solution also produced spectral peaks with 11,000 - 12,000 counts. However, a $1x10^{-7}$ M solution was tried and no peaks were observed for reasons that remain unclear.

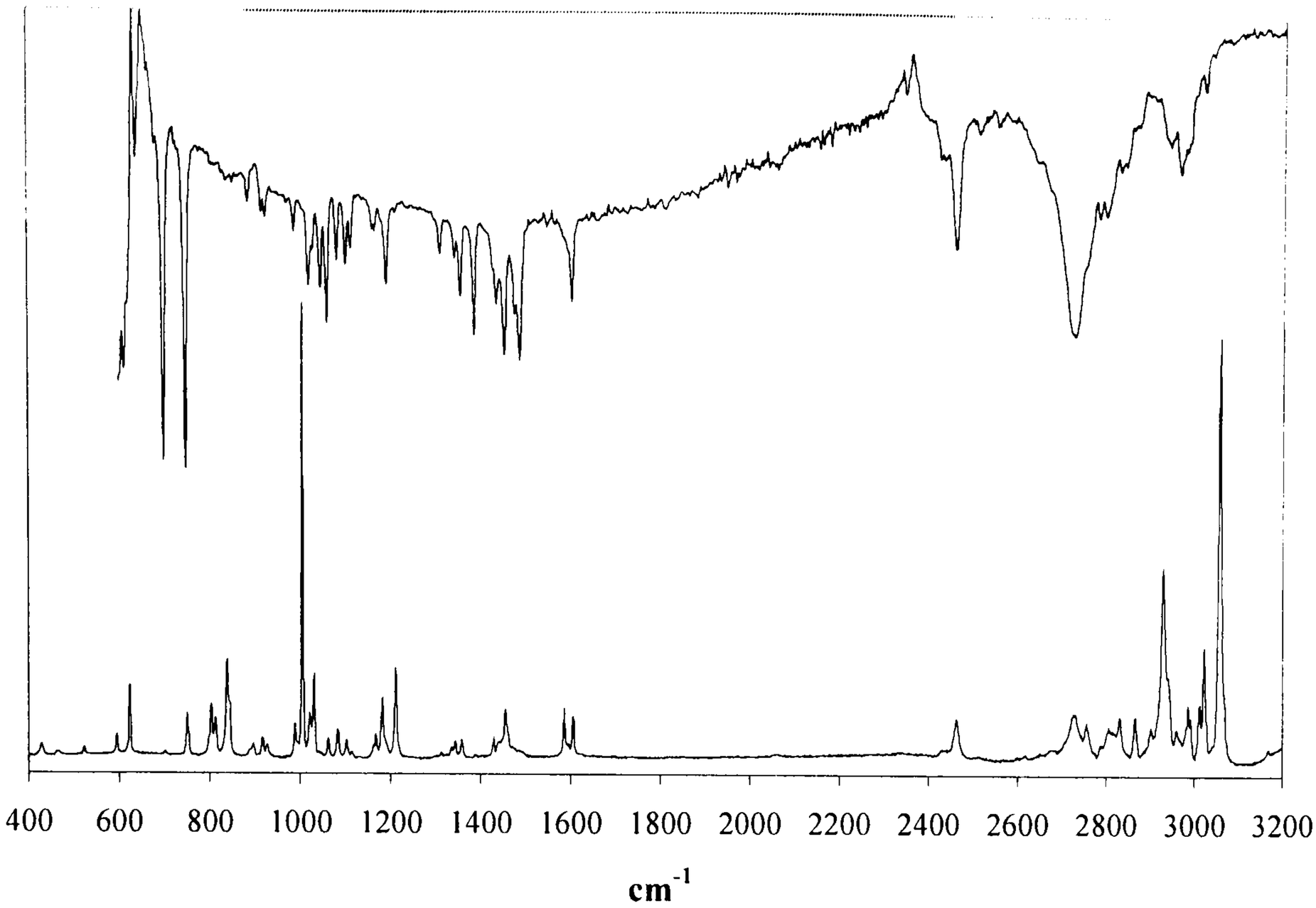

Figure 5.15: Raman (lower spectrum) and IR (upper spectrum) spectra of crystalline methamphetamine hydrochloride.

Table 5.1: Raman and IR peak position data and the molecular vibration associated with that peak for methamphetamine hydrochloride [Lin-Vien *et al* (1991), Moffat and Widdop (2004)].

Raman		**IR**	
Peak Position cm^{-1}	**Movement**	**Peak Position cm^{-1}**	**Movement**
632.2	Ring deformation, monosubstituted benzenes	747.0	CH_2 rock
750.6, 803.3	Ring Vibration	698.0, 1060.0	monosubstituted benzene
988.5, 1004.5, 1030.7	Trigonal ring breathing, monosubstitutes benzenes		
1083.4	CC Stretches, n-alkanes		
1211.5	Ring Vibration		
1455.4	CH_2 / CH_3 deformations		
1586.4, 1606	Ring Stretches		
2831.5, 2865.4	Symmetric CH_2 / CH_3 stretch		
2929.1	Anti-symmetric CH_2 stretch		
3022.6	CH_2 stretches		
3057.7	Aromatic CH stretch		

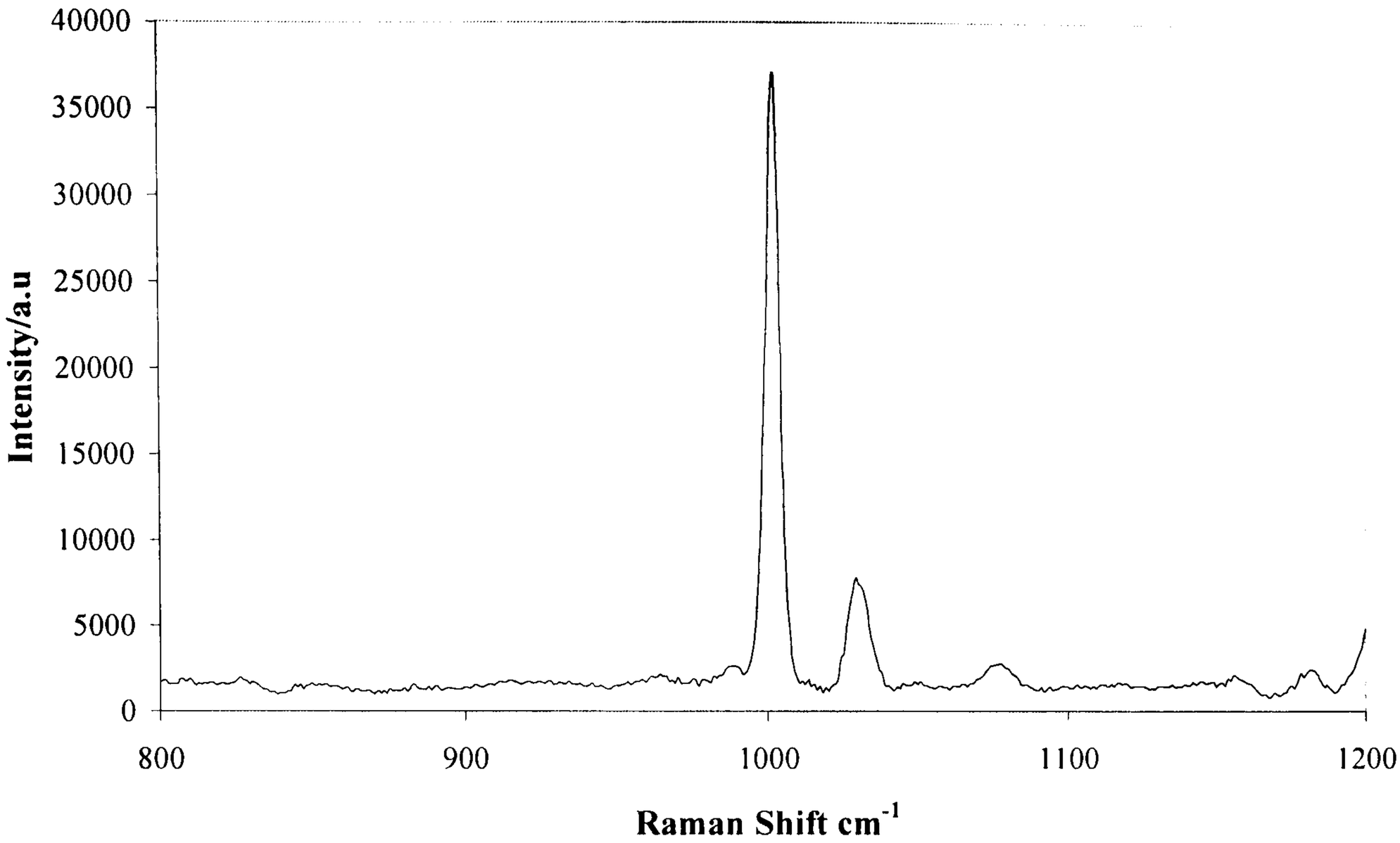

Figure 5.16: A SERS spectrum of a 1 µl volume of a $1x10^{-5}$ M aqueous methamphetamine solution.

5.4.3 MDEA

A 1 µl volume of a $1x10^{-7}$ M aqueous MDEA solution (Figure 5.17) was analysed and peaks were observed including the 1000 cm^{-1} peak $\pm$ 2 cm^{-1}. However, this result was only observed once even after repeat sample loading. This could be caused by the solution concentration or by the age of the solution used. Crystalline artefacts were observed on the surface of the substrate but no peaks were resolved upon spectrum capture.

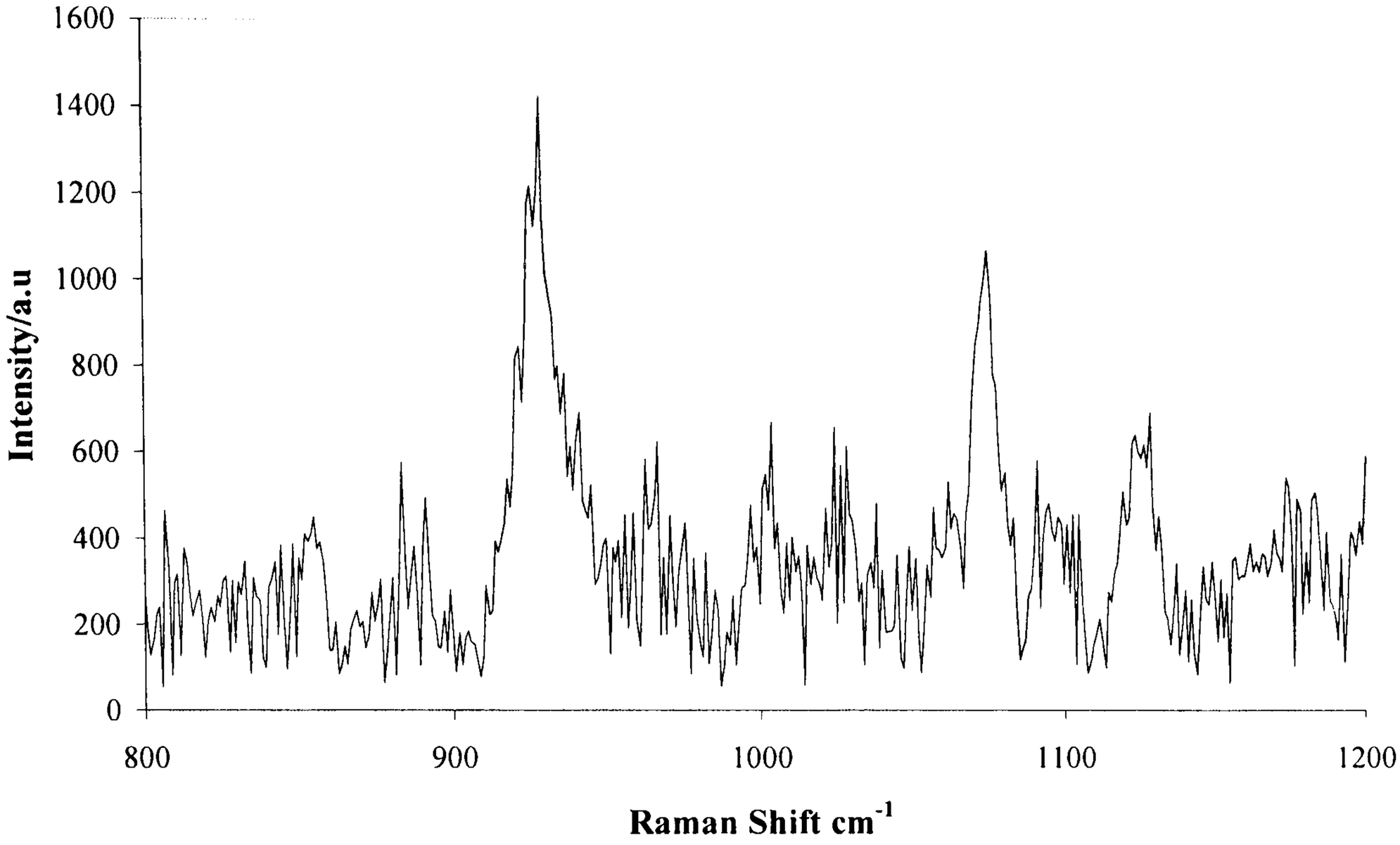

Figure 5.17: A SERS spectrum of a 1 μl volume of a $1x10^{-7}$ M aqueous MDEA solution. A peak at 1000 $cm^{-1} \pm 2$ cm^{-1} is just visible.

5.4.4 Cotton Swabs

A $1x10^{-6}$ M amphetamine solution was analysed following absorption onto a cotton swab and dabbing it onto the substrate surface. Spectral peaks were resolved and the characteristic peak at 1000 $cm^{-1} \pm 2$ cm^{-1} was also present (Figure 5.18). With continued analysis time the intensity of the peak observed increased to just under 1600 counts. Although the level of enhancement was not as great as has been observed before, the result is significant in several ways. Firstly, this indicates that it is possible to collect and load samples onto the substrate directly using a simple technique that could be employed for the collection of an oral fluid sample. Secondly, it indicates that sufficient sample volume can be transferred and analysed to observe the SERS activity of the aqueous solutions and lastly it shows that low concentrations of drug can be detected using this technique.

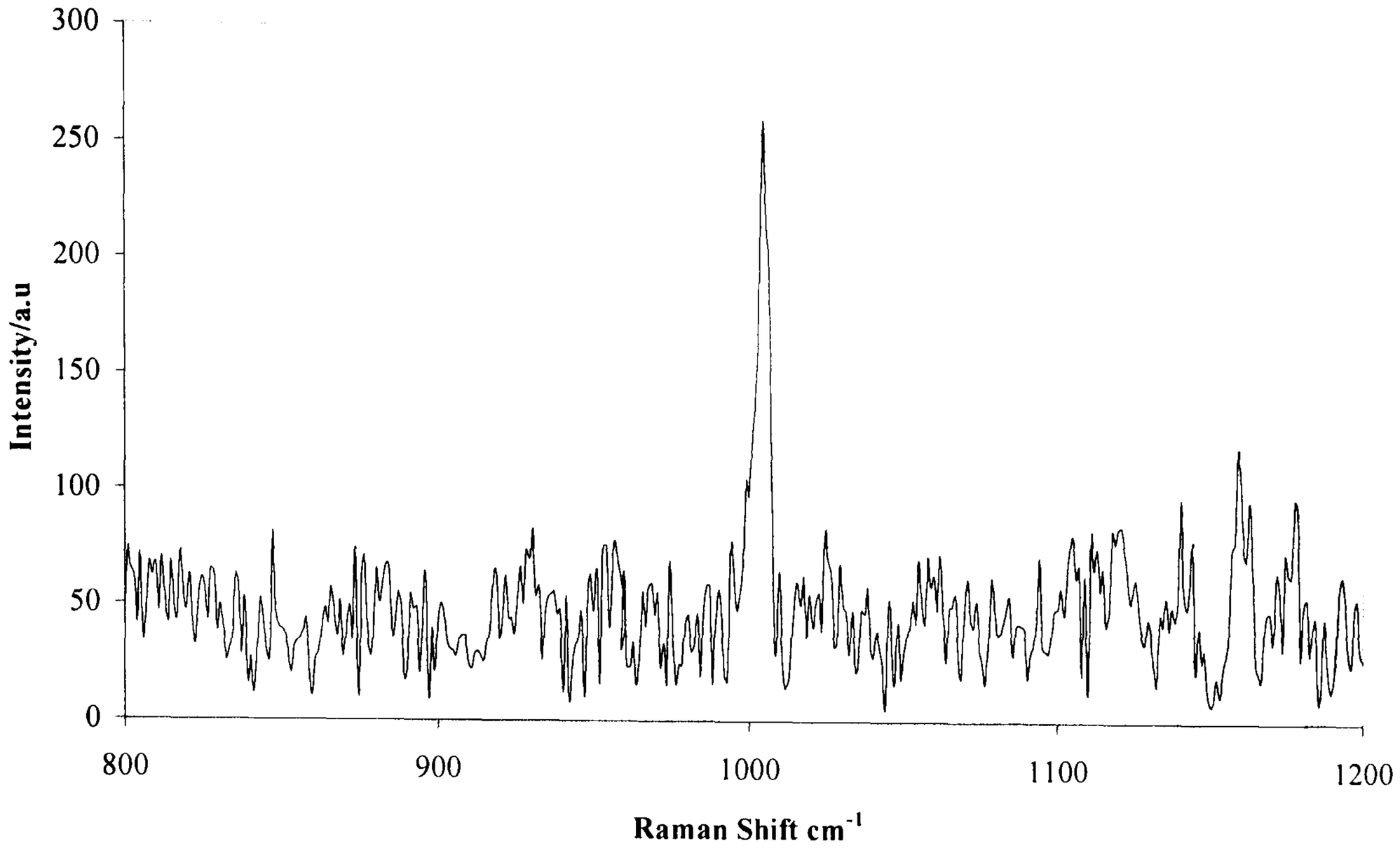

Figure 5.18: A SERS spectrum of $1x10^{-6}$ M aqueous amphetamine solution loaded onto a cotton swab and dabbed onto the surface of the substrate.

5.5 Conclusions

This experimental work has demonstrated the use of SERS to detect three phenethylamine derivatives through the use of silver based substrates other than colloid solutions or centrifuged colloid. The level of enhancement observed here using Ag/TiO_2 substrates in some cases exceeds that observed using both silver colloid and silver evaporated substrates.

Further research into the optimum working conditions of these substrates is required. The volume of solution used is a critical factor in observing the SERS effect at its greatest capacity. Tentative results from this experimental work carried out on the 633 nm laser system have indicated that this is a good wavelength of excitation for screening for the phenethylamines using Ag/TiO_2 substrates at least.

The characteristic amphetamine doublet peak so readily identified in amphetamine/silver colloid work was present in all the spectra recorded. This experimental work identified that surface enhancement of aqueous $1x10^{-6}$ M (368.49 ng/ml) amphetamine solution could again be observed on the Ag/TiO_2

substrates. Surface enhancement was also observed with a solution of methamphetamine at concentrations of $1x10^{-5}$ M (1856.9 ng/ml) and $1x10^{-6}$ M (185.69 ng/ml) and with MDEA at $1x10^{-7}$ M (24.37 ng/ml). In addition the 1 µl volume has been identified as the maximum volume that should be used, although to properly observe the drug/surface interaction and respective SERS effect a 0.5 µl volume is more efficient. At the present time solutions with a concentration of $1x10^{-7}$ M cannot be detected reproducibly using the Ag/TiO_2.

Timing of the collection of the spectra is also important because if taken too soon, little SERS activity is recorded and if taken too late only limited information is obtained if a thick layer of crystals have formed. The length of time taken for the sample to begin to evaporate may be reduced by using the cotton swabs instead of placing a bead of liquid on the surface of the substrate using a syringe. However, the cotton swab does not allow control of the volume of sample deposited onto the surface of the substrate so it can only be estimated.

The use of cotton swabs for sample application onto the surface of the substrate is a viable practical option both in terms of experimental and field work. It has demonstrated that SERS can be observed using this technique and at low concentrations.

5.6 Future Work

In the next chapter, Comparison of Silver and Gold Substrates for SERS Enhancement of Aqueous Amphetamine Solution, the SERS activity of several silver and gold substrates will be examined including; Ag/TiO_2, gold titanium dioxide (Au/TiO_2), sputtered silver, silver PVA, immobilised silver colloid and the commercially available Klarite substrate. These substrates will be investigated with $1x10^{-2}$ M (3.68 mg/ml) to $1x10^{-7}$ M (36.84 ng/ml) aqueous amphetamine solution. Additionally, the process of drop crystallisation in comparison to the SERS signal build-up will also be investigated. A UV pre-cleaning step will also be assessed for any improvements in the SERS signal.

Chapter 6

Comparison of Silver and Gold Substrates for SERS Enhancement of Aqueous Amphetamine Solution.

6.1 Introduction

In the previous chapter, application of aqueous amphetamine solution resulted in a bead of liquid on the surface. This indicated a large contact angle between the sample and the surface. Investigations were undertaken to reduce the contact angle to maximise the level of SERS signal captured from the sample.

To improve the contact angle the substrates were irradiated with UV light. It has been shown that the hydrophilic nature of the titania substrates is much improved by such a treatment, most likely by removing hydrophobic surface organic impurities by UV-driven photocatalytic processes Mills and Lee (2003).

The Ag/TiO_2 substrates were produced as previously described in Chapter 5.2.1 with a photodeposition time of 40 minutes and further information can be found in Mills *et al* (2004).

A comparative study was also undertaken investigating the SERS enhancement of different silver and gold surfaces. These included; Ag/TiO_2, Au/TiO_2, sputtered silver, silver PVA and immobilised silver colloid substrates and commercially available Klarite gold substrates. The lower limit of detection for these substrates was also assessed. This work was undertaken jointly with Martin Stewart at Strathclyde University.

A further method involving heating the Ag/TiO_2 substrates in an oven at 110°C for 3 minutes with the $1x10^{-4}$ M (0.03 mg/ml) aqueous amphetamine solution sample drop in position, showed no improvement in SERS signal versus previously tried methods. Limited spectral peak information was recorded. Consequently this method was not used in subsequent experiments.

6.2 Experimental

6.2.1 Ag/TiO_2 Substrate Preparation

The Ag/TiO_2 substrates were prepared using the method described in Chapter 5.2.1.

6.2.2 Au/TiO_2 Substrate Preparation

The Au/TiO_2 films were produced using a similar method as the Ag/TiO_2 films. The solgel films were prepared as previously described and then irradiated in a solution of $5x10^{-4}$ M gold chloride solution (50% methanol, 50% water). Once removed they were washed with purified water and left to air dry.

6.2.3 Sputtered Silver Substrate Preparation

The sputtered silver films were produced by placing a glass cover slip in an Edwards Coating Evaporator. The evaporator was evacuated to $5x10^{-5}$ mBar. The appropriate values were entered into the Intellimetrics IL 100 Thickness Monitor, which uses a quartz crystal oscillator to measure film thickness. The current at the molybdenum boat was increased until it glowed orange indicating the start of deposition. The deposition was undertaken at a slow rate of 0.01 nms^{-1} producing an even coat until the desired overall film thickness of 9 nm was reached. Once complete, the air was re-admitted to the chamber and the sample removed and stored in plastic bags until required for use [Stewart (2005)].

6.2.4 Silver PVA Substrate Preparation

The silver PVA films were prepared by stirring 0.40 g silver nitrate and 1.6 ml of 5% aqueous PVA solution for twenty-four hours at room temperature. The mixture was spin coated onto a glass cover slip at 400 revolutions per second for 30 seconds. The films were left to dry overnight at 60°C under vacuum and then dried at 100°C for 2 hours. Once dried the films were dipped for 20 minutes in a solution of w/w $FeSO_4$ (5 g $FeSO_4$ and 5 mls of water) to reduce the silver to Ag^0. The films were then dried at 110°C for 15 minutes before being washed thoroughly with purified water [Stewart (2005)].

The films were produced on pre-cleaned glass slides (cleaned with acidic permanganate solution for 1 hour and then rinsed with water several times and once with methanol). A solution of 2% APTMS ((3-Aminopropyl) trimethoxysilane) in 95% ethanol and 5% water was made and left for 10 minutes to settle. It was then poured into a slide bath containing the glass films for 10 minutes and gently shaken to ensure the films were evenly coated. The remaining silane solution was poured off and the films rinsed with methanol twice. Once complete they were placed in an oven held at 110°C for 1 hour to cure [Stewart (2005)].

After curing the films were rinsed again with methanol and transferred to a slide bath which was filled with methanol and placed in an ultrasonic bath to remove any silane traces. The slide bath was then rinsed with methanol twice and then distilled water several times. The films were then immersed in silver colloid for 16 hours. Once complete the remaining silver is poured off and the films dried on the bench before being stored in plastic bags [Stewart (2005)].

6.2.5 Klarite Substrate Preparation

Klarite substrates were purchased from Mesophotonics, Southampton. Klarite substrates are designed with a repetitive pattern at the sub-micorn scale. A layer of gold coats an underlying silicon surface which comprises regular arrays of holes. This regular pattern gives rise to photonic crystals which ultimately control the surface plasmon activity on the surface.

6.2.6 Spectral Collection

SERS spectra were recorded using the equipment described in Chapter 4.2.3.

6.2.7 SERS Analysis

All SERS spectra unless otherwise stated were recorded using the x50 microscope objective, for 5 seconds accumulation time. Solution concentrations of $1x10^{-2}$ M (3.68 mg/ml) $1x10^{-3}$ M (0.36 mg/ml) and $1x10^{-4}$ M (0.03 mg/ml) aqueous amphetamine solution were used for all studies. Additional solution concentrations of $1x10^{-5}$ M (3684.9 ng/ml), $8x10^{-6}$ M (2947.92 ng/ml), $6x10^{-6}$ M (2210.94 ng/ml), $4x10^{-6}$ M (1473.96 ng/ml), $2x10^{-6}$ M (736.98 ng/ml), $1x10^{-6}$ M (368.49 ng/ml),

$1x10^{-7}$ M (36.84 ng/ml) were used for the lower limit of detection study. A 0.5µl volume of sample solution was placed, using a syringe, directly onto the silver surface. For each substrate four spots of solution were analysed with three spectra collected from each spot. Blank substrate spectra were also taken to record the presence of any background activity within the substrate.

Recorded spectra were saved and peak height information recorded by measuring each peak positioned at 1000 cm^{-1} $\pm$ 2 cm^{-1}, a characteristic peak for aqueous amphetamine sulphate solution. The peak heights were recorded by measuring the same points on each spectrum, the lowest nearest peak count number, the top of the peak count number and then subtracting the two to obtain the response. The definition used as to what constitutes a peak was a response above a signal to noise ratio of 4. If less than 4 a 'no peak' was recorded and scored as 0 counts. However, the lack of a peak may be due to the response saturating the CCD.

6.2.8 Klarite Substrate Collection Parameters

Each batch was analysed using aqueous amphetamine sulphate solutions at a concentration range of $1x10^{-3}$ M to $1x10^{-7}$ M. A 0.5 µl volume of sample was placed in the corner of the substrate and analysed three times. Each substrate was tested with all five concentrations with the sample confined to the corners except for the $1x10^{-7}$ M which was loaded onto the centre of the substrate. The small volume of sample ensured the different concentrations did not overlap. The evaporated residue was located by a characteristic 'coffee ring' [Deegan *et al* (2000)] pattern left on the surface. A total of forty-eight Klarite substrates were analysed from 12 batches. Nine spectra were collected from each drug spot. Three background spectra prior to any sample loading were also recorded.

6.3 Results

6.3.1 UV Irradiation Pre-cleaned Ag/TiO_2

Following UV irradiation pre-cleaning as described in the introduction, 0.5 µl of $1x10^{-3}$ M aqueous amphetamine solution was placed on the substrate and immediately the contact angle between the sample and the substrate decreased and the sample wetted the substrate surface. When analysed with the Raman system the characteristic peak at 1000 cm^{-1} ± $2cm^{-1}$ associated with the presence of amphetamine was observed, Figure 6.1, showing an enhancement of approximately 14,000 counts.

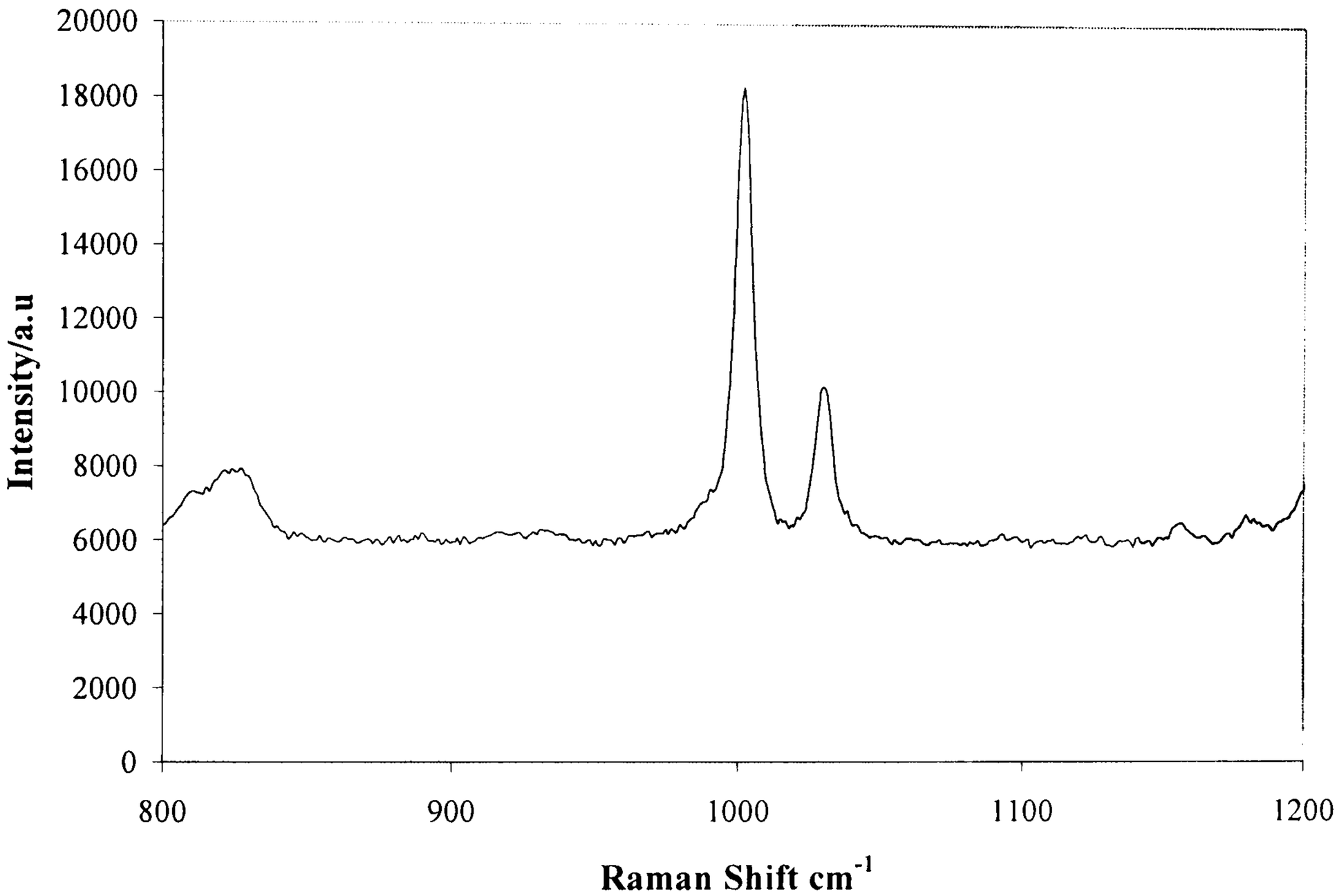

Figure 6.1: A spectrum of aqueous amphetamine solution with a Ag/TiO_2 substrate that has undergone pre-cleaning with spectroscopic methanol and 3 minutes UV irradiation.

Figure 6.2 is of a spot of $1x10^{-3}$ M aqueous amphetamine loaded onto an Ag/TiO_2 substrate with no surface pre-cleaning. This figure shows enhancement of approximately 5000 counts and only a single peak is visible in the spectrum. This peak is positioned at 989 cm^{-1} which is associated with the presence of amphetamine.

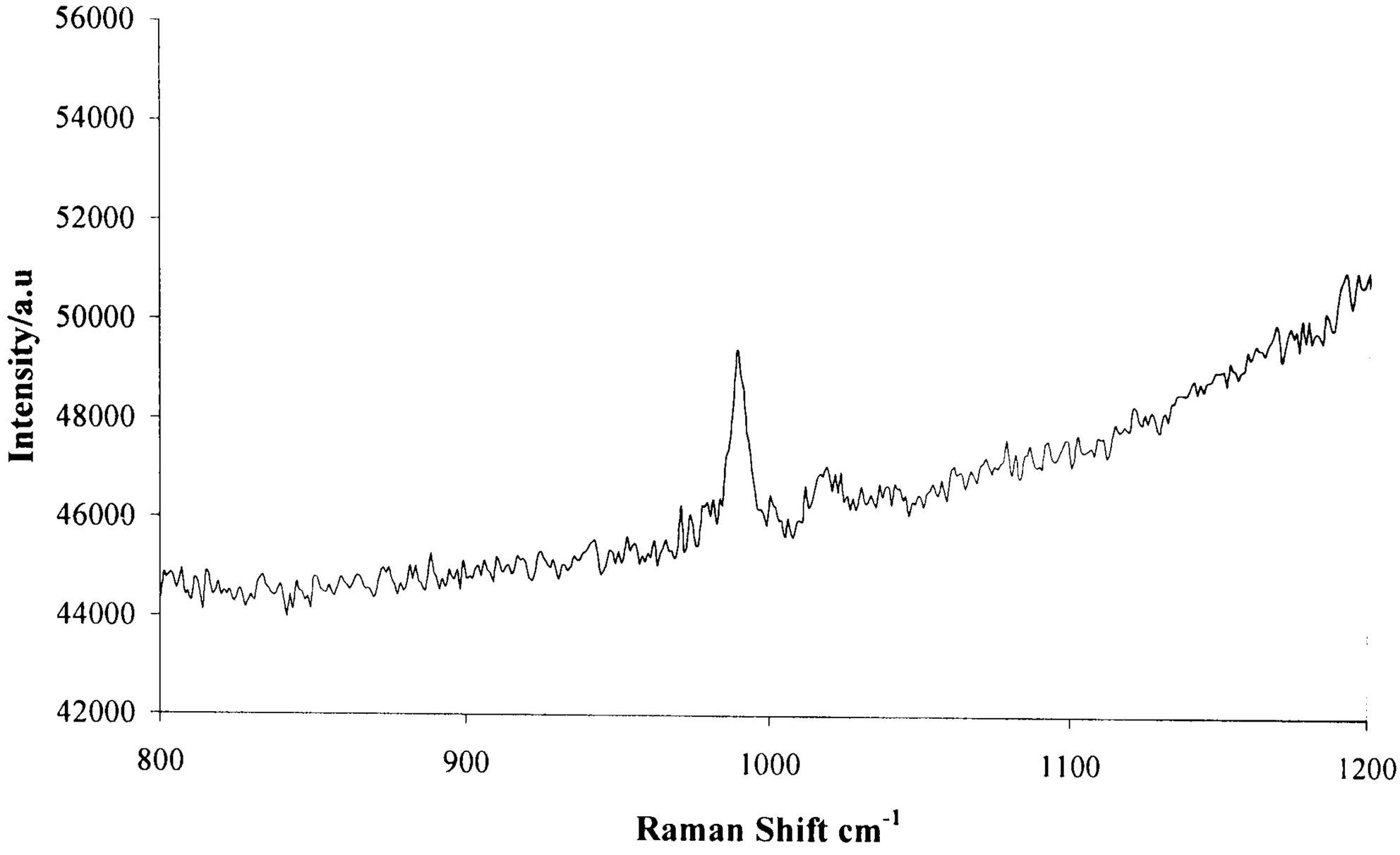

Figure 6.2: A spectrum of $1x10^{-3}$ M aqueous amphetamine solution with no pre-cleaning of the Ag/TiO_2 substrate.

In striking contrast to the results illustrated in Figure 6.2, Figure 6.1 reveals the Raman spectrum of a spot of the same solution spotted onto an Ag/TiO_2 substrate that has undergone pre-cleaning by soaking in spectroscopic methanol whilst being exposed to UV irradiation for 3 minutes. This figure shows peaks positioned at 1000 cm^{-1} and 1030 $cm^{-1} \pm 2cm^{-1}$ associated with the ring breathing and stretching modes. The peak at 1000 $cm^{-1} \pm 2cm^{-1}$ is the most characteristic peak used to identify the presence of the amphetamine. The levels of enhancement are significantly higher with approximately 11,000 counts and the background level was much reduced. This experiment shows that pre-cleaning of these substrates prior to sample loading and analysis significantly improves the observed enhancement by reducing the contact angle between the sample and the surface.

As noted earlier this reduction in contact angle is related to a rejuvenation of the substrate surface. Irradiation of the substrate with UV light in the presence of methanol appears to remove any hydrophobic organic species and, most probably removes any surface oxide or contaminants on the silver particles by photocatalysis of the TiO_2 layer [Mills and Lee (2003)] rendering it superhydrophylic. When the

aqueous sample is then placed on the freshly cleaned surface it readily wets. This wetting action improves the contact of the aqueous amphetamine sulphate solution with the silver, and so increases the SERS observed enhancement.

Most observations of the phenomenon of photoinduced superhydrophilicity [Wang *et al* (1997)] have been made using titania substrates only, whilst the Ag/TiO_2 substrates used in these experiments have a layer of photoreduced silver. However, the Ag layer is not continuous, enabling penetration of the UV to the lower TiO_2 (Figure 6.3). Additionally, the UV will photoregenerate the Ag^+ from any AgO formed on the surface of the Ag particles/layer, thus revealing binding sites for the drug to interact with, depending on the charged state of the drug.

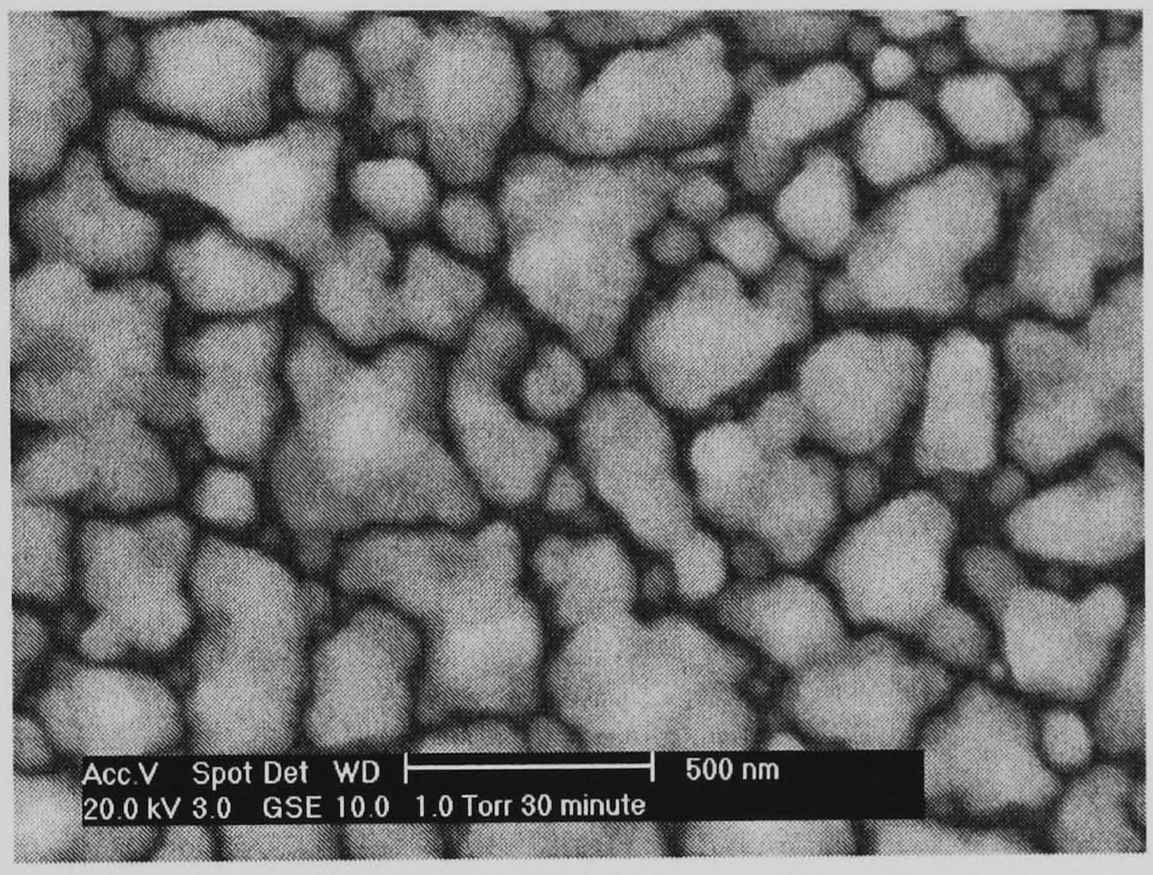

Figure 6.3: ESEM image of a substrate following 30 minutes photodeposition demonstrating the lack of continuity in the silver layer.

6.3.2 Ag/TiO_2 Silver Substrates

The Ag/TiO_2 substrates were examined for reproducibility within and between substrates with respect to levels of SERS enhancement for the $1x10^{-3}$ M aqueous amphetamine solution.

Figure 6.4 shows significant enhancement of the $1x10^{-3}$ M aqueous amphetamine with the doublet peak positioned at 1000 cm^{-1} and 1030 $cm^{-1} \pm 2$ cm^{-1} with approximately 44,500 counts of observed enhancement. Following on from this result a series of spots on the same substrate, at the same concentration were

analysed with three spectral collections per spot and the average SERS response calculated which can be found in Figure 6.5.

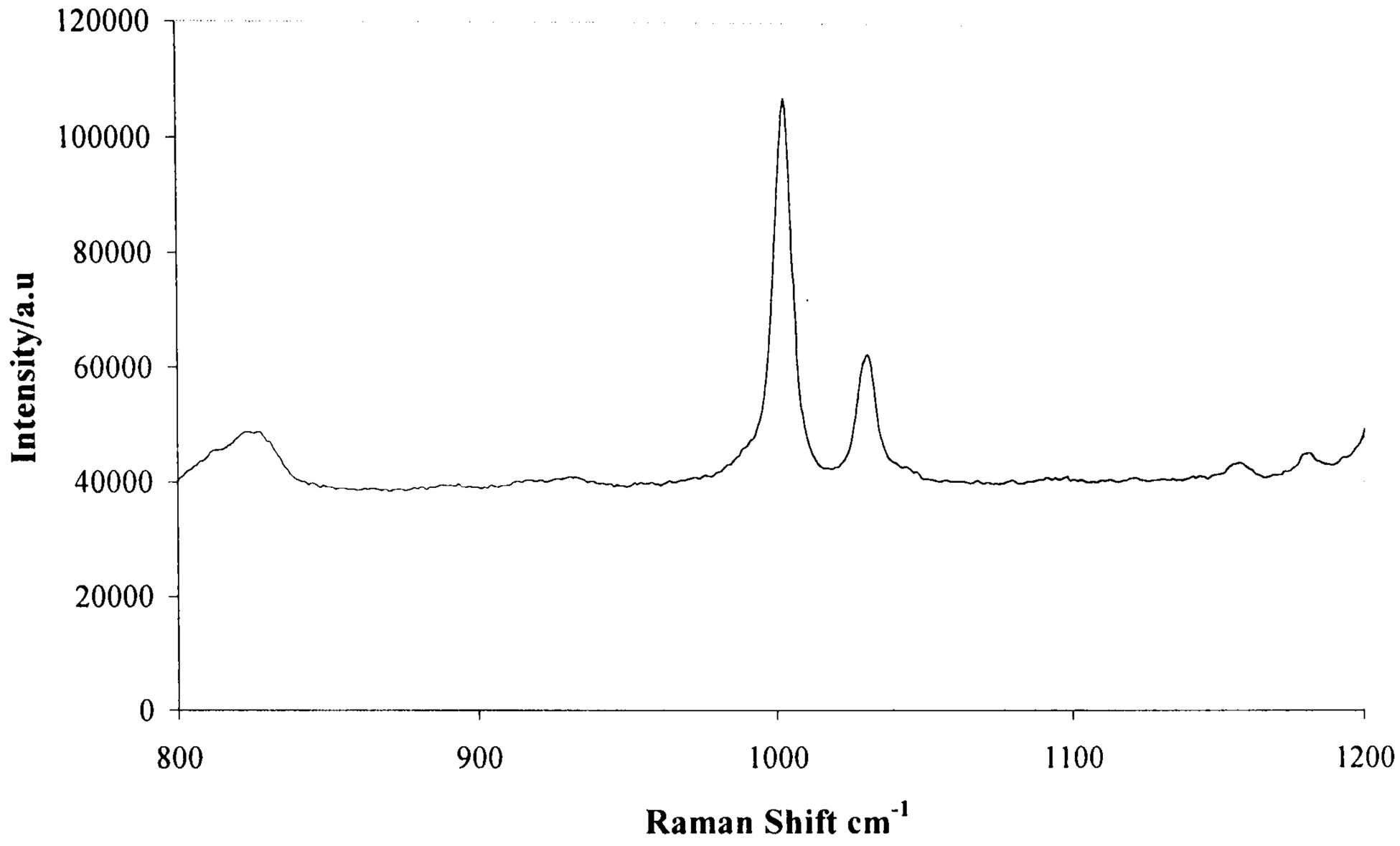

Figure 6.4: A spectrum of $1x10^{-3}$ M aqueous amphetamine sulphate spotted onto an Ag/TiO_2 substrate.

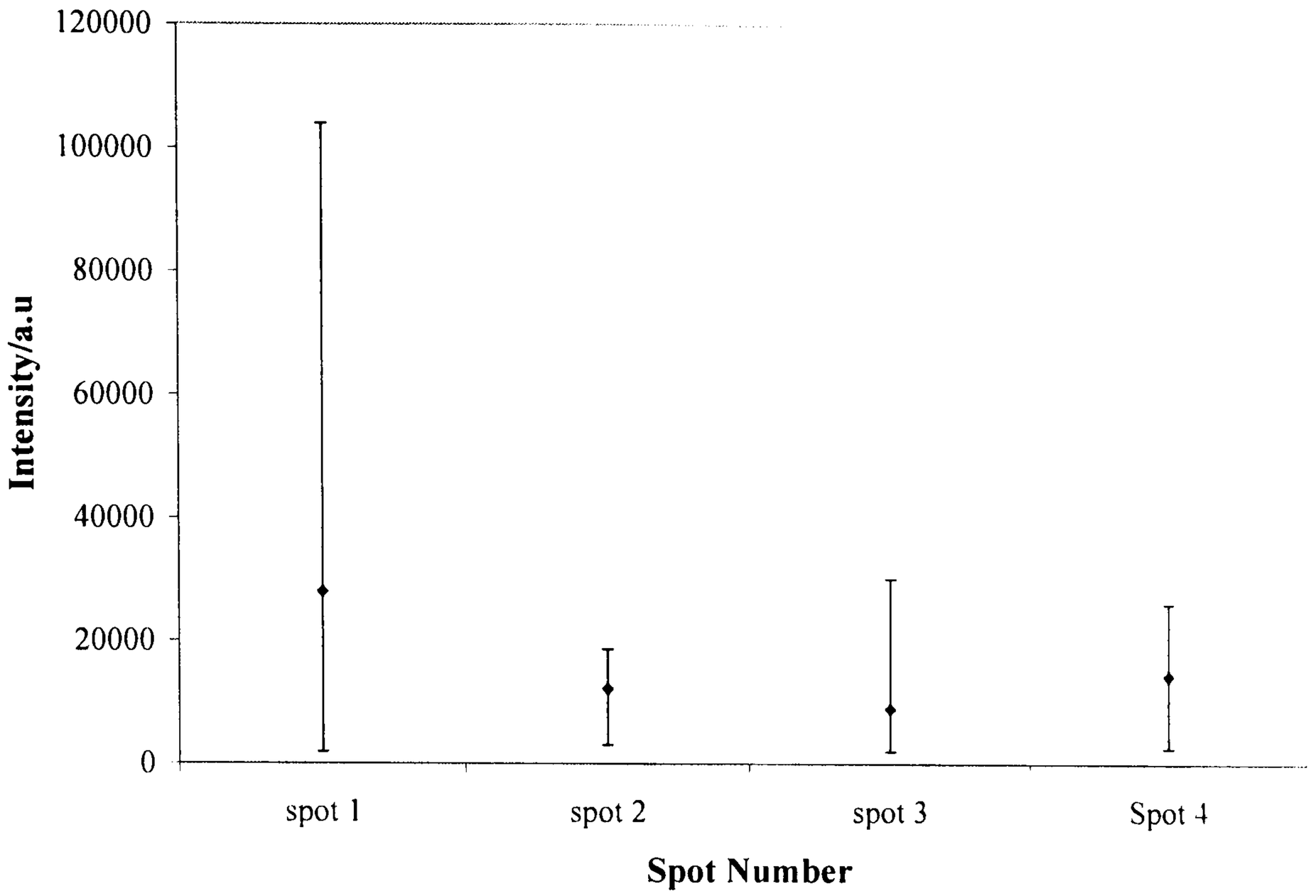

Figure 6.5: A graph showing the average intensity in counts (arbitrary units) of the SERS response observed for each spot of aqueous amphetamine solution analysed on the Ag/TiO_2 substrates. The error bars show the range in response of the weakest and strongest responses recorded from the same sample spot.

The average responses for spots 2, 3 and 4 are similar and also appear to have similar ranges in response. Spot 1 has the best response but a larger upper range variation than the others. A possible explanation for this is the SERS response has been recorded at a point where a monolayer of crystalline material has formed on the surface facilitating maximum surface enhancement. This may be due to chemical enhancement taking place involving an electronic interaction such as charge transfer where the electrons transfer from the molecules to the metal surface. It is possible that the area being interrogated contains a 'hot spot' resulting in very enhanced SERS peaks. However, as more crystalline material builds up field enhancement properties may also contribute to the SERS because this extends several tens of nanometers from the metal surface.

6.3.3 Establishing the Lower Limit of Detection for the Ag/TiO_2 Substrates

In efforts to determine the lower limit of detection aqueous solutions of amphetamine from $1x10^{-2}$ M to $1x10^{-5}$ M were examined for both reproducibility and sensitivity

(Figure 6.6). Three spectra were collected from four sample spots using three Ag/TiO_2 substrates. The variation in SERS signal with amphetamine concentration showed no clear trend over the range $10^{-2} - 10^{-5}$ M.

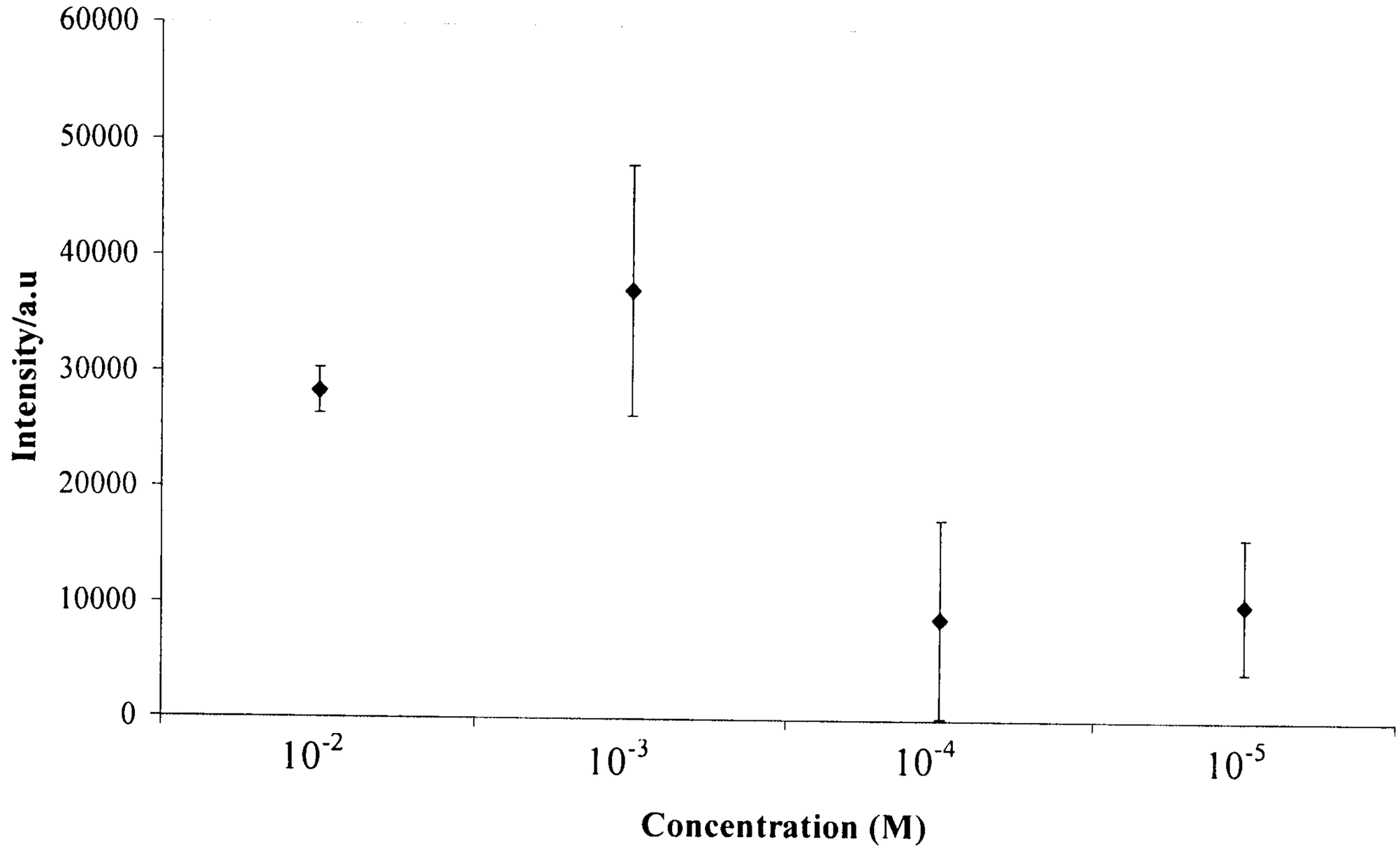

Figure 6.6: A graph showing the average intensity in counts (arbitrary units) of the SERS response observed for 4 concentrations of aqueous amphetamine solution ($1x10^{-2}$ M, $1x10^{-3}$ M, $1x10^{-4}$ M and $1x10^{-5}$ M) analysed on Ag/TiO_2 silver substrates. Three spectra were collected from four sample spots using three Ag/TiO_2 substrates. The error bars are ± 1 standard deviation from the mean.

More promisingly, at lower concentrations a reasonable trend was observed, as illustrated in Figure 6.7. Three spectra were collected from four sample spots using three Ag/TiO_2 substrates. Over the concentration range of $6x10^{-6}$ M to $8x10^{-7}$ M the SERS signal decreased with decreasing amphetamine concentration. However, over this concentration range the SERS signal appeared to be directly related to the logarithm of the amphetamine concentration, rather than being directly proportional to it. The lowest concentration detected in this experiment was estimated as ca. $8x10^{-7}$ M.

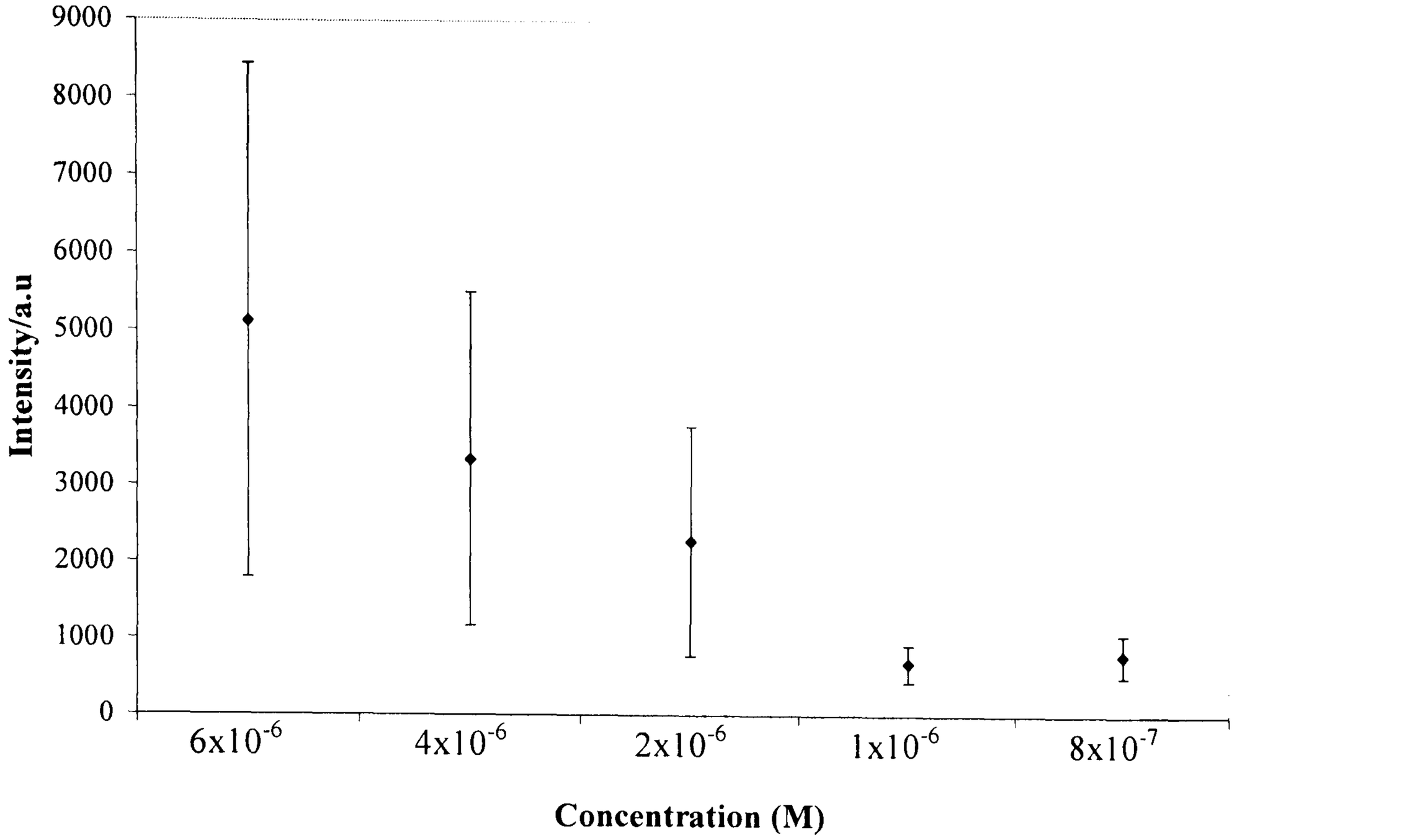

Figure 6.7: This graph shows the average intensity in counts (arbitrary units) of the SERS response observed for 5 concentrations of aqueous amphetamine solution ($6x10^{-6}$ M, $4x10^{-6}$ M, $2x10^{-6}$ M, $1x10^{-6}$ M and $8x10^{-7}$ M) analysed on Ag/TiO_2 substrates. Three spectra were collected from four sample spots using three Ag/TiO_2 substrates. The error bars are ± 1 standard deviation from the mean.

The lower limits of detection shown here with the cleaned Ag/TiO_2 substrates show potential for the application of roadside screening for drugs.

6.3.4 Sputtered Silver Substrates

In comparison to the $AgTiO_2$ substrates the sputtered silver substrates overall showed a good SERS response but with less reproducibility (Figure 6.8). Three spectra were collected from four sample spots using three sputtered silver substrates. The 1000 $cm^{-1} \pm 2\ cm^{-1}$ peak of the amphetamine solution was investigated. It is possible that the 9 nm thickness substrate examined was not the ideal to facilitate SERS enhancement with the aqueous amphetamine solution.

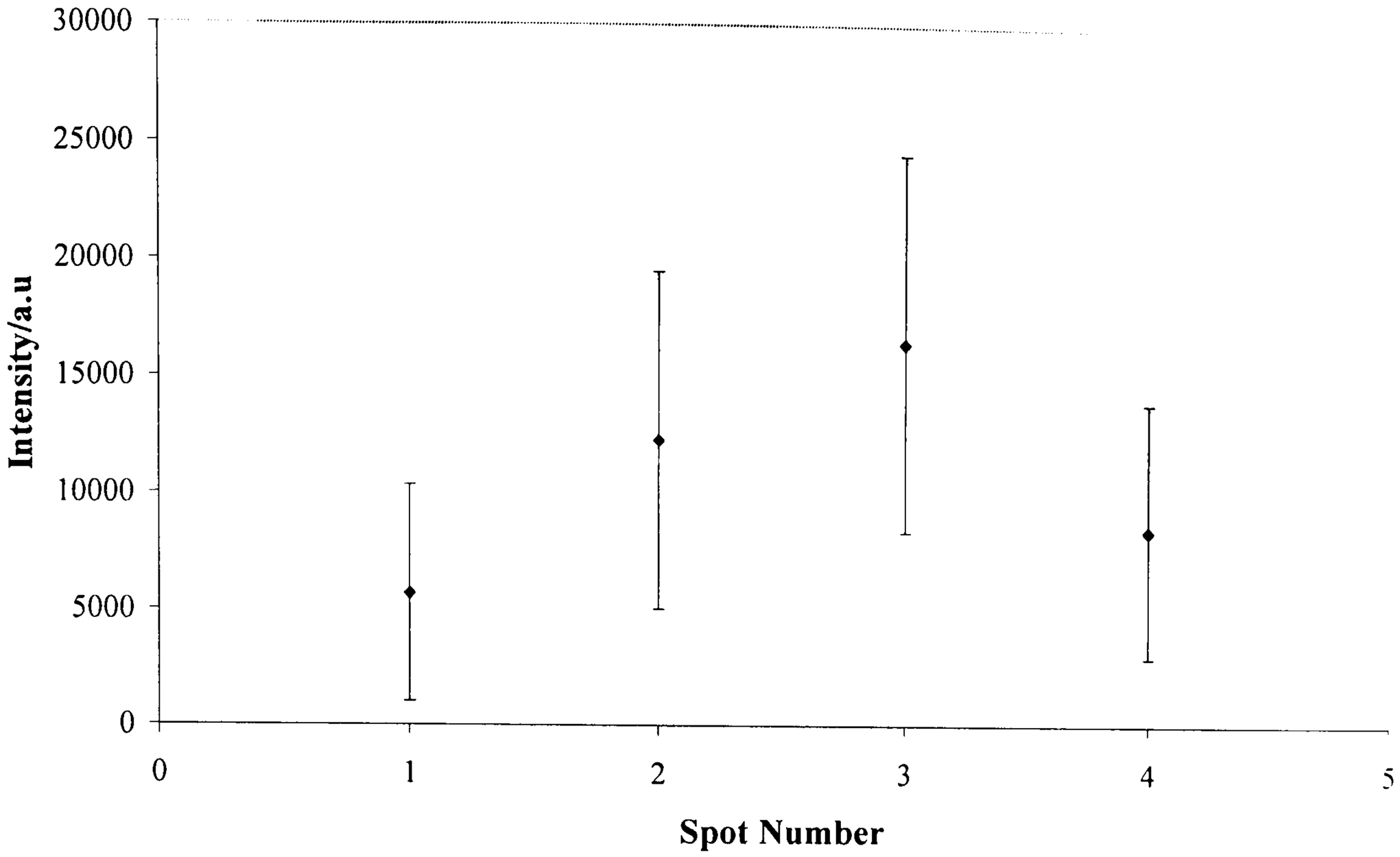

Figure 6.8: A graph showing the average intensity in counts (arbitrary units) of the SERS response observed for each spot of aqueous amphetamine solution ($1x10^{-3}$ M) analysed on the sputtered silver substrates. Three spectra were collected from four sample spots using three sputtered silver substrates. The error bars are ± 1 standard deviation from the mean.

Figure 6.9 is an example of the best spectrum recorded from the $1x10^{-3}$ M aqueous amphetamine solution using these surfaces. Whilst the level of enhancement recorded in this spectrum was approximately 20,000 counts the reproducibility of this level of enhancement was not consistent. It is also apparent that this surface when compared with the Ag/TiO_2 has similar capability to resolve the peaks associated with the presence of amphetamine sulphate. This is evidenced by the presence of the doublet peaks at 1000 cm^{-1} and 1030 cm^{-1} $\pm$ 2 cm^{-1} again associated with the ring breathing and stretching modes of this drug structure.

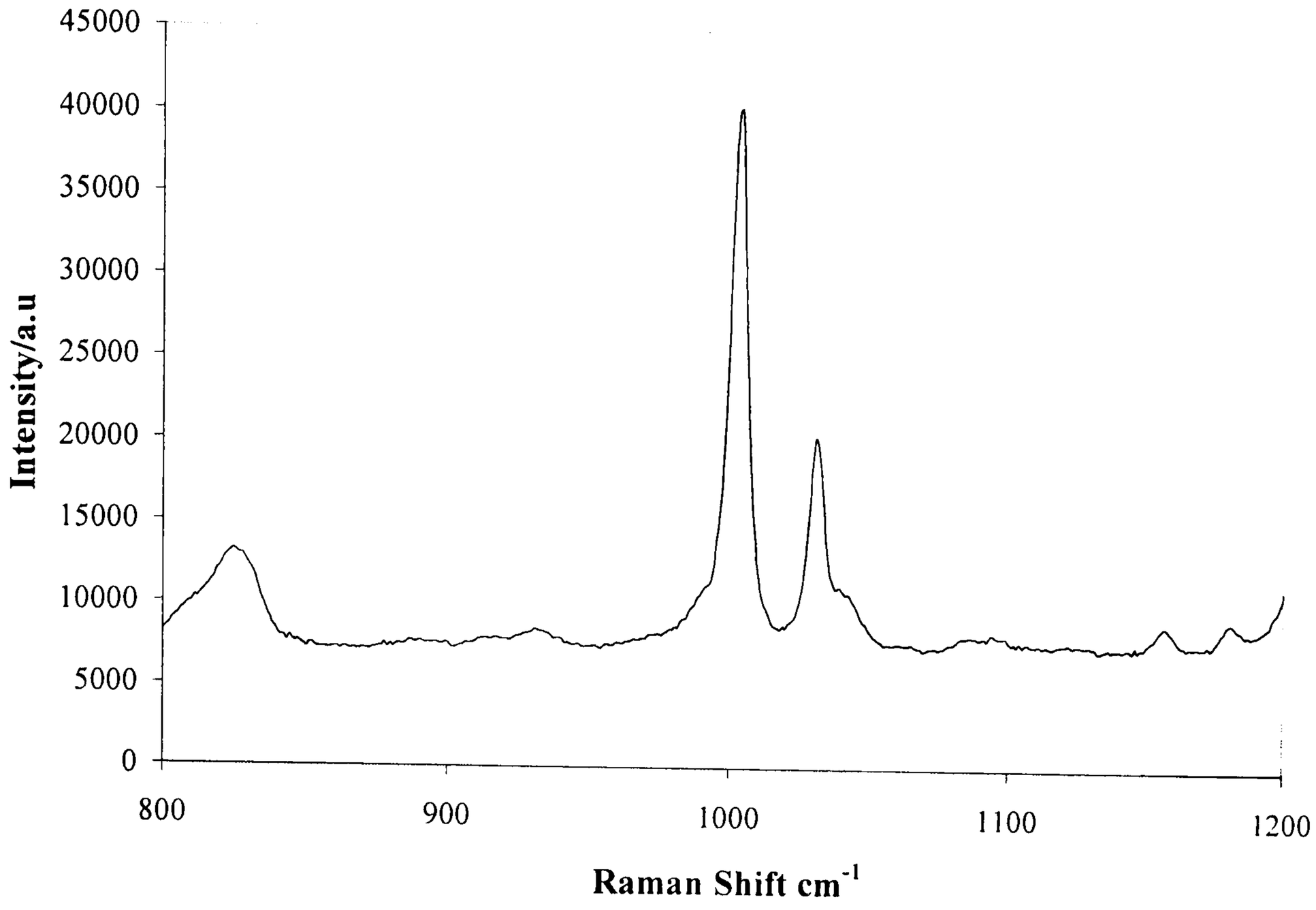

Figure 6.9: A spectrum recorded from the $1x10^{-3}$ M aqueous amphetamine solution spotted onto a sputtered silver substrates.

6.3.5 Au/TiO_2 Substrates

Au/TiO_2 substrates were prepared as previously described in the experimental section of this chapter. Work by Faulds *et al* (2002) reported the detection of amphetamine sulphate ($1x10^{-3}$ M to $1x10^{-5}$ M) with colloidal and evaporated gold and 785 nm excitation. Figure 6.10 is a spectrum of $1x10^{-3}$ M aqueous amphetamine solution on the Au/TiO_2 substrates. In comparison to the Ag/TiO_2 work the signal to noise ratio is poor and the level of SERS enhancement considerably lower. At lower concentrations were no SERS spectrum could be recorded for $1x10^{-3}$ M aqueous amphetamine solution. Consequently these substrates were no longer used. The lack of observed enhancement from these substrates is not understood but perhaps the coupling of the 633 nm wavelength with gold for this application is not as suitable as the Ag/TiO_2 substrates.

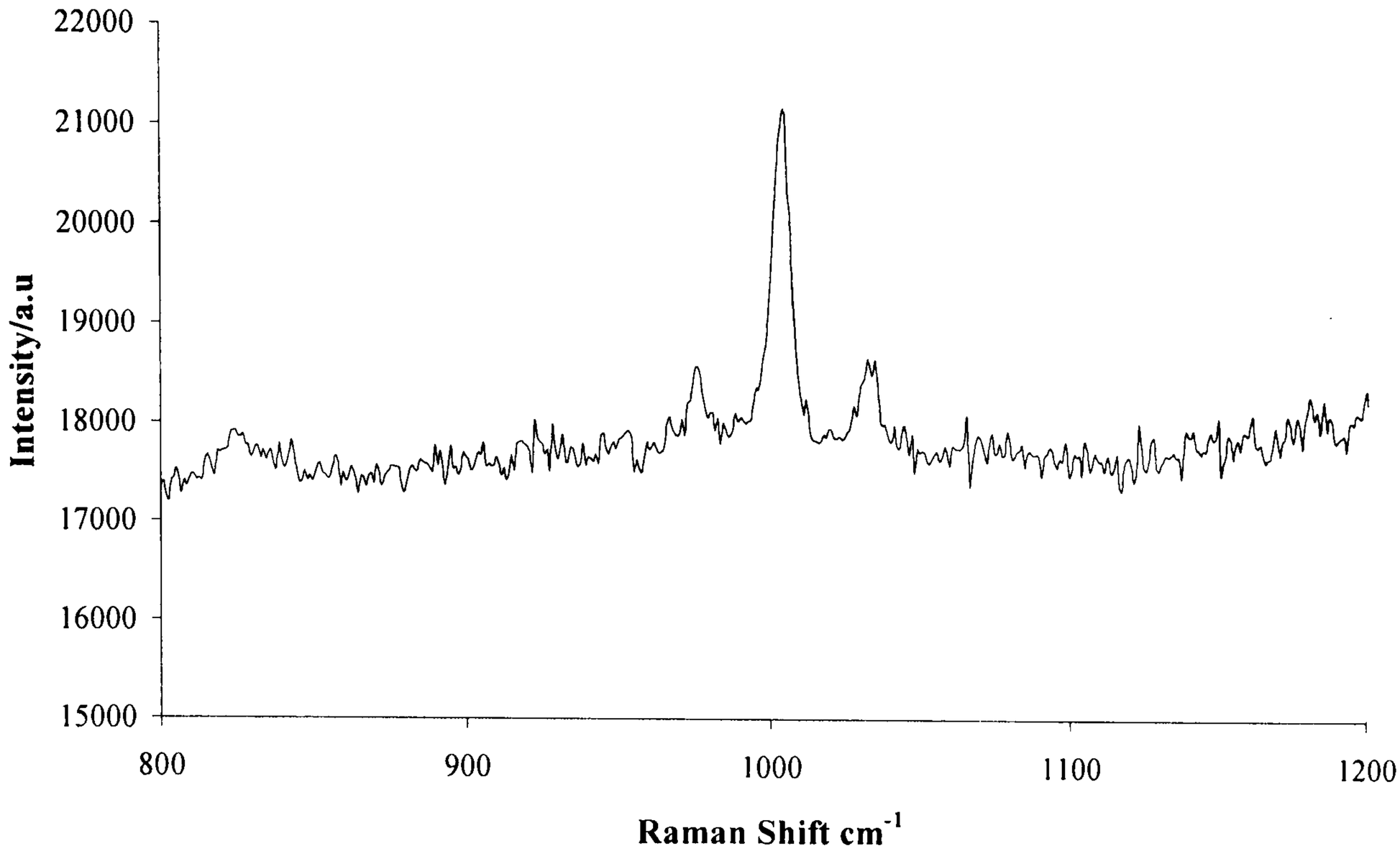

Figure 6.10: A spectrum recorded from the $1x10^{-3}$ M aqueous amphetamine solution spotted onto an Au/TiO_2 substrates.

6.3.6 Commercially Available Silver Klarite Surfaces From Mesophotonics

Klarite substrates are designed with a repetitive pattern at the sub-micorn scale. A layer of gold coats an underlying silicon surface which comprises regular arrays of holes. This regular pattern gives rise to photonic crystals which ultimately control the surface plasmon activity on the surface. Optimising and harnessing this activity is responsible for the observed SERS enhancement (Figure 6.11).

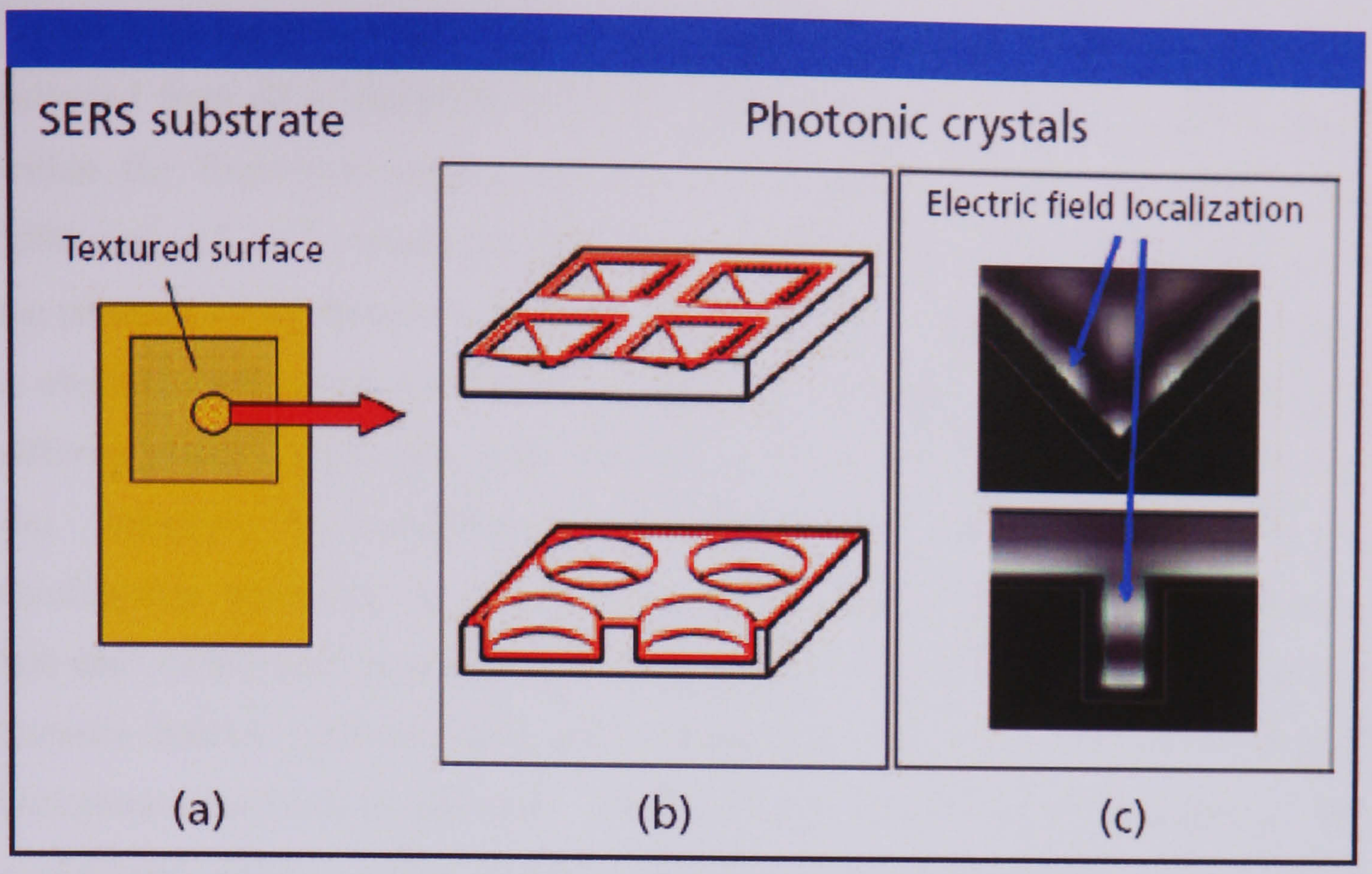

Figure 6.11: A diagram showing an example of a SERS substrate engineering (a). The textured surface can be structured with 2D periodic features having different shapes, geometry and size (b). The localisation of the laser electric field within the texture features as calculated by finite difference time domain for a ca. 1 μm wide pyramid and a ca. 0.5 μm wide cylindrical hole (c) [Netti and Stanford (2006)].

Four unrelated batches of Klarite gold substrates (N = 48) were purchased from Mesophotonics, Southampton (www.mespohotonics.com). Each batch was analysed with 633 nm using aqueous amphetamine solutions at a concentration range of $1x10^{-3}$ M to $1x10^{-7}$ M. A single 0.5 μl volume of sample was placed in the corner of the substrate and analysed three times. Each substrate was tested with all five concentrations with the sample confined to the corners except for the $1x10^{-7}$ M which was loaded onto the centre of the substrate. The small volume of sample ensured the different concentrations did not overlap. The evaporated residue was located by a characteristic 'coffee ring' [Deegan *et al* (2000)] pattern left on the surface. A total of forty-eight individual Klarite substrates were analysed from 12 batches. Nine spectra were collected from each drug spot. Three background spectra prior to any sample loading were also recorded.

Figure 6.12 represents an overview of the variable background Raman activity collected from all of the blank substrates prior to sample loading. There are areas within the fingerprint region that have very intense activity especially in the 1000 $cm^{-1} \pm 2$ cm^{-1} region where the characteristic molecular vibrations relating to the presence of amphetamine would be identified. The variability of the background is observed both within and between batches of substrates. Each batch represents a different manufacturing run, with all of the substrates within a batch from the same run. However, the variability within the batches of the background activity is considerable especially in Batch 4 which has broad spectral activity between 800 cm^{-1} - 1600 cm^{-1} in several substrates. This variability across the substrates and between batches prevents easy data management and application of a standard background subtraction protocol. This is compounded by the intensity of the background activity, which if subtracted from a sample spectrum could result in subtraction of peak data relating to the sample and not to the background.

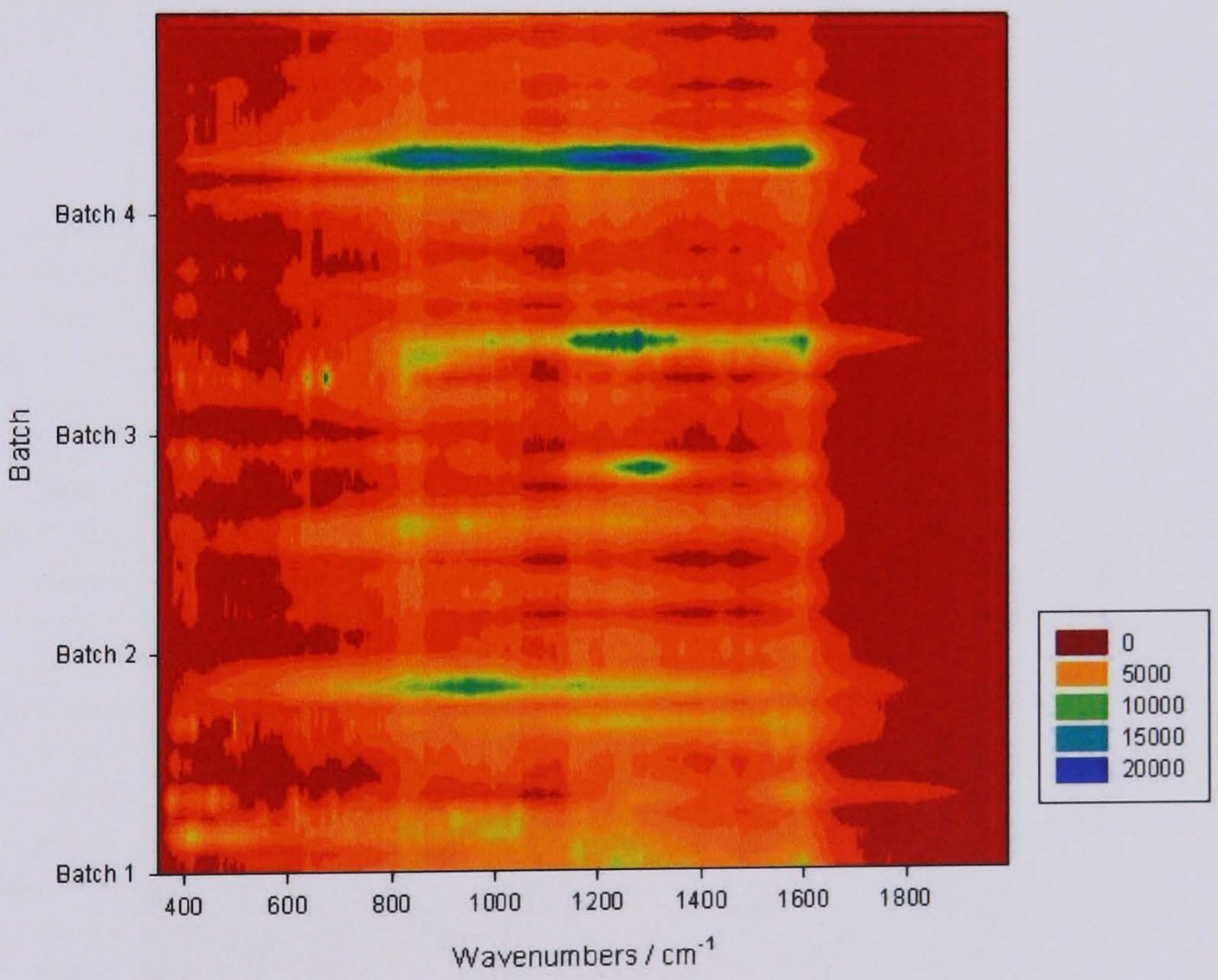

Figure 6.12: Background spectra collected from each substrate were initially averaged and then plotted for each substrate in each batch as a contour plot. All background spectra were taken pre-sample loading.

Following addition of the amphetamine sample to the substrate surface some SERS enhancement was observed especially with the $1x10^{-4}$ M solution which had the most pronounced enhancement. However, as indicated in Figure 6.13 whilst limited SERS enhancement can be observed with the $1x10^{-4}$ M and $1x10^{-5}$ M solutions, the inconsistencies in detection of the lower concentrations combined with low levels of enhancement, limits the usefulness and suitability of these substrates, with this sampling methodology for drug detection in aqueous solution.

Figure 6.13 represents an overall area map of the level of SERS enhancement recorded for each batch at each concentration (Y-axis) versus the Raman Shift (wavenumber /cm^{-1}, X-axis). Again, if the presence of a peak at 1000 cm^{-1} $\pm$2 cm^{-1} indicates a positive identification for amphetamine, the ability to make a qualitative identification ceases at $1x10^{-5}$ M. Although, caution must be applied when interpreting the data because the background spectra indicated an underlying peak activity at the same Raman Shift precluding conclusive identification of drug presence.

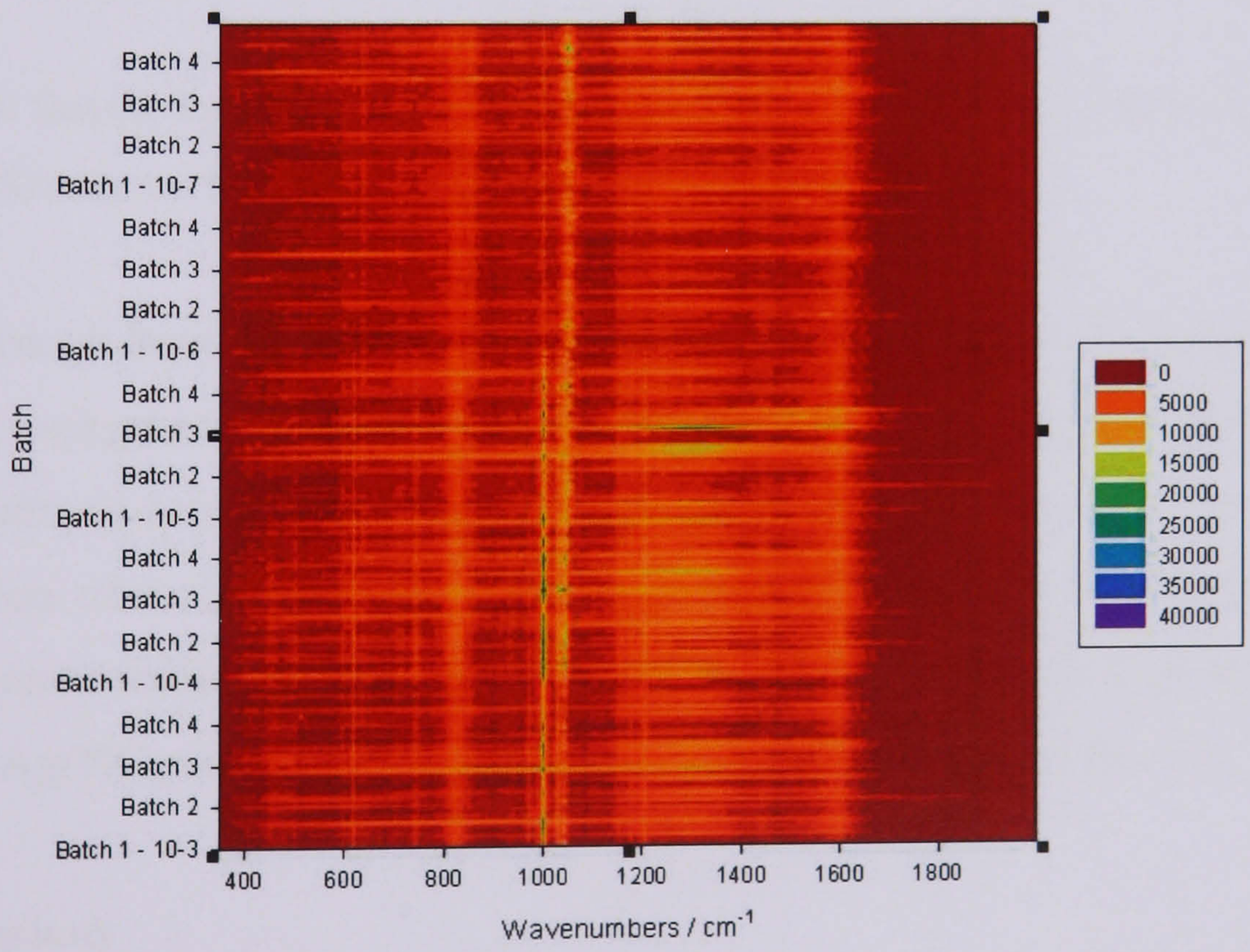

Figure 6.13: A contour map of the performance of the substrates in batch grouping at each concentration of aqueous amphetamine solution with 633 nm excitation.

Figure 6.14 the overall sensitivity of all of the batches of substrates to each concentration of amphetamine sulphate tested with 633 nm excitation. Poor sensitivity below $1x10^{-5}$ M is observed indicating insufficient lower limits of detection.

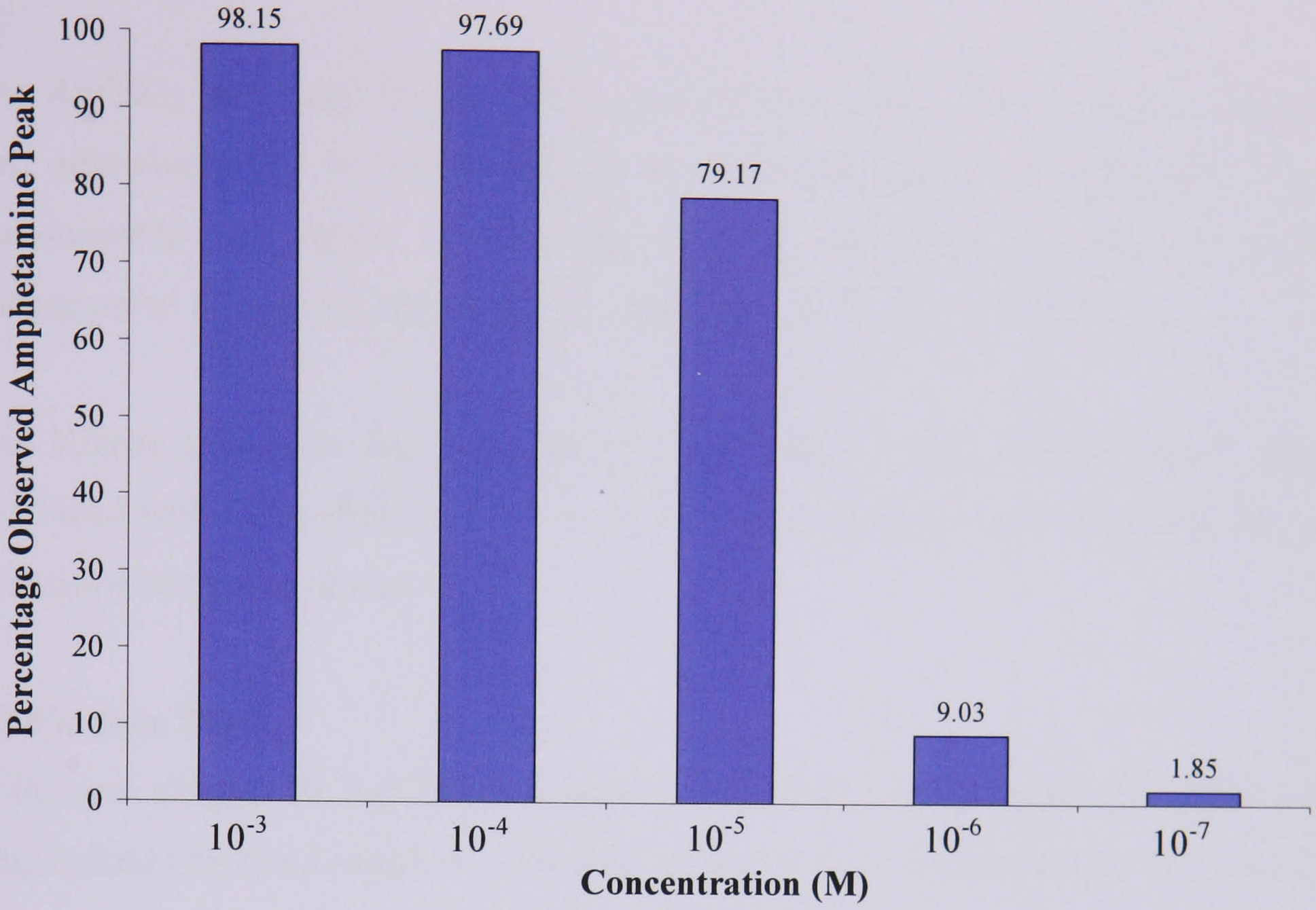

Figure 6.14: Sensitivity of all the substrates for each concentration of amphetamine solution tested with 633 nm excitation looking at the 1000 $cm^{-1} \pm 2\ cm^{-1}$.

The conclusions from this feasibility study were that the Klarite substrates significant underlying background activity precludes qualitative identification of the presence of a drug of interest below $1x10^{-5}$ M. The substrates could, at best, be used down to a concentration of $1x10^{-5}$ M which is two orders of magnitude above the desired $1x10^{-7}$ M concentration as detailed in the type approval specification for drug driving, a level the Ag/TiO_2 substrates are capable of providing a good response to.

6.4 Conclusions

Pre-cleaning of the Ag/TiO_2 substrates with spectroscopic grade methanol and UV lamp irradiation for 3 minutes reduces the contact angle of the solution of interest on the substrate surface assisting with the observation of SERS enhancement. This

reduction in contact angle allows greater substrate interaction between the sample and the silver particles to take place. As the sample re-crystalises on the substrate there is more opportunity for chemical and field enhancement to occur resulting in a larger SERS enhancement and better detection of lower concentrations of aqueous amphetamine.

The Ag/TiO_2 substrates demonstrated the most consistent SERS response with the best reproducibility in comparison to the other substrates investigated. They demonstrated low limits of detection and the possibility of detecting SERS enhancement of aqueous amphetamine solution at levels below $8x10^{-7}$ M.

The Klarite substrates had significant variable background activity which when combined with a detection limit of $1x10^{-5}$ M limits their usefulness for application as a roadside screening device.

6.5 Further Work

In the next chapter the Ag/TiO_2 substrates will be investigated further with blank and drug spiked oral fluid samples. Oral fluid collected from registered drug addicts will also be tested with these substrates and the results compared with confirmatory analysis results.

Chapter 7

Drug User Oral Fluid Samples

7.1 Introduction

The previous chapter concluded that the Ag/TiO_2 substrates demonstrated the most consistent SERS response and reproducibility in comparison to the other substrates investigated including those commercially available. The Ag/TiO_2 substrates also demonstrated low limits of detection and the possibility of detecting SERS enhancement of aqueous amphetamine solution at levels ca. $8x10^{-7}$ M. Whilst the substrates have demonstrated good results with aqueous drug solutions, it is necessary to establish if they will confer the appropriate sensitivity for detection of drugs in oral fluid.

The principle differences between the drug presentation in the oral fluid samples versus spiked oral fluid samples is the presence of complex metabolic products and conjugated parent drugs. The pH of the oral fluid sample may also influence the SERS enhancement factor achieved from the substrate [Farquharson *et al* (2005a)].

Farquharson *et al* (2005a) demonstrated the influence of pH with 1 mg/ml 5-fluoruracil (5-FU), which is a weak acid with a pKa of 7.93. The graph below (Figure 7.1) shows the effect of changing pH value ((A) 10.7, (B) 9.2, (C) 6.5, (D) 5.6 and (E) 4.3) on observed SERS enhancement and more specifically the observed peaks and positions. The peaks at 1234, 1400 and 1667 cm^{-1} decrease in intensity whereas the peak at 1335 cm^{-1} remains constant as the pH is adjusted to basic conditions. New peaks can also be observed between 1500 – 1650 cm^{-1}. However, it should be noted that the pH ranges represented exceed those observed in oral fluid (pH 5 – 8).

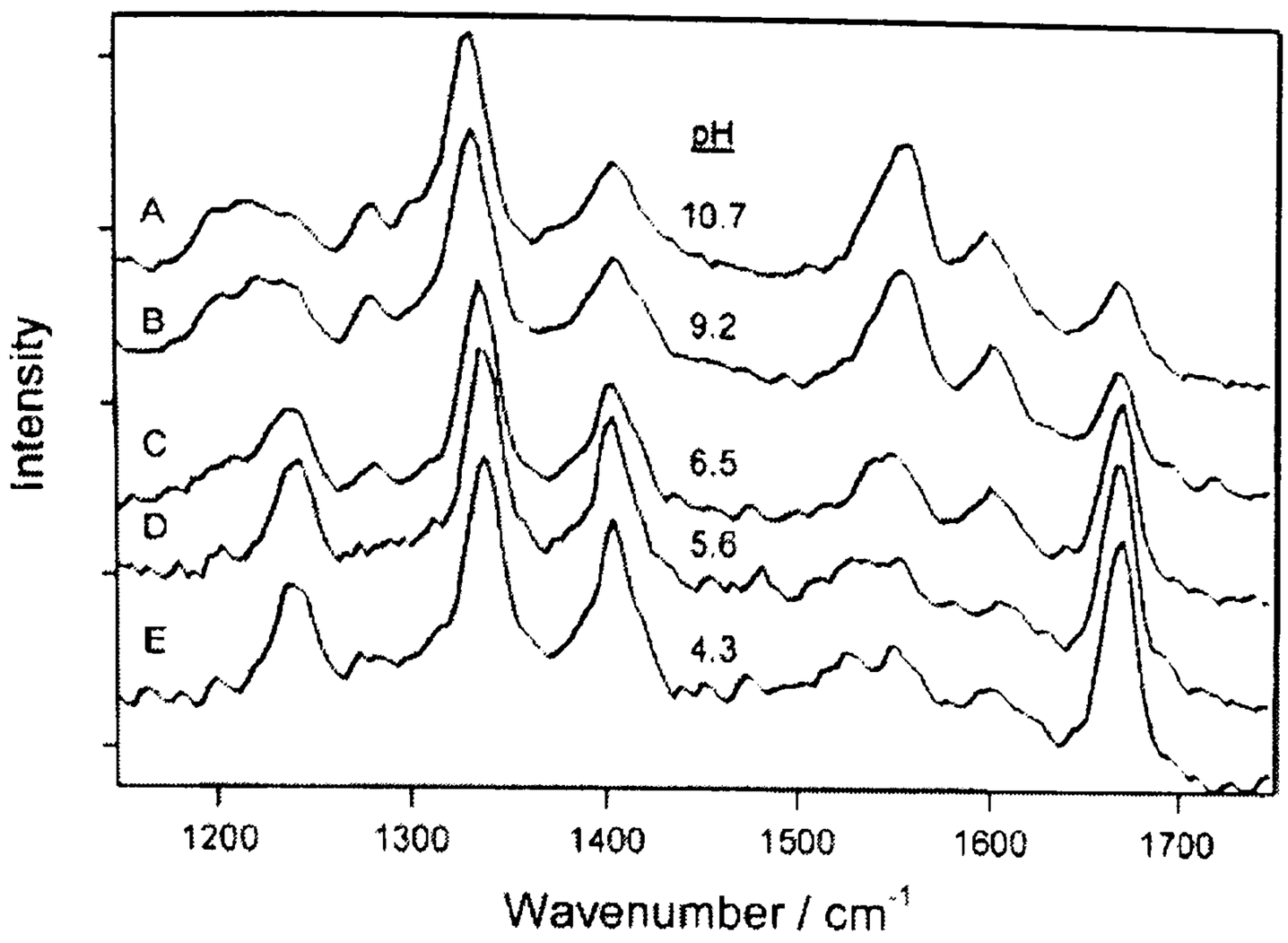

Figure 7.1: SERS spectra as a response to changing pH of aqueous 5-FU. ((A) 10.7, (B) 9.2, (C) 6.5, (D) 5.6, (E) 4.3). Reproduced from Farquharson *et al* (2005a).

In this chapter samples of oral fluid were collected from drug users registered in an NHS maintenance programme, Acorn. The necessary ethical permissions were obtained and a consented study undertaken. The subjects were recruited at random from the clinic and were commonly polydrug users although some were on methadone only maintenance programmes. The illicit drugs being investigated in these oral fluid samples include buprenorphine, cocaine, heroin, and methadone (Figure 7.2) which have not been investigated in the previous experimental work using SERS. Ecstasy consumption was also reported and these tablets often contain more than one phenethylamine (Chapter 3.4).

The subjects were also assessed for signs of impairment using the FIT tests (Chapter 1.1.1) and computerised versions of the Sustained Attention to Response Task (SART) and Critical Tracking Task (CTT). These are psychomotor tests currently under evaluation by the Home Office to provide a computerised non-subjective measure of impairment in drivers.

This study was completed in collaboration with the Human Psychopharmacology Research Unit (HPRU) at Surrey University and the Forensic Medicine Unit at Glasgow University.

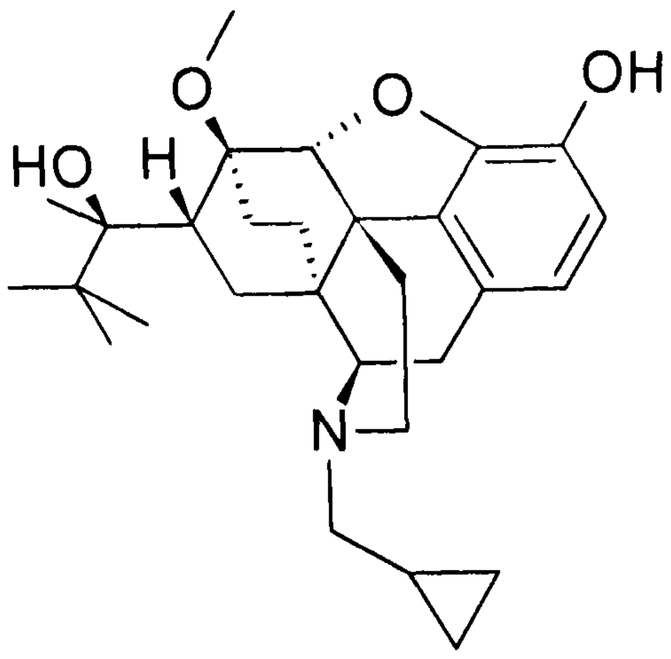

Buprenorphine

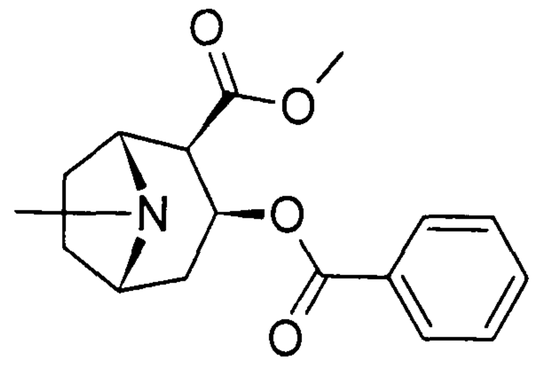

Cocaine

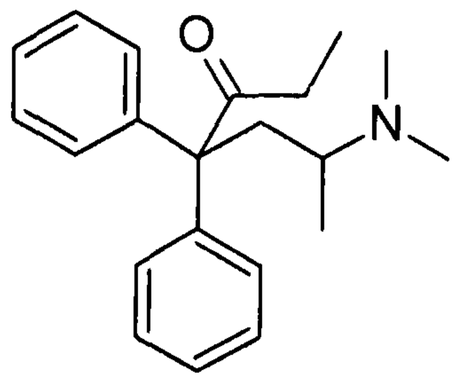

Methadone

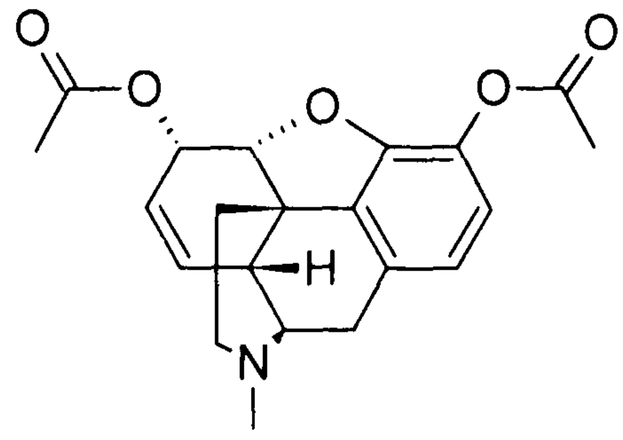

Heroin

Figure 7.2: The structures of buprenorphine, cocaine, heroin and methadone.

7.2 Experimental

7.2.1 Oral Fluid Volunteers

Thirty subjects (18 – 65 years inclusive) were identified by the treatment centre staff (Acorn) and recruited for the study. The subjects were pre-collected and transported to the testing facility. Each subject was assessed upon arrival to ensure capability to provide informed consent. The subjects who fulfilled the entry criteria and provided written informed consent were enrolled in the study (n = 30).

Thirty additional age and sex matched control subjects were recruited by HPRU to compare against the drug maintenance programme volunteers. They were subjected

to the same testing protocol but with the addition of a drugs of abuse urine screen, to ensure the subject had not used any illicit drugs prior to participating in the study.

All subjects performed a breathalyser test to ensure negative or low alcohol consumption. Oral fluid samples were collected using a Sarstedt cotton Salivette collection device. The collection device was placed in the oral cavity positioned between the cheek and the gum line to enable collection of un-stimulated oral fluid. Collection times were on average 5 minutes, but were dependent on the individuals' drug dose and the time since administration. Following collection the samples were stored at -80 °C until analysed. A self-assessment questionnaire was also completed to obtain information about any medicinal and non-medicinal substances, including tobacco and alcohol, consumed within the last twenty-four hours.

To remove the oral fluid from the collection device it was centrifuged at 4300 rpm for 20 minutes. This also caused any cellular debris to coalesce at the bottom of the tube leaving clear exudate at the top of the tube for analysis. A small volume (50µl) of the exudate was then decanted into a second tube and retained for the SERS analysis. The remaining sample was sent to an external laboratory (Forensic Medicine Unit, Glasgow University) for confirmatory LC/MS analysis.

Representatives from the 30 subjects will be presented in this chapter and discussed in detail. However, all subject samples were analysed in the same manner.

7.2.2 SART Test

The SART test assessed sustained attentional performance. Continuous stimulus in the form of road sign images were presented on a hand-held device. Subjects were required to respond to the presentation of every stimulus with a key press unless presented with the target stimulus ('PARK' sign) in which case they were required to withhold response. The subjects were informed that the target stimulus was a predefined road sign and were prompted after a wrong response. The primary response variable was the number of incorrect SART key presses to the no go 'PARK' sign.

7.2.3 CTT Test

The CTT test was an integrative task of cognitive and psychomotor function, comprising of tracking ability, divided attention and reaction time. The task required the user to track a moving ball with a PDA stylus. The movement of the target was controlled by an irregular sinusoidal function. The tracking error response measure was the root mean square of the difference between the centre of the target and the stylus. Whilst tracking was in progress a peripheral awareness task was included. This required the user to respond when symbols were presented on the screen by pressing a button. The primary response variables were: tracking error during each 30s section of the tracking task, tracking error following response to a peripheral stimuli (tracking post response) and reaction time to the peripheral stimuli. All data were captured electronically.

7.2.4 FIT Test

The standard police tests used at the roadside to screen drivers suspected of driving whilst impaired through drugs were undertaken. There were five psychophysical tests carried out; the pupillary examination, Rhomberg test (estimation of 30 seconds), walk and turn test, the one leg stand test and the finger to nose test. Additionally, horizontal and vertical gaze nystagmus tests were performed.

7.2.5 $AgTiO_2$ Substrate Preparation

The Ag/TiO_2 substrates were prepared using the method described in Chapter 5.2.1.

7.2.6 Spectral Collection

SERS spectra were recorded using the equipment described in Chapter 4.2.3.

7.2.7 Raman Analysis

Raman spectra from crystalline samples of the illicit drugs were collected for peak position comparison with the SERS spectra. Several crystals were placed on a glass slide and spectra (400 – 3200 cm^{-1}) captured using a x50 objective and a 30 second accumulation time with 633 nm laser excitation at 100% power.

7.2.8 SERS Analysis

All the oral fluid samples were analysed using the same collection parameters and sample volume as detailed in Chapter 6.2.7.

7.2.9 Spectral Processing

Post collection, all spectra were subject to baseline correction (auto levelling), peak picking (across the whole spectra), peak fitting (Gaussian and Lorentzian mix) and exportation of the final peak tables using Advanced Chemistry Development Inc Spec Manager 2006 (v 9.15).

7.2.10 GC/MS and LC/MS Methodology

The GC/MS and LC/MS method used was published by Wylie *et al* (2005a).

7.3 Results

7.3.1 Crystalline Drug Spectra

Crystalline Raman spectra of buprenorphine (Figure 7.3), cocaine (Figure 7.4), heroin (Figure 7.5) and methadone (Figure 7.6) and the accompanying peak data table (Tables 7.1 to 7.4 respectively) were captured to enable comparison with the SERS spectra for peak identification. The vibrational modes have been assigned where possible.

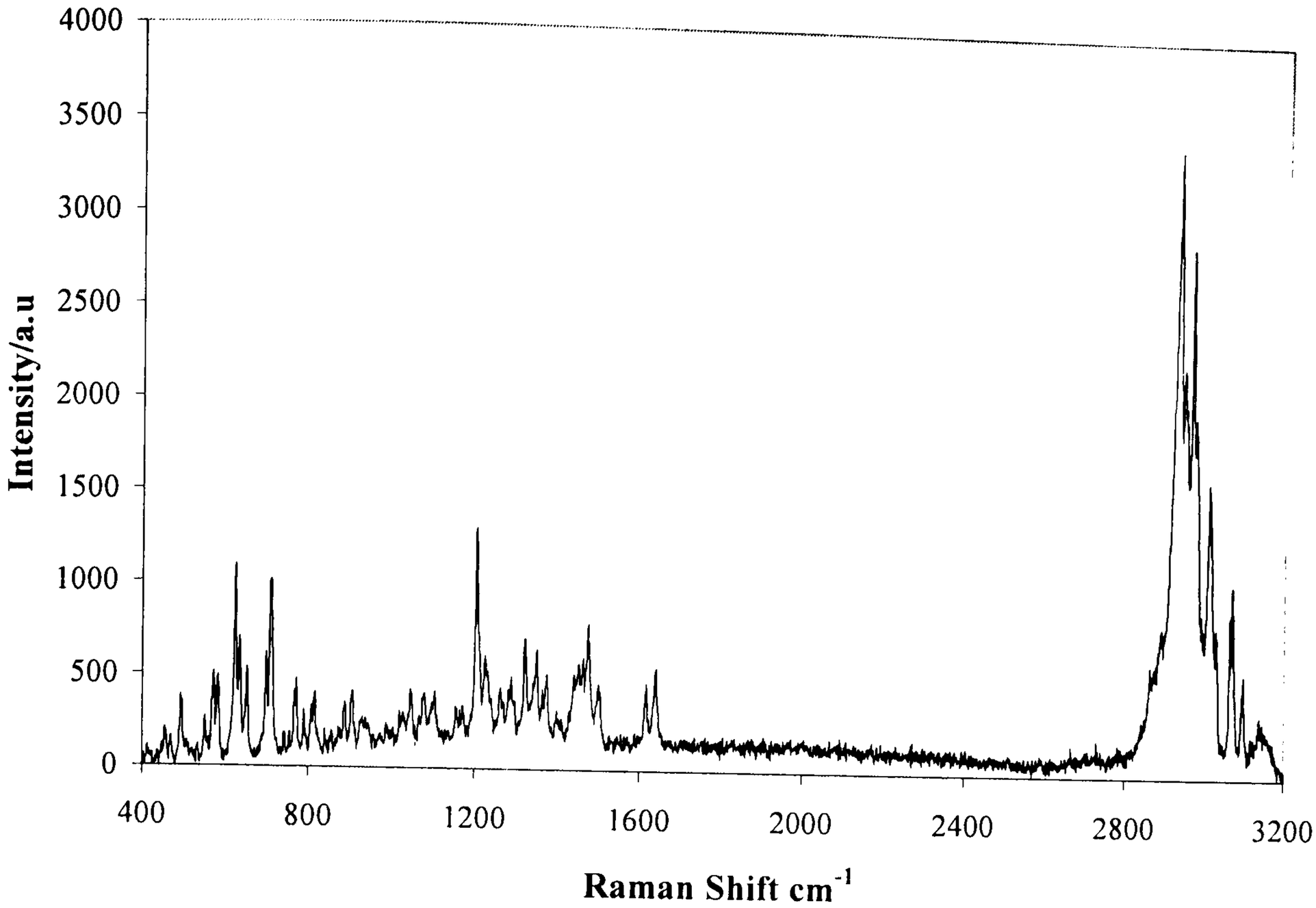

Figure 7.3: Raman spectrum of buprenorphine.

Table 7.1: Raman peak position data and molecular movement and strength (Weak (W), Medium (M), Strong (S), Very Strong (VS)) associated with that peak for buprenorphine [Lin-Vien *et al* (1991)].

Raman	
Peak Position cm^{-1}	**Movement**
624.17 (M)	Ring deformation
1203.98 (M)	Ring vibration or C-$(CH_3)_3$ stretch
1475.35 (M)	OCH_3 deformation
2929.1 (VS)	Anti-symmetric CH_2 stretch
2963.65 (S)	Anti-symmetric CH_3 stretch
3008.31 (M)	Aromatic CH stretch or Cyclopropane CH_2 symmetric stretch
3096.8 (W)	Cyclopropane CH_2 anti-symmetric stretch
3040.34 (W)	Cyclopropane CH_2 symmetric stretch

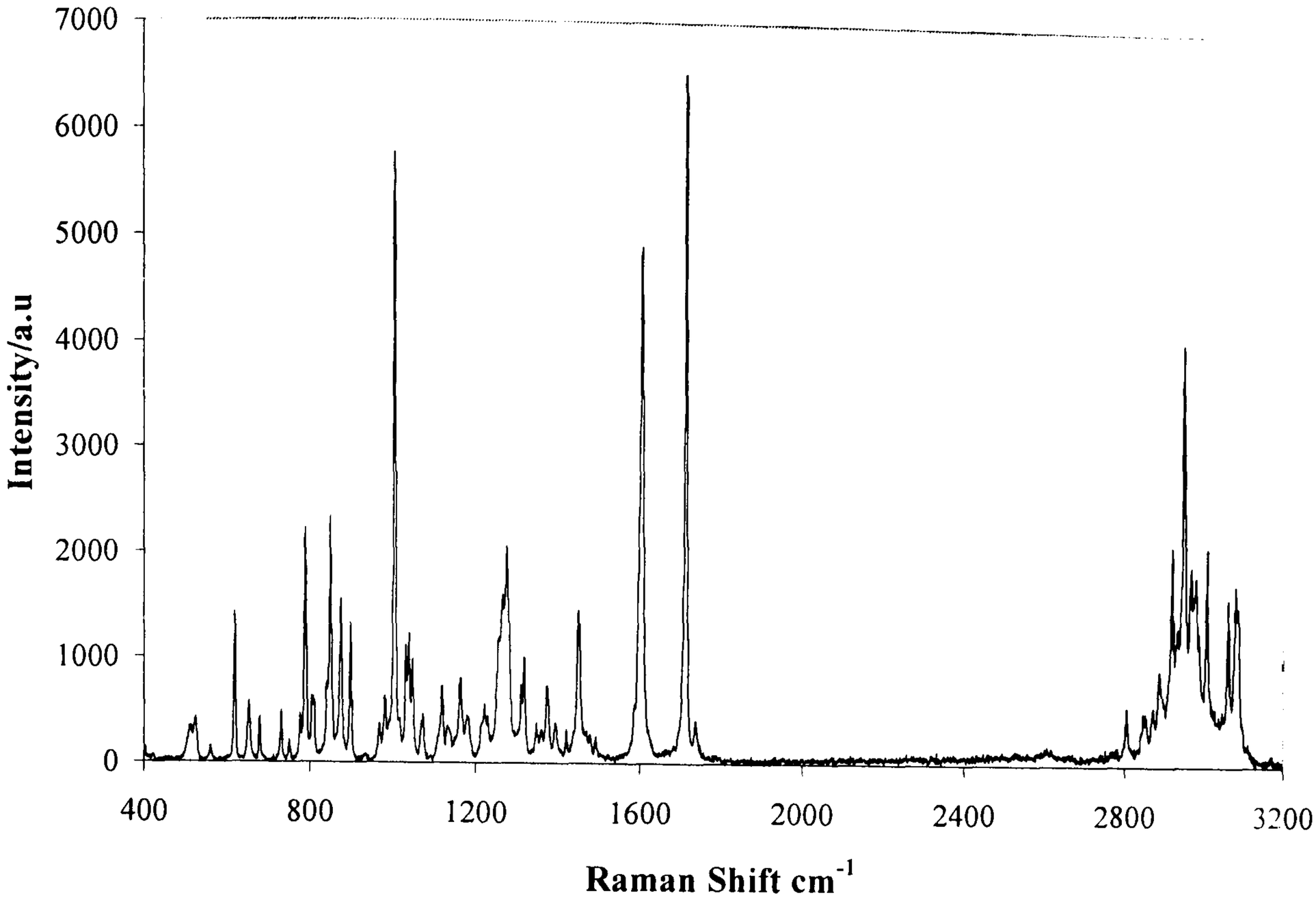

Figure 7.4: Raman spectrum of cocaine.

Table 7.2: Raman peak position data and molecular movement and strength (Weak (W), Medium (M), Strong (S), Very Strong (VS)) associated with that peak for Cocaine [Lin-Vien *et al* (1991)].

Raman	
Peak Position cm^{-1}	**Movement**
788.99 (M)	CH_2 Rock
849.51 (M)	Symmetric CNC stretch
1004.65 (S)	Trigonal ring breathing
1450.48 (W)	O-CH_3 deformation
1603.91 (S)	C=C stretch
1711.32 (VS)	C=O stretch
3007.01 (M)	C-O-CH_3
3079.47 (W)	C-O-CH_3

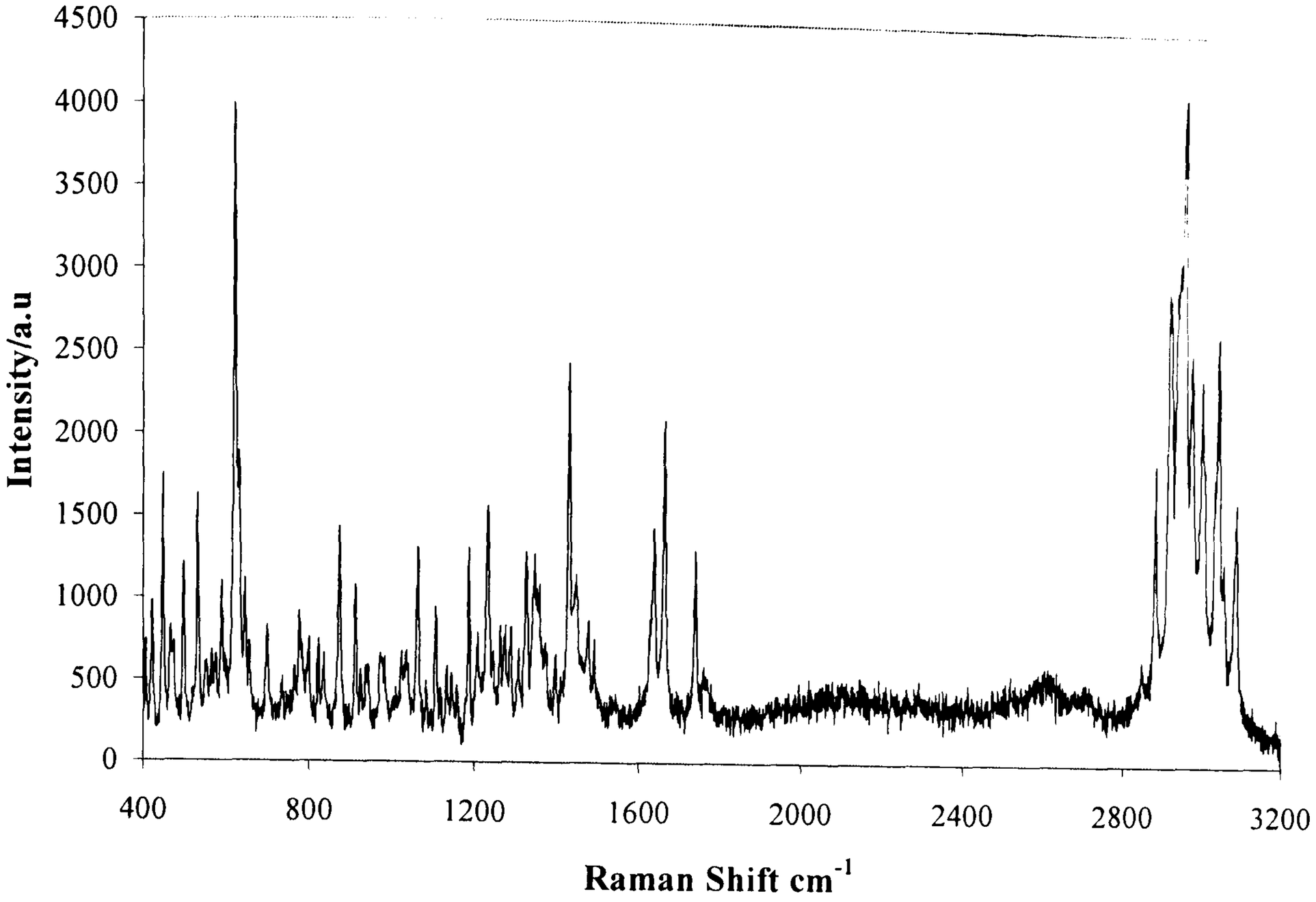

Figure 7.5: Raman spectrum of heroin.

Table 7.3: Raman peak position data and molecular movement and strength (Weak (W), Medium (M), Strong (S), Very Strong (VS)) associated with that peak for heroin [Lin-Vien *et al* (1991)].

Raman	
Peak Position cm^{-1}	**Movement**
621.06 (VS)	Ring deformation
873.38 (M)	Symmetric CNC stretch
912.59 (W)	Symmetric COC stretch
1062.62 (M)	Ring vibration
1233.11 (M)	Ring vibration
1638.01 (M)	C=O stretch or C=C stretch
1662.73 (M)	Amide I Band
1738.60 (M)	C=O stretch unconjugated ester
2881.70 (M)	Symmetric CH_3 stretch
2963.54 (M)	Anti-symmetric CH_3 stretch
3000.19 (M)	Aromatic CH stretch
3055.60 (M)	CH stretch

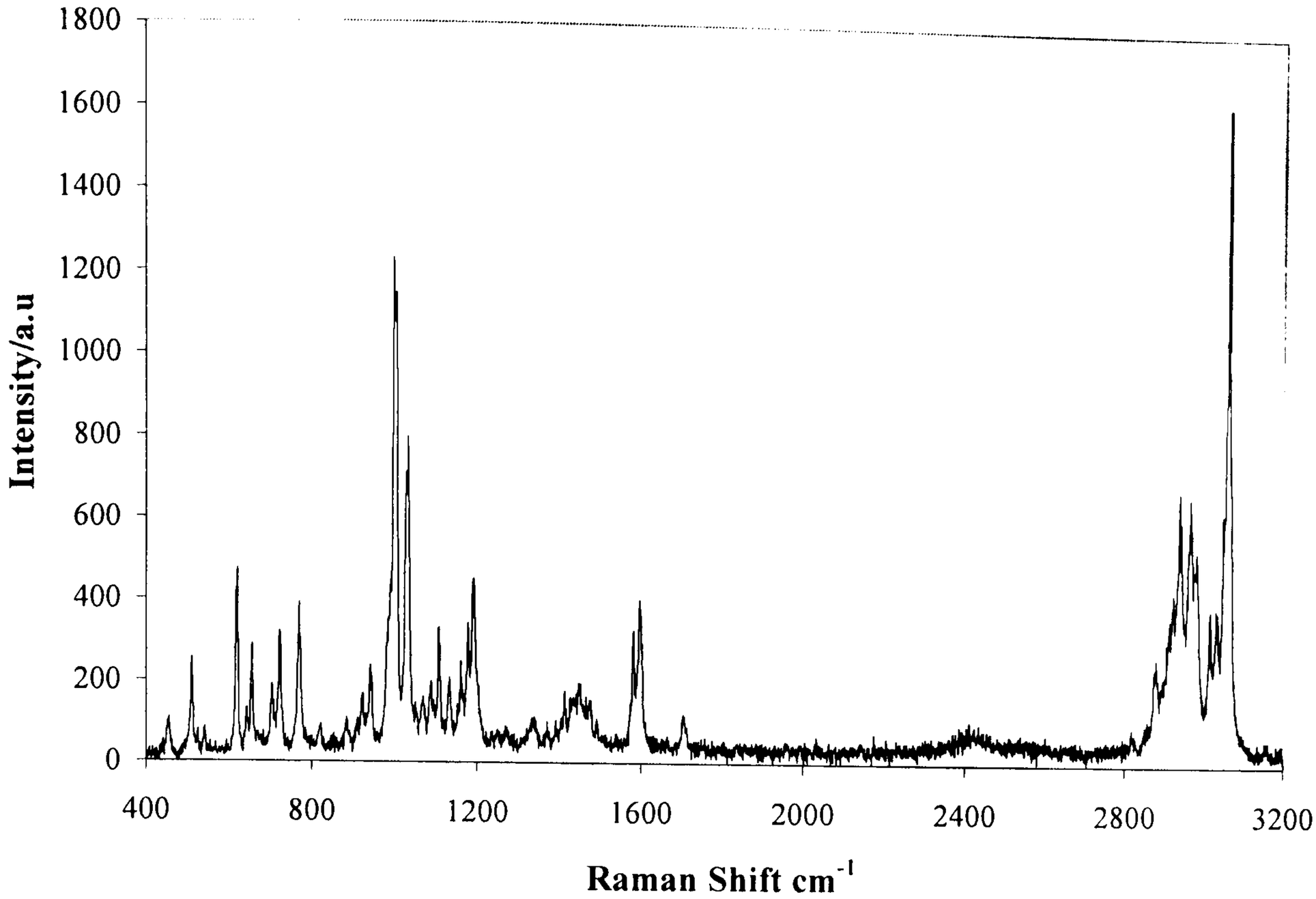

Figure 7.6: Raman spectrum of methadone.

Table 7.4: Raman peak position data and molecular movement and strength (Weak (W), Medium (M), Strong (S), Very Strong (VS)) associated with the that peak for methadone [Lin-Vien *et al* (1991)].

Raman	
Peak Position cm^{-1}	**Movement**
619.96 (W)	Ring deformation
998.35 (S)	Trigonal ring breathing
1004.25 (S)	Trigonal ring breathing
1028.69 (M)	In-plane CH deformation
1032.06 (M)	Ring vibration
1582.38 (W)	C=C stretch
1596.71 (M)	Primary amine
2922.35 (W)	Primary amine
2965.33 (M)	Anti-symmetric CH_3 stretch
3047.08 (M)	Aromatic CH stretch
3061.41 (VS)	Aromatic CH stretch

7.3.2 SERS From Blank Oral Fluid

A blank oral fluid spectrum is shown in Figure 7.7. This spectrum shows an absence of any distinct peaks within the fingerprint region but there is a strong peak at 2114.4 cm^{-1}. This peak is thought to be a thiocyanate peak [Farquharson *et al* (2005a)] which is present in oral fluid as an antibacterial agent [Ermans *et al* (1972)]. Farquharson *et al* (2005a) prepared samples of thiocyanate and performed SERS analysis using silver doped solgels. A broad thiocyanate peak at 2095 cm^{-1} (range ca. 2000 – 2200 cm^{-1}) was observed in Farquharson *et al* (2005a) work. If the range of the peak is considered then the peak observed in this work falls within position confirming the presence of the thiocyanate component C-N stretch.

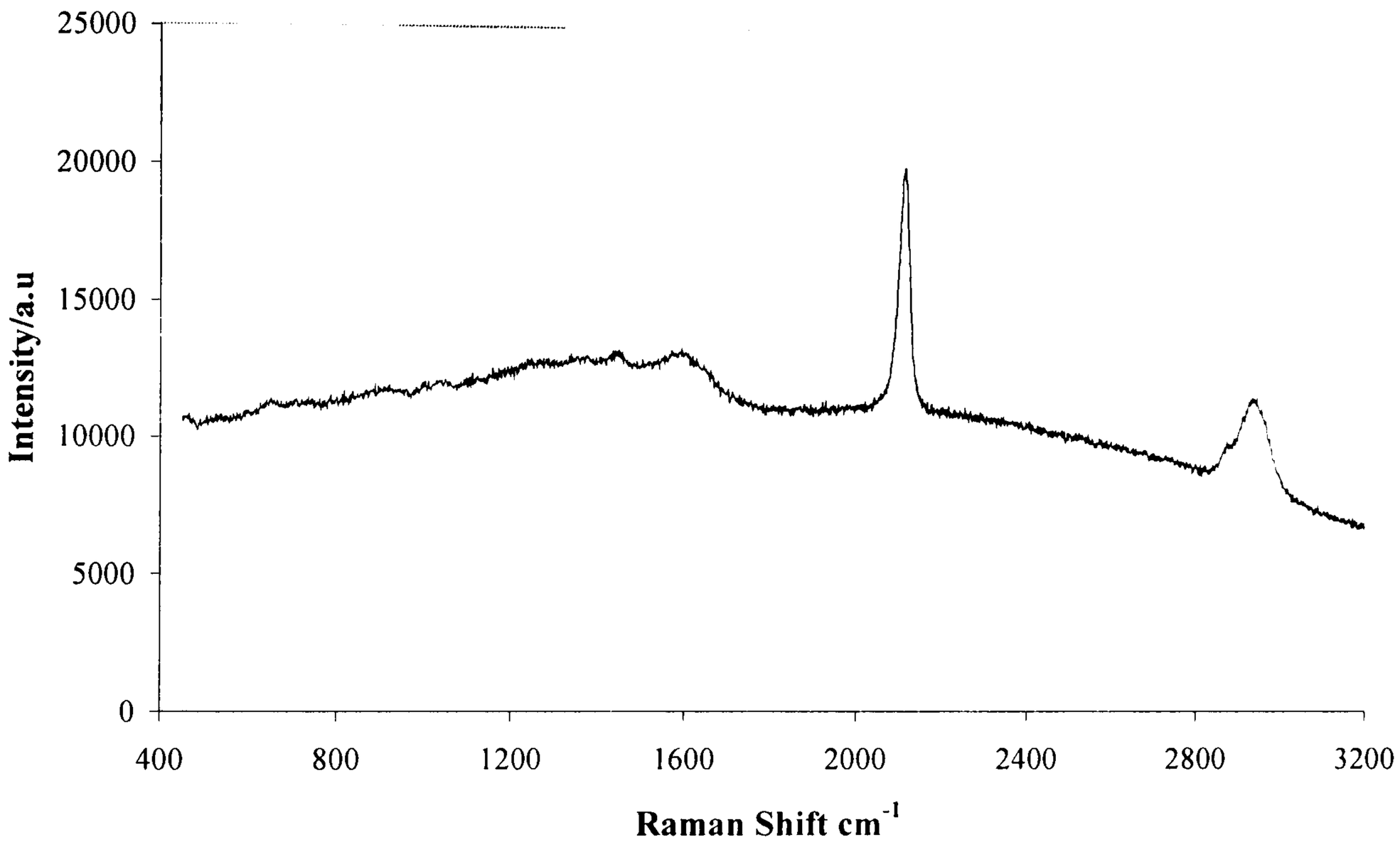

Figure 7.7: SERS spectrum of a blank oral fluid sample.

7.3.3 SERS From Oral Fluid Samples From Drug User Subject 14

Subject 14, a representative of the 30 subjects, self reported consuming methadone and ibuprofen (Table 7.5). However, the confirmatory analysis (Table 7.6) indicated that not only were methadone and its major metabolite 2-ethylidene-1,5-dimethyl-3,3-diphenylpyrrolidine (EDDP) present, but additionally trace quantities of buprenorphine, its metabolite (norbuprenorphine) and MDMA were also present in the oral fluid sample. The concentration of methadone observed is slightly higher than the typical therapeutic range expected (Chapter 1.2) but may reflect advances in

therapeutic regimes. The buprenorphine concentration also reflects expected therapeutic levels [Moffat and Widdup (2005)]. Although the lack of admission by the subject reflects that self-assessment questionnaires cannot be relied upon for honest reporting.

Table 7.5: Self-assessment questionnaire of drugs identified as consumed by subject 14.

Drug	**Taken**
Methadone	Daily – 75 mls
Ibuprofen	500 mg

Table 7.6: LC/MS confirmatory analysis results for oral fluid sample from subject 14.

Drug	**Concentration (ng/ml)**	**Concentration (M)**
Methadone	1909	$6.17x10^{-6}$
EDDP	6	$2.16x10^{-8}$
Buprenorphine	54	$1.11x10^{-7}$
Norbuprenorphine	55	$1.33x10^{-7}$
MDMA	28	$1.21x10^{-7}$

Despite readily identifying the drugs using confirmatory analysis methods, interpretation of the SERS spectrum (Figure 7.8) was complex. There are several peaks present which, where possible, have been assigned (Table 7.7). The thiocyanate peak is readily observed in Figure 7.8 confirming the authenticity of the oral fluid sample.

Figure 7.8 demonstrates the complexity of interpreting SERS spectra of oral fluid samples from poly-drug users. It is possible that the pH of the oral fluid sample inhibited the SERS enhancement mechanism [Farquharson *et al* (2005a)] limiting the observed vibrational movements of the drugs. These results reflect that at this time the Ag/TiO_2 substrates demonstrate sensitivity close to the concentration detection requirements, as specified in the type approval specification, especially for MDMA (30 ng/ml or $1.30x10^{-7}$) when applied to oral fluid samples that have undergone in-vivo metabolism. This subject was classified as impaired using the FIT test.

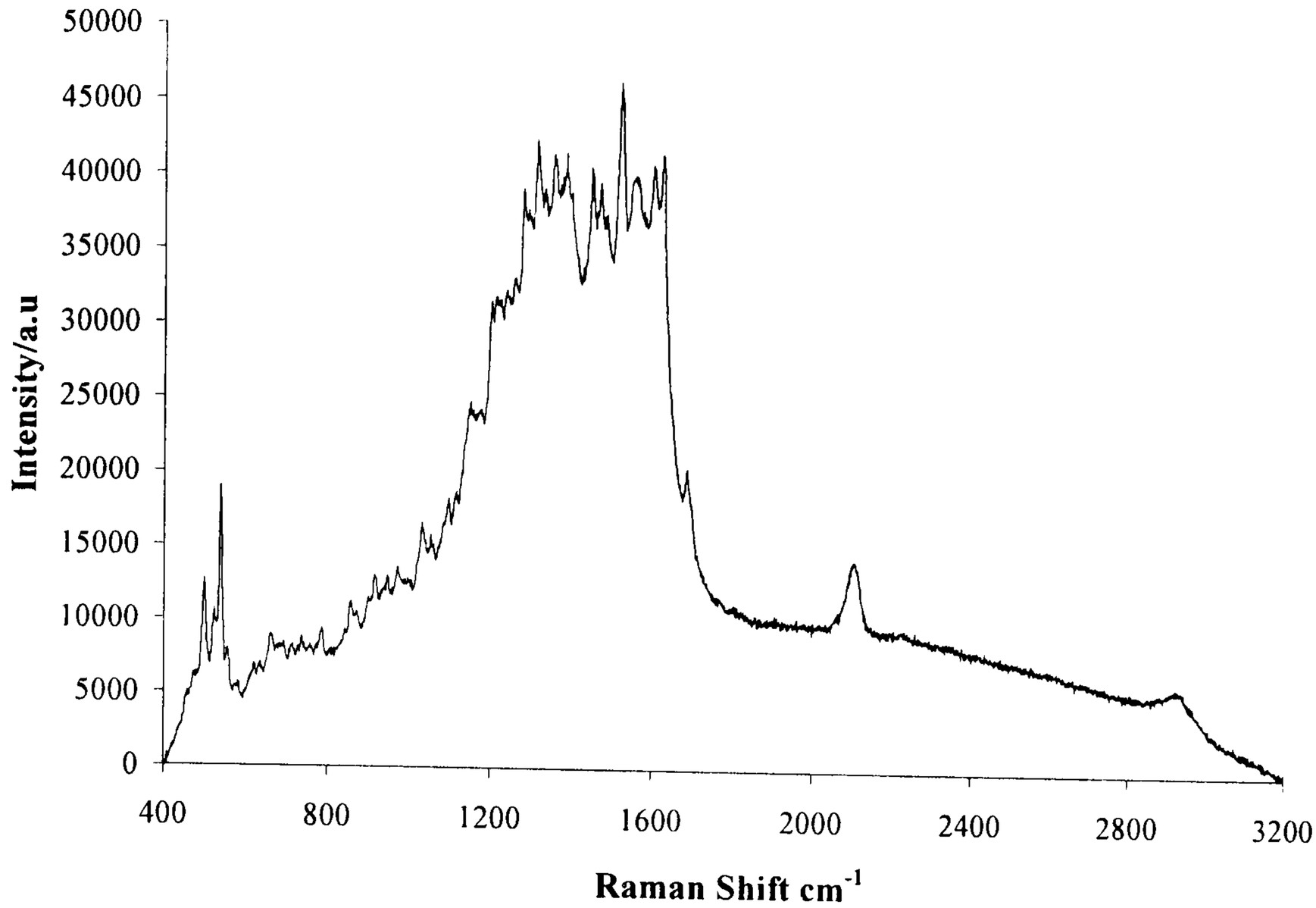

Figure 7.8: SERS spectrum of oral fluid sample from subject 14 known to contain methadone, EDDP, buprenorphine, nor-buprenorphine and MDMA.

Table 7.7: Observed SERS peaks in the oral fluid from subject 14, the associated vibrational movement, strength (Weak (W), Medium (M), Strong (S), Very Strong (VS)) and possible drug assignment [Lin-Vien *et al* (1991)].

Peak Position cm^{-1}	**Movement**	**Drug**
915.61 (W)	Symmetric COC Stretch	Unknown
1030.61 (M)	Trigonal ring breathing/ring vibration/in-plane CH deformation	Methadone
1148.13 (M)	CC stretch	Unknown
1209.40 (S)	Ring vibration	Buprenorphine
1274.88 (S), 1308.46 (VS)	Amide III band/CH_2 twist/CH_2 rock/in-plane CH deformation	MDMA
1350.43 (S)	CH deformation	Unknown
1381.49 (S)	CH_3 symmetric deformation	Unknown
1596.38 (S)	NH_2 scissors	Methadone
1618.20 (S)	NH_2 scissors	MDMA
1684.52 (S)	Amide I band	Unknown

7.3.4 SERS From Oral Fluid Samples From Drug User Subject 16

Subject 16, a representative of the 30 subjects, self reported consuming a number of illicit and prescription drugs (Table 7.8). The buprenorphine and the cocaine were confirmed as present in the oral fluid sample by LC/MS analysis (Table 7.9). Additional confirmation of the cocaine consumption is obtained from its major metabolite benzoylecgonine, which was detected at a high concentration. The concentrations detected for cocaine reflect those found in drivers suspected of drug driving by Oliver *et al* (2006) (Chapter 1.2).

A metabolite of diazepam, desmethyldiazepam, was only found when the cotton swabs were washed with solvent and the extract analysed. It is believed that the cotton swabs readily retained this drug preventing its detection following the centrifugation step. This indicates the importance of choosing an appropriate swabbing material that does not retain the drugs on the fibres [Drummer (2008)].

The lack of detection of the heroin, cannabis and nitrazepam reflects the time interval between consumption and sample collection. These drugs will have been fully metabolised so any active drug or active metabolite will have been eliminated.

Table 7.8: Self-assessment questionnaire of drugs identified as consumed by subject 16.

Drug	Taken
Buprenorphine	Daily - 8 mg
Crack Cocaine	3 hrs prior – unknown amount
Heroin	10 hrs prior – unknown amount
Cannabis	10 hrs prior – unknown amount
Diazepam	12 hours prior
Nitrazepam	48 hrs prior
Venlafaxine Excell	Daily – 225 mg (none today)
Nicotine	Daily – 20 – 30 cigarettes

Table 7.9: LC/MS confirmatory analysis results for oral fluid sample from subject 16.

Drug	Concentration (ng/ml)	Concentration (M)
Buprenorphine	32	$6.85x10^{-8}$
Cocaine	3170	$9.33x10^{-6}$
Benzoylecgonine	8028	$2.775x10^{-5}$
desmethyldiazepam	4 ng/swab	-

Despite the ability to readily identify the drugs using confirmatory analysis methods it was not possible to detect any drugs using the SERS method (Figure 7.9). It was only possible to identify the thiocyanate peak (Table 7.10). The reasons for this are not wholly understood at this time. The high oral fluid concentration for cocaine is expected following the self-report of 3 hours since consumption. Additionally, it is common to have oral contamination following the use of smoked crack cocaine. The basic nature of the drug sees it readily partition into the acidic oral fluid [Cone *et al* (1993), Navarro *et al* (2001)]. However, the samples were stored without the addition of a pH buffer and Ventura *et al* (2008) have shown statistically significant degradation of cocaine to benzoylecgonine in the absence of a buffer. This is reflected in the elevated benzoylecgonine concentration detected by LC/MS. It is also likely that further degradation has occurred with prolonged storage (-80 ^{o}C) between collection and the SERS analysis (18 months). The confirmatory LC/MS analysis was undertaken earlier than the SERS analysis. This subject was also classified as impaired by the FIT test.

It is also possible that the pH of the oral fluid sample inhibited the SERS enhancement mechanism [Farquharson *et al* (2005a)]. Stimulant drugs such as cocaine cause a reduction in oral fluid flow. This reduction in flow reduces the pH. The pH in turn influences the ionisation state of the drug which interferes with the drug-surface interaction [Farquharson *et al* (2005a)]. This effect might explain the lack of detection of the benzoylecgonine. These results may also reflect that at this time the Ag/TiO_2 substrates do not have the required sensitivity when applied to oral fluid samples containing high concentrations of cocaine and benzoylecgonine that have undergone in-vivo metabolism.

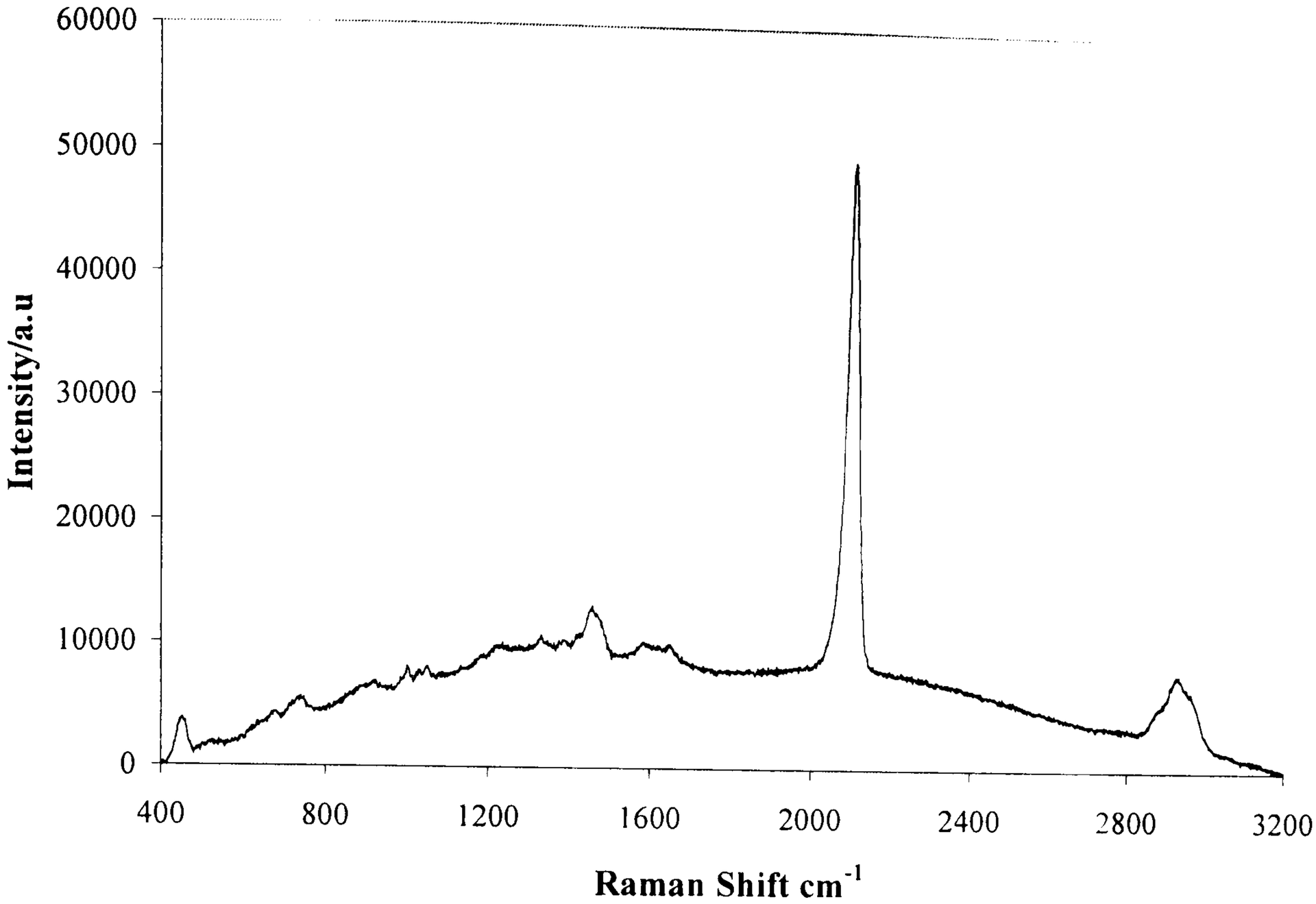

Figure 7.9: SERS spectrum of oral fluid sample from subject 16 known to contain buprenorphine, cocaine, benzoylecgonine and desmethyldiazepam.

Table 7.10: Observed SERS peaks in the oral fluid from subject 16, the associated vibrational movement, strength (Weak (W), Medium (M), Strong (S), Very Strong (VS)) and possible drug assignment [Lin-Vien *et al* (1991)].

Peak Position cm^{-1}	**Movement**	**Drug**
2107.59 (VS)	C-N stretch	Thiocyanate ion

Farquharson *et al* (2005b) demonstrated that by adjusting the pH of oral fluid in the presence of a drug it was possible to improve the SERS enhancement achieved using SERS-active sol-gels. The SERS-active sol-gel is forced into a negative charge state by passing 5 mM hydrochloric acid solution through the sol-gel. The oral fluid sample is then analysed using the charged sol-gel and the improved enhancement observed (Figure 7.10). When repeated with a blank oral fluid sample suppression of the thiocyanate peak is observed (Figure 7.10). It appears that the charging of the sol-gel preferentially binds the drugs improving the overall sensitivity of the system. However, the original amount of thiocyanate was unknown so the true success is undetermined.

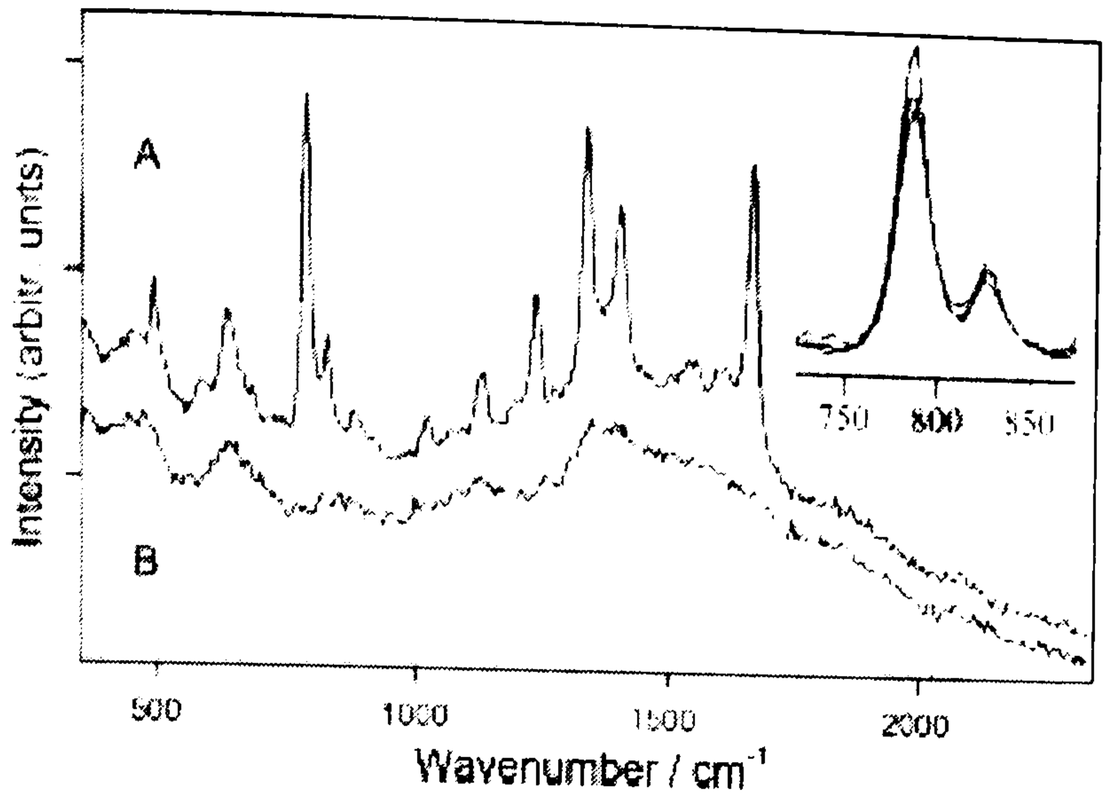

Figure 7.10: SERS spectra of 5-FU (50 μg/ml) following pH adjustment of the sol-gel with 5 mM hydrochloric acid (A) and a blank oral fluid sample (B). Reproduced from Farquharson *et al* (2005 b).

7.3.5 Control Oral Fluid Samples

All of the control samples (n = 30) contained no drugs as confirmed by LC/MS analysis. The SERS analysis produced the thiocyanate ion peak in all of the spectra and no other distinct peaks, providing further confirmation of the drug negative control samples.

7.3.6 SART and CTT Results

The subjects were divided into 4 groups control, no illicit drugs (buprenorphine and methadone), illicit drugs and poly-drugs (Table 7.11). Discriminant analysis of impaired and non-impaired subjects using a non-parametric tri-weight kernel statistical procedure combining age, gender and the primary response variables of the SART and CTT tests was undertaken. The results are summarized in Table 7.12. The 'n' number is out of the total for each drug grouping.

The results (Table 7.12) show that using the response variables from the SART and CTT test in combination with age and gender it is possible to demonstrate a low false negative rate (n = 7) and a low false positive rate (n = 5). Whilst a low false positive rate is desirable to reduce time wasting for both the police and drivers, a low false negative rate is imperative to prevent drug drivers evading detection.

Table 7.11: Drug groupings for the subjects

	Acorn	Control	Total
Control	0	30	30
No illicit Drugs	6	0	6
Illicit Drugs	13	0	13
Poly-drug	11	0	11

Table 7.12: Discriminant analysis of the no drug, drug, poly-drug combination using CTT and SART variables in combination with age and sex.

	Control	No illicit Drugs	Illicit Drugs	Poly-drug
Control	42.9% (n = 12)	39.2% (n = 11)	17.9% (n = 5)	0.0%
No illicit Drugs	0.0%	100% (n = 6)	0.0%	0.0%
Illicit Drugs	23.1% (n = 3)	15.4% (n = 2)	61.5% (n = 8)	0.0%
Poly-drug	0.0%	18.2% (n = 2)	36.3% (n = 4)	45.5% (n = 5)

7.4 Conclusions

This work demonstrates that at this time variable results with the Ag/TiO_2 substrates to obtain a qualitative SERS spectrum of oral fluids known to contain drugs are observed. The reasons for this are not fully understood. Representatives from the full thirty subjects were chosen but all samples were analysed in the same manner. Overall the split between successful drug detection and non-detection in the subject was 40:60 respectively. The lack of SERS enhancement could relate to the pH of the oral fluid sample interfering with the SERS enhancement mechanism [Farquharson *et al* (2005a)], a lack of sensitivity of particular drugs with this substrate or degeneration of the samples.

Interestingly, using SERS it was possible to detect the thiocyanate peak at ca. 2100 cm^{-1} in the blank and drug user samples. This can be used not only to authenticate a true oral fluid sample against an adulterated sample but also confirms that some SERS enhancement was occurring.

This work also confirms that SERS has a role within drug detection in oral fluid samples. The successful detection of methadone and buprenorphine, used to treat

heroin addiction, was at concentrations associated with therapeutic use, representing lower concentration drugs. The detection of MDMA in the oral fluid sample not only showed promise for the detection of illicit drugs, but did so at the concentration detailed in the draft type approval specification for roadside drug screening devices.

The CTT and SART data also show tentative indications that these tests could be used to provide an impartial assessment of driver impairment with low false positive and false negative results.

Chapter 8

Conclusions and Future Work

Initial work investigated ecstasy tablet composition to identify what drugs and excipients might be present in oral fluid samples obtained from users. The data showed the presence of phenethylamine derivatives and excipients in the seized ecstasy tablets. However, on closer inspection of the absolute peak positions it is not possible to categorically distinguish between the phenethylamine derivative(s) present in the samples when in a mixture. The phenethylamine derivatives average peak position data per tablet showed detectable variability in the intensity per batch but consistency within sub-batches, tentatively indicating that the tablets originate from the same clandestine laboratory. This is further supported by the average peak responses of the excipients and the reproducibility observed within associated sub-batches. Overall this study showed that ecstasy tablet composition profiling can be undertaken with some degree of success using Raman spectroscopy. It also showed that a mixture of phenethylamines and excipients are present in the tablets which might appear in the oral fluid of users.

Initial SERS research focused on achieving enhancement of aqueous drug solutions with silver and gold colloid. It is necessary to identify a suitable aggregating agent for the illicit drugs and their metabolites in aqueous samples to observe the SERS signal. The electron donating/withdrawing nature of the functional groups needs to be considered as well, as demonstrated through the lack of observed enhancement with the PMA solutions. It is also clear that the volume and concentration of the aggregating agent used has a direct influence on the SERS activity and the spectral data observed. Tentative results show the 633 nm laser system is an appropriate excitation wavelength for screening for amphetamine and the phenethylamines due to a greater spectral overlap with the plasmon resonance band for the silver colloidal particles. Overall a lack of reproducibility when using both the silver and gold colloid was observed. Therefore, alternative SERS enhancement mechanisms were sought.

Research continued investigating the detection of three phenethylamine derivatives using silver based substrates. The level of enhancement observed using Ag/TiO_2 substrates exceeded that observed using both silver colloid and silver evaporated substrates. The volume of solution used is also a critical factor in observing the SERS effect at its greatest capacity. A 0.5 µl volume was the most efficient volume to observe the drug/surface interaction and respective SERS effect. This work demonstrated SERS detection of aqueous $1x10^{-6}$ M (368.49 ng/ml) amphetamine solution with the Ag/TiO_2 substrates. Surface enhancement was also observed with a solution of methamphetamine at concentrations of $1x10^{-5}$ M (1856.9 ng/ml) and $1x10^{-6}$ M (185.69 ng/ml) and with MDEA at $1x10^{-7}$ M (24.37 ng/ml).

Timing of the spectral collection is also important, too soon and little SERS activity is recorded, too late and only limited information is obtained if a thick layer of crystals have formed. The length of time taken for the sample to begin to evaporate may be reduced by using the cotton swabs instead of placing a bead of liquid on the surface of the substrate using a syringe. The use of cotton swabs for sample application onto the surface of the substrate is a viable practical option for both experimental and field work. It has demonstrated that SERS can be observed using this technique and at low concentrations.

Pre-cleaning of the Ag/TiO_2 substrates with spectroscopic grade methanol and UV lamp irradiation reduced the contact angle of the solution on the substrate surface assisting with the observation of SERS enhancement. This reduction in contact angle allows greater substrate interaction between the sample and the silver particles to take place. As the sample re-crystalises on the substrate there is more opportunity for chemical and field enhancement to occur resulting in a larger SERS enhancement and better detection of lower concentrations of aqueous amphetamine.

The Ag/TiO_2 substrates demonstrated the most consistent SERS response with the best reproducibility in comparison to the other substrates investigated. The Ag/TiO_2 substrates demonstrated low limits of detection and the possibility of detecting SERS enhancement of aqueous amphetamine solution at levels below $8x10^{-7}$ M.

However, at this time variable results with the Ag/TiO_2 substrates with oral fluid samples known to contain drugs were observed. The reasons for this are not fully understood. The lack of SERS enhancement could relate to the pH of the oral fluid sample interfering with the SERS enhancement mechanism [Farquharson *et al* (2005a)], a lack of sensitivity of particular drugs with this substrate or degeneration of the samples. Interestingly, using SERS it was possible to detect a thiocyanate peak at ca. 2100 cm^{-1} in the blank and drug user samples which could be used to authenticate a true oral fluid sample against an adulterated sample. It also indicates that some SERS enhancement was occurring.

This work also confirms that SERS has a role within drug detection in oral fluid samples. The successful detection of methadone and buprenorphine, used to treat heroin addiction, was at concentrations associated with therapeutic use, representing lower concentration drugs. The detection of MDMA in the oral fluid sample not only showed promise for the detection of illicit drugs, but did so at the concentration detailed in the draft type approval specification for roadside drug screening devices.

Further work with the ecstasy tablets includes investigating separation of the phenethylamine derivatives. This might include looking at other Raman fingerprint regions for alternative characteristic peaks to distinguish them. Additionally, cooling the sample to approximately 77 K might improve the peak resolution as temperature effects cause peak broadening [Otto (2006)]. Spatially Offset Raman [Matousek and Parker (2006)] is another method that could be tried. This enables penetration through the tablet facilitating analysis of different layers within the tablets. However, none of these methods will have an added advantage over the method described unless better separation of the phenethylamine derivatives is achieved.

Future work with the Ag/TiO_2 substrates includes further assessment of the substrates with more poly-drug profiles. Investigations of oral fluid samples spiked with drugs at a known concentration across a range of pH values representative of those found in the oral cavity should be undertaken. This will enable assessment of the possible effects of pH on the Ag/TiO_2 substrates and any interference to the

SERS enhancement mechanism. If pH is found to be significantly influential on when SERS can and cannot be observed it may be necessary to explore chemical functionalisation. This could promote preferential orientation binding of the drug to the Ag/TiO_2 substrates to facilitate observation of the SERS signal at all times.

References

ACPO Press release 2007, Drink and drug driving remains a problem. January 2007. www.acpo.police.uk

Adrian F. Charge-transfer effects in surface enhanced Raman scattering. *J. Chem. Phys.* 1982, **77**, 5302-5314

Ahern A., Garrell R. Insitu photoreduced silver nitrate as a substrate for surface enhanced Raman spectroscopy. *Anal. Chem.* 1987, **59**, 2813-2816

Angebranndt M., Winefordner J. Surface enhanced Raman spectroscopy on copper hydrosols. *Talanta* 1992, **63**, 569-572

Aps J., Martins L. Review: the physiology of saliva and transfer of drugs into saliva. *For. Sci. Rev.* 2005, **150**, 119-131

Asher S., Johnson C. Raman Spectroscopy of a coal liquid shows that fluorescence interference is minimised with ultraviolet excitation. *Science* 1984, **225**, 311-313

Bell S., Beattie J., McGarvey J., Peter K., Sirimuthu N., Speers S. Development of sampling methods for Raman analysis of solid dosage forms of therapeutic and illicit drugs. *J. Raman Spec.* 2004, **35**, 409-417

Bell S., Barrett L., Burns D., Denis A., Speers J. Tracking the distribution of ecstasy tablets by Raman composition profiling: a large scale feasibility study. *Analyst*, 2003, **128**, 1331-1355

Bell S., Spence S. Disposable, stable media for reproducible surface-enhanced Raman spectroscopy. *Analyst* 2001, **126**, 1-3

Bell S., Burns D., Dennis A., Speers S. Rapid analysis of ecstasy and related phenethylamines in seized tablets by Raman spectroscopy. *Analyst* 2000a, **125**, 541-544

Bell S., Burns D., Dennis A., Matchett L., Speers S. Composition profiling of seized ecstasy tablets by Raman spectroscopy. *Analyst* 2000b, **125**, 1811-1815.

Birke R.L., Lombardi J.R., in *Spectroelectrochemistry Theory and Practise*, Gale R.J., (ed) Plenum, New York 1988, 263-328

Brookhuis K.A., De Waard D., Pernot L. A driving simulator study on driving performance and traffic safety after multiple drug use, consisting of MDMA and various other psychoactive compounds. *International Conference on Alcohol Drugs and Traffic Safety* 2000

Busto U., Bendayan R., Sellers E. Clinical pharmacokinetics of non-opiate abused drugs. *Clin. Pharmacokinet.* 1989, **16**, 1-26

Cho A. Ice: a new dosage form of an old drug. *Science* 1990, **249**, 631-634

Cinta S., Iliescu T., Astilean S., David L., Cozar O., Kiefer W. 1,4-Benzodiazepine drugs adsorption on the Ag colloidal surface. *J. Mol. Struc.* 1999, **482-483**, 685-688

Codon J., Smith N. British Crime Survey Findings 229. Home Office, UK. December 2003

Cone E. Saliva testing for drugs of abuse New York Academy of Sciences 1993; 694: 1-348 Malamud D., Tabak L., (eds) NYAS

Cook C., Jeffcoat A., Hill J., Pugh D., Patetta P., Sadler B. Pharmacokinetics of methamphetamine self administered to human subjects by smoking S-(+)-methamphetamine hydrochloride. *Drug Metab. Dispos.* 1993, **21**, 717-723

Crouch D. Oral fluid collection: the neglected variable in oral fluid testing. *For. Sci. Int.* 2005, **150**, 165-173

Dawes C. Physiological factors affecting salivary flow rate, oral sugar clearance and the sensation of dry mouth in man. *J. Den. Res.* 1987, **66**, 648-653

De la Torre R., Farre M., Ortuno J., Mas M., Brenneisen R., Roset P. Non-linear pharmacokinetics of MDMA (ecstasy) in humans. *B. J. Clin. Pharm.* 2000, **49**, 104-109

Deegan R., Bakajin O., Dupont T., Huber G., Nagel S., Witten T. Contact line deposition in a evaporating drop. *Phys. Rev. E.* 2000, **62**, 756-765

Del Rio M., Alvarez F. Illegal drugs and driving. *J. Traff. Med.* 1995, **23**, 1-5

Drummer O.H. *The forensic pharmacology of drugs of abuse,* Arnold Publishers, London, 2001

Drummer O. Introduction and review of collection techniques and applications of drug testing of oral fluid. *Therap Drug Monit.* 2008, **30**, 203-6

Eatman F., Maggio A., Pocelinko R., Botenbaum H., Geither H., Glover W., Macasieb T., Holazo A., Weinfield R., Kaplin S. Blood and salivary concentrations of sulfamethoxazole and trimethoprim in man. *J. Pharmacokinet. Biopharm.* 1977, **5**, 615-624

Ermans A., Delange F., Van der Velden M., Kinaert J. Human Development and the Thyroid Gland. Relation to Endemic Cretinism. Stanbury J., Kroc R. (eds) Plenum Press: New York 1972

Fallon J. Kicman A., Henry J., Milligan P., Cowan D., Hutt A. Stereospecific analysis and enentiomeric disposition of 3,4-methylenedixymethamphetamine ("Ecstasy") in humans. *Clin. Chem.* 1999, **45**, 1058-1069

Farquharson S., Shende C., Inscroe F., Maksymiuk P. Gift A., Analysis of 5-fluorouracil in saliva using surface-enhanced Raman spectroscopy. *J. Raman Spectrosc.* 2005a, **36**, 208-212

Farquharson S., Gift A., Shende C., Maksymiuk P., Inscroe F., Murran J. Detection of 5-fluorouracil in saliva using surface-enhanced Raman spectroscopy. *Vib. Spec.* 2005b, **38**, 79-84

Faulds K. Detection of drugs of abuse by surface enhanced Raman scattering. PhD Thesis Strathclyde University April 2003

Faulds K., Smith W., Graham D., Lacey R. Assessment of silver and gold substrates for the detection of amphetamine sulfate by surface enhanced Raman scattering (SERS). *Ana.* 2002, **127**, 282-286

Fleischmann M., Hendra P., McQuillan A. Raman spectra of pyridine adsorbed at a silver electrode. *J. Phys. Lett.* 1974, **26**, 163-166

Gao X., Wan C., He T., Li J., Xin H., Liu F., Surface-enhanced Raman-scattering and enhanced fluorescence of dyes on silver chloride sols. *Chem. Phys Lett.* 1984, **112**, 465-468

Gardiner D.J., Graves P.R., *Practical Raman Spectroscopy*, Springer -Verlag, London 1989

Giccovazzo C., Monaco H., Viterbo D., Scordari F., Gilli G., Zanotti G. Catti M. *Fundamentals of crystallography*. Giccovazzo C., (eds) 1992 Oxford University Press

Glennon R.A., Young R., Dukat M., Cheng Y. Initial characterization of PMMA as a discriminative stimulus. *Pharmacol. Biochem. Behav*. 1997, **57**, 151-158

Grabar K., Freeman R., Hommer M., Natan M. Preparation and characterisation of gold colloid monolayers. *Anal. Chem*. 1995, **67**, 735-743

Haeckel R. Interpretation of salivary drug concentrations. Application of saliva in laboratory medicine. *J. Clin. Chem. Clin. Biochem.* 1989, **27**, 221-252

Horvath E., Mink J., Kristof J. Surface-enhanced Raman spectroscopy as a technique for drug analysis. *Mikrochim. Acta.* 1997, **14**, 745-746

Hubball J. The use of chromatography in forensic science. *Adv. Chromatogr.* 1992. **32**, 131-172

Jones, J., McLaughlin C., Littlejohn D., Sandler D., Graham D.. Smith E. Quantitative assessment of surface enhanced Raman scattering for the analysis of dyes on colloidal surfaces. *Ana. Chem.* 1999, **71,** 596-601

Jusko W., Milsap R. Pharmacokinetic principles of drug distribution in saliva. *The New York Academy of Sciences* 1993, **694,** 1-348 Malamud D., Tabak L., (eds) NYAS, New York

Karpov S., Popov A., Slabko V. Laser-induced photochromic reactions of metallic colloidal silver. *Quantum Electronic Conference* 1996, **96**, 76-76

Kidwell D., Holland J., Athanaselis S. Testing for drugs of abuse in saliva and sweat. *J. Chromatogr. B. Biomed. Sci. Appl.* 1998, **713**, 111-135

King L., Clarke K., Orpet A., Cone E., Darwin W. Amphetamine profiling in the UK. *Forensic Sci Int.*, 1994, **69**, 65-75

Kintz P. The role of saliva and sweat in detecting cases of driving under the influence. Group Road Traffic and Drugs Strasbourg 19-21 April 1999

Krueger H., Vollrath M. Effects of cannabis and amphetamines on driving simulator performance of recreational drug users in the natural field. ICADTS 2000.

Lamping S. The detection of drugs of abuse in aqueous solution using Raman spectroscopy: a comparative study between the optical and racemic forms of amphetamine, methylenedioxyamphetamine and methylenedioxymethamphetamine aqueous solutions using Raman spectroscopy. MSc Degree in Forensic Science, Kings College London. August 1999

Lamping S. Raman spectroscopy profiling of ecstasy tablets. Home Office. Published www.belspo.be/belspo/fedra/proj.asp?l=en&COD=DR/272006

Lee P.C., Meisel D., Adsorption and surface enhaced Raman of dyes on silver and gold sols. *J. Phys. Chem.*, 1982, **86**, 3391-3395

Lee S., Guan Z., Xu H., Moskovits M. Surface enhanced Raman spectroscopy and nanogeometry: the plasmonic origin of SERS. *J. Phys. Chem. C.* 2007, **111**, 17985-17988

Lewis I., Daniel N., Chaffin N., Griffiths P., Tungol M. Raman spectroscopic studies of explosive materials - towards a fieldable explosives detector. *Spectrochim. Acta, Part A.* 1995, **51**, 1985-2000

Lin-Vien D., Colthrup N., Fateley W., Grasselli J. The handbook of infrared and Raman characteristic frequencies of organic molecules, 1991 Academic Press. London

Litter M. Heterogeneous photocatalysis- Transition metal ions in photocatalytic systems. *Appl. Catal. B: Environ.* 1999, **23**, 89-114

Logan B., Couper F. 3,4-Methylenedioxymethamphetamine – effects on human performance and behaviour. *For. Sci. Rev.* 2003, **15**, 12-28

Logan B. Methamphetamine – effects on human performance and behaviour. *For. Sci. Rev.* 2002, **14**, 135-151

Macpherson W. The Stephen Lawrence Inquiry, report of an inquiry by Sir William Macpherson of Cluny. Home Office, February 1999

Mandel I. The diagnostic uses of saliva. *J. Oral Pathol. Med.* 1990, **19**, 119-125

Mannich C., Jacobson W. Hydrophenylalkylamines and dihydroxyphenylalkylamine. *Berichte*, 1910, **43**, 189-197

Martin S., Wan S., Knight J. Quantitative determination of entiomeric compounds I-simultaneous measurement of the optical isomers of amphetamine in human plasma and saliva using chemical ionization mass spectrometry. *Biomed. Mass Spec.* 1977, **4**,118-121

Martindale, *The Extra Pharmacopoeia 31st Edition*, Reynolds J. (eds) The Royal Pharmaceutical Society London 1993

Matousek P., Parker A. Bulk Raman analysis of pharmaceutical tablets. *App. Spectros.* 2006, **60**, 1353-1357

McCreery R. *Raman Spectroscopy for Chemical Analysis*, Wineforder J. (eds) Whiley-Interscience, New York, 2000

McLaughlin C., Graham D., Smith W. Comparison of resonant and non-resonant conditions on the concentration dependence of surface enhanced Raman scattering from a dye adsorbed on silver colloid. *J. Phys Chem. B.* 2002, **106**, 5408-5412

Meier M., Wokaun A. Enhanced fields on large metal particles: dynamic depolarization. *Opt. Lett.* 1983, **8**, 581-583

Mills A., Hill G., Graham D., Smith W., Hodgen S., Halfpenny P., Faulds K., Robertson P. Characterisation of novel Ag on TiO_2 films for surface enhanced Raman scattering. *App. Spec.* 2004, **58**, 922-928

Mills A., Lee S. Platinum group metals and their oxides in semiconductor photosensitisation. *Platinum Met. Rev.* 2003, **47**, 2-12

Mills A., LeHunte S. An overview of semiconductor photocatalysis. *J. Photochem. Photobiol. A* 1997, **108**, 1-35

Moffat A., Widdop B. *Clarkes Analysis of Drugs and Poisons*. 3rd Ed, Pharmaceutical Society of Great Britain, London 2004

Morgan M. Recreational use of "ecstasy" (MDMA) is associated with elevated impulsivity. *Neuropsychopharm.* 1998, **19**, 252-264

Mortier K., Clawaert A., Lambert W., Van Bocxlaer J., Van den Eeckhaut E., Van Peteghem C., De Leenheer A. Simultaneous quantitative determination of opiates, amphetamine, cocaine, benzoylecgonine in oral fluid by liquid chromatography quadrupole time of flight mass spectrometry. *Rapid Commun. Mass Spectrom.* 2001, **15**, 1773-1775

Moskovits M. Surface Enhanced Raman Spectroscopy a brief perspective, *Topics in Applied Physics, Surface Enhanced Raman Scattering, Springer Berlin.* 2006, 1-17 Kneipp K., Moskovits M., Kneipp H. (eds)

Munro C., Smith W., Garner M., Clarkson J., White P. Characterization of the surface of a citrate reduced colloid optimized for use as a substrate for surface enhanced Raman scattering. *Langmuir* 1995, **11**, 3712-3720

Navarro M., Pichini S., Farre M., Ortuno J., Roset P., Segura J., De la Torre R. Usefulness of saliva for measurement of 3,4-methylenedioxmethamphetamine and its metabolites: correlation with plasma drug concentrations and effect of salivary pH. *Clin. Chem.* 2001, **47**, 1788-1795

Negishi N., Iyoda T., Hashimoto K., Fujishama A. Preparation of transparent TiO_2 thin-film photocatalyst and its photocatalytic activity. *Chem Lett* 1995, **24**, 841-842

Netti C. and Stanford H. Applications of reproducible SERS substrates for trace level detection, www.spectroscopymag.com, June 1, 2006

Nic Daeid N., Waddell R. The analytical and chemometric procedures used to profile illicit drug seizures. *Talanta* 2005, **67**, 280-285

Norrod K., Sudnik L., Rousell D., Rowlen K. Quantitative comparison of five SERS substrates: sensitivity and limit of detection. *Appl. Spectros.* 1997, **51**, 994-1001

Oliver J., Seymour A., Wylie F., Torrence H., Anderson R., Monitoring the effectiveness of UK field impairment tests. Department for Transport Road Safety Research Report No. 63. March 2006

O'Neal C., Crouch D., Robins D., Fatal A. The effects of collection methods on oral fluid codeine concentration. *J. Anal. Toxicol.* 2000, **24**, 536-542

Otto A. The First International Symposium on Surface Enhanced Raman Scattering 2006 Nishinomiya, Japan

Otto A., Raman-spectra of (CN)- absorbed at a silver surface. *Surf. Sci.* 1978, **75**, L392-L396

Pandey K., Schatz G. A detailed analysis of the Raman enhancement mechanisms associated with the interaction of a Raman scatterer with a resonant metal cluster – results for LIN-H2. *J. Chem. Phys.* 1984, **80**, 2959-2972

Perez R., Ruperez A., Laserna J., Evaluation of silver substrates for surface-enhanced Raman detection of drugs banned in sport practises, 1998, **376**, 255-263

Persson B., Ryberg R. Vibrational ineraction between molecules adsorbed on a metal-surface-the dipole-dipole interaction. *Phsy. Rev. B* 1981, **24**, 6954-6970

Quinn D., Wodak A., Day R. Pharmacokinetic and pharmacodynamic principles of illicit drug use and treatment of illicit drug users. *Clin. Pharmacokinet.* 1997, **33**. 344-400

Rang H.,Dale M., Ritter J. Pharmacology, 3rd Edition, Churchill Livingstone, Edingurgh 1995

Raman C., Krishnan K. A new type of secondary radiation *Nature*, 1928, **121**. 501

Railway and Transport Safety Act 2003 (c. 20) HMSO. London

Raymon L. Advanced Pharmacology Workshop. The International Association of Forensic Toxicologists Meeting, Melbourne, Australia. 2003

Research Technology Branch, National Institute on Drug Abuse. Drug concentrations and driving impairment. *JAMA.* 1985, **254**, 2618-2621

Ritchie R. Plasma losses by fast electrons in thin films. *Phys. Rev.* 1957, **106**, 874-881

Road Traffic Act. 1988 Chapter 52 HMSO. London. Reprinted 1991

Roe S., Man L., Drug misuse declared: findings from the 2005/2006 British Crime Survey. *Home Office Statistical Bulletin.* October 2006

Romberg R., Needleman S., Snyder J., Greedan A. Methamphetamine and amphetamine derived from the metabolism of Selegiline. *J. Forens. Sci.* 1995, **40**, 1100-1102

Ruperez A., Montes R., Laserna J., Identification of stimulant drugs by surface enhanced Raman spectroscopy on colloidal silver. *Vib. Spec.* 1991, **2**, 145-154

Ryder A. Surface enhanced Raman scattering for narcotic detection and applications to chemical biology. *Curr. Op. Chem. Biol.* 2005, **9**, 1-5

Ryder A. Classification of narcotics in solid mixtures using principal component analysis and Raman spectroscopy. *J. Forensic Sci* 2002, **47**, 275-284

Sagmuller B., Schwarze B., Brehm G., Trachta G., Schneider S. Identification of illicit drugs by a combination of liquid chromatography and surface-enhanced Raman scattering spectroscopy. *J. Mol. Struct.* 2003, **661-662**, 279-290

Samyn N., De Boeck G., Wood M., Lamers C., De Waard D., Brookhuis K., Verstraete A., Riedel W. Plasma, oral fluid and sweat wipe ecstasy concentrations in controlled and real life conditions. *Forens. Sci. Int.* 2002, **128**, 90-97

Sands H., Hayward I., Kirkbride T., Bennett R., Lacey R., Batchelder D. UV-excited resonance Raman Spectroscopy of narcotics and explosives. *J. Forens. Sci.* 1998, **143**, 509-513

Schechter M., MDMA as a discriminative stimulus: isomeric comparisons. *Pharmacol Biochem. Behav* 1987, **27**, 41-44

Schepers R., Oyler J., Joseph R., Cone E., Moolchan E., Huestis M. Methamphetamine and amphetamine pharmacokinetics in oral fluid and plasma after controlled oral methamphetamine administration to human volunteers. *Clin. Chem.* 2003, **49**, 121-123

Schifano F. Dangerous driving and MDMA (Ecstasy) abuse. *J. Serotonin Res.* 1995, **1**, 53-57

Schlegel V., Cotton T. Silver island films as substrates for enhanced Raman scattering: effect of deposition rate on intensity. *Anal. Chem.* 1991, **53**, 241-247

Semin D. Rowlen K. Influence of vapor deposition parameters on SERS active AG film morphology and optical properties. *Anal. Chem.* 1994, **66**, 4324-4331

Seymour A., Oliver J. A study of alcohol and drugs in impaired and fatally injured drivers in the West of Scotland. *J. Traffic Med.* 2000, **28**, 32-37

Shulgin A.T., The background and chemistry of MDMA. *J. Psychoactive Drugs* 1986, **18**, 291-304

Siegel I. The role of saliva in drug monitoring; *Anal. N. Y. Acad. Sci.* 1993, **694**, 1-348 Malamud D., Tabak L. (eds) Pub NYAS

Smith E., Dent G., Modern Raman Spectroscopy a practical approach, John Wiley and Sons Ltd, London, 2005

Smith F. Detection of amphetamine in bloodstains, semen, seminal stains, saliva, and saliva stains. *Forensic Sci. Int.* 1981, **17**, 225-228

Sonderman N., Kower K. Screening experiments of ecstasy street samples using Near Infrared Spectroscopy. *Forensic Sci. Int.* 1999, **106**, 147-156

Stewart M. PhD thesis Development and characterisation of novel photocatalytically prepared SE(R)RS substrates. 2005, Strathclyde University, Glasgow

Sudnik L., Norrod K., Rowlen K. SERS active Ag films from photoreduction of Ag^{+} on TiO_2. *Appl. Spectrosc.* 1996, **50**, 422-424

Sulk R., Corcoran R., Carron K. Surface-enhanced Raman scattering detection of amphetamine and methamphetamine by modification with 2-mercaptonicotinic acid. *App. Spec.* 1999, **53**, 954-959

Sutherland W., Laserna J., Angebranndt M., Winefordner J. Surface enhanced Raman analysis of sulfa drugs on colloid silver dispersion. *Ana. Chem.* 1990, **62**, 689-693

TICTAC: version 4:3 July (1999). J. Ramsey. The Stationary Office

The Misuse of Drugs Act 1971 (Modification) Order 2001 SI 3932 London

The Misuse of Drugs Act 1971 (Amendment) Order 2006 SI 3331 London

Valter K., and Arrizabalaga P. *Designer Drugs Directory,* Elsevier Science, Amsterdam 1998

Van Duyne R., Hulteen J., Treichel D. Atomic force microscopy and surface enhanced Raman spectroscopy. I. Ag island films and Ag film over polymer nanosphere surfaces supported on glass. *J. Phys Chem.* 1993, **99**, 2101-2115

Ventura M., Pichini S., Ventura R., Zuccaro P., Pacifici R., De la Torre R. Stability studies of principal illicit drugs in oral fluid: preparation of reference materials for external quality assessment schemes. *Ther. Drug. Monit.* 2007, **29**, 662-665

Verstraete A., Raes E., Rosita II report. March 2006 www.rosita.org

Vollenweider F., Gamma A., Liechti M., Huber T. Psychological and cardiovascular effects and short term sequelae of MDMA ("ecstasy") in MDMA naïve healthy volunteers. *Neuropsychopharm.* 1998, **19**, 241-251

Vo-Dinh T. Surface-enhanced Raman spectroscopy using metallic nanostructures, 1998, **17**, 557-582

Walsh J.M. An evaluation of oral fluid for point of collection testing devices. *J. Ana. Tox.* 2003, **27**, 429-439

Wan S., Martin S., Azarnoff D. Kinetics salivary excretion of amphetamine isomers and effects of urinary pH. *Clin. Pharmacol. Ther.* 1978, **23**, 585-590

Wang R., Hashimoto K., Fujishima A., Chikuni M., Kojima E., Kitamura M., Shimohigoshi M., Watanabe T. Light induced amphilic surfaces. *Nature*. 1997, **388**, 431-432

Wang Y., Li Y., Zhang Z., An D. Surface-enhanced Raman scattering of some water insoluble drugs in silver hydrosols. *Spectro. Chim. Acta.* 2003, **59**, 589-594

World Drug Report 2008, United Nations Office on Drugs and Crime, United Nations Publication 2008

World Drug Report 2006, United Nations Office on Drugs and Crime, United Nations Publication 2006

Wylie F., Torrance H., Anderson R., Oliver J. Drugs in oral fluid Part I. Validation of an analytical procedure for licit and illicit drugs in oral fluid. *For. Sci. Int.* 2005a, **150**, 191-198

Wylie F., Torrance H., Seymour A., Buttress S., Oliver J. Drugs in oral fluid Part II. Investigation of drugs in drivers. *For. Sci. Int.* 2005b, **150**, 199-204

Xu H., Bjerneld E., Kall M., Borjesson L. Spectroscopy of single hemoglobin olecules by surface enhanced Raman scattering. *Phys Rev Letters* 1999, **83**, 4357-4360

Zeman E., Schatz G.C. An accurate electromagnetic theory study of surface enhancement factors for AG, AU, CU, LI, NA, AL, GA, IN, ZN and CD. *J. Phys. Chem.* 1987, **91**, 634-643